

10-2-2009

# Discovery of a Novel Ring Fragmentation Reaction; Efficient Preparation of Tethered Aldehyde Ynoates and N-Containing Heterocycles; Radical Addition Approach to Asymmetric Amine Synthesis

Cristian Draghici  
*University of Vermont*

Follow this and additional works at: <http://scholarworks.uvm.edu/graddis>

---

## Recommended Citation

Draghici, Cristian, "Discovery of a Novel Ring Fragmentation Reaction; Efficient Preparation of Tethered Aldehyde Ynoates and N-Containing Heterocycles; Radical Addition Approach to Asymmetric Amine Synthesis" (2009). *Graduate College Dissertations and Theses*. Paper 70.

This Dissertation is brought to you for free and open access by the Dissertations and Theses at ScholarWorks @ UVM. It has been accepted for inclusion in Graduate College Dissertations and Theses by an authorized administrator of ScholarWorks @ UVM. For more information, please contact [donna.omalley@uvm.edu](mailto:donna.omalley@uvm.edu).

**DISCOVERY OF A NOVEL RING FRAGMENTATION REACTION;  
EFFICIENT PREPARATION OF TETHERED ALDEHYDE YNOATES  
AND N-CONTAINING HETEROCYCLES;  
RADICAL ADDITION APPROACH TO ASYMMETRIC AMINE SYNTHESIS**

A Dissertation Presented

by

Cristian Draghici

to

The Faculty of the Graduate College

of

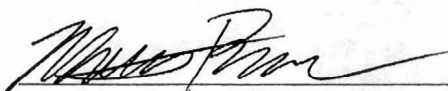
The University of Vermont

In Partial Fulfillment of the Requirements  
for the Degree of Doctor of Philosophy  
Specializing in Chemistry

May, 2009

Accepted by the Faculty of the Graduate College, The University of Vermont, in partial fulfillment of the requirements for the degree of Doctor of Philosophy specializing in Organic Chemistry.

**Thesis Examination Committee:**

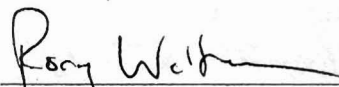


Matthias Brewer, Ph.D.

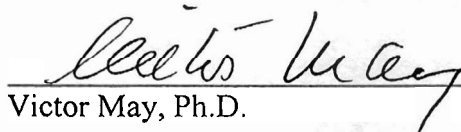
Advisor



José S. Madalengoitia, Ph.D.

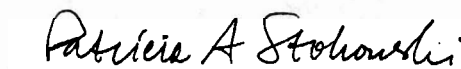


Rory Waterman, Ph.D.



Victor May, Ph.D.

Chairperson



Patricia A. Stokowski, Ph.D.

Interim Dean, Graduate College

Date: February 27, 2009

## ABSTRACT

This dissertation describes the development of a novel ring fragmentation reaction in which cyclic  $\gamma$ -silyloxy- $\beta$ -hydroxy- $\alpha$ -diazoesters undergo efficient rupture of the C $_{\beta}$ -C $_{\gamma}$  bond when treated with tin tetrachloride to provide tethered aldehyde ynoate products with varying tether length, in high yield.

Tethered aldehyde ynoates are versatile intermediates and this functional group combination is unique to this fragmentation. The synthetic utility of tethered aldehyde ynoates is highlighted by their predisposition to undergo facile intramolecular [1,3]-dipolar cycloaddition reactions in presence of bistrimethylsilyl- $\alpha$ -amino acids to provide 2,5-dihydropyroles. The ability to quickly assemble such structural motifs encouraged studies on the synthesis of steroidal alkaloid solanidine.

A new method for the *N*-amination of oxazolidiones with NH<sub>2</sub>Cl was investigated and provides efficient access to acyl hydrazines. However, the full scope of the reaction has not been yet fully explored.

The study of isopropyl radical additions to *N*-acylhydrazones and comparison of several stereocontrol elements on the oxazolidinone moiety revealed that all are effective.

## CITATION

Material from this dissertation has been published in the following form:

Draghici, C., Brewer, M.. (2008). Lewis acid promoted carbon-carbon bond cleavage of  $\gamma$ -silyloxy- $\beta$ -hydroxy- $\alpha$ -diazoesters. *Journal of the American Chemical Society*, 130, 3766-3767.

*Pentru Ion, Veronica si Oana cu dragoste*

## ACKNOWLEDGMENTS

I would like to express my gratitude to Professor Matthias Brewer for allowing me the independence to formulate my own ideas and the support to push them to new understanding.

I thank Professor Gregory K. Firestad for his guidance and support, and Dr. Jean-Charles Marié for the time he took to carefully answer every single question I had in my first year as a graduate student.

I am indebted to Dr. Paul A. Krapcho and Dr. Martin Kuehne for offering me almost limitless access to two of the most remarkable minds in chemistry.

I thank Jodi Wyman, Ali Bayir, Nezar Al Bataineh, Dr. Qiufeng Huang, and in particular, Irfan Mohammad Javed and Derek Laws, for their company, support and scientific insights over the years.

With my deepest feelings I thank Katrin Sara Sadigh for the love and encouragement with which she has provided me from the onset.

I would like to thank Jeff Powers and Michelle LaMalfa for their unlimited support and friendship.

I would also like to thank the Kishes for their love and support and for welcoming me as part of the family.

Finally, I am sincerely grateful to my parents, Ion and Veronica Draghici, and my sister, Oana Draghici, for having the courage and the heart to allow me to pursue my dreams on another continent. Without their presence, this work would not have been possible.

## TABLE OF CONTENTS

	Page
CITATION.....	ii
ACKNOWLEDGMENTS .....	iv
LIST OF FIGURES .....	ix
LIST OF TABLES .....	x
1. Chapter 1: Background .....	1
1.1. The Chemistry of $\alpha$ -Diazo Carbonyl Compounds.....	1
1.1.1. Structure of $\alpha$ -diazo carbonyl compounds.....	1
1.1.2. Reactivity profile of $\alpha$ -diazo carbonyl compounds .....	3
1.1.3. Reactivity profile of vinyl cation species generated from $\beta$ -hydroxy- $\alpha$ -diazo carbonyl compounds .....	10
1.1.4. Thermal stability of diazo compounds.....	13
1.1.5. Conclusions.....	14
1.2. Heterolytic Carbon-Carbon (C-C) bond cleavage reactions.....	14
1.2.1. Classification of heterolytic fragmentation reactions .....	16
1.2.2. Alkyne-forming fragmentation reactions of acyclic systems .....	20
1.2.3. Alkyne-forming fragmentation reactions of cyclic systems .....	22
1.2.4. Miscellaneous transition metal induced fragmentations.....	24
1.2.5. Conclusions.....	26
2. Chapter 2: Discovery of a new mode of reactivity for diazo-esters .....	27
2.1. Novel approach to keto-furans with an unexpected result.....	27



2.2.	Hypothesis.....	33
2.3.	Testing the hypothesis.....	33
2.4.	Optimization of reaction conditions.....	35
2.4.1.	Lewis Acid Screening.....	35
2.4.2.	Temperature Effect .....	36
2.4.3.	Solvent Effect.....	37
2.4.4.	Concentration Effect .....	37
2.5.	Synthesis of ring fragmentation precursors .....	37
2.5.1.	Synthesis of $\alpha$ -silyloxy ketones.....	38
2.5.2.	Synthesis of the requisite $\gamma$ -silyloxy- $\beta$ -hydroxy- $\alpha$ -diazo esters .....	42
2.5.3.	Determination of stereochemical outcome of ethyl lithio-diazoacetate addition to cyclic $\alpha$ -silyloxy ketones.....	44
2.6.	Fragmentation results.....	48
2.7.	Discussion of proposed reaction mechanisms .....	51
2.8.	Exploring the versatility of the fragmentation protocol.....	60
2.9.	Pursuit of alternate fragmentation strategies.....	65
2.10.	Future perspective.....	69
2.10.1.	Expanding the utility of the novel fragmentation reaction .....	69
2.11.	Conclusions.....	73
3.	Chapter 3: Tethered aldehyde ynoates – useful synthetic intermediates .....	74
3.1.	Background.....	74
3.1.1.	Previously reported preparative routes to tethered aldehyde ynoates.....	74
3.1.2.	Recent applications of tethered aldehyde ynoates .....	76

3.1.3. Intramolecular [1,3]-dipolar cycloaddition reactions of tethered alkynyl aldehydes.....	79
3.2. Intramolecular [1,3]-dipolarcycloadditions of tethered aldehyde ynoates with stabilized and unstabilized azomethine ylides .....	89
3.2.1. Intramolecular reactions with stabilized azomethine ylides .....	89
3.2.2. Intramolecular reactions with unstabilized azomethine ylides .....	93
3.2.3. Development of a one pot ring fragmentation / [1,3]-dipolar cycloaddition reaction protocol .....	100
3.2.4. Conclusions and future perspective .....	101
3.3. Applications towards the synthesis of steroidal alkaloid solanidine .....	103
3.3.1. Background .....	103
3.3.2. Application of fragmentation / [1,3] – dipolarcycloaddition protocol towards the synthesis of solanidine .....	107
3.4. Conclusions.....	120
4. Chapter 4: Radical Addition Approach to Asymmetric Amine Synthesis .....	121
4.1. Background.....	121
4.2. Design and synthesis of chiral <i>N</i> -acylhydrazones .....	130
4.2.1. Synthesis of chiral <i>N</i> -acylhydrazones .....	132
4.2.2. Effect of varying the stereocontrol element in radical additions to <i>N</i> -acylhydrazones.....	137
4.3. Conclusions.....	138
5. Chapter 5: Experimental Procedures .....	140
5.1. General.....	140

5.2. Experimental procedures for the preparation of new $\alpha$ -silyloxy and $\alpha$ -alkoxy ketones .....	141
5.3. Experimental procedures for the preparation $\gamma$ -hydroxy- $\beta$ -silyloxy- $\alpha$ -diazoesters and $\gamma$ -hydroxy- $\beta$ -alkoxy- $\alpha$ -diazoesters.....	148
5.4. Experimental procedures for the preparation of fragmentation products .....	158
5.5. Procedures for the preparation of <i>N</i> -containing heterocycles via [1,3]-dipolar cycloaddition reactions .....	164
5.6. Miscellaneous procedures.....	171
5.7. Tin-Mediated Radical Addition to Hydrazones.....	173
REFERENCES .....	177
APPENDIX.....	187

## LIST OF FIGURES

	Page
Figure 1.1. The first $\alpha$ -diazo carbonyl compound .....	1
Figure 1.2. Postulated configurations for diazo compounds.....	2
Figure 1.3. Diazo contributing resonance structures .....	3
Figure 1.4 ‘ <i>Destabilized</i> ’ vinyl cation .....	11
Figure 2.1. Alkenyl diazonium salt 117: a fragmentable system.....	31
Figure 2.2. X-ray crystal structure of 157s .....	44
Figure 2.3. X-ray crystal structure of 158s .....	45
Figure 2.4. Long range “W” coupling .....	46
Figure 2.5. ROESY NOE’s of steroid derived diazoester 159a.....	47
Figure 2.6. Chelation of transition metals to the diazo functional group .....	53
Figure 2.7. Energy diagram .....	59
Figure 2.8. Alternate fragmentation precursors .....	61
Figure 3.1. Conformational constraints in [1,3]-dipolarcycloaddition reactions.....	82
Figure 3.2. Proposed steric effect of the neighboring groups on the stereoselectivity of ethyl lithio-diazoacetate addition.....	109
Figure 3.3. Remaining challenges in the synthesis of solanidine. ....	115
Figure 4.1. Nucleophilic addition to C=N bonds.....	121
Figure 4.2. Radical addition to C=N bonds. ....	122
Figure 4.3. Approaches to stereocontrol for radical addition to C=N bonds.....	129
Figure 4.4. (a) Design of a hypothetical N-linked auxiliary approach for stereocontrolled radical addition to C=N bonds, with Lewis acid (LA) chelation inducing a rigid, electronically activated radical acceptor. (b) Implementation with N-acylhydrazones derived from 4-benzyl-2-oxazolidinone. ....	131

## LIST OF TABLES

	Page
Table 2.1. Optimization of reaction conditions .....	36
Table 2.2. Ethyl lithio-diazoacetate addition to $\alpha$ -silyloxy ketones .....	43
Table 2.3. Fragmentation results.....	49
Table 2.3. Fragmentation results continued.....	50
Table 2.4. Synthesis of alternate fragmentation precursors.....	62
Table 3.1. Optimization of reaction conditions .....	92
Table 3.2. Synthesis of $\alpha$ -silyloxy and $\alpha$ -alkoxy ketones 346a, 346b, 346c.....	112
Table 3.2. Ethyl lithio-diazoacetate addition to steroid derived differentially protected $\alpha$ -silyloxy and $\alpha$ -alkoxy ketones.....	113
Table 4.1. Diastereoselectivity in tin-mediated radical additions of isopropyl iodide with propionaldehyde hydrazone.....	138

## 1. CHAPTER 1: BACKGROUND

### 1.1. The Chemistry of $\alpha$ -Diazo Carbonyl Compounds

The preparation of the first aliphatic substance to contain the diazo functional group, ethyl diazoacetate (**1**, Figure 1.1), by Curtius<sup>1</sup> in 1883 marked the beginning of a prolific period of time in organic synthesis. For more than 100 years, diazo compounds have been shown to react differently when treated with Lewis and Brønsted acids, transition metals or when irradiated with light, which lead to the development of a wide array of synthetically useful chemical transformations.

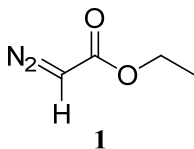


**Figure 1.1. The first  $\alpha$ -diazo carbonyl compound**

Diazo compounds can be generally divided in two main categories: unstabilized aliphatic diazos and  $\alpha$ -diazo carbonyl compounds. Grounds for such classification are given by the fact that the two groups differ drastically as far as their overall stability, reactivity and methods of preparation are concerned. It is commonly understood that unstabilized aliphatic diazo compounds are less stable and require more elaborate methods of preparation than the  $\alpha$ -diazo carbonyl counterparts. Structural, reactivity and stability aspects of  $\alpha$ -diazo carbonyl compounds shall be discussed in the following sections as they pertain to the topics embodied in this dissertation work.

#### 1.1.1. Structure of $\alpha$ -diazo carbonyl compounds

The structure of diazo compounds was the subject of debate for many years after their discovery. Initially, Curtius<sup>2</sup> suggested diazirine **2** (Figure 1.2) as the preferred configuration of diazo compounds, while Thiele,<sup>3</sup> in 1911 proposed the open configuration as represented by structure **3**. In 1935 Boersch<sup>4</sup> used the data gathered from an electron diffraction experiment to partially settle the debate in favor of the linear arrangement.

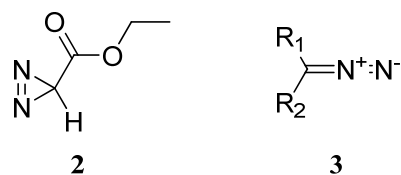
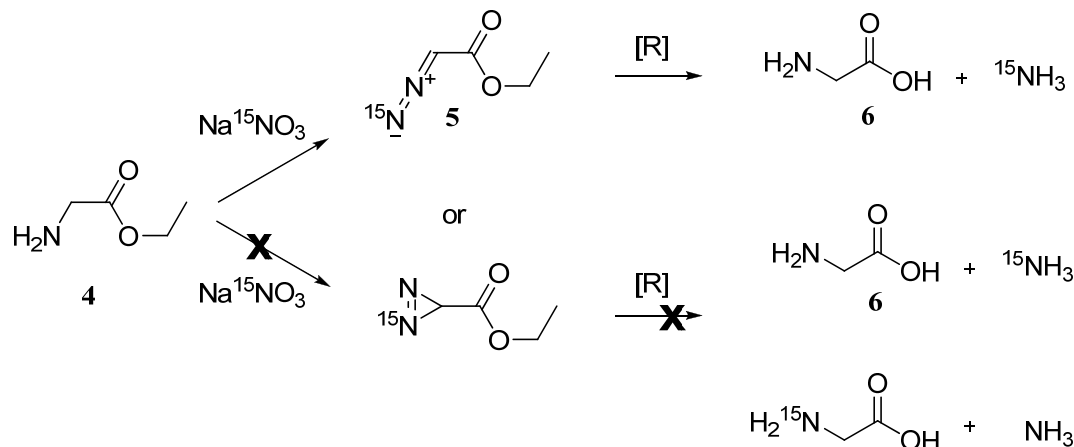


**Figure 1.2. Postulated configurations for diazo compounds**

The correct structure of diazo compounds was not fully elucidated until 1957 when a chemical experiment was devised to prove the open structure for ethyl diazoacetate<sup>5</sup>. Note that in diazirine structure **2** (Figure 1.2) the two nitrogens occupy indistinguishable positions, while in the open diazo configuration **3**, they reside in distinct locations.

The experiment began with diazotization of ethyl glycinate (**4**) with  $^{15}\text{N}$ -labeled sodium nitrate to provide labeled ethyl diazoacetate (**5**) which was subsequently reductively cleaved to glycine (**6**) and ammonia (Scheme 1.1). The fact that the labeled  $^{15}\text{N}$  was exclusively released as ammonia and none was found incorporated into glycine proved the linear structure. If diazirine structure (**2**) were correct, than a statistical distribution of the label would have been expected.

Scheme 1.1.



### 1.1.2. Reactivity profile of $\alpha$ -diazo carbonyl compounds

With a linear geometry diazo compounds have three main contributing resonance structures represented as 7, 8 and 9 (Figure 1.3). These resonance forms help to explain why diazos undergo transformations via three main paths: carbene and carbenoid reactions, [1,3]-dipolar cycloadditions and electrophilic, and nucleophilic substitutions at the  $\text{C}(\alpha)$  position. Examples of each reaction manifold are given and discussed below.

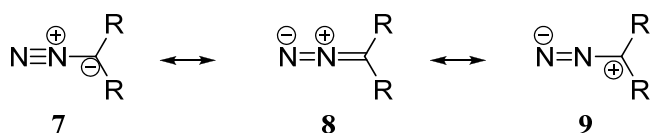


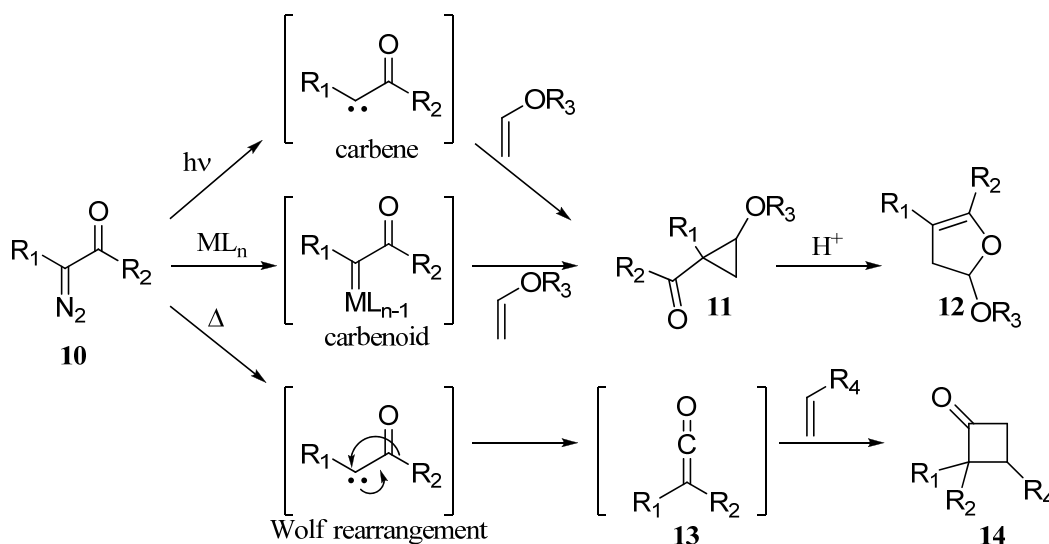
Figure 1.3. Diazo contributing resonance structures

$\alpha$ -Diazo carbonyl compounds (e.g 10, Scheme 1.2) have the ability to form carbenes when irradiated with light and carbenoid type species when treated with transition metals. These highly reactive species can be trapped intermolecularly by electron rich olefins to form substituted cyclopropanes (e.g 11) and unsaturated furans



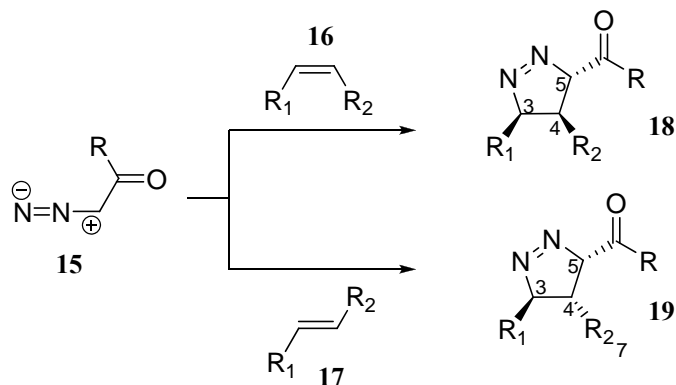
(e.g. **12**).  $\alpha$ -Diazo carbonyls can also thermally decompose to generate carbenes, which then undergo a Wolf type rearrangement to give rise to highly reactive ketene species (e.g. **13**, Scheme 1.2).<sup>6,7</sup> Alkenes can trap ketenes via a [2+2] cycloaddition reactions to yield substituted cyclobutanones (e.g. **14**).

Scheme 1.2.



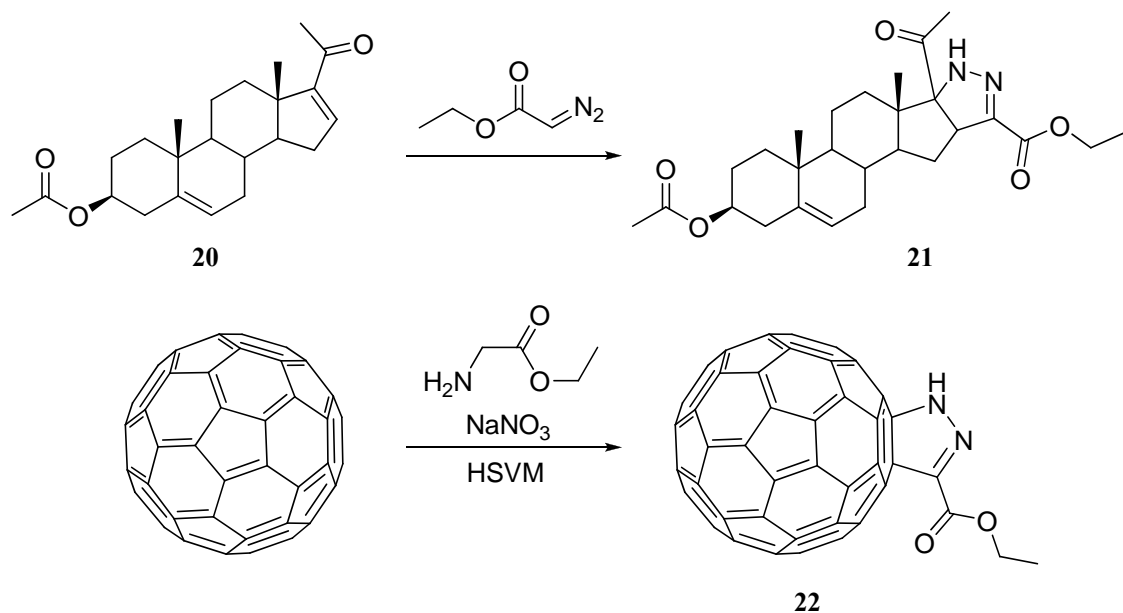
$\alpha$ -Diazo carbonyl compounds have also been shown to participate in [1,3]-dipolar cycloaddition reactions. These are transformations that occur via a concerted mechanism in which resonance form **15** (Scheme 1.3) adds across dipolarophiles such as alkenes (e.g. **16** and **17**) to provide pyrazolines (e.g. **18** and **19**). The addition to the dipolarophile is stereospecific and the relative configuration of the dipolarophile is conserved in the cycloadduct. Thus, the [1,3]-dipolar cycloaddition of *cis* alkene **16** with diazocarbonyl **15** provides the appropriate 3,4-*cis*-, 4,5-*trans*-relative configuration in the cycloadduct **18**, while that of *trans* alkene **17** affords the 3,4-*trans*-, 4,5-*cis*- pyrazoline **19**.<sup>8</sup>

Scheme 1.3.



As early as 1954 Riegel and Mueller reported the addition of ethyl diazoacetate to 3 $\beta$ -acetoxy-5,16-pregnadiene-20-one (**20**, Scheme 1.4),<sup>9,10</sup> an extension of the well known addition of diazomethane to 16-dehydro-20-keto steroids, which affords the corresponding pyrazoline carboxylic ester (**21**).<sup>11</sup>

Scheme 1.4.

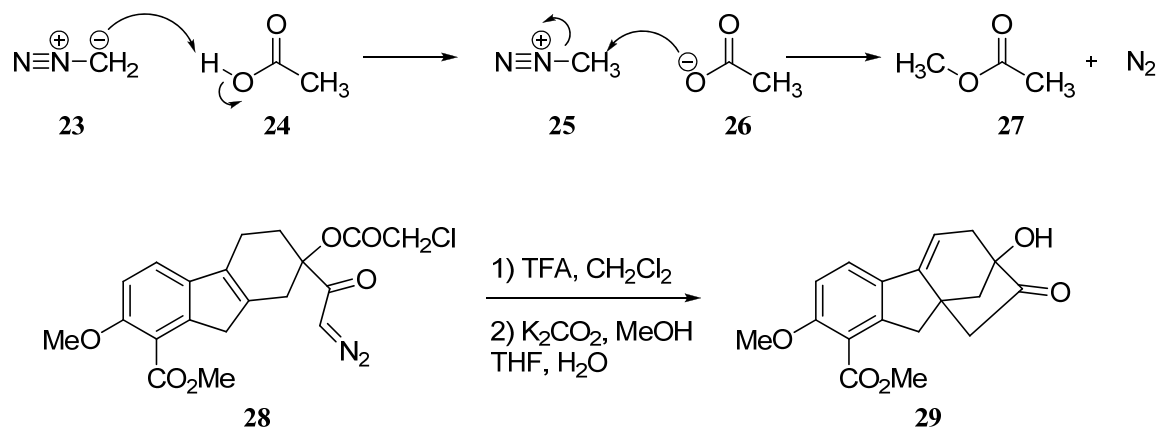


In an interesting application of this reactivity, Wang<sup>12</sup> and coworkers also took advantage of the ability of ethyl diazoacetate to readily undergo a [1,3]-dipolar cycloaddition reaction to prepare [60]Fullerene-fused pyrazoline **22**.

Reactions of diazo species which invoke electrophilic and nucleophilic substitution at the C( $\alpha$ ) position have also found application in synthesis. Until recently this reactivity profile has mainly found use in reactions of diazo compounds with protic acids to form diazonium ions, which subsequently react further. The pre-eminent example of this is the use of diazomethane for the esterification of carboxylic acids (Scheme 1.5). In this reaction, diazomethane (**23**) initially acts as a base to deprotonate carboxylic acid **24** forming the carboxylate ion **26** and methyl diazonium ion **25**. The electrophilic methyl diazonium ion then undergoes nucleophilic attack by the carboxylate ion to provide methyl ester **27** and molecular nitrogen. This process is a highly unique chemical transformation as it represents a complete transposition in reactivity of one atom of a reagent; an atom that was initially moderately nucleophilic becomes highly electrophilic.

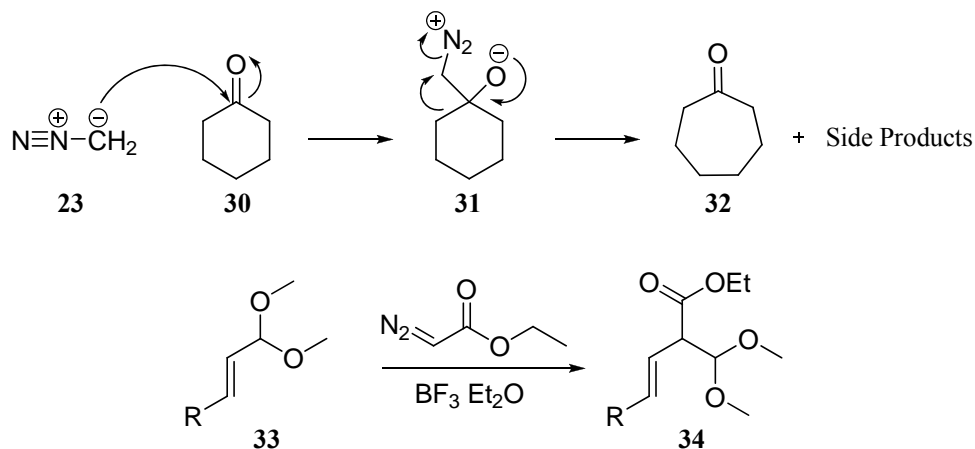
This reactivity switch is key to the  $\alpha$ -substitution transformations that diazo compounds undergo and has been used in intramolecular reactions. For example, the acid-induced conversion of 4-diazoacetylcyclohexane **28** into bicyclo[3.2.1]octanone **29** in 89 % yield over two steps after hydrolysis of the chloroacetate group proceeds by intramolecular cyclization of an olefin onto a diazonium ion (Scheme 1.5).<sup>13</sup>

Scheme 1.5.



The ability of unstabilized diazo compounds to act as competent nucleophiles is highlighted in their reactions with acid chlorides to provide  $\alpha$ -carbonyl diazo species and with ketones and aldehydes to provide the homologated carbonyl compounds.<sup>14</sup> Such types of transformations can lead to either preservation or loss of the diazo functional group during the course of the reaction. As an example of the latter case, nucleophilic attack of diazo methane (23, Scheme 1.6) onto the carbonyl group of cyclohexanone (30) yields diazonium betaine 31, which undergoes a Tiffeneau-Demajnov-type rearrangement<sup>15,16</sup> to provide homologated ketone 32 with loss of molecular nitrogen. The difficulty encountered with this type of reaction is that a mixture of products is observed when unsymmetrical carbonyl compounds are used; epoxide formation is a common side reaction, and multiple homologation is often unavoidable. However this reaction can be improved when run in the presence of a Lewis acid such as boron trifluoride, which is important to note because it highlights the use of Lewis acids in the presence of alkyl diazo species.<sup>17-19</sup>

Scheme 1.6.

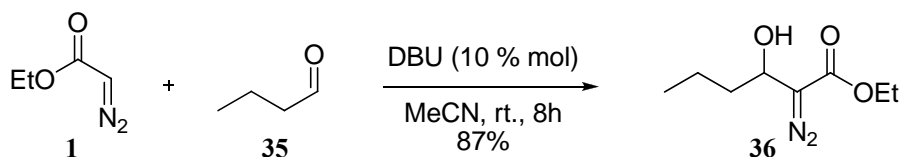


$\alpha$ -Diazo carbonyl compounds are less nucleophilic than unstabilized diazos, but are still competent nucleophiles for highly reactive electrophiles. The nucleophilic additions of alkyl diazoacetates onto carboxonium ions generated from carbonyls and triethyloxonium tetrafluoroborate accompanied by loss of the diazo functional group serve as a good examples.<sup>20</sup> Doyle<sup>21</sup> and co-workers utilized this reactivity to prepare  $\beta,\gamma$ -unsaturated esters (e.g. **34**, Scheme 1.6) by Lewis acid catalyzed homologation of ethyl diazoacetate (**1**) with  $\alpha,\beta$ -unsaturated acetals (e.g. **33**).

Additionally,  $\alpha$ -diazo carbonyl compounds have also been shown to be suitable nucleophiles for condensations with less reactive electrophiles, in the presence of mild bases. For example, Wang<sup>22</sup> recently reported the nucleophilic addition of ethyl diazoacetate (**1**, Scheme 1.7) to butyraldehyde (**35**) promoted by catalytic amounts of 1,8-diazabicyclo[5.4.0]undec-7-ene (DBU) to provide  $\beta$ -hydroxy- $\alpha$ -diazoester **36** in 87% yield. It is important to note that nucleophilic additions of  $\alpha$ -diazo carbonyl compounds to ketones, generally less reactive than aldehydes, do not occur under such

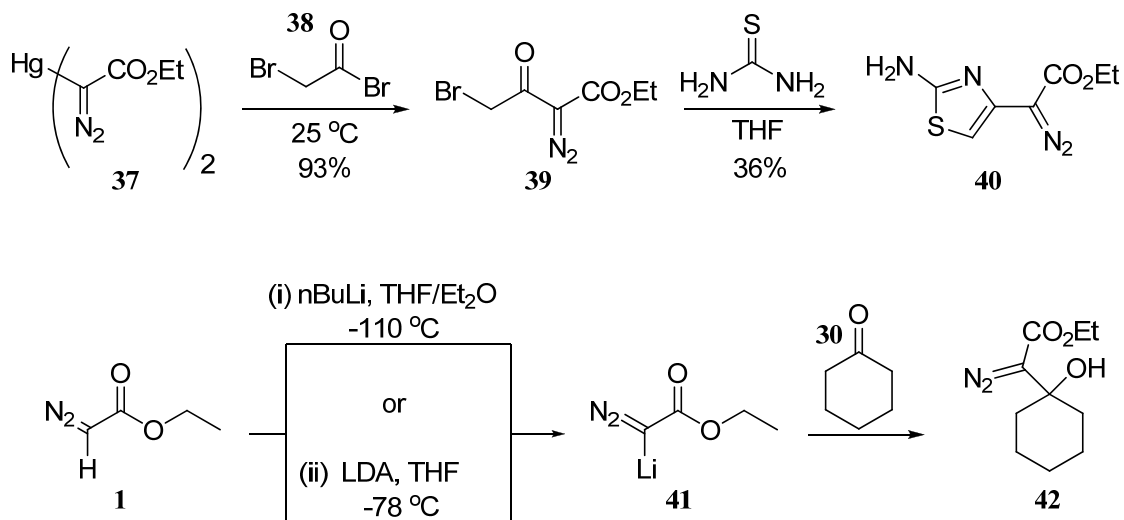
mild conditions, and promoting such transformations requires much stronger acyldiazomethane nucleophiles.

Scheme 1.7.



The high C( $\alpha$ )H-acidity allows acyldiazomethanes to undergo efficient metallation reactions,<sup>23</sup> and provide highly reactive nucleophiles (e.g **37** and **41**, Scheme 1.8) which efficiently add to a variety of electrophiles with preservation of N<sub>2</sub> functional group. This class of reactions is known as ‘electrophilic diazoalkane substitutions.’<sup>24,25</sup> One such example is the acylation of diazomercurial reagent **37**<sup>26</sup> (Scheme 1.8) with bromoacetyl bromide **38** to form bromodiazoester **39**, which further reacts with thiourea to provide 2-amino diazothiazole **40** in 36% yield.<sup>27</sup>

Scheme 1.8.



Another example of a highly reactive and commonly used metallo-acyldiazomethane nucleophile is ethyl lithio-diazoacetate (**41**, Scheme 1.8). This can be easily accessed in situ via metallation of ethyl diazoacetate (**1**) with: (i)<sup>28</sup> butyllithium in ether or THF/ether at -110°C or (ii)<sup>29</sup> lithium diisopropylamide (LDA) in THF at -78°C. Ethyl lithio-diazoacetate (**41**) adds to less reactive electrophiles such as cyclohexanone (**30**) to afford  $\beta$ -hydroxy- $\alpha$ -diazo esters (e.g. **42**).<sup>29</sup> This transformation is of importance as it emerged as a viable method for the efficient preparation of a new set of  $\beta$ -hydroxy- $\alpha$ -diazo ester derivatives found to undergo an unprecedented fragmentation reaction that shall be discussed in this dissertation work.

$\beta$ -Hydroxy- $\alpha$ -diazo carbonyl compounds (e.g. **42**, Scheme 1.8) have been shown to be valuable synthetic intermediates which undergo a wide range of transformations.<sup>30-34</sup> Notably, a recent study revealed that the reaction of diazo carbonyl compounds with  $\text{BF}_3 \cdot \text{OEt}_2$  in various solvents affords an unusual array of products, seemingly involving vinyl cation intermediates (e.g. **43**, Figure 1.4).<sup>29,35</sup> The following section will present some important aspects concerning these species as they appear to play an important role in the outcome of the newly developed reaction presented in this dissertation work.

### **1.1.3. Reactivity profile of vinyl cation species generated from $\beta$ -hydroxy- $\alpha$ -diazo carbonyl compounds**

The chemistry of carbenium ions has been extensively studied since the turn of the last century.<sup>36,37</sup> Major methods used for the generation of vinyl cations consist of: electrophilic addition to the triple bond of acetylenes<sup>38-41</sup> or the cumulene bond of

allenes;<sup>42,43</sup> intramolecular participation of acetylenic<sup>44,45</sup> and allenyl<sup>46-48</sup> bonds in solvolysis reactions; and ionization of suitable vinylic derivatives.<sup>49-52</sup> More recently Padwa<sup>29</sup> reported a detailed study regarding the generation and rearrangement of ‘*destabilized*’ vinyl cations (e.g. **43**, Figure 1.4; species in which an electron withdrawing group is attached directly to the carbon atom bearing the positive charge) employing the use of the diazo functional group.

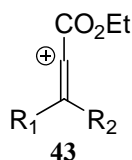
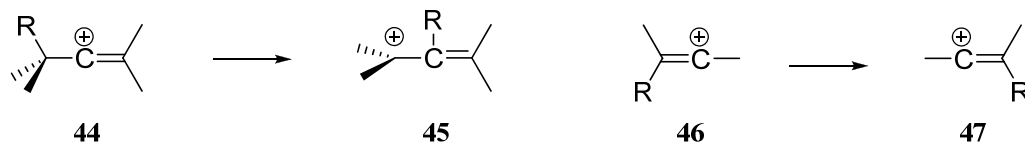


**Figure 1.4 ‘Destabilized’ vinyl cation**

The sp-hybridized carbon atom of a vinyl cation possesses an empty  $\pi$ -orbital. As a result, atoms possessing nonbonding pairs of electrons, multiple bonds, and  $\sigma$ -bonds react rapidly with these reactive intermediates. For example, the solvolysis of vinyl derivatives in oxygen-containing solvents typically affords vinyl ethers and ketones as products which is the consequence of solvent participation.<sup>53,54</sup>

**Scheme 1.9.**

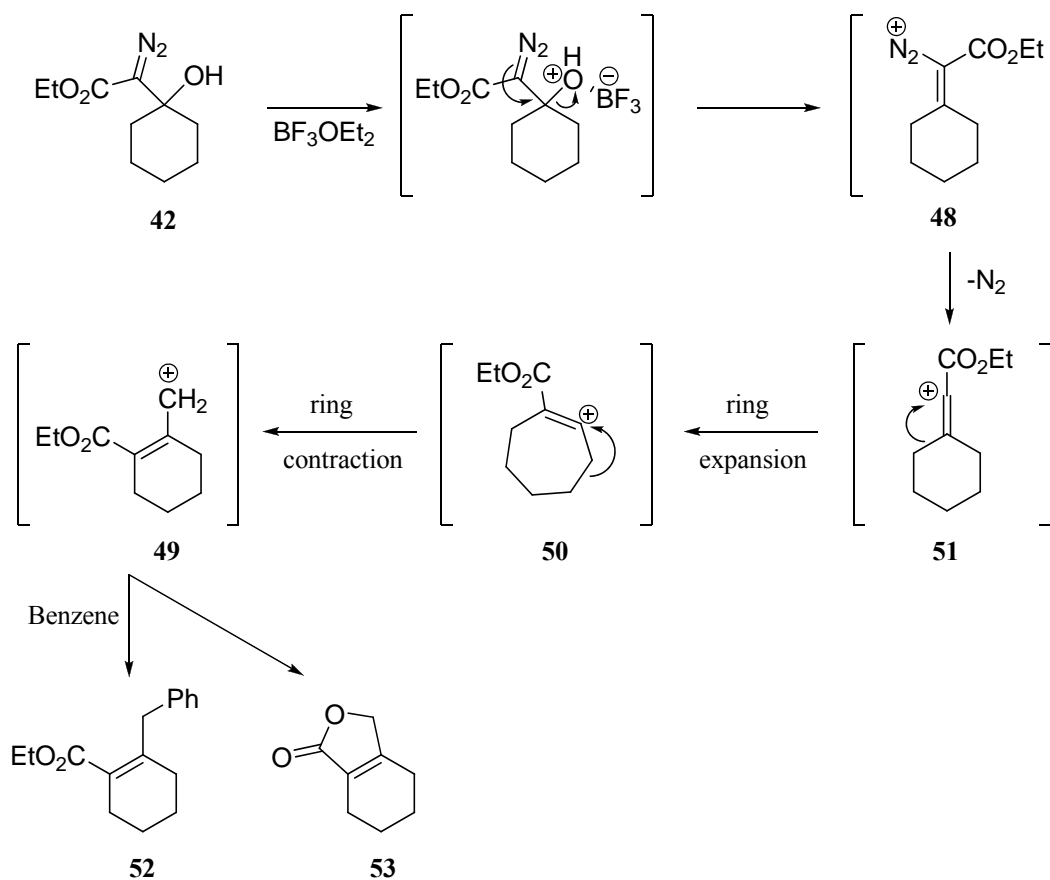


Vinyl cations can also undergo reactions with the electrons of C-H and C-C  $\sigma$ -bonds. The deprotonation and rearrangement of vinyl cations to produce alkynes are examples of such  $\sigma$ -bond reactions. Rearrangement of these unsaturated cations can be



classified in two general categories: (a) migration to the double bond with the formation of an allylic cation (**44** → **45**, Scheme 1.9) and (b) migration of an alkyl group across the double bond whereby one vinyl cation is isomerized to another (**46** → **47**). These rearrangements occur whenever a more stable ion is formed from a less stable progenitor.

**Scheme 1.10.**



The pre-eminent example of this is the reaction of  $\beta$ -hydroxy- $\alpha$ -diazo ester **42** (Scheme 1.10) which is thought to proceed via complexation of the alcohol functionality with boron trifluoride etherate followed by elimination of the alcohol to

generate cycloalkylidene diazonium salt **48**. Loss of nitrogen produces a highly reactive, *destabilized*, linear vinyl cation (e.g. **51**). Ring expansion via a 1,2-methylene shift leads to the formation of a more stable, bent cycloalkenyl vinyl cation (e.g. **50**). A subsequent 1,2-methylene shift results in ring contraction ultimately leading to a stable allylic cation (e.g. **49**). This cation is either trapped by solvent or undergoes cyclization with the adjacent ester group to give a lactone (e.g. **53**).<sup>29</sup>

#### 1.1.4. Thermal stability of diazo compounds

Diazo compounds are considered sensitive and/or thermolabile, and there have been many documented cases of accidents caused by explosions involving this class of organic compounds. However, without differentiation, stating that *all* diazo compounds are as sensitive and/or thermolabile could be quite untrue. The complexity of the field of thermal decomposition of diazo compounds was very early recognized by Staudiger and Gaule who stated:<sup>55</sup> “More complex than the acid-initiated decomposition is indeed the behavior of diazo compounds when decomposed by heat... general rules could *not* be found.” This statement remains valid even today.

The pathway by which diazo compounds decompose becomes clearer when considering valence structures **7**, **8** and **9** (Figure 1.3). The former is of special importance for the elimination of nitrogen. However, it has become common knowledge that substituents with electron acceptor character capable of stabilizing **7** by delocalization of the negative charge, increase the thermal stability of diazo alkanes.  $\alpha$ -Diazo carbonyl compounds are examples of such class of thermally stable materials that generally exhibit relatively long shelf lives.

### 1.1.5. Conclusions

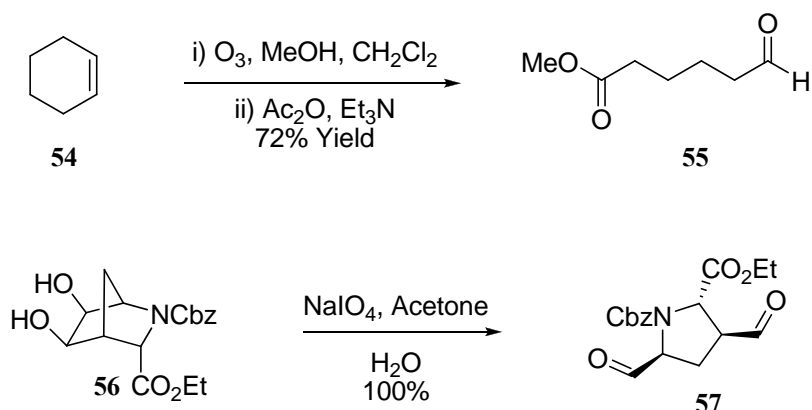
The variety of conditions under which diazo compounds have been shown to react over a period of more than 100 years suggests how versatile this class of organic compounds truly is. Such incessant exploration has generated a wealth of knowledge concerning synthetic uses and the reactivity and stability of both unstabilized aliphatic diazo and  $\alpha$ -diazo carbonyl compounds. This has allowed chemists to utilize diazo compounds as a key functional group in the development of novel synthetic methods which, in turn, serve in the synthesis of complex natural products. The dissertation work presented herein will provide insight into one such new synthetic application of  $\alpha$ -diazo carbonyl compounds.

### 1.2. Heterolytic Carbon-Carbon (C-C) bond cleavage reactions

The development of new synthetic methods that allow for stereo-, chemo- and regioselective assembly of complex organic molecules via C-C bond forming events has been a major focus of research in organic synthesis. In contrast, transformations which involve the cleavage of C-C bonds have received much less attention, but have without a doubt emerged as important and versatile synthetic tools.<sup>56</sup>

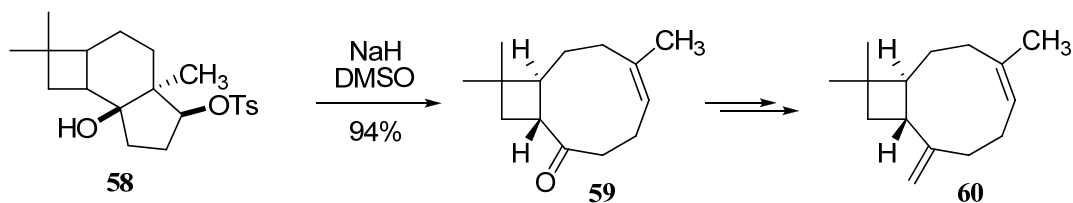
Fragmentation reactions have the ability to unmask latent functional groups under chemoselective reaction conditions and ring fragmentations are particularly useful because they result in two newly formed functional groups tethered at a predefined distance determined by ring size. One such example is the ozonolysis of cyclohexane (**54**, Scheme 1.11), a widely used protocol for the synthesis of useful intermediates such as methyl 6-oxohexanoate (**55**).<sup>57</sup>

**Scheme 1.11.**



Additionally, fragmentation reactions of cyclic systems offer stereochemical advantages as well. For example, sodium periodate mediated oxidative cleavage of azabicyclodiol **56** (Scheme 1.11) provides dialdehyde **57** in great yield and with preservation of the preexisting stereochemical information.<sup>58</sup> This is of importance because installing the same stereocenters using other synthetic methods could prove to be a much more difficult task.

**Scheme 1.12.**



As early as 1964 E. J. Corey and co-workers<sup>59</sup> recognized the ability of C-C bond cleavage reactions to provide carboskeletal frameworks otherwise challenging to prepare, and successfully utilized a Grob-type fragmentation of a ring fused C-C bond to quickly access macrocyclic ketone **59** (Scheme 1.12) starting from tricyclic sulfonate

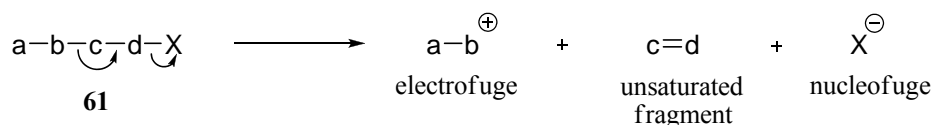
58. Ketone **59** subsequently served as a key intermediate in the total synthesis of caryophyllene (**60**).

The following section will serve as brief overview of Grob-type C-C cleavage reactions and will explore relevant characteristics of these types of transformations as they pertain to the discovery of a novel Lewis acid promoted ring fragmentation<sup>60</sup> described in this dissertation work.

### 1.2.1. Classification of heterolytic fragmentation reactions

Fragmentations were first introduced as a new class of reactions by C. A. Grob in the 1950's and they were classified as transformations which involve the cleavage of a molecule (as symbolized by **61**, Scheme 1.13) into three fragments: a nucleofuge, an unsaturated fragment and an electrofuge.<sup>61</sup>

Scheme 1.13.



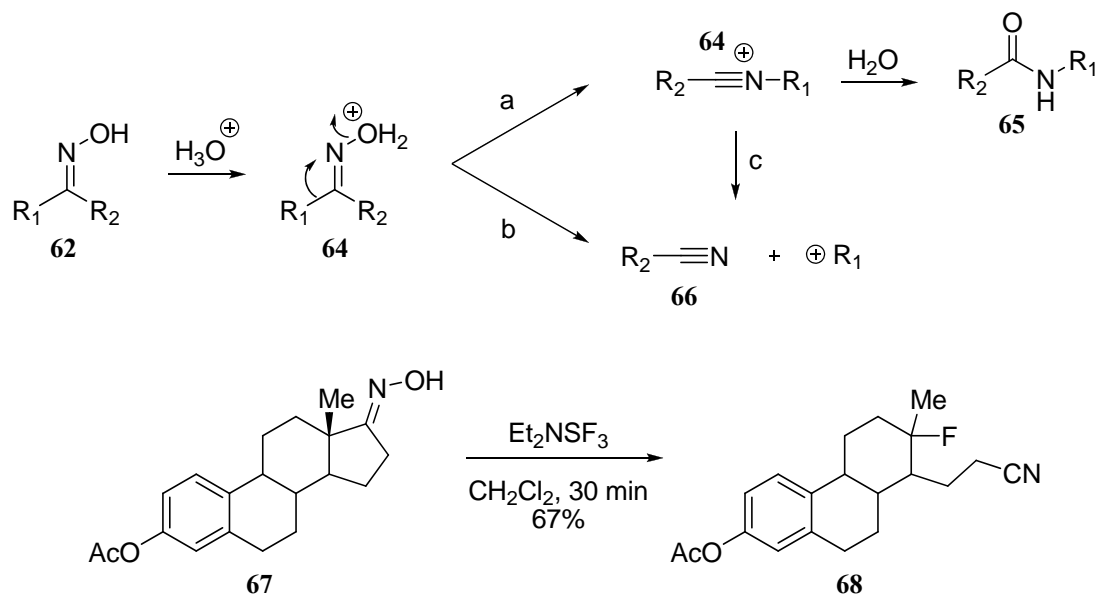
In heterolytic fragmentation reactions, 'X' leaves with the electron pair by which it was originally attached to the rest of the molecule as a nucleofuge, typically a halide, carboxylate or sulfonate anion. Neutral nucleofugal fragments have also been found to participate in fragmentations and usually derive from diazonium, oxonium, ammonium and sulfonium groups. The departure of 'X' results in electron deficiency on atom 'd', thus leading to heterolytic cleavage of the bond between atoms 'b' and 'c' and formation of an unsaturated fragment **c=d** and a fragment **a-b**. The latter leaves without the bonding electron pair as an electrofuge, becoming one unit of charge more

positive in the process. Typical electrofugal fragments are carbonyl compounds, carbon dioxide, imonium, carbonium and acylium ion, olefins, diimine and nitrogen.

The ease with which an electrofugal fragment is formed will depend on the stabilization of the incipient positive charge on 'b' due to the inductive or conjugative effect of 'a'. The structural unit **a-b** is frequently a hydroxyl, amino, alkyl or aryl group. The displacement of electrons from 'a' towards 'b' promotes the release of the unsaturated fragment **c=d**. Variations of nucleofugal, unsaturated fragments and electrofugal groups have lead to the development of a variety of heterolytic C-C bond cleavage reactions and the one generally accepted classification protocol is based on the nature of the unsaturated fragment released.

Frequently encountered unsaturated fragments are alkenes, acetylenes, imines and nitriles and transformation shown in Scheme 1.12 serves as a relevant example of an alkene forming fragmentation reaction. Additionally, nitrile-forming reactions have also been observed and are associated with reactions of ketoximes (e.g. **62**, Scheme 1.14). It is well known that if the hydroxyl group of **62** is converted into a more active nucleofugal group a Beckmann rearrangement<sup>62</sup> (route a) generally takes place. That is, the group that is trans to the hydroxyl moiety (i.e. R<sub>1</sub>) migrates to form nitrilium ion **64** which can further react with water to form an amide (e.g. **65**). However, if R<sub>1</sub> is an active electrofugal group it may be wholly or partially removed, with simultaneous formation of a nitrile (e.g. **66**, path b, Scheme 1.14). Processes of this type are frequently referred to as Beckmann fragmentations.

Scheme 1.14.

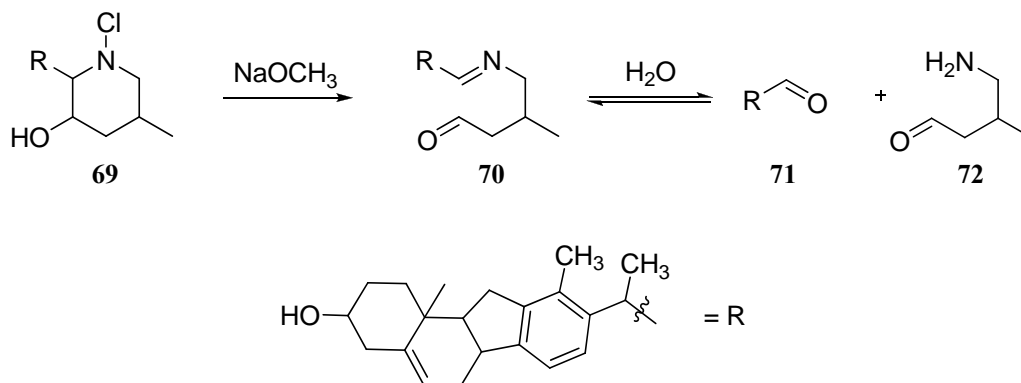


Generally, the presence of substituents at the position  $\alpha$  to the oximino carbon capable of stabilizing a carbocation can bias the reactivity of ketoximes in favor of nitrile (e.g. **66**) formation. For example the fragmentation of steroid derived ketoxime **67** (Scheme 1.14) mediated by diethylaminosulfur trifluoride provides fragmented fluorinated carbonitrile **68** in 67% yield while Beckman rearrangement type products (e.g **65**) are not observed.<sup>63</sup>

The existence of efficient and reliable methods for the preparation of imines, such as condensations of primary amines with aldehydes and ketones (e.g. **71** + **72**  $\rightarrow$  **70**, Scheme 1.15) has obviated the need for fragmentation reactions which lead to such products. However, these transformations have been observed and utilized in the degradation of  $\beta$ -amino alcohols (e.g **69**).<sup>64</sup> Specifically,  $\beta$ -hydroxy-*N*-chloro amine **69**

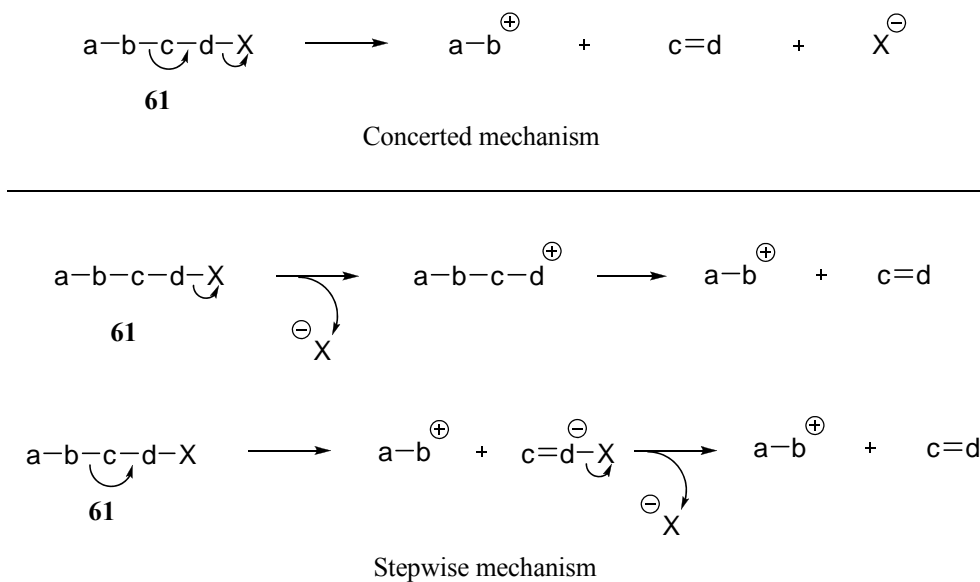
was found to undergo fragmentation in the presence of a base to provide imine **70**, which can further hydrolyze to aldehyde **71** and the respective primary amine **72**.

**Scheme 1.15.**



Fragmentation reactions which result in the formation of an alkyne are of special interest as they include the newly developed fragmentation reaction discussed in this dissertation work, and will be discussed separately in Sections 1.2.2 and 1.2.3.

**Scheme 1.16.**



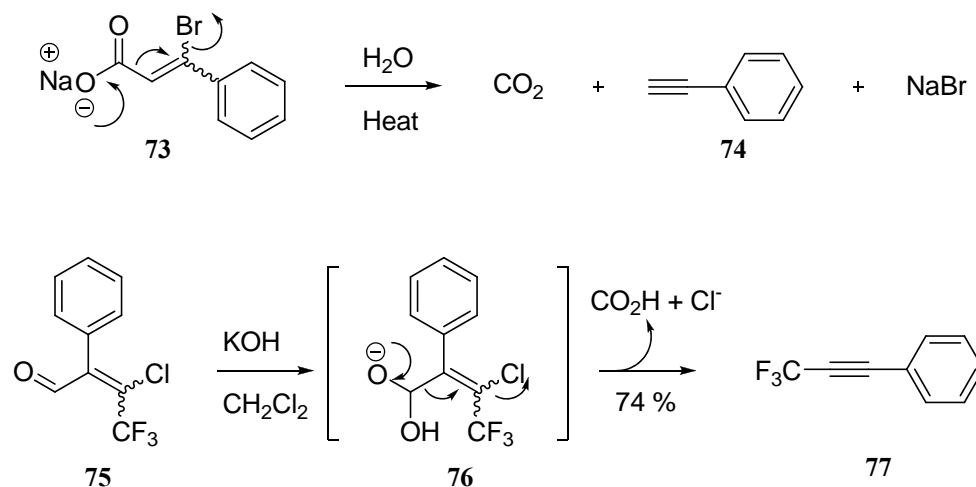


Finally, beside the categorization model described above based on the nature of the unsaturated fragment released, heterolytic fragmentation reactions can also be classified according to mechanistic criteria and these differ in the order in which the fragments are released. Thus one-step and two-step processes can be distinguished depending on whether **a-b** and 'X' depart simultaneously from **c-d** or whether **a-b** or 'X' depart successively (Scheme 1.16).

### 1.2.2. Alkyne-forming fragmentation reactions of acyclic systems

Alkyne-forming fragmentations are not as numerous as C-C cleavage reactions that lead to the formation of olefins, probably because in order to form an alkyne, the nucleofugal group must be attached to an unsaturated carbon atom and therefore ionizes with difficulty. Consequently, a reaction takes place only when the nucleofugal activity of 'X' is particularly high or when **a-b** is an extremely active electrofugal group.

Scheme 1.17.



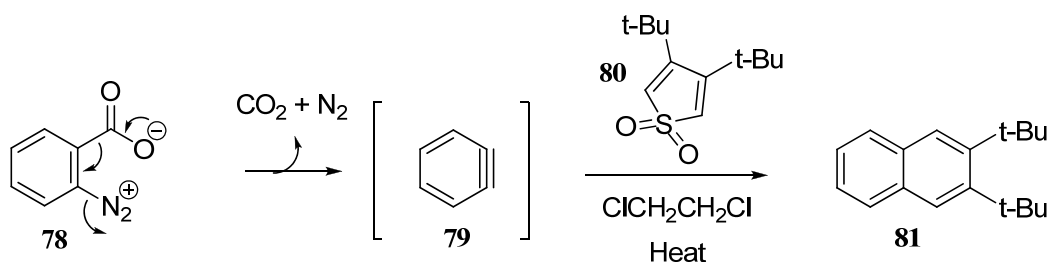
An example of the latter is represented by the fragmentation of  $\alpha,\beta$ -unsaturated  $\beta$ -haloacids (e.g. **73**, Scheme 1.17).<sup>65</sup> In this transformation the sodium salts of both *cis*-

and *trans*- $\beta$ -bromocinnamic acid (**73**) was found to undergo C-C bond cleavage via decarboxylation when heated in water, to produce phenylacetylene (**74**) as the main product.

More recently, Laurent<sup>66</sup> and co-workers were able to induce the fragmentation of  $\beta$ -halogenated  $\alpha,\beta$ -unsaturated carbonyl compound **75** upon the addition of a nucleophile. Thus in the presence of potassium hydroxide, 3-chloro-4,4,4-trifluoro-2-phenylbut-2-enal (**75**, Scheme 1.17) decomposes into formic acid and alkyne **77**. The reactive substrate is assumed to be the anion of the aldehyde hydrate **76**.

Alkyne-forming fragmentations may include, at least formally, certain reactions used in the preparation of benzyne (**79**, Scheme 1.18). This unstable intermediate is formed by mild decarboxylation of diazotized anthranilic acid (**78**)<sup>67</sup> and can be readily trapped intermolecularly via a [4+2] cycloaddition with 3,4-di-*tert*-butylthiophene 1,1-dioxide (**80**) to afford 2,3-di-*tert*-butylnaphthalene (**81**).<sup>68</sup> Such reaction is important to note because it highlights one of the few examples in which a diazo functional group participates as a nucleofuge in the fragmentation of a C-C bond followed by the formation of an alkyne.

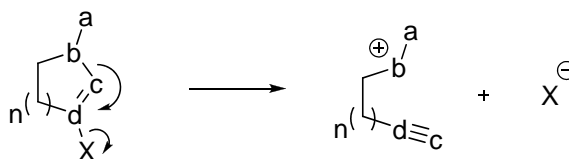
Scheme 1.18.



### 1.2.3. Alkyne-forming fragmentation reactions of cyclic systems

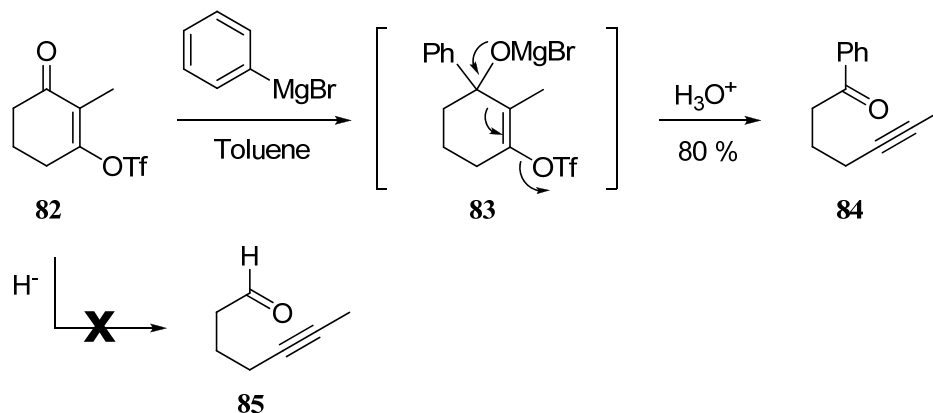
Because ring fragmentations lead to a substantial change in a molecule's architecture, they are not always obvious retrosynthetic disconnects, but can efficiently provide functionalized synthetic intermediates and can greatly simplify a synthetic sequence. Thus fragmentations of cyclic systems have emerged as ideal methods for the construction of new materials and complex molecules. Systems suitable for such transformations have the general configuration: electrofuge (**a-b**), unsaturated fragment (**c-d**) and nucleofuge 'X' as shown in Scheme 1.19.

Scheme 1.19.



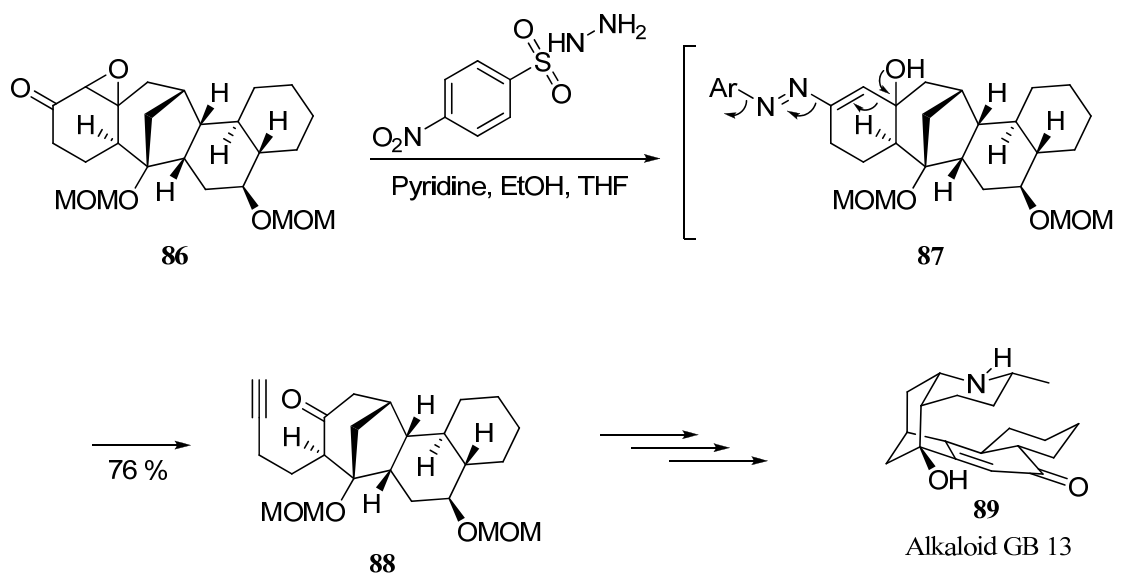
Dudley and co workers<sup>69</sup> have recently reported the fragmentation of cyclic vinylogous triflates (**82**, Scheme 1.20) which yields a variety of acyclic acetylenic compounds (e.g. **84**). The reaction is proposed to proceed through a 1,2-addition of phenyl magnesium bromide to the carbonyl group of the triflate **82** to form tetrahedral alkoxide intermediate **83**. Subsequently, a Grob-type fragmentation effects C-C bond cleavage to yield 1-phenylhept-5-yn-1-one (**84**) in 80 % yield. A wide array of nucleophiles such as organolithium, lithium enolates and their analogs as well as lithium amides were also shown to induce fragmentation in good yields. However, the use of hydride reagents as nucleophiles was unsuccessful and thus no acyclic tethered acetylenic aldehydes (e.g. **85**, Scheme 1.20) were formed.

Scheme 1.20.



In principle, the fragmentation of vinilogs triflates is synonymous to the Eschenmoser-Tanabe<sup>70-73</sup> fragmentation which was recently utilized by Mander and McLachlan<sup>74</sup> in the total synthesis of galbulimima alkaloid GB 13 (**89**, Scheme 1.21).

Scheme 1.21.



Specifically, treatment of epoxy ketone **86** with *p*-nitrobenzenesulfonylhydrazide in protic media is thought to produce intermediate **87**, which can

subsequently undergo fragmentation and give tethered acetylenic ketone **88** in 76 % yield.

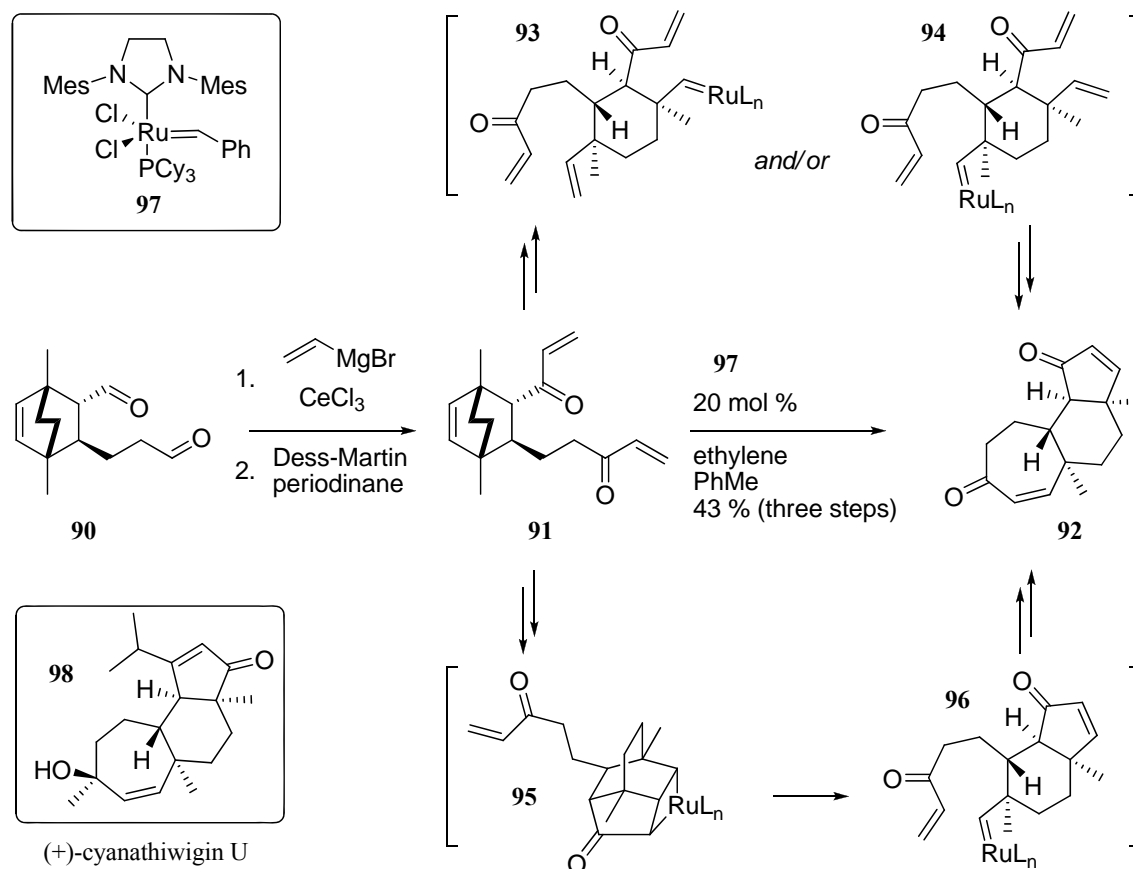
#### 1.2.4. Miscellaneous transition metal induced fragmentations

Recent advances in synthetic chemistry have allowed for the development of methods which induce the cleavage of C-C bonds utilizing transition metals. Such transformations differ mechanistically from the Grob-type fragmentations outlined above, and often feature transition metal complexes as reactive intermediates. For example, Phillips and co-workers tapped into the versatility of ruthenium based alkylidene complexes and developed a ring-opening-ring-closing metathesis of bicyclo[2.2.2]octenes which yields decalins and hydrindanes in reasonable yields.<sup>75</sup> Furthermore, this methodology was successfully implemented in the total synthesis of (+)-cyanathiwigin U (**98**, Scheme 1.22).<sup>76</sup>

The process involves treatment of dialdehyde **90** (Scheme 1.22) with vinylmagnesium bromide and reoxidation with Dess-Martin periodinane to provide bis-enone **91**, which sets the stage for the key two directional tandem ring-opening-ring-closing metathesis sequence. Exposure of **91** to catalyst **97**, under an atmosphere of ethylene, provides tricycle **92** in 43% yield for the three steps from aldehyde **90** and establishes a concise route to the carbocyclic skeleton of (+)-cyanathiwigin U (**98**). Several pathways that lead from **90** to **92** can be envisioned. Initial ring-opening metathesis of the bicyclo[2.2.2]octene leads to intermediates **93** or **94**, which can subsequently undergo ring-closing metathesis to provide **92**. Alternatively, initial metathesis of the endo enone, followed by reaction with the olefin of the

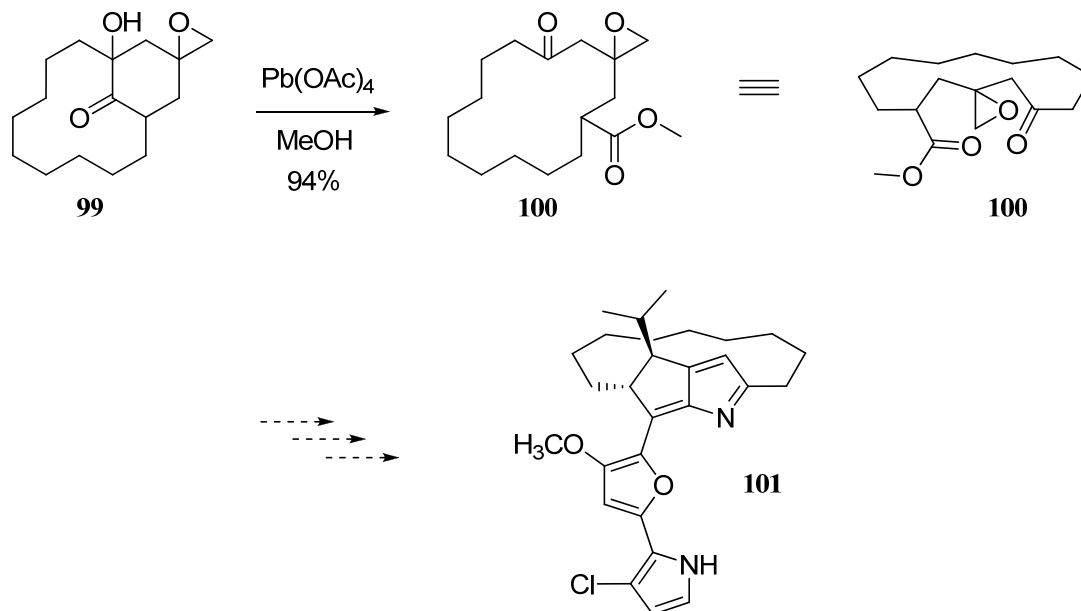
bicyclo[2.2.2]octene, leads to metallacyclobutane **95**, which upon ring opening yields **96**, which can undergo a subsequent ring-closing metathesis to provide **92**.

Scheme 1.22.



Furthermore, Dudley and co-workers<sup>77</sup> recently utilized a lead mediated oxidative cleavage to induce C-C bond fragmentation and subsequent ring expansion, a key step envisaged in the total synthesis of roseophilin (**101**, Scheme 1.23). More specifically, treatment of  $\alpha$ -hydroxy ketone **99** with lead tetraacetate in MeOH affords macrocyclic ketoester **100**.

**Scheme 1.23.**



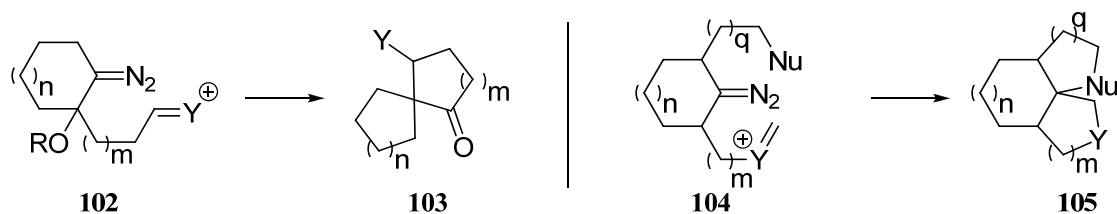
### 1.2.5. Conclusions

Fragmentation reactions hold a special position in organic synthesis because of their ability to quickly and efficiently provide access to complex frameworks that are otherwise difficult to prepare. They are excellent methods for the synthesis of novel materials and natural products but unfortunately, relatively few synthetically valuable fragmentation reactions are known. Therefore, development of new methodology involving such transformations could prove very useful. Dissertation work presented herein will provide insight into the development of a novel Lewis acid mediated ring fragmentation reaction.

## 2. CHAPTER 2: DISCOVERY OF A NEW MODE OF REACTIVITY FOR DIAZO-ESTERS

The initial goal of my research was to develop new methodology that would utilize the reactivity of diazo compounds to form complex polycycles containing all-carbon quaternary centers via tandem reactions. Specifically, we envisioned that intramolecular nucleophilic attack of a diazo species onto a carboxonium or iminium ion would provide diazonium intermediates that would undergo further intramolecular reaction [either carboskeletal rearrangement (**102**  $\rightarrow$  **103**) or nucleophilic trapping (**104**  $\rightarrow$  **105**), Scheme 2.1]. This methodology was envisioned to provide a variety of polycyclic scaffolds containing all-carbon quaternary centers.

Scheme 2.1.

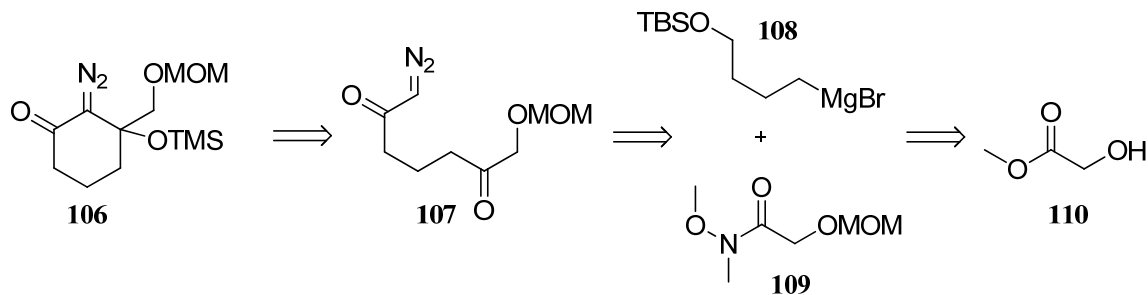


### 2.1. Novel approach to keto-furans with an unexpected result

While numerous methods are known for the synthesis of all-carbon spirocycles (**103** and **105**),<sup>78-80</sup> developing methodology to form quaternary stereo centers via a stereospecific tandem reaction from simple starting materials would be a significant advancement. Thus, I directed my attention towards the synthesis of the first test substrate, cyclic  $\alpha$ -diazo ketone **106** (Scheme 2.2).



Scheme 2.2.



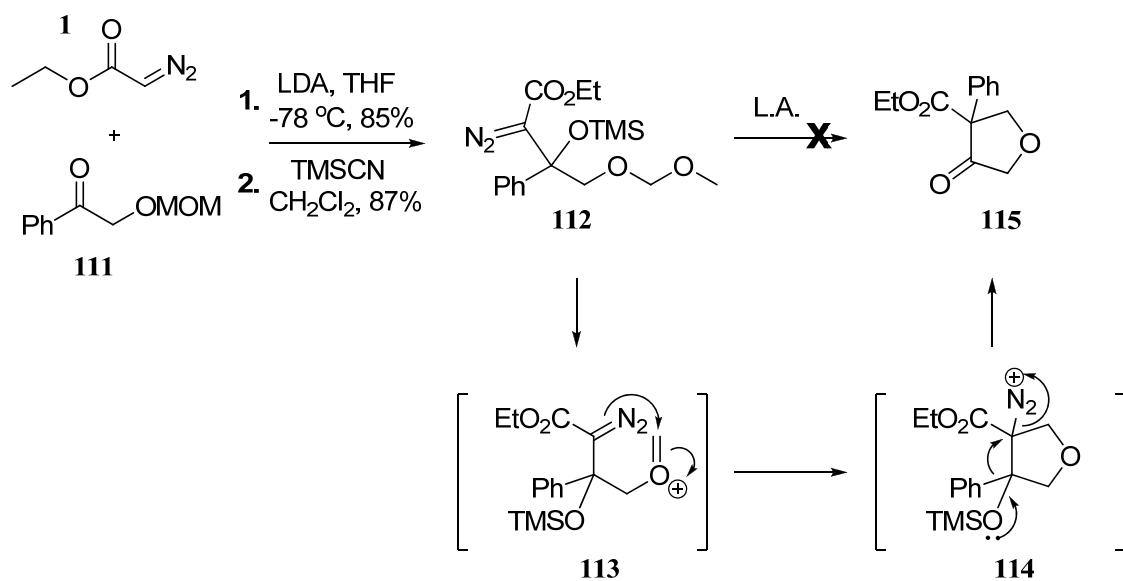
Access to  $\alpha$ -diazo cyclohexanone **106** was envisioned via the key retrosynthetic steps highlighted in Scheme 2.2. An intramolecular cyclization of diazo **107** followed by protection of the resulting tertiary alcohol would provide desired cyclic diazo ketone **106**. In turn, diazo ketone **107** would be derived from the Grignard addition to Weinreb amide **109**, which is available in two steps from commercial methyl 2-hydroxyacetate (**110**).

The forward synthesis proved to be unproductive and, overall, plagued by low conversions in the latter stages. So, I shifted my efforts to the synthesis of a simpler test substrate. Acyclic  $\alpha$ -diazo ester **112** (Scheme 2.3) emerged as a viable candidate. The synthesis of diazo ester **112** was efficiently achieved via nucleophilic addition of ethyl lithio-diazoacetate into phenyl ketone **111** and subsequent trimethylsilyl protection of the ensuing tertiary alcohol with TMS-CN.

While diazo ester **112** would not provide access to all-quaternary carbon spirocycles, it still offers the required functional group arrangement desired to test the initially proposed chemical transformation sequence. In effect, I hypothesized that a Lewis acid would cleave the methoxymethyl ether of **112** to provide carboxonium ion

**113** (Scheme 2.3). Nucleophilic attack of the diazo would provide diazonium intermediate **114** that could undergo silyloxy assisted phenyl migration with loss of molecular nitrogen to yield ketofuran **115**.

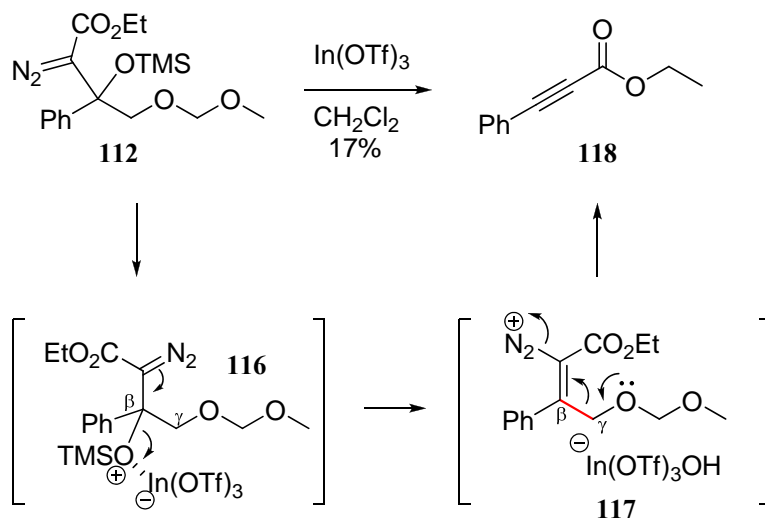
Scheme 2.3.



All attempts to induce ketofuran formation in the presence of various Lewis acids were unsuccessful and often led to complex mixtures of products. However, the reaction of  $\alpha$ -diazoester **112** with indium(III) triflate provided ethyl 3-phenylpropiolate (**118**, Scheme 2.4), which was isolated from a complex mixture of products in 17% yield. This find was critical, as it prompted us to inquire about the path taken by diazo ester **112** during the reaction to arrive to observed aryl alkyne **118**.

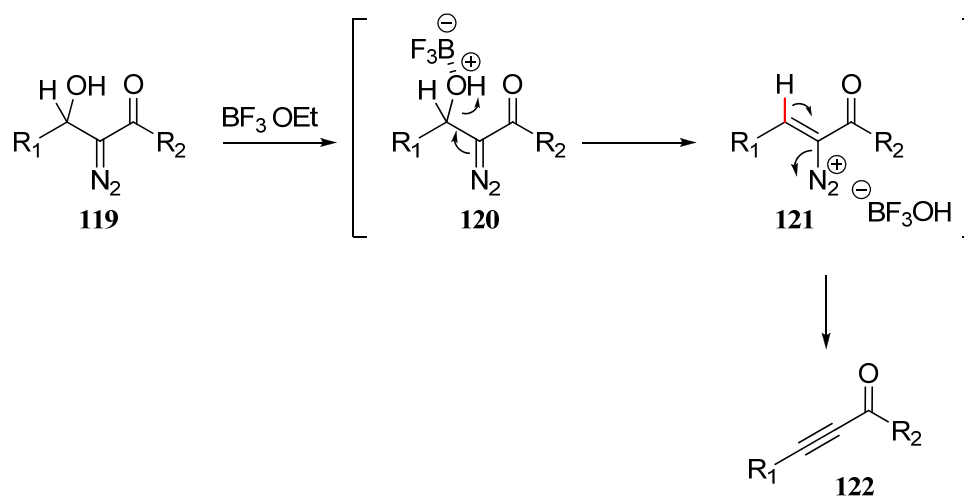
Mechanistically, the formation of ynoate **118** appeared to involve the loss of the  $\beta$ -silyloxy group, loss of molecular nitrogen, and fragmentation of the C <sub>$\beta$</sub> -C <sub>$\gamma$</sub>  bond (highlighted in red) (Scheme 2.4).

Scheme 2.4.



A careful review of the literature revealed that Padwa and co-workers<sup>29</sup> had described a similar reaction in which treatment of acyclic  $\alpha$ -diazo ketone **119** (Scheme 2.5) with boron trifluoride etherate complex in polar solvents such as acetonitrile resulted in the formation of the acylacetylene **122**.

Scheme 2.5.



Padwa rationalized their transformation as proceeding *via* coordination of the secondary alcohol with boron trifluoride etherate followed by elimination and generation of the alkenyldiazonium salt **121** (Scheme 2.5). Deprotonation of **121** with extrusion of molecular nitrogen, would afford alkyne **122**.

Though both processes described in Scheme 2.4 and 2.5, invoke similar reactive intermediates [*i.e.* alkenyldiazonium salts **117** (Scheme 2.4) and **121** (Scheme 2.5)], there is one striking difference; diazonium intermediate **121** undergoes a C-H (highlighted in red – Scheme 2.5) bond cleavage to afford alkyne **122**, while diazonium intermediate **117** yields alkyne **118** *via cleavage of a C-C bond* (highlighted in red – Scheme 2.4).

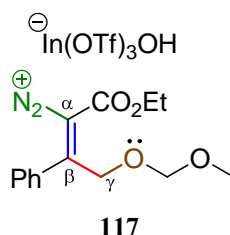


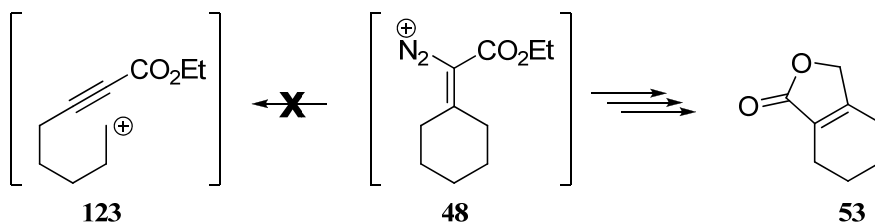
**Figure 2.1. Alkenyl diazonium salt 117: a fragmentable system**

Further scrutiny of the two reactive intermediates revealed a key structural difference as well: the presence of an alkoxy functional group at the C<sub>γ</sub> of **117**. This feature completes the requirements for a system capable of undergoing *C-C bond fragmentation* according to the criteria outlined by Grob (see Section 1.2.1);<sup>61</sup> specifically, the presence of an electrofuge – alkoxy group (**brown**); an unsaturated

fragment – C<sub>α</sub>–C<sub>β</sub> fragment (blue); and an electrofuge – diazonium ion (green) (Figure 2.1).

Moreover, in the presence of Lewis acids, β-hydroxy α-diazo esters were proposed to undergo alkenyldiazonium salt (**48**, Scheme 1.10, Section 1.1.3) formation and subsequent carbocation rearrangements to yield lactones such as **53**. To this date such intermediates had *not* been observed to undergo any type of ring cleavage reactions (**48** → **123**, Scheme 2.6).

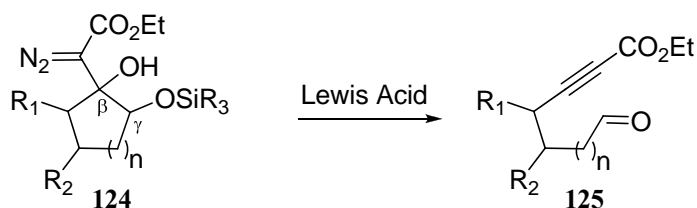
Scheme 2.6.



## 2.2. Hypothesis

The formation of **118** from diazo **112** (Scheme 2.4) allowed us to hypothesize that cyclic  $\gamma$ -silyloxy- $\beta$ -hydroxy- $\alpha$ -diazo esters (e.g. **124**) would undergo efficient Lewis acid mediated rupture of the  $C_\beta$ - $C_\gamma$  bond and lead to the formation of tethered aldehyde ynoates (**125**, Scheme 2.7). This would be of importance because there are few synthetically useful ring fragmentations available (see Section 1.2).

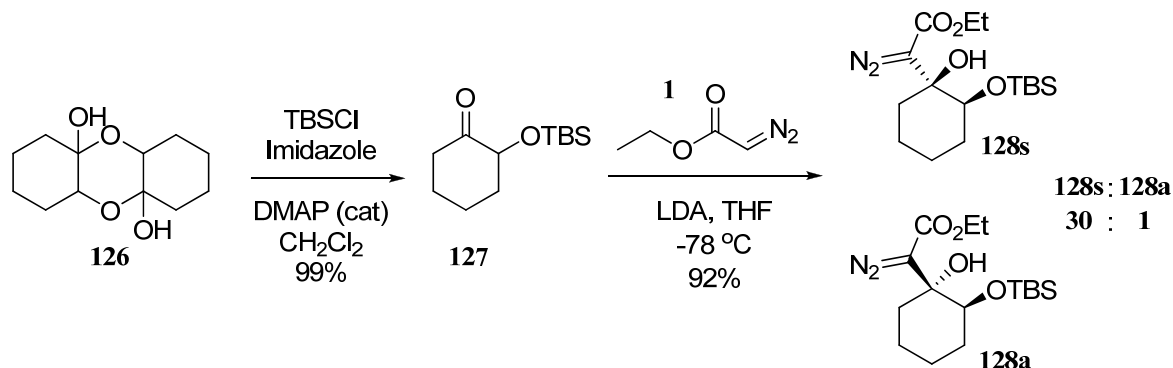
Scheme 2.7.



## 2.3. Testing the hypothesis

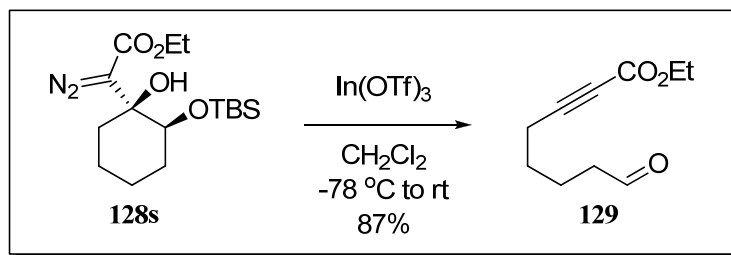
Cyclic  $\gamma$ -silyloxy- $\beta$ -hydroxy- $\alpha$ -diazo ester **128** (Scheme 2.8) emerged as leading candidate to test the hypothesis, mainly due to the ease with which it could be prepared. In effect, addition of ethyl lithio-diazoacetate to 2-(tert-butyl-dimethyl-silyloxy)cyclohexanone (**127**), which in turn was easily accessed in one step from commercially available 2-hydroxy cyclohexanone dimer (**126**), provided desired diazo ester **128** in 92% yield. It is important to note that addition of ethyl lithio-diazoacetate to ketone **127**, resulted in a 30:1 mixture of *syn* (**128s**) and *anti* (**128a**) diastereomers (for stereochemical assignment see Section 2.5.3). The two were subsequently separated by chromatography and the major *syn* diastereomer (**128s**) was carried on for further testing.

Scheme 2.8.



Gratifyingly, treatment of ethyl 2-((1*S*,2*S*)-2-(TBS)-1-hydroxycyclohexyl)-2-diazoacetate (**128s**) with freshly dried indium(III) triflate resulted in observable gas evolution and provided ethyl 8-oxooct-2-ynoate (**129**) in 87% as the only product (Scheme 2.9). Though pleased with this result, the reaction appeared to provide the desired fragmentation in reduced yields when older batches of indium(III) triflate were employed. Finding suitable reaction conditions which would promote ring fragmentation with good levels of consistency became my first main focus in optimizing this reaction.

Scheme 2.9.



## 2.4. Optimization of reaction conditions

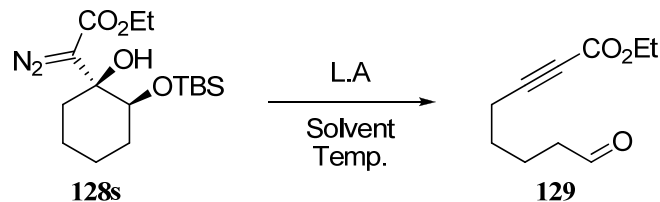
### 2.4.1. Lewis Acid Screening

Identifying a better suited Lewis acid served as a starting point. Ideally, the Lewis acid of choice would: (i) promote fragmentation in stoichiometric or catalytic amounts with good to excellent conversions; (ii) be readily and inexpensively available from commercial sources; (iii) be easy to purify and store for long periods of time; (iv) present low levels of toxicity as a reactant and as a byproduct of the reaction.

The results of a Lewis acid screen are presented in Table 2.1. In the end I discovered that a freshly-prepared 1M solution of tin tetrachloride induced the desired fragmentation in high yield and with good levels of consistency (Entry 10). Furthermore, reducing the quantity of tin tetrachloride to 10 mol % competently promoted the fragmentation reaction, although product yield was reduced (Entry 11). Older batches of tin tetrachloride did provide more complex product mixtures, but fresh solutions were easily attained by distillation of pure commercially available tin tetrachloride. Additionally, a 1M solution of tin tetrachloride in  $\text{CH}_2\text{Cl}_2$  could be stored under inert atmosphere for prolonged period without loss of reagent efficacy. The use of  $\text{BF}_3 \cdot \text{OEt}_2$  (Entry 2) as a Lewis acid provided complex product mixtures as did  $\text{MgBr}_2 \cdot \text{OEt}_2$  (Entry 3), scandium(III) triflate (Entry 4), and anhydrous  $\text{HCl}$  (Entry 9). Dibutyl tin dichloride (Entry 8), titanium (IV) isopropoxide (Entry 5) and lithium perchlorate (Entry 6) failed to promote the reaction (Table 2.1).



**Table 2.1.Optimization of reaction conditions**



Entry	Lewis Acid	Mol %	Temperature	Solvent	%Yield
1	In(OTf) <sub>3</sub>	100	-78 °C to rt	CH <sub>2</sub> Cl <sub>2</sub>	87 <sup>a</sup>
2	BF <sub>3</sub> ·OEt <sub>2</sub>	100	-78 °C to rt	CH <sub>2</sub> Cl <sub>2</sub>	Undetermined <sup>b</sup>
3	MgBr <sub>2</sub> ·OEt <sub>2</sub>	100	-78 °C to rt	CH <sub>2</sub> Cl <sub>2</sub>	0
4	Sc(OTf) <sub>3</sub>	100	-78 °C to rt	CH <sub>2</sub> Cl <sub>2</sub>	Undetermined <sup>b</sup>
5	Ti( <i>i</i> PrO) <sub>4</sub>	100	-78 °C to rt	CH <sub>2</sub> Cl <sub>2</sub>	No Rxn.
6	LiClO <sub>4</sub>	100	-78 °C to rt	CH <sub>2</sub> Cl <sub>2</sub>	No Rxn.
7	SnCl <sub>4</sub> <sup>c</sup>	100	-78 °C to rt	CH <sub>2</sub> Cl <sub>2</sub>	92 <sup>a</sup>
8	<i>n</i> Bu <sub>2</sub> SnCl <sub>2</sub>	100	-78 °C to rt	CH <sub>2</sub> Cl <sub>2</sub>	No Rxn.
9	HCl	100	-78 °C to rt	CH <sub>2</sub> Cl <sub>2</sub>	0
<b>10</b>	<b>SnCl<sub>4</sub><sup>c</sup></b>	<b>100</b>	<b>0 °C</b>	<b>CH<sub>2</sub>Cl<sub>2</sub></b>	<b>94<sup>a</sup></b>
11	SnCl <sub>4</sub> <sup>c</sup>	10	0 °C	CH <sub>2</sub> Cl <sub>2</sub>	85 <sup>a</sup>
12	SnCl <sub>4</sub> <sup>c</sup>	100	0 °C	Toluene	93 <sup>a</sup>
13	SnCl <sub>4</sub> <sup>c</sup>	100	0 °C	DMF	No Rxn.
14	In(OTf) <sub>3</sub>	100	0 °C	DMF	No Rxn.

Note: <sup>a</sup> % yield determined after chromatography. <sup>b</sup> reaction monitored by GC and **129** detected along within a complex mixture of products. <sup>c</sup> used as a 1M solution in CH<sub>2</sub>Cl<sub>2</sub>.

#### 2.4.2. Temperature Effect

Initially, a typical fragmentation protocol involved adding tin tetrachloride to a stirred solution of ethyl 2-((1S,2S)-2-(TBS)-1-hydroxycyclohexyl)-2-diazoacetate (**128s**) in CH<sub>2</sub>Cl<sub>2</sub> at -78 °C. Upon warming, gas evolution was observed to occur when the temperature reached -20 °C. Subsequent trials revealed that fragmentation occurs cleanly in the presence of tin tetrachloride at ice water bath temperature (0 °C) in high yields (Entry 10, Table 2.1).

### 2.4.3. Solvent Effect

A partial solvent screen showed that changing the solvent from CH<sub>2</sub>Cl<sub>2</sub> to toluene had little effect on the reaction (Entry 10 and 11), whereas dimethyl formamide (DMF) (Entry 13 and 14) inhibited the reaction completely. This was attributed to the ability of such solvent to strongly bind to Lewis acids such as tin tetrachloride and indium(III) triflate and render them inactive.

### 2.4.4. Concentration Effect

Initial reaction protocol required a reactant concentration of 0.1 M in the respective solvent. Even though such concentrations were not detrimental to the reaction outcome, it was observed that more consistent results were obtained when the reactions were performed at lower concentrations, such as 0.05 M.

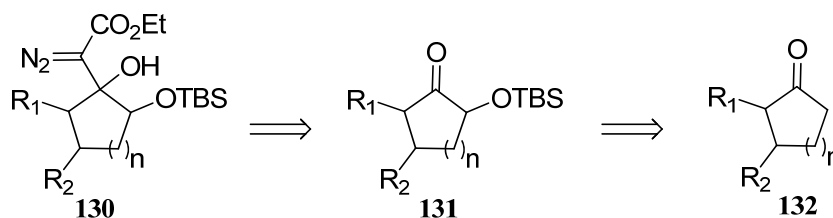
## 2.5. Synthesis of ring fragmentation precursors

Having found appropriate conditions under which  $\gamma$ -silyloxy- $\beta$ -hydroxy- $\alpha$ -diazo ester (**128s**) fragmented to consistently provide tethered aldehyde ynoate **129** in great yield, the next task became to prepare additional fragmentation precursors. By design, candidates would possess structural features that would allow for a thorough test of generality of this novel ring fragmentation. Thus, varying ring size, functionality enclosed within the ring and complexity of molecule to be fragmented was believed to provide adequate insight to the general scope of the reaction.

The synthesis of the desired cyclic  $\gamma$ -silyloxy- $\beta$ -hydroxy- $\alpha$ -diazo esters (e.g. **130**, Scheme 2.10) aimed to utilize the well established ethyl lithio-diazoacetate addition to the appropriate  $\alpha$ -silyloxy ketones (e.g. **131**). Access to the latter was

envisioned via a Rubottom<sup>81</sup> oxidation protocol starting with readily available cyclic ketones (e.g. **132**).

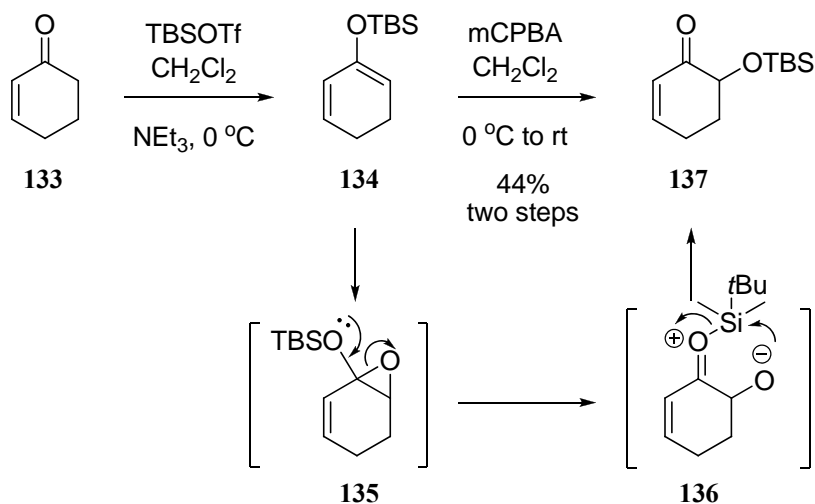
Scheme 2.10.



### 2.5.1. Synthesis of $\alpha$ -silyloxy ketones

The Rubottom oxidation protocol proved to be a facile method for the synthesis of three of the desired  $\alpha$ -silyloxy ketones. Thus, the synthesis of 6-(tert-butyldimethylsilyloxy)cyclohex-2-enone (**137**, Scheme 2.11) was achieved as follows.

Scheme 2.11.

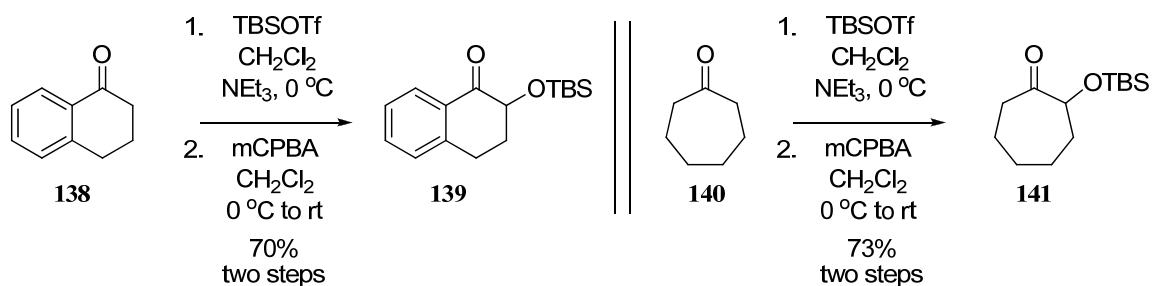


Treatment of cyclohexenone (**133**) with *t*-butyldimethylsilyl triflate (TBSOTf) in the presence of triethyl amine provided quantitative yield of silylenol ether **134**. Subsequent oxidation of the electron rich double bond of the silylenol ether with *m*-

chloroperoxybenzoic acid (mCPBA) initially provided epoxy silane **135**, which underwent rearrangement through zwitterionic intermediate **136** to give the desired  $\alpha$ -silyloxy ketone **137** in 44% yield over two steps. This reaction did not require purification of silylenol ether **134** which was carried through the oxidation step as crude material.

The oxidation of the silylenol ethers obtained from  $\alpha$ -tetralone (**138**) and cycloheptanone (**140**) also took place under the same conditions and provided the corresponding  $\alpha$ -siloxy ketones **139** and **141** in 70% and 73% yield respectively (Scheme 2.12).

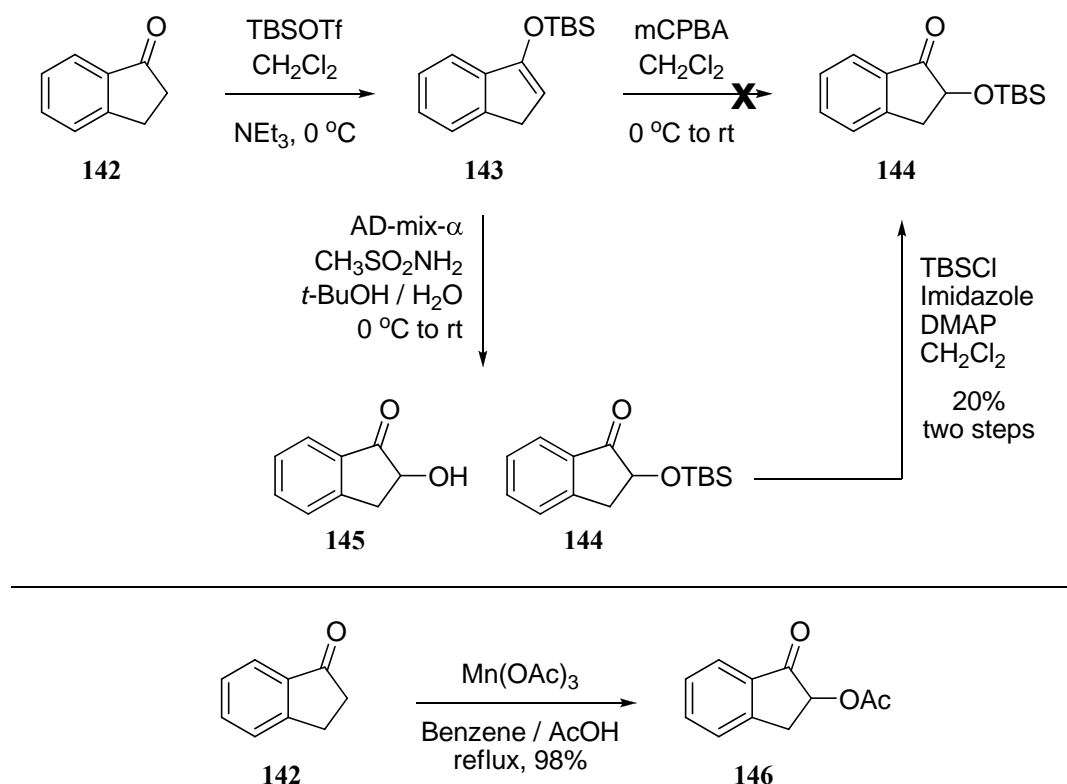
Scheme 2.12.



Unfortunately, the same cannot be said for the oxidation of the enoxysilane derived from 1H-indenone (**143**, Scheme 2.13) which did not provide the desired  $\alpha$ -silyloxy ketone **144**. Alternate strategies were explored, and although most attempts were unsuccessful in providing the desired transformation, it was found that treatment of silylenolether **143** with AD-mix- $\alpha$ , under Sharpless<sup>82</sup> asymmetric dihydroxylation conditions, provided a mixture of  $\alpha$ -hydroxy and  $\alpha$ -silyloxy ketones **145** and **144**. Subsequent protection of the free alcohol gave desired 2-(TBS)-2,3-dihydro-1H-inden-

1-one (**144**), albeit in low yield. It is worth mentioning that there are other protocols for the  $\alpha$ -oxidation of 1-indanone (**142**), such as the Mn(III) acetate mediated oxidation of enones (Scheme 2.13),<sup>83</sup> but I did not pursue these because there was no need for large quantities of silyloxy ketone **144**.

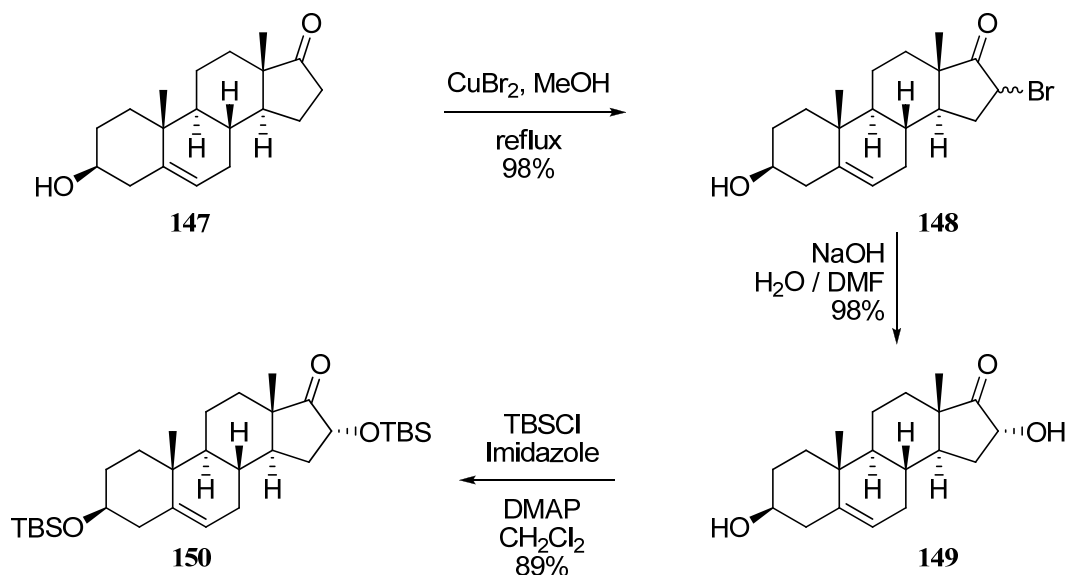
Scheme 2.13.



Another desirable  $\alpha$ -silyloxy ketone was envisioned to derive from commercially available dehydroepiandrosterone (**147**, Scheme 2.14). Previously reported methods provided facile access to enantiomerically pure  $\alpha$ -hydroxy ketone **149**.<sup>84-86</sup> Bromination of dehydroepiandrosterone (**147**) with  $\text{CuBr}_2$  in MeOH afforded an epimeric mixture of  $\alpha$ -bromo ketone **148**, and subsequent controlled stereoselective

alkaline hydrolysis with DMF as buffer, provided  $\alpha$ -hydroxy ketone **149** in high yields. The synthesis of desired  $\alpha$ -silyloxy ketone **150** was accomplished by protecting both secondary alcohols as the tert-butyldimethylsilylethers in 89% yield after chromatography. As a technical note, it is worth mentioning that carrying the crude  $\alpha$ -bromo ketone **148** through the hydrolysis step also affords alcohol **149** with good conversions.

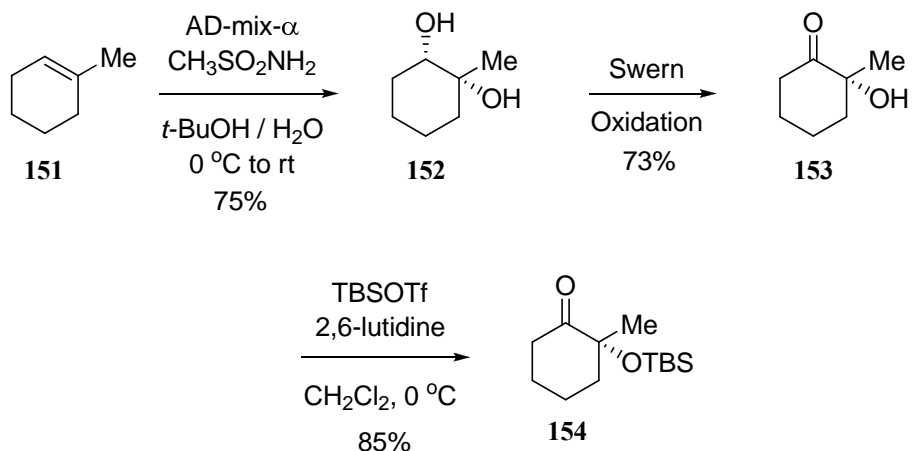
Scheme 2.14.



Preparation of  $\alpha$ -methyl- $\alpha$ -silyloxy cyclohexanone **154** (Scheme 2.15) was accomplished starting with Sharpless asymmetric dihydroxylation of 1-methylcyclohex-1-ene (**151**) which provided (1R,2S)-1-methylcyclohexane-1,2-diol (**152**) in 75% yield. Subsequent oxidation of the secondary alcohol utilizing the Swern protocol provided  $\alpha$ -methyl- $\alpha$ -hydroxy cyclohexanone **153** in 73% yield, and TBS

protection of the tertiary alcohol concluded the synthetic sequence to provide the desired (R)-2-(TBS)-2-methyl- cyclohexanone (**154**) in 85% yield.

Scheme 2.15.



### 2.5.2. Synthesis of the requisite $\gamma$ -silyloxy- $\beta$ -hydroxy- $\alpha$ -diazo esters

All of the requisite  $\gamma$ -silyloxy- $\beta$ -hydroxy- $\alpha$ -diazo esters were accessed by the addition of ethyl lithio-diazoacetate to the corresponding  $\alpha$ -silyloxy ketones. All reactions gave the desired fragmentation precursors in good yields as mixtures of *syn* and *anti* diastereomers as summarized in Table 2.2.

The diastereomeric mixtures of  $\gamma$ -silyloxy- $\beta$ -hydroxy- $\alpha$ -diazo esters **158** and **159** (Entries 4 and 5) were separated by chromatography and a selective crystallization from MeOH allowed for the isolation of the major *syn* diol diastereomer of  $\gamma$ -silyloxy- $\beta$ -hydroxy- $\alpha$ -diazo ester **157** (Entry 3). All other fragmentation precursors were isolated as mixtures of the two diastereomers and submitted to fragmentation conditions as such.

Table 2.2. Ethyl lithio-diazoacetate addition to  $\alpha$ -silyloxy ketones

Entry	$\gamma$ -silyloxy- $\beta$ -hydroxy $\alpha$ -diazoester	Compound # <i>syn:anti</i> <sup>a,b</sup>	yield <sup>c</sup>
1		<b>155s : 155a</b> 11 : 1	91%
2		<b>156s : 156a</b> 11 : 1	87%
3		<b>157s : 157a</b> 5 : 1	91%
4		<b>158s : 158a</b> 1 : 2.8	88%
5		<b>159s : 159a</b> 1.2 : 1	84%
6		<b>160s : 160a</b> N.A.	95%

Note: <sup>a</sup> *syn* / *anti* designation refers to relative stereochemistry of the diaol moiety.

<sup>b</sup> ratios determined by analysis of the <sup>1</sup>H NMR of the crude reaction mixture.

<sup>c</sup> yields are reported for the mixture of diastereomers after chromatography.



### 2.5.3. Determination of stereochemical outcome of ethyl lithio-diazoacetate addition to cyclic $\alpha$ -silyloxy ketones

X-ray quality crystals were successfully obtained from concentrated oils of  $\gamma$ -silyloxy- $\beta$ -hydroxy- $\alpha$ -diazo esters **157s** and **158s**. These were submitted for X-ray analysis to the University of California–Irvine X-ray facility and data obtained revealed the *syn* diol relative stereochemistry for the two compounds (Figure 2.2 and 2.3).

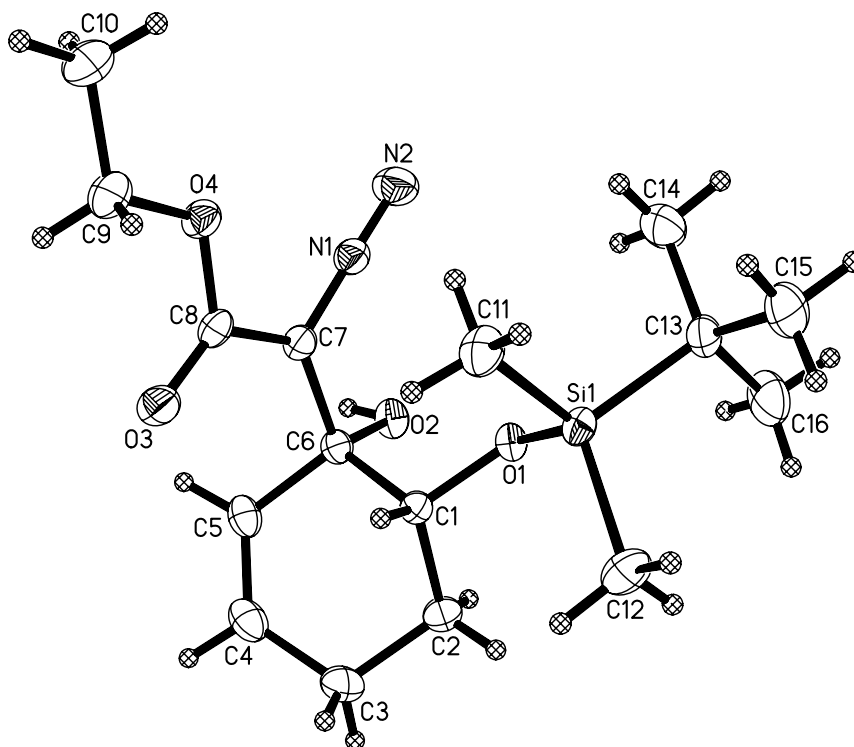


Figure 2.2. X-ray crystal structure of **157s**

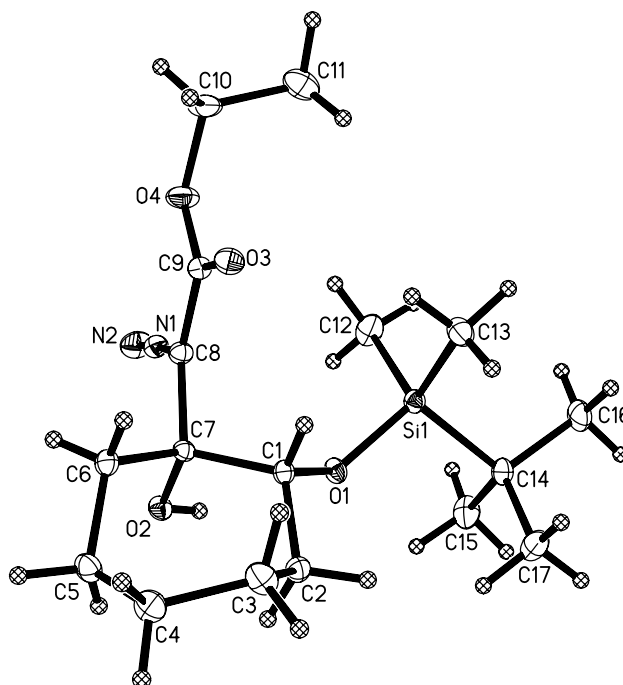
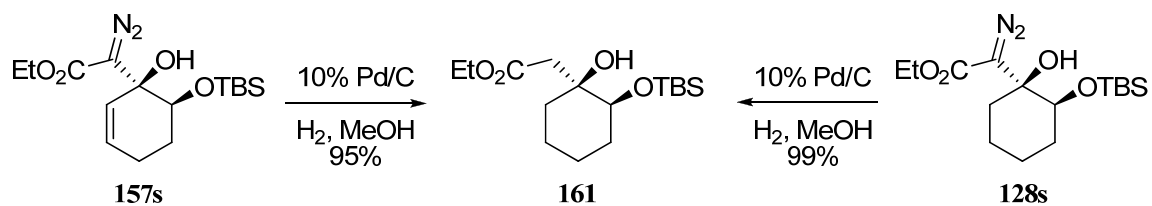


Figure 2.3. X-ray crystal structure of **158s**

The relative *syn* diol stereochemistry of  $\gamma$ -silyloxy- $\beta$ -hydroxy- $\alpha$ -diazo ester **128s** (Scheme 2.16) was determined by efficiently reducing both  $\gamma$ -silyloxy- $\beta$ -hydroxy- $\alpha$ -diazo esters<sup>33</sup> **128s** and **157s** in presence of 10% palladium on charcoal under an atmosphere of hydrogen to the identical saturated  $\gamma$ -silyloxy- $\beta$ -hydroxy ester **161**.

Scheme 2.16.



Close scrutiny of the  $^1\text{H}$  NMR spectra acquired for the pure *syn* isomers of  $\gamma$ -silyloxy- $\beta$ -hydroxy- $\alpha$ -diazo esters **158s**, **128s** and **157s** (Figure 2.4) revealed one interesting trend. The proton of the hydroxyl group appears as a *sharp* doublet ( $J = 2.2$  Hz) in the  $^1\text{H}$  NMR of both **158s** and **128s** and as a sharp singlet in the  $^1\text{H}$  NMR of **157s**. Since the carbon bearing the hydroxyl group is quaternary, the splitting pattern can only be attributed to a long range type coupling, such as a “W” coupling. To explain this phenomenon we considered the possibility of hydrogen bonding between the hydroxyl and the adjacent oxygen of the silyloxy group which would create a rigid conformation in which the H-O-C-C- $\text{H}_{\text{axial}}$  coplanar “W” arrangement is achieved as highlighted in red (Figure 2.5). The coplanar arrangement is also clearly visible in the X-ray crystal structure of **158s** (Figure 2.3).

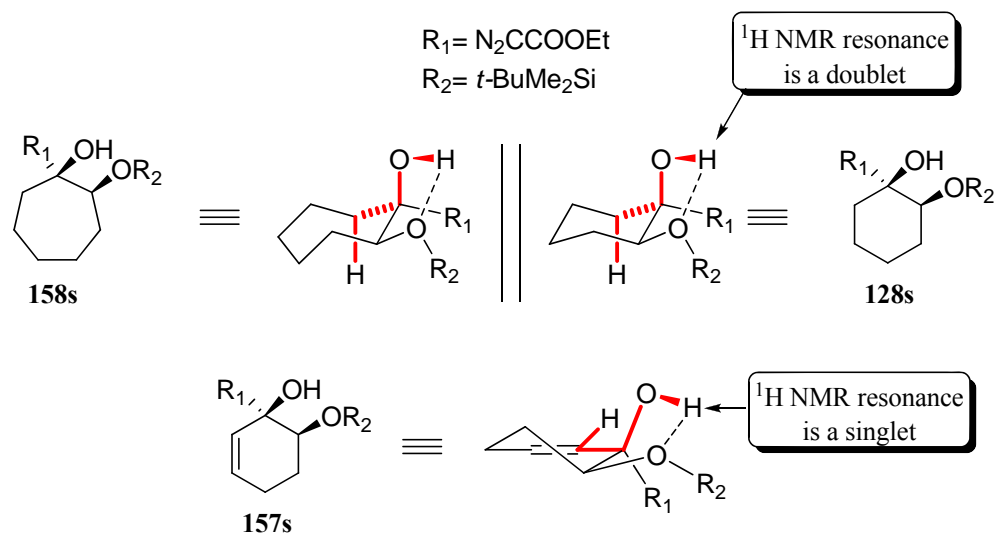
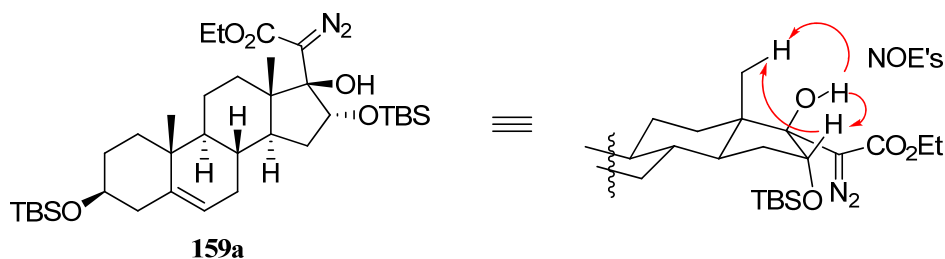


Figure 2.4. Long range “W” coupling

Unsaturated  $\gamma$ -silyloxy- $\beta$ -hydroxy- $\alpha$ -diazo esters **157s** lacks the coplanar “W” arrangement and the proton of the hydroxyl group is not split; the peak appears as a

*sharp* singlet (Figure 2.4). Furthermore, comparison of  $^1\text{H}$  NMR spectra of the major **158a** and the minor **158s** diastereomers of the cycloheptanone derived diazoester, revealed that the hydroxyl shift of the *anti* diastereomer appears as a *broad* singlet and downfield from the hydroxyl shift of the *syn* diastereomer.

Based on the  $^1\text{H}$  NMR spectral information gathered and described above, it was tentatively concluded that in general *syn*  $\gamma$ -silyloxy- $\beta$ -hydroxy- $\alpha$ -diazo esters would display a sharp “OH” peak in the  $^1\text{H}$  NMR spectrum while the *anti*  $\gamma$ -silyloxy- $\beta$ -hydroxy- $\alpha$ -diazo esters would display a broad “OH” peak further downfield. Furthermore, if a H-O-C-C- $\text{H}_{\text{axial}}$  coplanar “W” arrangement is possible, the proton of the hydroxyl moiety would appear as a *sharp* doublet in the  $^1\text{H}$  NMR spectra of the respective diazoesters. Thus *syn* : *anti* diastereomer ratios of all  $\gamma$ -silyloxy- $\beta$ -hydroxy- $\alpha$ -diazo esters which were isolated as inseparable mixtures, were determined in favor of one isomer or the other based on the trend highlighted above.



**Figure 2.5. ROESY NOE's of steroid derived diazoester 159a**

The correct absolute stereochemistry of the minor diastereomer of  $\gamma$ -silyloxy- $\beta$ -hydroxy- $\alpha$ -diazo ester **159a** (Figure 2.5) was determined through full 2D NMR characterization. Analysis of the COSY, HMQC, TOCSY and HMBC spectra allowed

for assignment of all spectral frequencies to the corresponding protons and carbons and the analysis of the ROESY spectrum provided the necessary information for stereochemical assignments. Relevant ROESY NOE signals are highlighted in Figure 2.5.

## 2.6. Fragmentation results

To test the generality of the newly discovered ring fragmentation, previously optimized reaction conditions were applied to the newly synthesized  $\gamma$ -silyloxy- $\beta$ -hydroxy- $\alpha$ -diazo esters shown in Table 2.2; overall the reaction appeared to be quite general. Tin mediated fragmentation of cyclohexanone derivative **128s** provided ethyl 8-oxooct-2-ynoate (**129**) in 94% yield (Entry 1, Table 2.3) while 1-tetralone derivative **155** and 1-indanone derivative **156** provided the corresponding homologous aryl-substituted ynoates **162** and **163** in 95% and 71% yield, respectively (Entries 2 and 3). The highly conjugated (*Z*)-ethyl 8-oxooct-4-en-2-ynoate (**164**) was formed in 97% yield from cyclohexenone derivative **157s** (Entry 4). Diastereomeric cycloheptanone derivatives **158s** and **158a** fragmented as well to provide 9-oxonon-2-ynoate (**165**) in 91% and 76%, respectively (Entries 5 and 6). The more structurally complex dehydroisoandrosterone derivative **159s** fragmented to provide desired aldehyde ynoate **166** in 76% yield (Entry 7). This example is notable because the steroid-derived product would not be straightforward to prepare by other means. On the other hand, the fragmentation of the dehydroisoandrosterone derived **159a** provided the same product in a very low 5% yield (Entry 8). This interesting result will be discussed in more detail in Section 2.7.

**Table 2.3. Fragmentation results**

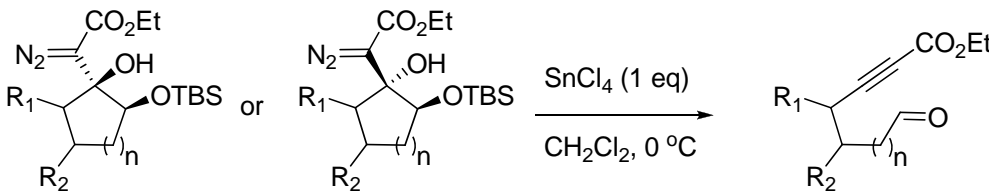
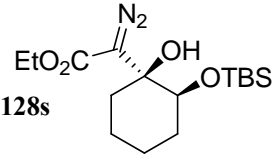
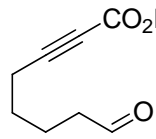
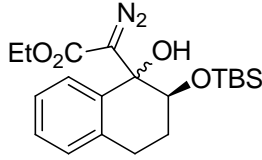
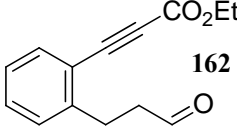
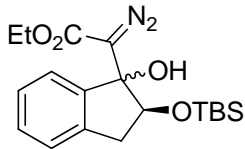
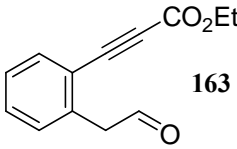
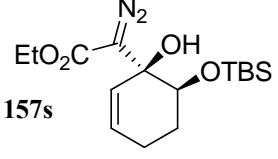
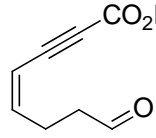
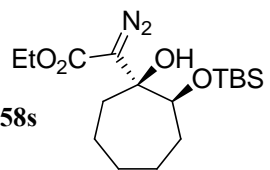
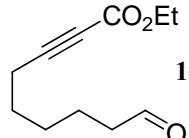
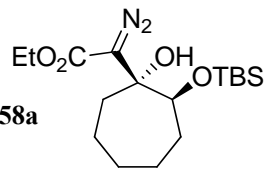
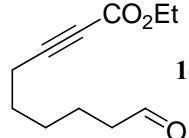
			
Entry	$\gamma$ -silyloxy- $\beta$ -hydroxy $\alpha$ -diazoester <sup>a</sup>	Tethered aldehyde ynoate	yield <sup>b</sup>
1 <sup>c</sup>	<b>128s</b> 	 <b>129</b>	94%
2	<b>155</b> 	 <b>162</b>	95%
3	<b>156</b> 	 <b>163</b>	71%
4	<b>157s</b> 	 <b>164</b>	97%
5	<b>158s</b> 	 <b>165</b>	91%
6	<b>158a</b> 	 <b>165</b>	76%

Table 2.3. Fragmentation results continued

Entry	$\gamma$ -silyloxy- $\beta$ -hydroxy $\alpha$ -diazoester <sup>a</sup>	Tethered aldehyde ynoate	yield <sup>b</sup>
7	 159s	 166	76%
8	 159a	 166	5%
9	 160	 167	27%

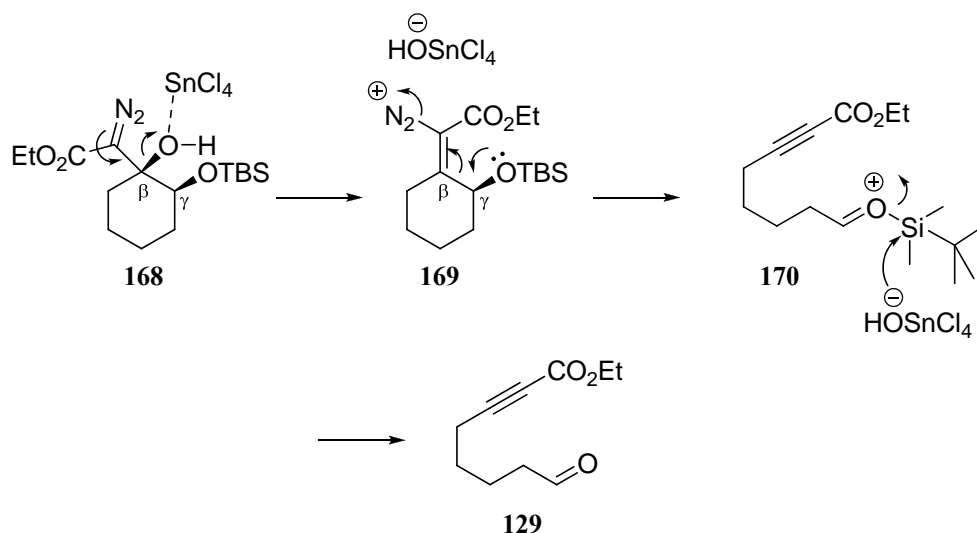
Note: <sup>a</sup> Reactions performed on 100 mg scale for all diazo esters. <sup>b</sup> yields are reported for chromatographically isolated fragmentation products. <sup>c</sup> **128s** undergoes efficient fragmentation even on 1 gram scale without significant loss in yield.

Finally, the 2-methyl-2-silyloxycyclohexanone derivative **160** fragmented to the tethered ketone ynoate **167** in only 27% yield, highlighting one potential limitation encountered with this new reaction (Entry 9).

## 2.7. Discussion of proposed reaction mechanisms

Formation of aldehyde ynoates by fragmentation of  $\gamma$ -silyloxy- $\beta$ -hydroxy- $\alpha$ -diazo esters appears to involve the loss of the diazo,  $\beta$ -hydroxyl and *t*-butyldimethylsilyl moieties. The mechanism we originally proposed was based on Padwa et al.'s report<sup>29</sup> that  $\beta$ -hydroxy- $\alpha$ -diazoesters react with  $\text{BF}_3 \cdot \text{OEt}_2$  to provide vinyl diazonium species, and ultimately vinyl cations, via elimination of the  $\beta$ -hydroxyl group (see Scheme 1.10, Section 1.1.3). We believe that  $\gamma$ -silyloxy- $\beta$ -hydroxy- $\alpha$ -diazo esters react similarly with tin tetrachloride to provide vinyl diazonium **169** (Scheme 2.17) in which the  $\text{C}_\beta\text{-C}_\gamma$  bond and the C-N bond are coplanar. As molecular nitrogen leaves, lone pair donation from the  $\gamma$ -oxygen atom would result in  $\text{C}_\beta\text{-C}_\gamma$  bond fragmentation to provide ynoate **170**. Subsequent loss of the *t*-butyldimethylsilyl group would provide tethered aldehyde ynoate **129**.

Scheme 2.17.





The mechanism described above assumes monochelation of tin tetrachloride to the free tertiary alcohol to induce diazo assisted elimination with formation of vinyl diazonium (**168**  $\rightarrow$  **169**). If this was indeed true, the fragmentation should occur with all  $\gamma$ -silyloxy- $\beta$ -hydroxy- $\alpha$ -diazo esters indifferent of diastereomer utilized, *syn* or *anti*, producing similar results. Such trend is not however observed as becomes evident when considering the following. Fragmentation of the cycloheptanone derived *syn* diol diastereomer **158s** yields **165** in 91% while a reduced yield of 76% is observed for the *anti* diol diastereomer **158a** (Table 2.3). Reduced yields are also observed for the fragmentation of a mixture of *syn* and *anti* diastereomers of cyclohexenone derivative **157** while pure *syn* diastereomer **157s** affords desired **164** in 97% yield.

Such results suggest that the reaction path to tethered aldehyde ynoates is more complex than what the mechanism in Scheme 2.17 describes. Thus, alternate mechanisms must be considered, and this section attempts to present some plausible pathways by which tethered aldehyde ynoates can be obtained starting from  $\gamma$ -silyloxy- $\beta$ -hydroxy- $\alpha$ -diazo esters and tin tetrachloride.

Similar to the mechanism proposed in Scheme 2.17, another possible mechanism which involves the loss of the diazo,  $\beta$ -hydroxyl and *t*-butyldimethylsilyl moieties with formation of a vinyl cation, invokes a tin tetrachloride bischelate model (Scheme 2.18). Metal chelation to the diazo functional group is a well known, phenomenon<sup>87</sup> and generally occurs via: (i) coordination to the terminal nitrogen or (ii) coordination to the  $\pi$ -bond of the diazo group to form a  $\eta^2$ -complex (Figure 2.6).

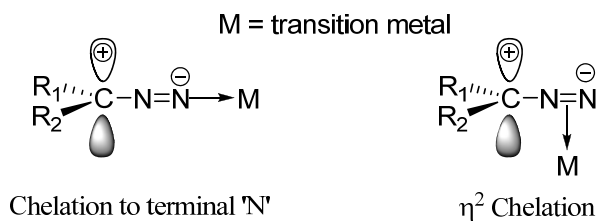
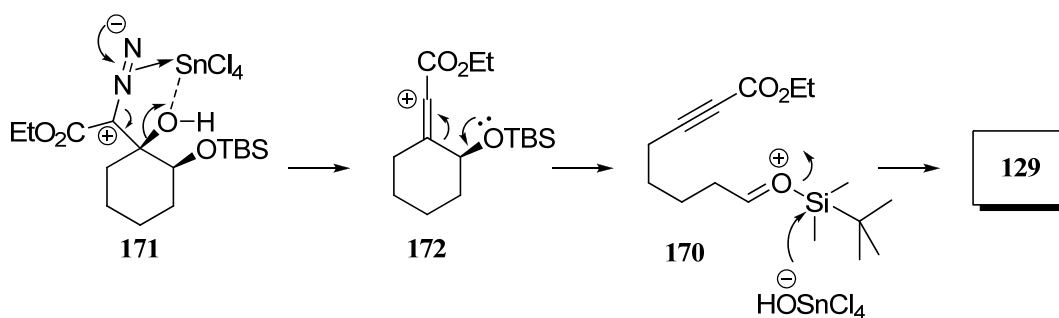


**Figure 2.6. Chelation of transition metals to the diazo functional group**

In order to address any steric concerns that may contradict the occurrence of a bischelate tin complex involving the diazo moiety, all such models invoked in mechanisms proposed herein are assumed to occur via  $\eta^2$ -complexation of tin to the diazo functional group. Thus, assuming the possibility of forming a hexacoordinate tin complex such as **171**, synchronous loss of molecular nitrogen and elimination of the hydroxyl group could be envisioned as key step towards the formation of vinyl cation **172**. Such species is then primed for C-C bond cleavage to provide fragmented intermediate **170**, which upon loss of *t*-butyldimehtylsilyl group would provide **129**.

**Scheme 2.18.**



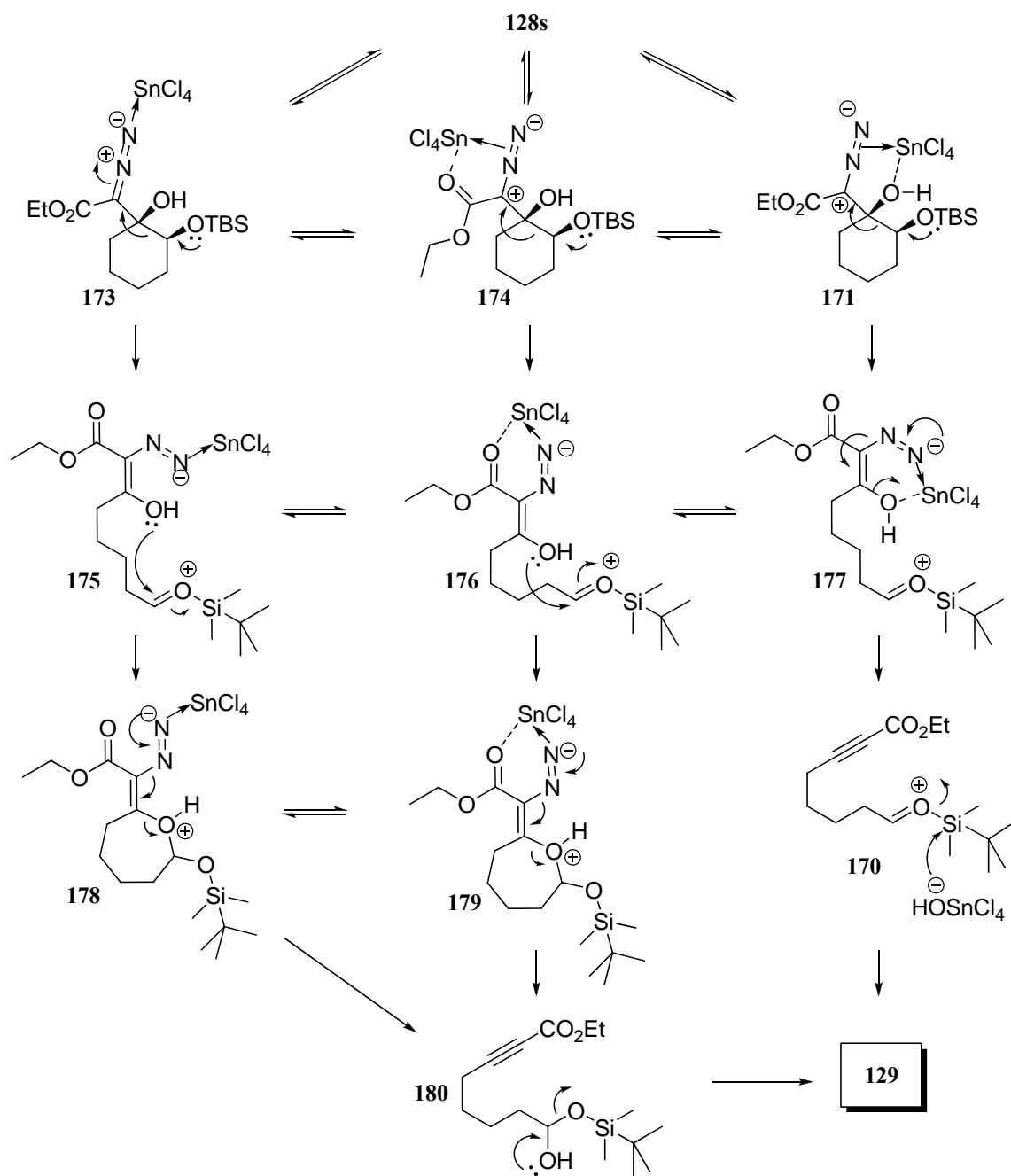
Postulated bischelate **171** (Scheme 2.18) may provide some explanation for the observed difference in yield between the fragmentations **158s** and **158a** as it takes into account the stereochemistry present in the molecule. It is possible that a more efficient

bischelation of tin to the diazo and hydroxyl group occurs in the *syn* diastereomer case and a less efficient one with the *anti* diastereomer. However, the origin of such differentiation is still unclear.

It is important to note that both mechanisms described in Schemes 2.17 and 2.18 involve the loss of the diazo and hydroxyl moieties with formation of a vinyl cation and subsequent cleavage of the C-C bond. Another possible pathway that can be postulated involves the fragmentation of the C-C bond prior to loss of the diazo and hydroxyl functional groups and a series of possible mechanisms describing such a transformation are depicted in Scheme 2.19. Tin could form three possible intermediates, that are in equilibrium, in the presence of  $\gamma$ -silyloxy- $\beta$ -hydroxy- $\alpha$ -diazoester **128s**: monochelate **173** and bischelates **174** and **171**. Both **173** and **174** could undergo C-C bond cleavage to yield the similar fragmented products, diaza enols **175** and **176**. A subsequent intramolecular cyclization could provide silyloxy acetals **178** or **179**, which upon loss of molecular nitrogen would yield silyloxy hemiacetal **180**. Elimination of silyloxy moiety would finally provide the desired tethered aldehyde ynoate **129** (Scheme 2.19).

Yet another possible path would involve tin tetrachloride bischelated diaza enol **177**, which instead of intramolecular acetal formation could undergo synchronous tin mediated loss of molecular nitrogen and elimination of the hydroxyl group to provide ynoate **170**; loss of *t*-butyldimehtylsilyl moiety would provide tethered aldehyde ynoate **129**.

Scheme 2.19.



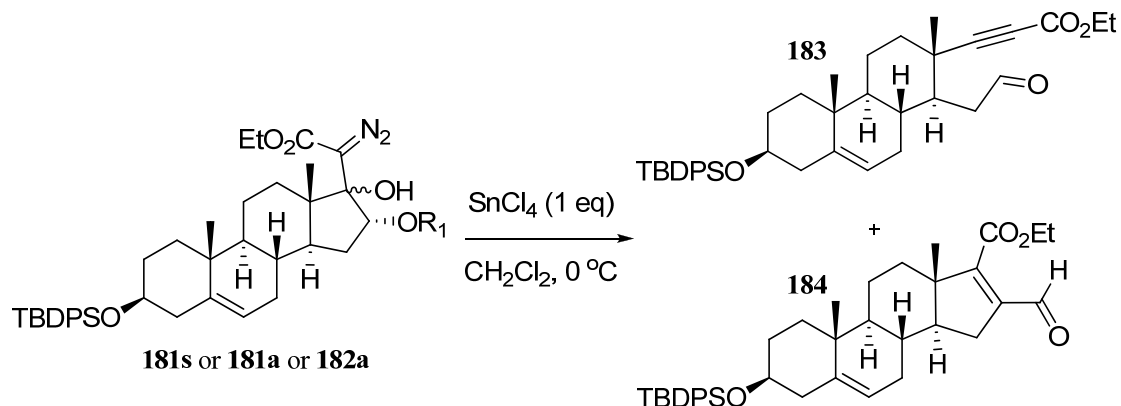
While all proposed mechanisms described herein explain formation of **129**, there is, at this point, *no* evidence to support or negate any of them. Further studies

aimed towards the identification of possible reactive intermediates are required. In situ React-IR and variable temperature  $^1\text{H}$  and  $^{119}\text{Sn}$  NMR experiments could provide necessary insight for the elucidation of such intermediates. Additionally, incorporating an  $^{18}\text{O}$  labeled hydroxyl group into the fragmentation precursor **128s**, could provide useful information about the potential existence of intermediates such as **178** or **179**. In our initial studies which were performed at  $-78\text{ }^\circ\text{C}$  we observed rapid loss of coloration and formation of a transparent reaction mixture upon the addition of Lewis acid to the bright yellow diazo ester **128s** solution in  $\text{CH}_2\text{Cl}_2$ . This suggests that chelation of tin tetrachloride to the diazo moiety is a possibility as this would disrupt conjugation which is often the cause for the observed intense colors associated with diazo compounds.

Finally, another relevant result worth discussing is the fragmentation of dehydroisoandrosterone derivative **159s** and **159a** which provided the desired aldehyde ynoate with drastically different yields (76% and 5% respectively, entries 7 & 8, Table 2.3). Additionally, fragmentation of **159s** also led to the formation of an unexpected minor aldehyde byproduct while **159a** provided that same byproduct as the major constituent of more complex crude reaction mixture. Further inquiry directed us towards the synthesis of differentially protected *syn* and *anti*  $\gamma$ -silyloxy- $\beta$ -hydroxy- $\alpha$ -diazo ester **181s** and **181a** respectively ( $\text{R}_1 = \text{TES}$ , Scheme 2.20). Again, *syn* diastereomer **181s** provided desired ynoate **183** in 74% yield and unexpectedly  $\alpha,\beta$ -unsaturated ester **184** in 18% yield. The *anti* diastereomer **181a** allowed for the

isolation  $\alpha,\beta$ -unsaturated ester **184** from a more complex mixture of compounds as the major product in 50% yield.

Scheme 2.20.



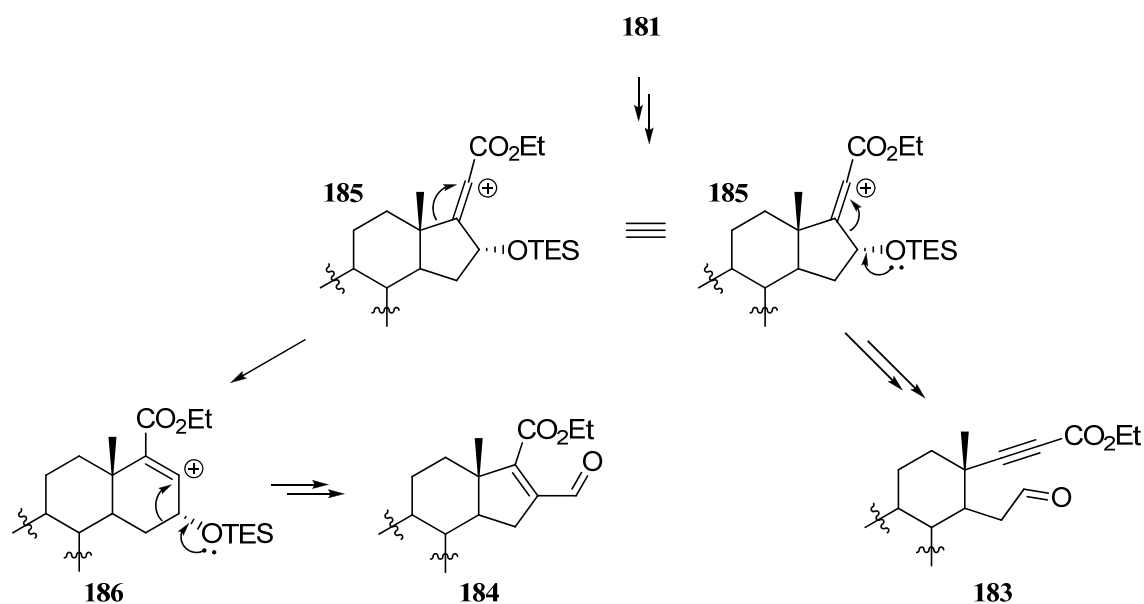
R <sub>1</sub>	Diastereomer	Compound #	<b>183</b> (%yield)	<b>184</b> (%yield)
TES	<i>syn</i>	<b>181s</b>	74	18
TES	<i>anti</i>	<b>181a</b>	5	50
TBDPS	<i>anti</i>	<b>182a</b>	5	51

Furthermore the attempted fragmentation of the *anti* diastereomer **182a** (R<sub>1</sub>= TBDPS) also provided a complex mixture of products out of which  $\alpha,\beta$ -unsaturated ester **184** was isolated as the major product in 51% yield. The similar yields, obtained for the reaction of both **181a** and **182a**, seem to suggest that altering the steric bulk around the reaction center has little effect on the reaction outcome. Such statement can also be valid for the comparison of the fragmentation results of  $\gamma$ -*t*-butyldimethylsilyloxy derivative **159s** (Entry 7, Table 2.3) and  $\gamma$ -triethylsilyloxy

derivative **181s** (Scheme 2.20), both providing tethered aldehyde ynoates **166** and **183** in almost identical 76% and 74% yield, respectively.

The observed formation of  $\alpha,\beta$ -unsaturated ester **184** demanded a plausible mechanistic explanation and initially a path from vinyl cation **185** was considered (Scheme 2.21). If ring expansion were to occur (**185**  $\rightarrow$  **186**), instead of the more likely C-C bond cleavage (**185**  $\rightarrow$  **183**), vinyl cation **185** would be formed and  $\gamma$ -silyloxy assisted alkyl migration would provide the rearranged  $\alpha,\beta$ -unsaturated ester **184**, upon subsequent loss of silyloxy moiety.

Scheme 2.21.



However, such mechanism presumes that formation of both **184** and **183** occurs from a common intermediate such as vinyl cation **185**, which cannot be correct because the experimental data shows that the reaction of the *syn* diastereomer leads to the formation of tethered aldehyde ynoate **183** as a major product while the *anti*

diastereomer led to the formation of  $\alpha,\beta$ -unsaturated ester **184** as a major product. A common intermediate cannot explain this result. Two different reactive intermediates, each accessible from both the *syn* and *anti* diastereomers via energetically different pathways, must form. Energy diagram represented in Figure 2.7 depicts these potential paths, but it should be noted that the relative energy differences have no empirical support.

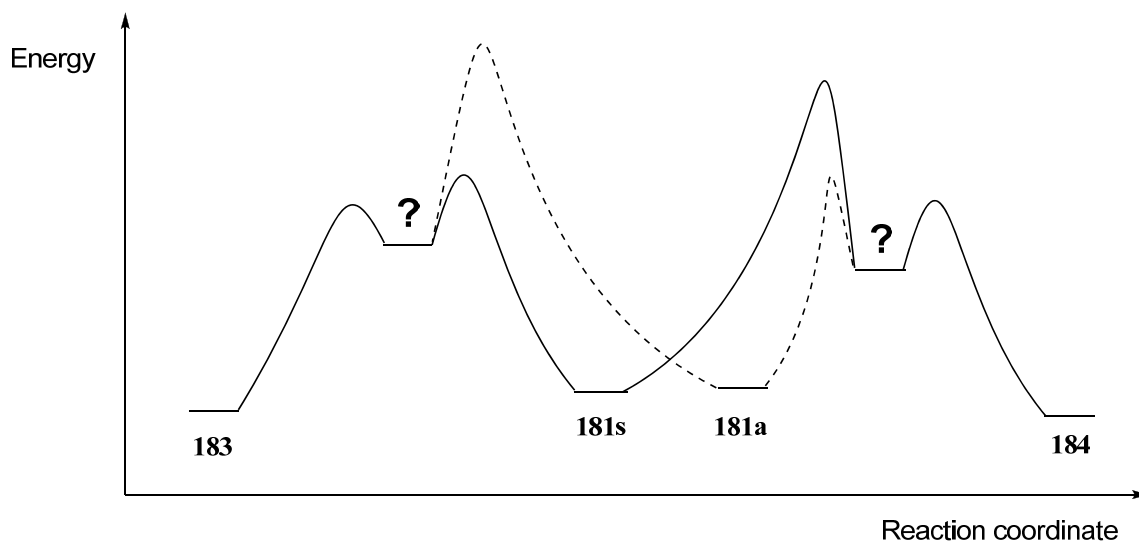
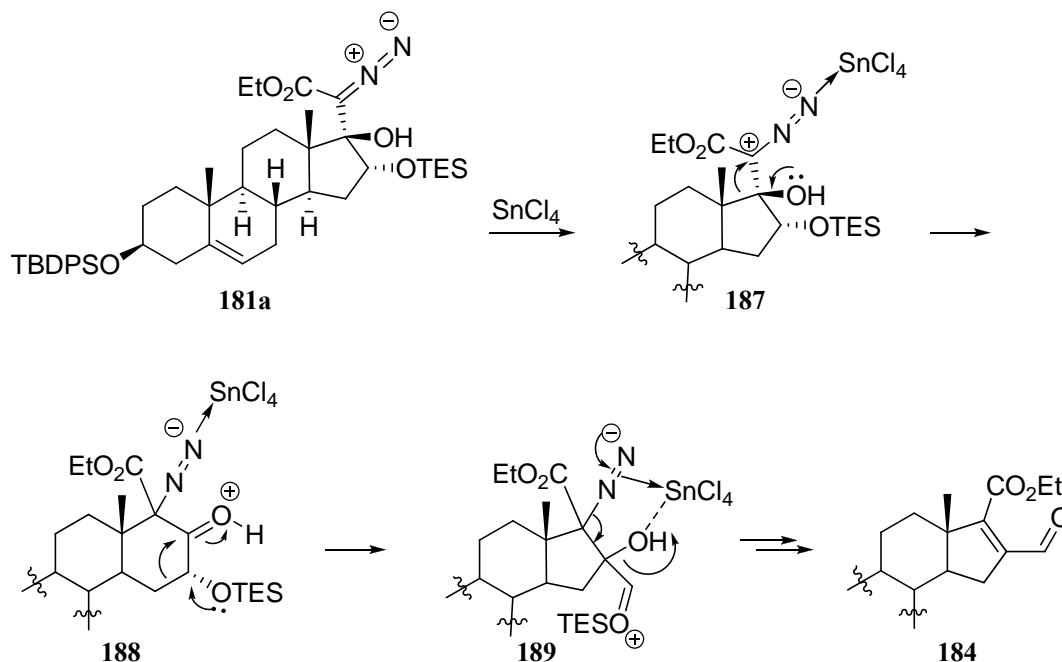


Figure 2.7. Energy diagram

An alternate hypothetical mechanism, which may explain formation of  $\alpha,\beta$ -unsaturated ester **184** is highlighted in Scheme 2.22 and invokes a  $\beta$ -hydroxyl promoted ring expansion to give intermediate **188**. Subsequent alkyl migration would afford **189** which, upon loss of molecular nitrogen, the hydroxyl and triethylsiloxy groups would, provide  $\alpha,\beta$ -unsaturated ester **184**.



Scheme 2.22.



At this time there is no empirical data to support any of the postulated mechanisms or offer explanation for the preference exhibited by the *syn* diastereomer to provide aldehyde ynoate **183** as the major product and *anti* diastereomer to give  $\alpha,\beta$ -unsaturated ester **184** as the major product. Revealing the identity of key reactive intermediates which lead to the formation of the observed products would clearly be necessary in order to disprove any mechanistic hypothesis presented herein. The use of in situ React-IR and variable temperature  $^1\text{H}$  and  $^{119}\text{Sn}$  NMR experiments could potentially shed some light on the matter.

## 2.8. Exploring the versatility of the fragmentation protocol

Having discovered that the fragmentation of various  $\gamma$ -silyloxy- $\beta$ -hydroxy- $\alpha$ -diazoesters proceeded in good to excellent yields, I set out to establish if other

structural alterations would have any effect on the reaction outcome. Fragmentation precursors such as the diazo esters presented in Figure 2.8 emerged as good test substrates. Whereas diazo esters **190a**, **190b** and **190c** were expected to afford the same tethered aldehyde ynoate product, substrates **191** and **192** were designed to test the possibility of providing fragmented products bearing different combinations of functional groups.

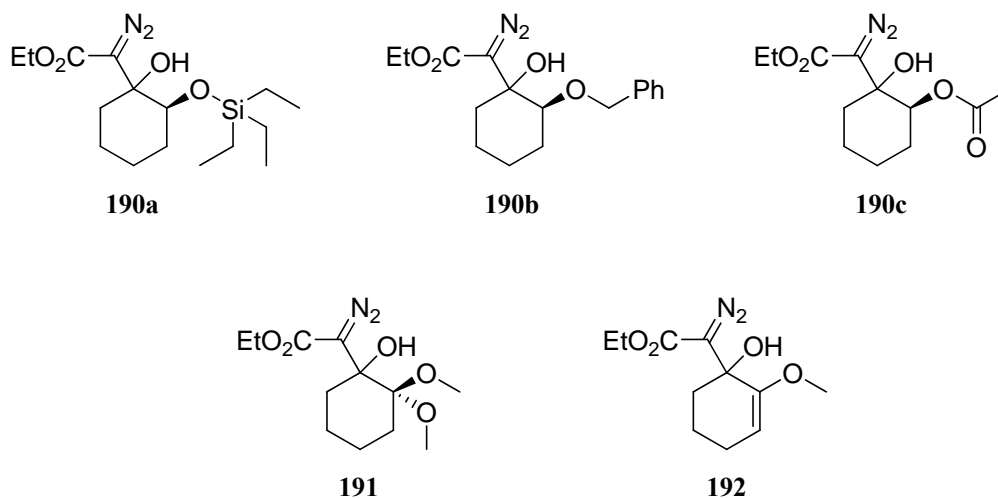
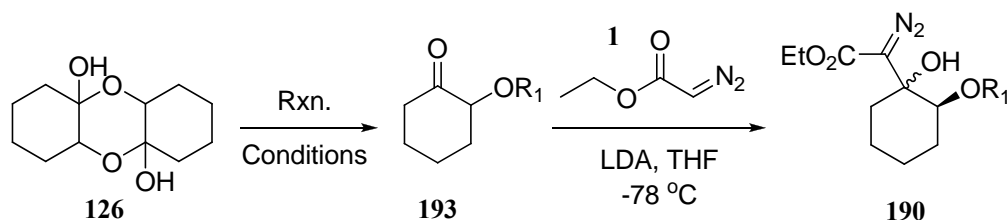


**Figure 2.8. Alternate fragmentation precursors**

The synthesis of the fragmentation precursors bearing various  $\gamma$ -OH protecting groups began with commercially available cyclohexanone dimer (**126**). Differentially protected  $\alpha$ -hydroxy ketones were obtained via silylation, benzylation and acetylation of the free alcohol, and subsequent ethyl lithio-diazoacetate addition provided the desired fragmentation precursors in good yields as mixtures of *syn* and *anti* diastereomers (results are summarized in Table 2.4).

Table 2.4. Synthesis of alternate fragmentation precursors

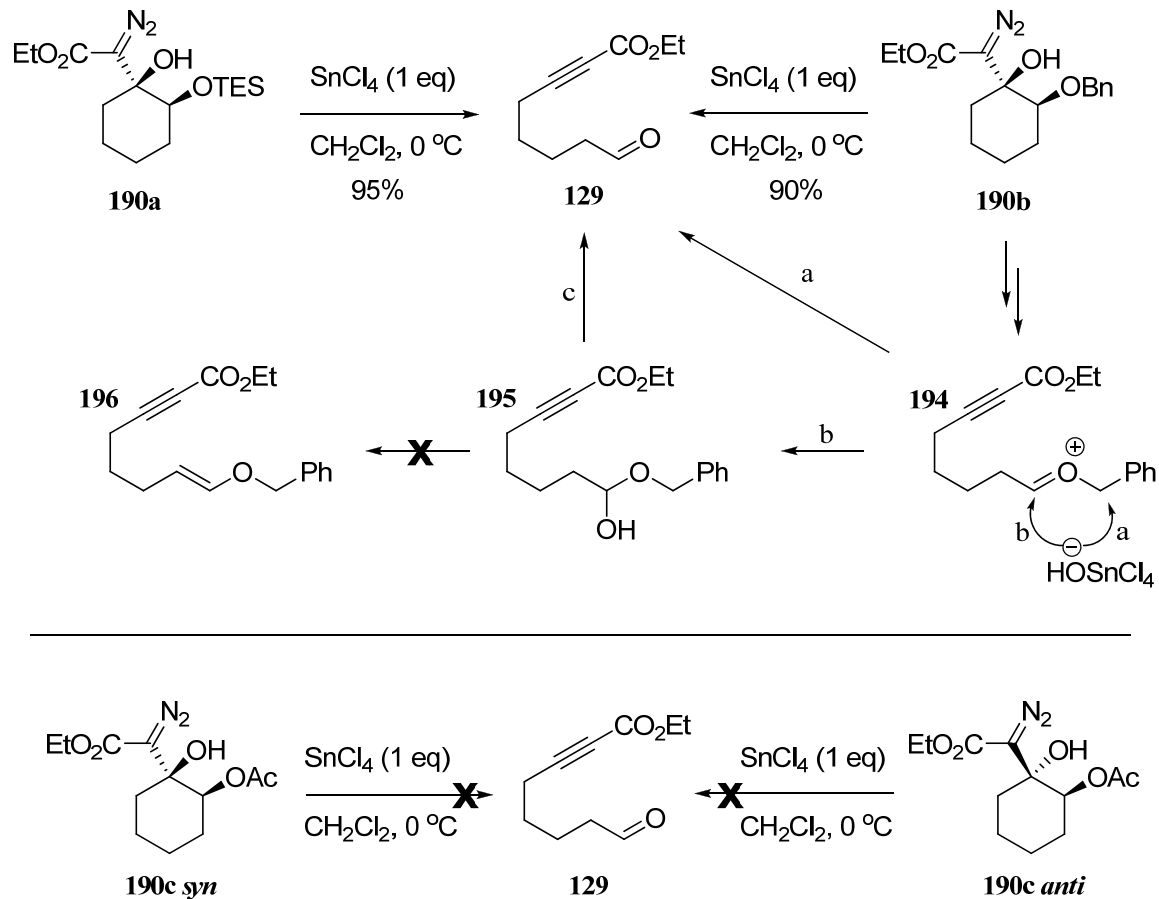


Entry	R <sub>1</sub>	Rxn. Conditions	$\alpha$ -OR Ketone (yield) <sup>a</sup>	$\alpha$ -diazo ester (yield) <sup>a</sup>	<i>syn</i> : <i>anti</i> <sup>b</sup>
1	TES	TESCl, Imidazole DMAP, CH <sub>2</sub> Cl <sub>2</sub>	<b>193a</b> (88%)	<b>190a</b> (94%)	20 : 1
2	Bn	BnOH, Toluene HCl, Reflux	<b>193b</b> (47%)	<b>190b</b> (92%)	20 : 1
3	Ac	Ac <sub>2</sub> O, reflux	<b>193c</b> (97%)	<b>190c</b> (89%)	1.4 : 1 <sup>c</sup>

Note: <sup>a</sup> yields are reported after chromatography. <sup>b</sup> ratios determined by analysis of the <sup>1</sup>H NMR of the crude reaction mixture. <sup>c</sup> ratio assigned tentatively by comparison of <sup>1</sup>H NMR spectra with known *syn* and *anti* diastereomer spectra.

Gratifyingly, both  $\gamma$ -triethylsilyloxy- $\beta$ -hydroxy- $\alpha$ -diazoacetate **190a** and  $\gamma$ -benzyloxy- $\beta$ -hydroxy- $\alpha$ -diazoacetate **190b** underwent tin mediated ring fragmentation to provide ethyl 8-oxooct-2-ynoate (**129**) in good yields (Scheme 2.23). Even though pleased with the result, the fragmentation of the benzyloxy derivative **190b** was somewhat intriguing, because it was expected that such substrate may provide access to (E)-ethyl 8-(benzyloxy)oct-7-en-2-ynoate (**196**) rather than the observed tethered aldehyde ynoate **129**. It is possible that intermediate **194** undergoes either loss of benzyloxy moiety (path 'a') to provide **129** or hemiacetal formation (path 'b'). The latter can further react and undergo tin mediated elimination of benzyloxy moiety to provide the observed product **129** without  $\alpha$ -elimination to form **196**.

Scheme 2.23.

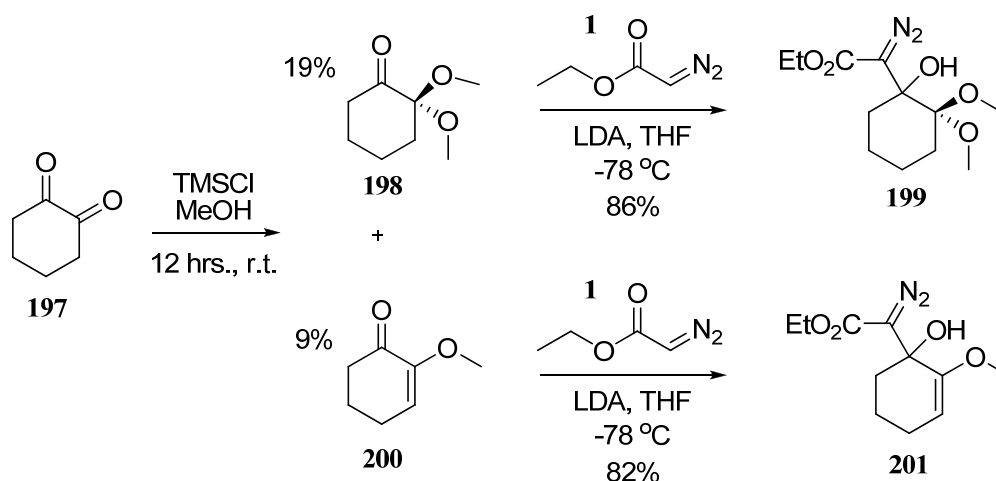


The fragmentation of either *syn* or *anti* diastereomers of  $\gamma$ -acetoxy- $\beta$ -hydroxy- $\alpha$ -diazoacetates **190c** (Scheme 2.23), was met with lower levels of success. When subjected to tin tetrachloride, complex mixtures of products were observed, and the desired aldehyde ynoate was only identified by  $^1\text{H}$  NMR.

The synthesis of  $\gamma$ -methoxycyclohex-2-enyl diazoester **201** and  $\gamma$ -dimethoxycyclohexyl diazo ester **199** began with commercially available cyclohexane-1,2-dione (**197**, Scheme 2.24). Treatment of **197** with  $\text{TMSCl}$  in  $\text{MeOH}$  provided a mixture of 2,2-dimethoxycyclohexanone (**198**) and 2-methoxycyclohex-2-enone (**200**)

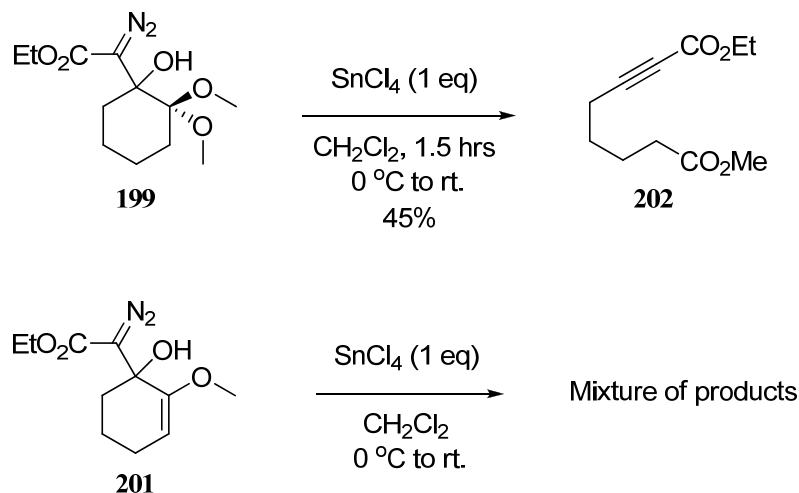
which were isolated in 19% and 9% yields respectively. Subsequent ethyl-lithio diazoacetate addition to ketones **198** and **200** provided diazo fragmentation precursors **199** and **201** in good yields.

Scheme 2.24.



When  $\gamma$ -dimethoxycyclohexyl diazo ester **199** was subjected to tin mediated fragmentation, the reaction appeared to occur at a much slower rate and less clean than what was previously observed for the fragmentation of  $\gamma$ -silyloxy- $\beta$ -hydroxy- $\alpha$ -diazoesters. However, the expected 1-ethyl 8-methyl oct-2-ynedioate (**202**, Scheme 2.25) was observed and subsequently isolated by chromatography in 45% yield. It should be noted that even though isolated in modest yields under unoptimized reaction conditions, promoting formation of **202** was highly gratifying because it highlighted the broad scope and versatility of this novel fragmentation protocol. On the other hand, the reaction of  $\gamma$ -methoxycyclohex-2-enyl diazoester **201** with tin tetrachloride provided a complex mixture of products, none of which have been thus far identified (Scheme 2.25).

Scheme 2.25.



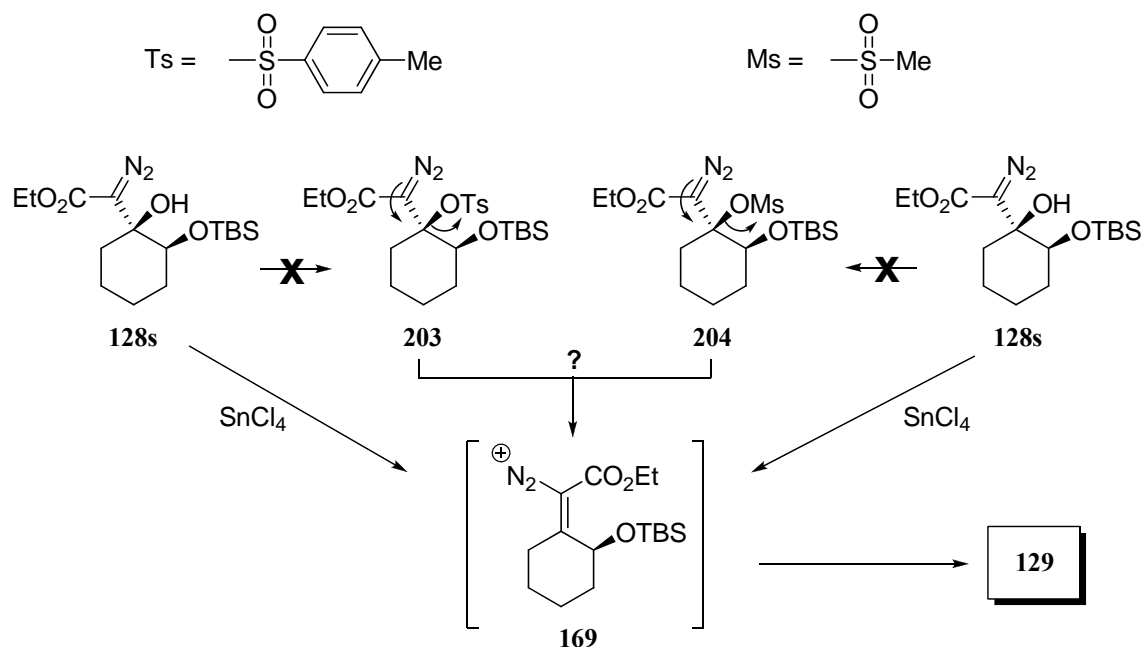
In conclusion, the fragmentation reaction appears to tolerate  $\gamma$ -triethylsilyloxy and benzyloxy groups providing the desired tethered aldehyde ynoates in good yields, while the presence of an acetoxo group at the  $\text{C}_\gamma$  position inhibits the reaction. Furthermore,  $\gamma$ -bismethoxy- $\beta$ -hydroxy- $\alpha$ -diazoester **199** was shown to also undergo tin mediated cleavage of the  $\text{C}_\beta$ - $\text{C}_\gamma$  bond to provide tethered ynedionate **202** in modest yields. Overall these results expand the general scope and attest to the synthetic potential of this novel reaction.

## 2.9. Pursuit of alternate fragmentation strategies

Based on the initial assumption that the fragmentation of  $\gamma$ -silyloxy- $\beta$ -hydroxy- $\alpha$ -diazoester **128s** occurs with initial formation of a vinyl diazonium intermediate (e.g. **169**, Scheme 2.26) and subsequent cleavage of the  $\text{C}_\beta$ - $\text{C}_\gamma$  bond, the idea of potentially developing a Lewis acid free version emerged. In effect, it was envisioned that vinyl diazonium species **169** could be accessed from  $\gamma$ -silyloxy- $\beta$ -*p*-toluenesulfonate- $\alpha$ -

diazoester **203** or  $\gamma$ -silyloxy- $\beta$ -methanesulfonate- $\alpha$ -diazoester **204** via elimination of the *p*-toluenesulfonate or methanesulfonate moieties.

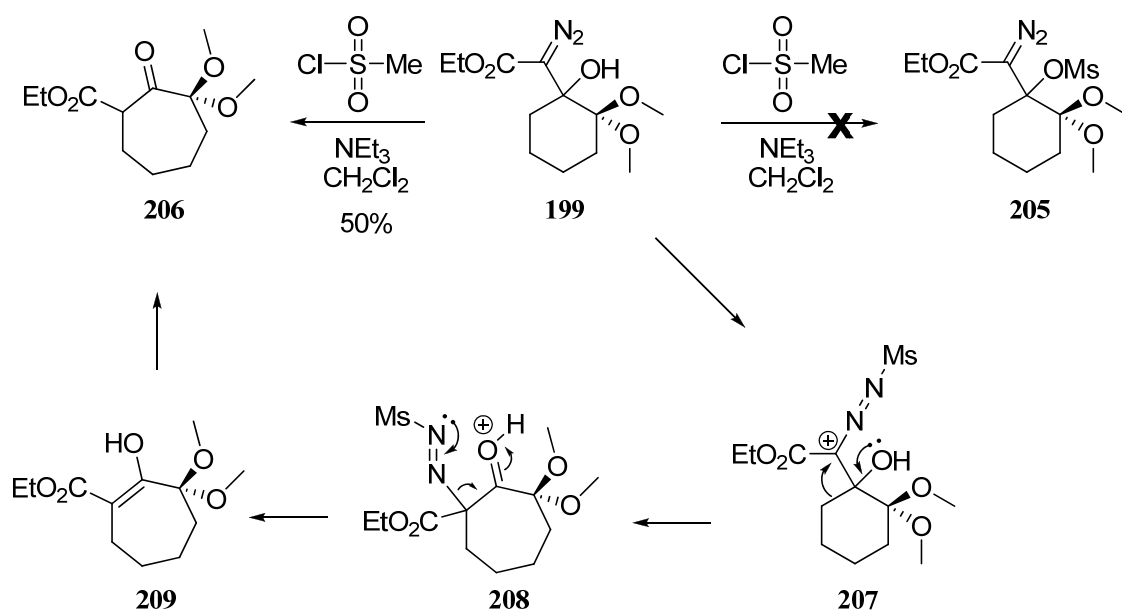
Scheme 2.26.



All attempts to synthesize the prospective fragmentation precursors **203** and **204** were unsuccessful, and often only led to the recovery of the starting materials from the reaction mixtures. Low nucleophilicity of the tertiary alcohol due to steric hindrance around the reaction center was considered as a likely cause for the lack of success encountered. Notably, the attempt to trap the lithio-oxyanion resulted from the addition of ethyl lithio-diazoacetate to the respective ketone with chloro *p*-toluenesulfonate or chloro methanesulfonate also failed. Reactions resulted in the isolation of undesired free alcohol and none of the desired sulfonates (e.g. **203** or **204**) were detected.

An unexpected result was observed, however, when  $\gamma$ -bismethoxycyclohexyl diazo ester **199** was treated with methanesulfonyl chloride and triethylamine in an attempt to access  $\beta$ -methanesulfonate **205**. Analysis of the crude reaction mixture revealed ketoester **206** as a major component which was subsequently isolated in 50% yield. Thus diazo ester **199** appeared to undergo ring expansion rather than the desired mesitylation of the tertiary alcohol. A mechanistic explanation assumes the potential mesitylation of the diazo moiety with formation of an intermediate such as **207**, which can undergo hydroxyl assisted alkyl migration to provide diaza intermediate **208**. Loss of molecular nitrogen and subsequent tautomerization would afford the empirically observed ethyl 3,3-dimethoxy-2-oxocycloheptanecarboxylate (**206**).

Scheme 2.27.



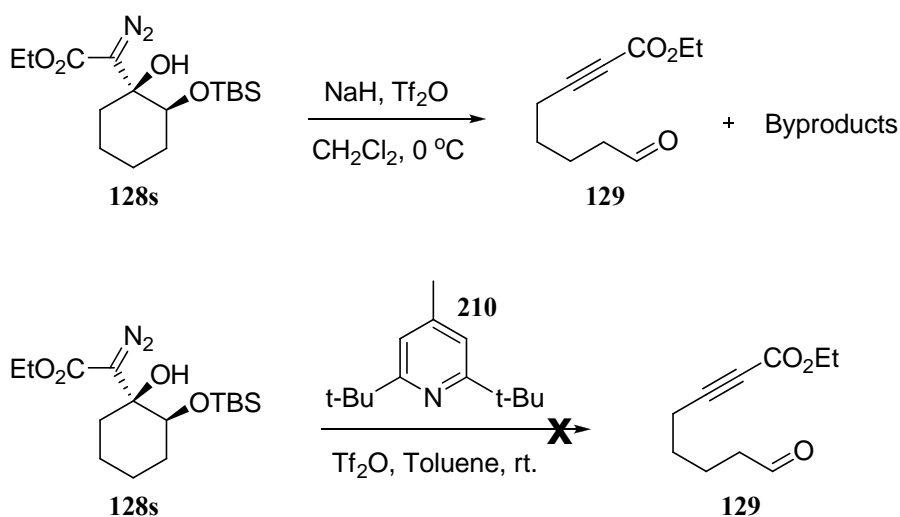
The reactivity exhibited by diazoester **199** in the presence of methanesulfonyl chloride seems to suggest that the most nucleophilic site in the molecule is the terminal



nitrogen of the diazo group. This reactivity profile may be of importance when considering the postulated mechanisms for the fragmentation of  $\gamma$ -silyloxy- $\beta$ -hydroxy- $\alpha$ -diazoesters presented in Section 2.7.

Other attempts to increase the electrofugality of the  $\beta$ -hydroxyl moiety included the treatment of  $\gamma$ -silyloxy- $\beta$ -hydroxy- $\alpha$ -diazoester **128s** with trifluoromethanesulfonic anhydride ( $\text{ Tf}_2\text{O}$ ), which resulted in observable gas evolution and formation of the desired tethered aldehyde ynoate **129** as determined by the analysis of the  $^1\text{H}$  NMR of the crude reaction mixture (Scheme 2.28).

Scheme 2.28.



However, the reaction was never clean and always provided undesired byproducts. Buffering the reaction with 2,6-di-*tert*-butyl-4-methylpyridine (**210**) completely inhibited the reaction and no desired fragmentation was observed, which raises the possibility that the prior result was due to trace acid present.

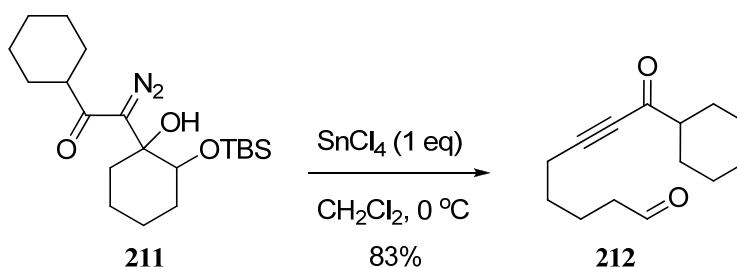
Although a Lewis acid free variant of the novel fragmentation reaction is appealing for both chemical and procedural reasons, development of a robust and reliable protocol has thus far failed.

## 2.10. Future perspective

### 2.10.1. Expanding the utility of the novel fragmentation reaction

The successful fragmentation of  $\gamma$ -silyloxy- $\beta$ -hydroxy- $\alpha$ -diazoesters has encouraged current investigations, conducted by Ali Bayir, aimed towards the fragmentation of  $\gamma$ -silyloxy- $\beta$ -hydroxy- $\alpha$ -diazoketones (e.g. **211**, Scheme 2.29) to provide tethered aldehyde ynones (e.g **212**). For example, cyclohexyl diazo ketone **211** was found to react cleanly in the presence of tin tetrachloride to provide 8-cyclohexyl-8-oxooct-6-ynal (**212**) in 83% isolated yield. The fragmentation of diazo ketones is expected to allow access to a wide range of aldehyde ynones, varying in ketone substituent and tether length.

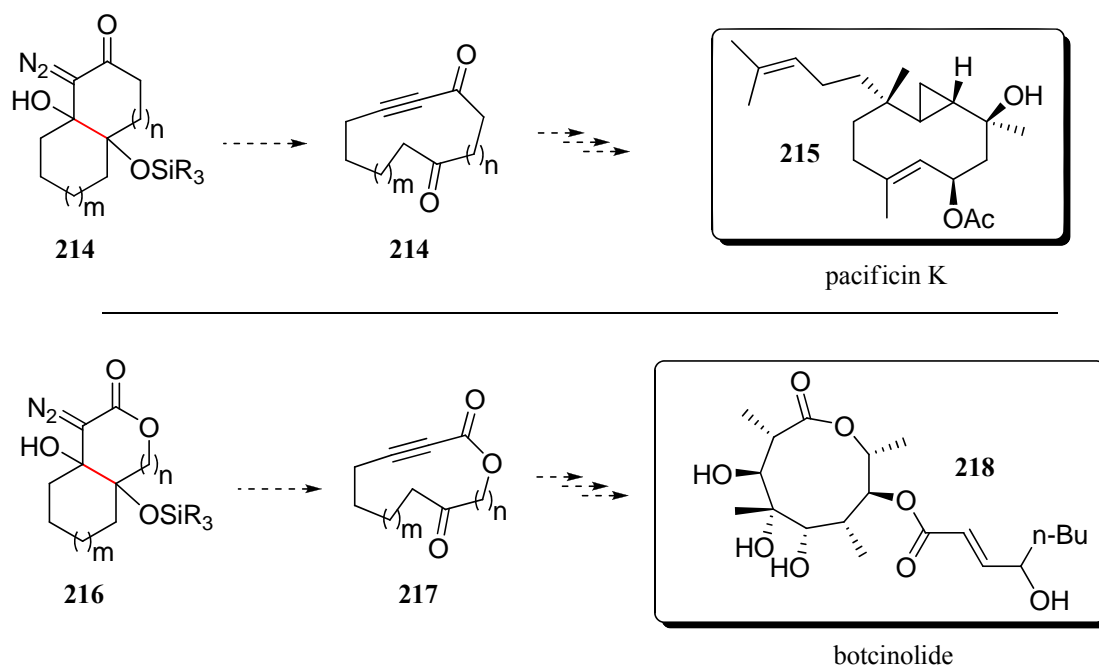
Scheme 2.29.



While numerous methods are known for the synthesis of macrocyclic ketones and lactones,<sup>88,89</sup> developing methodology that utilizes the novel C-C bond cleavage reaction to provide such products would be a significant advancement. Bicyclic  $\gamma$ -

silyloxy- $\beta$ -hydroxy- $\alpha$ -diazo species such as **213** and **216** (Scheme 2.30) can be envisioned as fragmentation precursors that can afford macrocyclic yne-diketones (e.g. **214**) or macrocyclic yne-ketolactones (e.g. **217**) via fragmentation of the ring fusion C-C bond (highlighted in red).

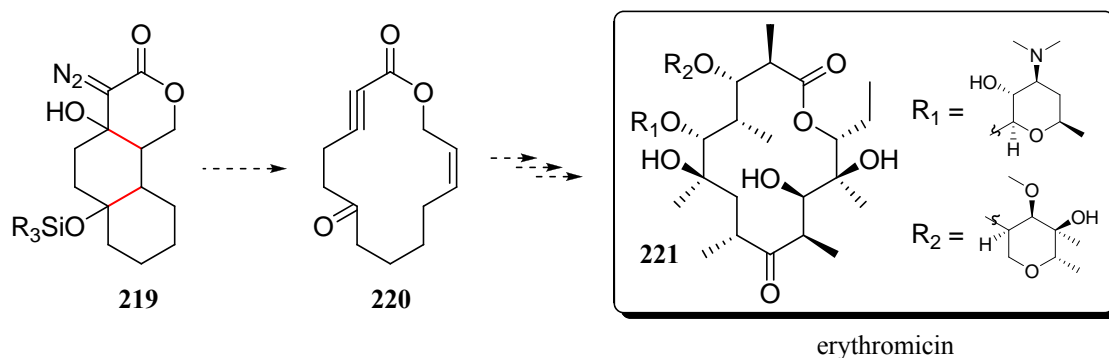
Scheme 2.30.



Quick and efficient access to various macrocyclic frameworks could be key steps in the total synthesis of complex natural products. Thus a more functionalized yne-diketone with the carboskeleton of **214** could serve as an intermediate in the synthesis of prenylbicyclogermacrane diterpenoids such as pacificin K (**215**),<sup>90</sup> while yne-ketolactones such as **217** could provide the carboskeletal framework found in botcinolide (**218**).<sup>91</sup>

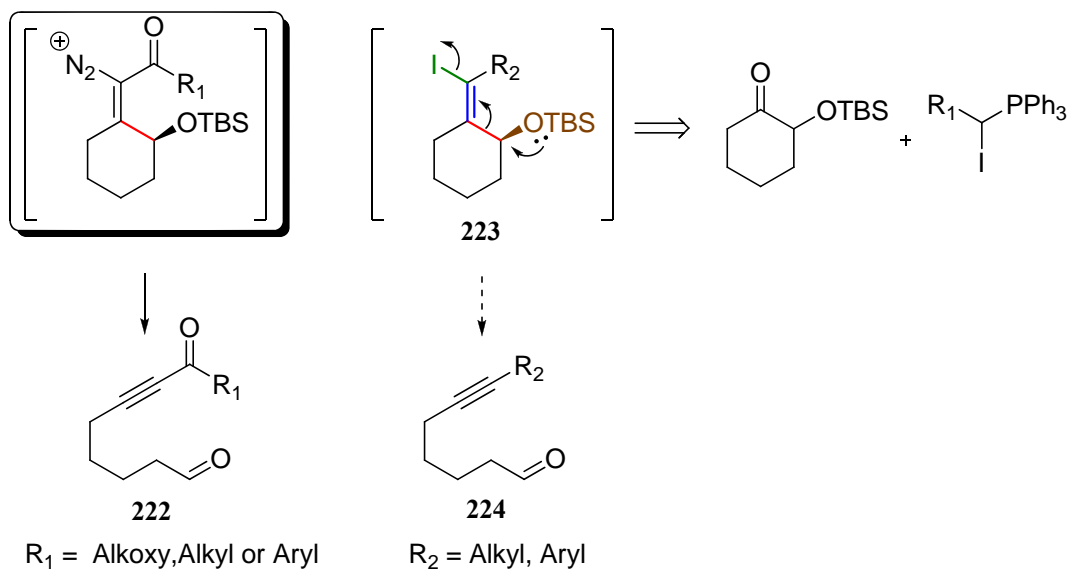
Furthermore, the possibility of extending such reactivity to involve the cleavage of not one but two ring fused C-C bonds to provide macrocyclic products (**219**  $\rightarrow$  **220**, Scheme 2.31) can also be imagined. The macrocyclic framework that would be revealed following such transformation is a common structural motif found in potent antibiotics such as erythromycin (**221**).

Scheme 2.31.



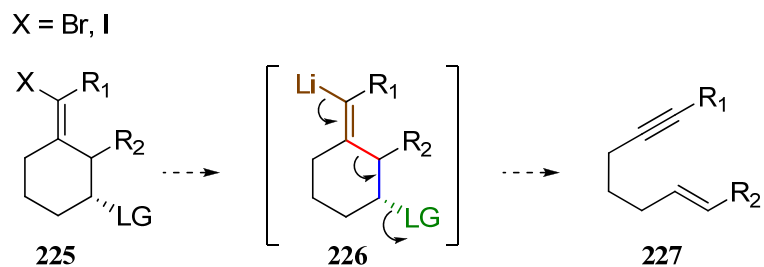
A limitation of the methodology discussed herein is that all fragmented products formed contain the ynone or ynoate functional group (e.g. **222**, Scheme 2.32). Compounds bearing an alkyl or aryl alkyne moiety would have to arrive from structurally different fragmentation precursors. Similar to vinyl diazonium intermediates, vinyl iodides (e.g. **223**) could be envisioned as potential fragmentation precursors that may undergo cleavage of a C-C bond to provide tethered alkyne aldehydes such as **224**.

Scheme 2.32.



Exocyclic vinyl halides of type **225** (Scheme 2.33) can be further envisioned as potential fragmentable systems. Lithium-halide exchange<sup>92</sup> could provide vinyl lithium intermediates (e.g. **226**) which contain all the required components for a system that may undergo a ring cleavage reaction: nucleofugal fragment (green), middle fragment (blue) and electrofugal fragment (brown). The resulting unsaturated products (e.g. **227**) could be of synthetic value and serve as useful organic intermediates.

Scheme 2.33



## 2.11. Conclusions

The Lewis acid promoted fragmentation of  $\gamma$ -silyloxy- $\beta$ -hydroxy- $\alpha$ -diazoesters provides a simple and efficient way to prepare tethered aldehyde ynoates with varying tether length. Tethered aldehyde ynoates are versatile intermediates<sup>93-99</sup> and this functional group combination is unique to this fragmentation. The synthetic utility of such products will be discussed in more detail in Chapter 3; particularly, their predisposition to undergo facile intramolecular [1,3]-dipolar cycloaddition reactions and their application towards the synthesis of the steroidal alkaloid solanidine.

For mechanism elucidation, further studies aimed towards identification of possible reactive intermediates which lead to the formation of tethered aldehyde ynoates are clearly necessary in order to disprove any mechanistic hypothesis presented herein. Future examinations of possible mechanistic pathways may include React-IR and/or variable temperature  $^1\text{H}$  and  $^{119}\text{Sn}$  NMR experiments to help elucidated such intermediates. Fully understanding the mechanisms by which this reaction occurs may help design complex molecules that can undergo efficient fragmentation.

### 3. CHAPTER 3: TETHERED ALDEHYDE YNOATES – USEFUL SYNTHETIC INTERMEDIATES

In Chapter 2 of this dissertation, I presented the successful development of a novel tin mediated ring fragmentation of  $\gamma$ -silyloxy- $\beta$ -hydroxy- $\alpha$ -diazoesters which allows for the efficient preparation of tethered aldehyde ynoates. In this chapter, I will describe the work carried out looking at how these fragmentation products can be used to build more complex systems. The presence of two reactive functional groups tethered together attracted our attention to intramolecular reactions; specifically [1,3]-dipolar cycloaddition reactions of stabilized and unstabilized azomethine ylides with pendant ynoates to provide N-containing polycyclic heterocycles. Additionally, developing this reactivity could be of significant importance because it could be utilized to efficiently assemble the heterocyclic core of natural products such as steroidal alkaloids solanidine and demisidine.

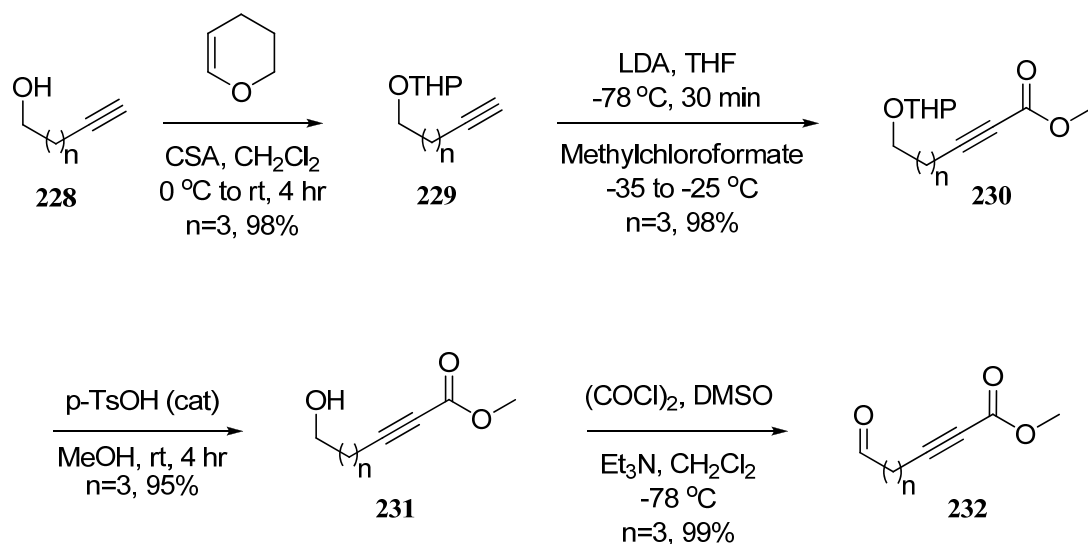
#### 3.1. Background

##### 3.1.1. Previously reported preparative routes to tethered aldehyde ynoates

A careful review of the recent literature revealed alkynyl alcohols<sup>100</sup> (e.g. **228**, Scheme 3.1) as common starting materials for the synthesis of various aldehyde ynoates differing by alkane tether length. For example, Marino<sup>93</sup> and co-workers reported the preparation of methyl 7-oxohept-2-ynoate (**232**, n=3, Scheme 3.1) by initially protecting the primary alcohol **228** (n=3) with tetrahydropyran (THP) and subsequently acylating the in situ formed alkynyl acetylide<sup>95</sup> with methyl chloroformate to afford alkynyl ester **230** (n=3). Removal of the THP protecting group

with catalytic amount of *p*-toluenesulfonic acid in methanol provided primary alcohol **231** (*n*=3) which upon oxidation under Swern conditions gave the desired tethered aldehyde ynoate **232** (*n*=3) in excellent yield.

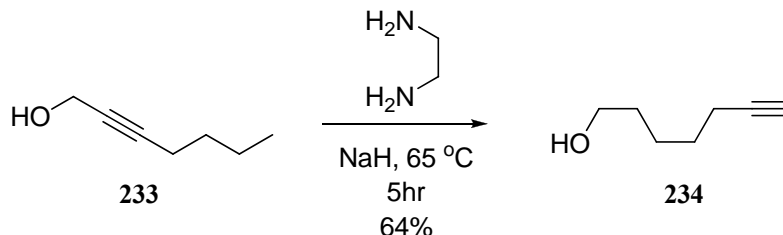
Scheme 3.1.



Although the method highlighted above provides efficient access to the desired tethered aldehyde ynoates (e.g. **232**), it is limited in applicable scope by the availability of the alkynyl alcohols used as starting materials (e.g. **228**). While 4-pentyn-1-ol (**228**, *n*=2) and 5-hexyn-1-ol (**228**, *n*=3) are commercially available, alkynyl alcohols bearing longer alkane tethers (*n*=4 or higher) have to be synthetically prepared. This is generally achieved by a base mediated transposition<sup>101</sup> of the alkyne moiety of propargylic alcohols (e.g. **233**, Scheme 3.2) to provide the requisite terminal alkynes (e.g. **234**).<sup>102</sup>

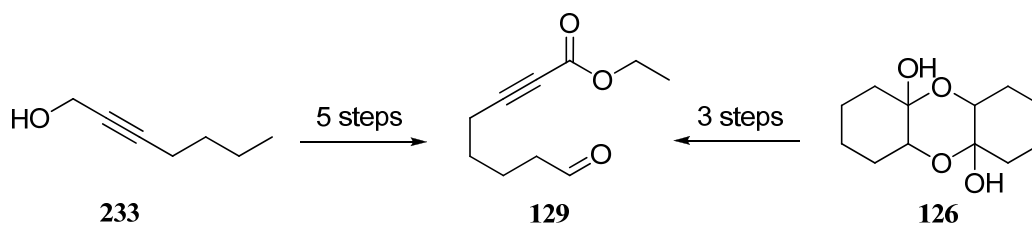


**Scheme 3.2.**



The preparation of ethyl 8-oxooct-2-ynoate (**129**) by the methods just described would require at least five synthetic steps. On the other hand, our fragmentation protocol efficiently provides the same product in only three steps (Scheme 3.3). Of greater concern however is the fact that while the route from propargylic alcohols works well for simple systems, it is not well suited to prepare functionalized aldehyde ynoates. To this respect our ring fragmentation reaction can be considered a much better option.

**Scheme 3.3.**

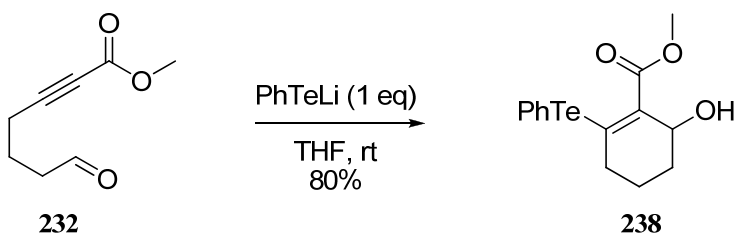
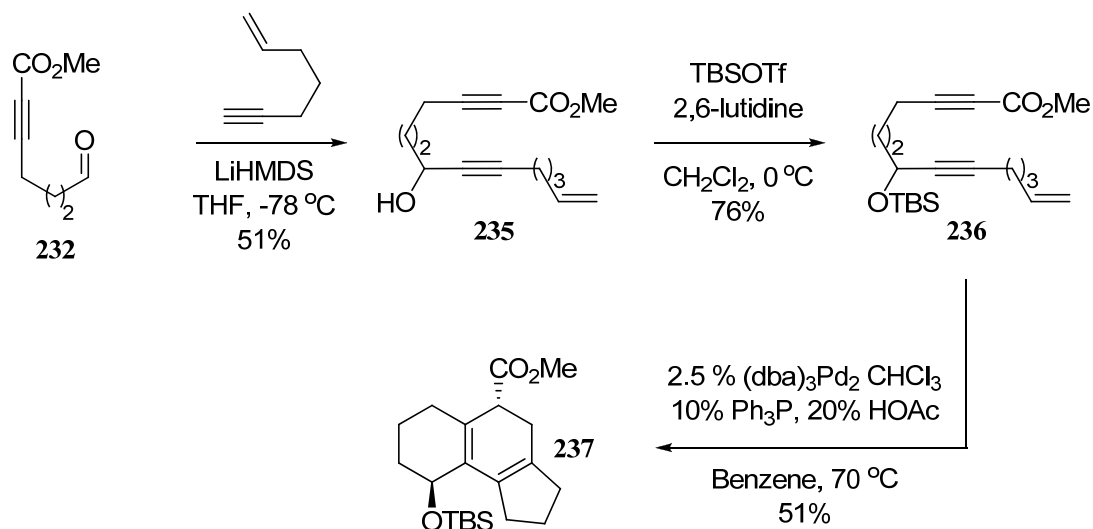


### 3.1.2. Recent applications of tethered aldehyde ynoates

Tethered aldehyde ynoates are useful synthetic intermediates that undergo various transformations based on the unique functional group arrangement that they possess. For example, Trost and co-workers<sup>95</sup> used ynoate **232** (Scheme 3.4) as a key intermediate in the synthesis of enediyne **235**, which in turn underwent a palladium

catalyzed diastereoselective cycloisomerization to provide tricyclic diene **237** in 51 % yield.

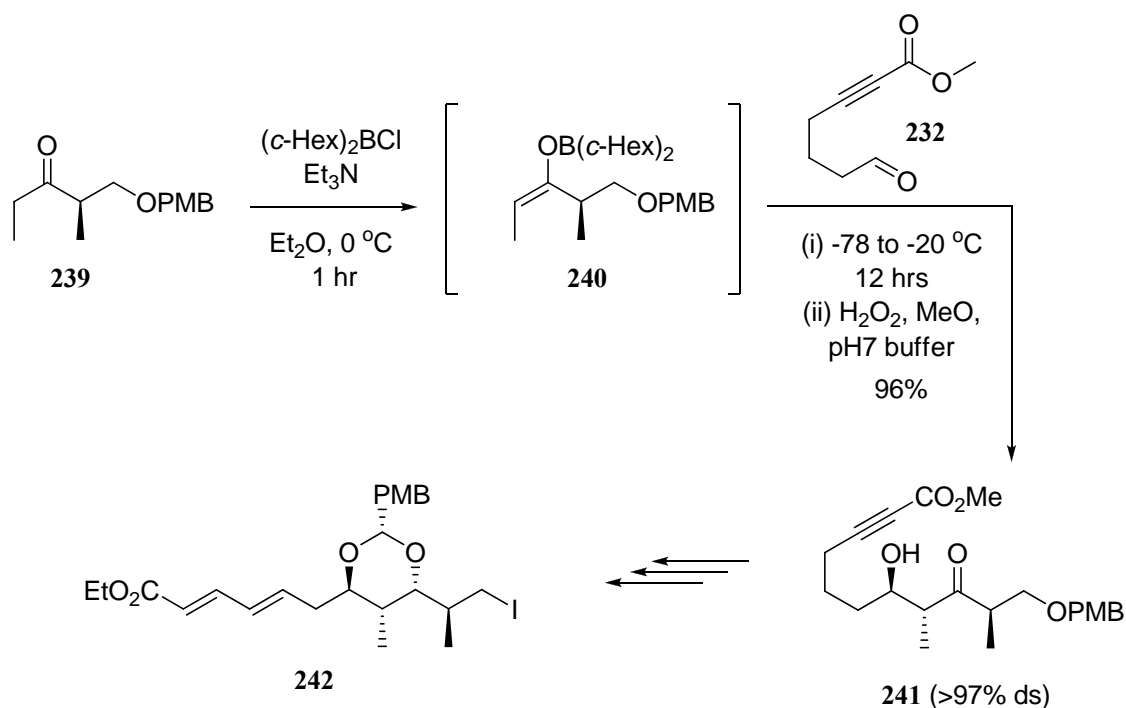
Scheme 3.4.



Additionally, Marino<sup>93</sup> and co-workers recently reported the intramolecular ‘electrotelluration’ of tethered alkynyl esters (e.g **232**, Scheme 3.4). For example, lithium phenyl tellurolate ( $\text{PhTeLi}$ ) added by Michael addition to **232** to provide a vinyl anion intermediate which was subsequently trapped intramolecularly by the internal aldehyde to provide vinylic telluride **238** in 80% yield. Vinylic tellurides can be further transmetalated to lithium,<sup>103</sup> copper,<sup>104</sup> or zinc<sup>105</sup> derivatives that can be employed in other C-C bond forming reactions.

Tethered aldehyde ynoates have also been used as functional intermediates in the synthesis of natural products. For example, Paterson<sup>99</sup> and co-workers used aldehyde **232** (Scheme 3.5) as a coupling partner in the aldol reaction with (*E*)-enol borinate **240** which gave the desired *anti-anti* aldol adduct **241** in 96% yield with greater than 97% diastereoselectivity. Notably, the acetylenic ester was carried through this reaction without difficulty, and ultimately provided access to (*E,E*)-diene ester moiety desired in the advanced synthetic intermediate **242**. Subunit **242** was subsequently utilized in the assembly of marine macrolide aplyronine A.<sup>106</sup>

Scheme 3.5.



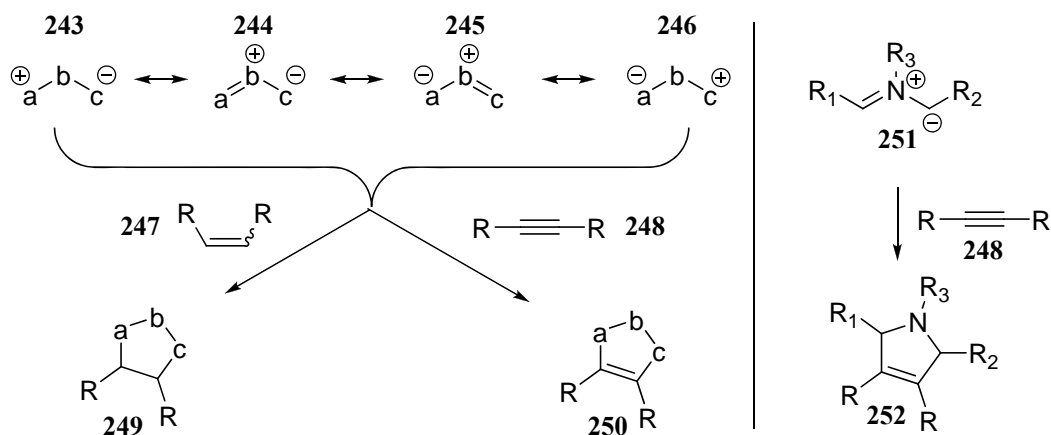
All reactions mentioned in this section attest to the synthetic value of tethered aldehyde ynoates. However, the true synthetic potential of these bi-functional

compounds has not yet been fully explored because of the unavailability of functionalized alkynyl esters.

### 3.1.3. Intramolecular [1,3]-dipolar cycloaddition reactions of tethered alkynyl aldehydes

Of particular importance to the work described in this chapter is the reactivity of [1,3]-dipoles with pendant alkynes because we consider tethered aldehyde ynoates as great candidates for intramolecular dipolarcycloadditions reactions that would allow for the efficient assembly of complex polycyclic heterocycles. The addition of [1,3]-dipoles (e.g. **243** and corresponding resonance structures, Scheme 3.6) to dipolarophiles (e.g. **247** or **248**) is a classic reaction in organic chemistry that has emerged as one of the most important methods for the preparation of five-member rings (e.g. **249** or **250**).

Scheme 3.6.



Changing the nature of the atoms (i.e. *a*, *b* and *c*) has led to the development of a wide variety of [1,3]-dipoles of which the most important are: nitrones, azomethine imines, azomethine ylides, carbonyl ylides, ozone, azides, nitrile ylides and diazo

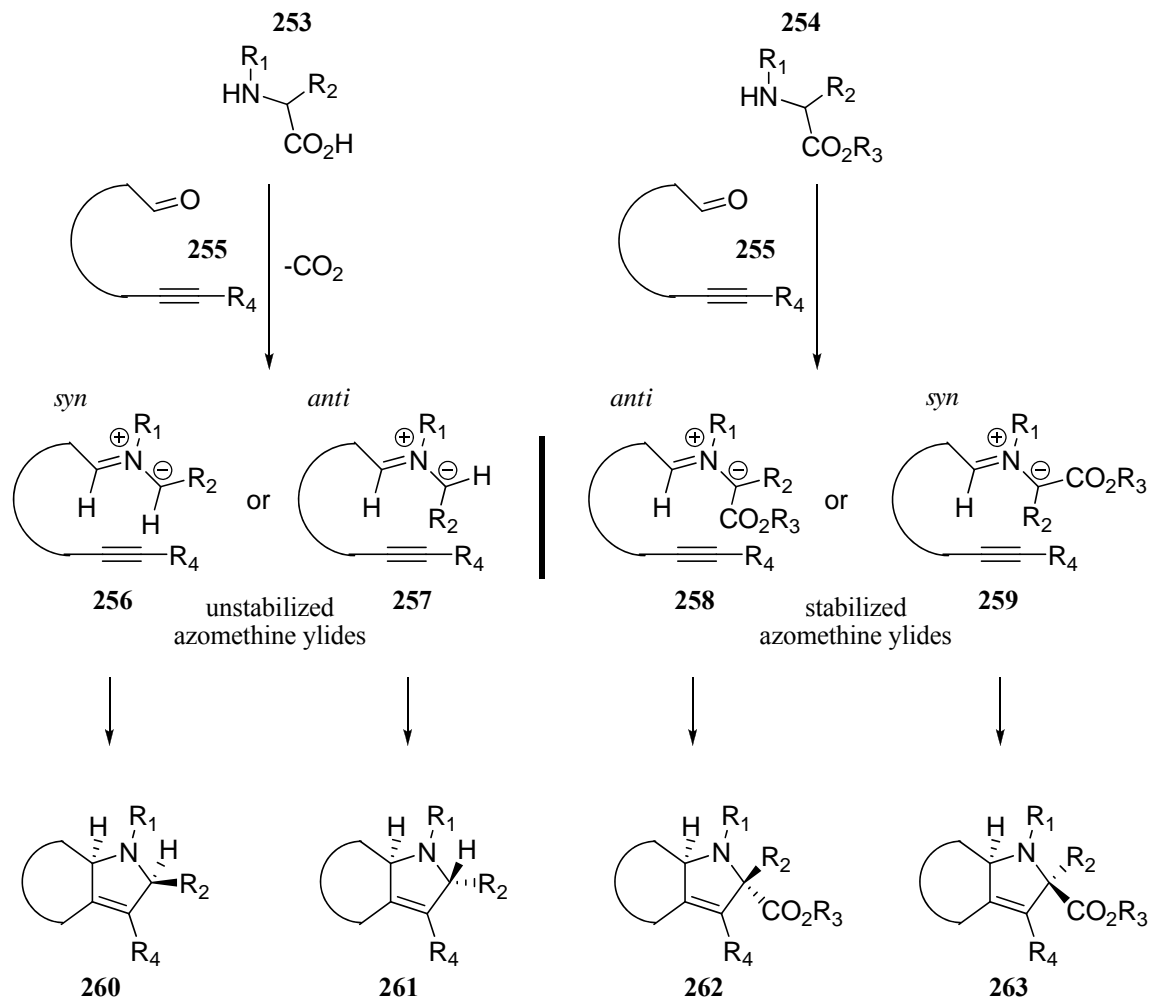
alkanes. The reactivity of all the species mentioned above has been extensively studied and thoroughly reviewed.<sup>107-112</sup>

Azomethine ylides (e.g. **251**, Scheme 3.6) are an especially important class of [1,3]-dipole that efficiently react with dipolarophiles (e.g. **248**) to provide N-containing heterocyclic cycloadducts, specifically pyrrolidines and 2,5-dihydropyrroles (e.g. **252**). A number of methods have been developed for the generation of azomethine ylides, including proton abstraction from imine derivatives of  $\alpha$ -amino acids, thermolysis or photolysis of aziridines and the thermal ring opening of 4-oxazolines.<sup>108,112</sup>

To understand the work presented in this dissertation, only pertinent aspects concerning the generation of unstabilized (e.g. **256**, Scheme 3.7) and stabilized (e.g. **258**) azomethine ylides by the condensation of aldehydes (e.g. **255**) with secondary  $\alpha$ -amino acids (e.g. **253**) and secondary  $\alpha$ -amino esters (e.g. **254**) and their subsequent participation in intramolecular [1,3]-dipolar cycloadditions with pendant alkynes to provide bicyclic (or polycyclic) N-containing heterocycles (e.g. **260**, **261**, **262** and **263**) need be considered.

Let us first consider the mechanism of a [1,3]-dipolar cycloaddition of an azomethine ylide with a  $\pi$ -system. This process involves a total of six  $\pi$  electrons [ $\pi 4_s + \pi 2_s$ ] and takes place by a thermally allowed suprafacial process in accord to the Woodward-Hoffmann rules.<sup>109,113,114</sup> For a suprafacial process, the two developing C-C bonds are formed to the same face of the azomethine ylide and to the same face of the dipolarophile. It is generally accepted that the cycloaddition is concerted with both C-C  $\sigma$ -bonds being formed at the same time.<sup>107</sup>

Scheme 3.7.



In the case of the addition of azomethine ylides to alkynes, evidence in favor of the concerted nature of the mechanism comes from the stereospecificity of the cycloaddition; the relative orientation of the substituents on the [1,3]-dipole correlates with the relative stereochemistry of these groups in the cycloadduct. Thus, *syn* dipoles (e.g. **256** or **259**, Scheme 3.7) lead to 3,4-*cis*-disubstituted 2,5-dihydropyrole products (e.g. **260** or **263**) and *anti* dipoles (e.g. **257** or **258**) lead to 3,4-*trans*-disubstituted 2,5-dihydropyrole products (e.g. **261** or **262**).

Steric and electronic effects also play an important role in [1,3]-dipolar cycloaddition reactions and may influence the regioselectivity. In intramolecular cycloaddition reactions conformational constraints normally dictate that only one regioisomer can be formed, and this is clearly beneficial in terms of enhancing the selectivity of the process (Figure 3.1).

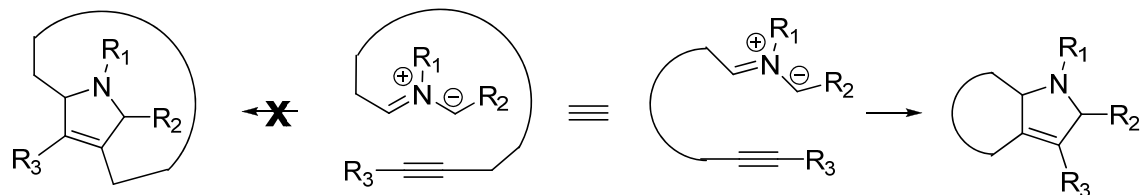
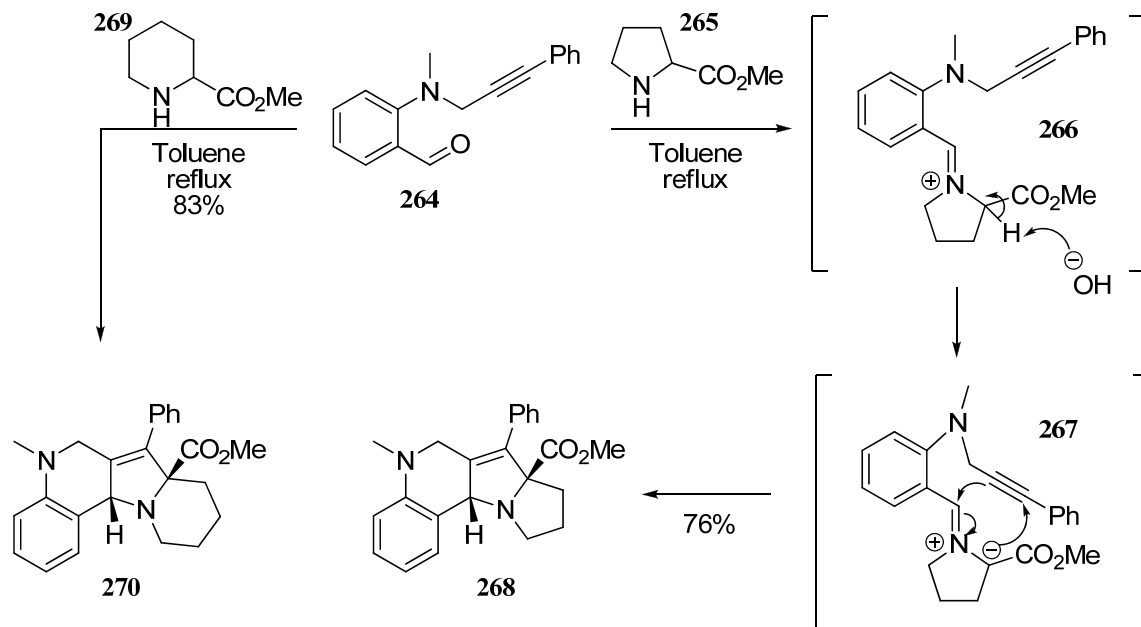


Figure 3.1. Conformational constraints in [1,3]-dipolar cycloaddition reactions.

Perhaps the most common method for the generation of stabilized azomethine ylides is the reaction of an aldehyde with a secondary amine bearing an electron-withdrawing group, such as a carboxylic ester, on the  $\alpha$ -carbon. For example, *N*-propargylic 2-aminobenzaldehyde **264** (Scheme 3.8) has been shown to condense with methyl prolinates (**265**) to form the iminium ion **266**, which readily undergoes deprotonation to the ylide **267**. Subsequent intramolecular cycloaddition of the ensuing [1,3]-dipole **267** affords the tetracyclic cycloadduct **268** in 76% yield. Note that a single stereoisomer, corresponding to the *cis* stereochemistry of the ring junction hydrogen atom and the methyl ester group is formed.<sup>115</sup> In similar fashion, the same *N*-tethered aldehyde **264** undergoes cycloaddition reaction in the presence of methyl pipecolate (**269**) to provide the corresponding polycyclic heterocycle **270** in 83% yield.

Scheme 3.8.

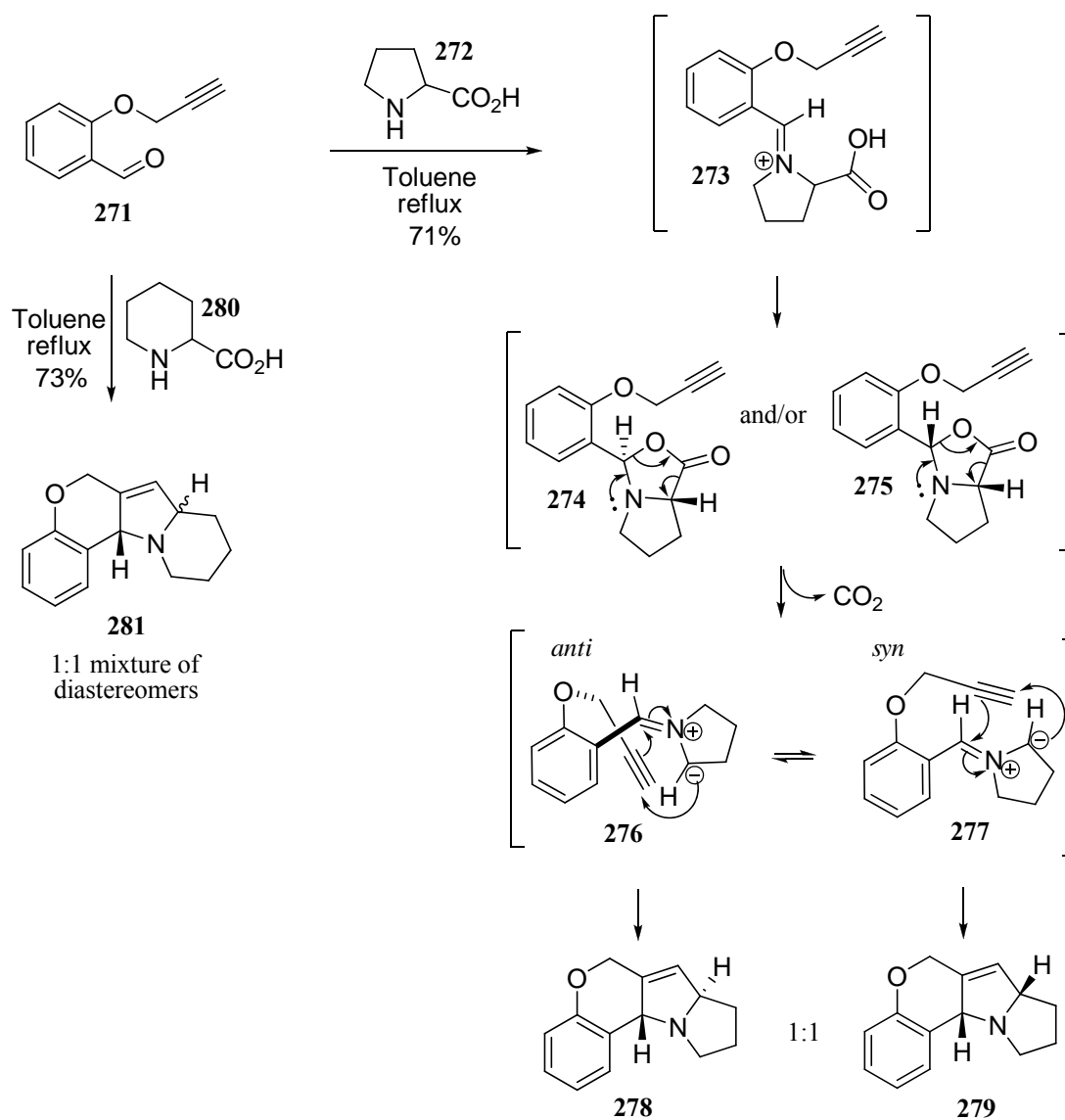


The condensation of aldehydes with secondary  $\alpha$ -amino acids affords the requisite unstabilized azomethine ylides after decarboxylation. For example, treating aldehyde **271** (Scheme 3.9) with proline provides oxazolidine-5-one **274** which loses carbon dioxide to yield the unstabilized azomethine ylide **276**. The pendant alkyne subsequently reacts with the [1,3]-dipole and affords the desired heterocyclic cycloadducts as a 1:1 mixture of diastereomers, arising from the *syn* and *anti* dipoles **276** and **277** respectively.<sup>115</sup> The stereochemical outcome of the reaction depends on the stereochemistry of the oxazolidine-5-one, which dictates the stereochemistry (*syn* or *anti*) of the newly formed azomethine ylide. Thus, oxazolidine-5-one **275** (Scheme 3.9) provides the corresponding *syn* dipole **277**, while oxazolidine-5-one **274** affords the *anti* dipole **276**. These azomethine ylides however, may undergo stereomutation if both: (i)



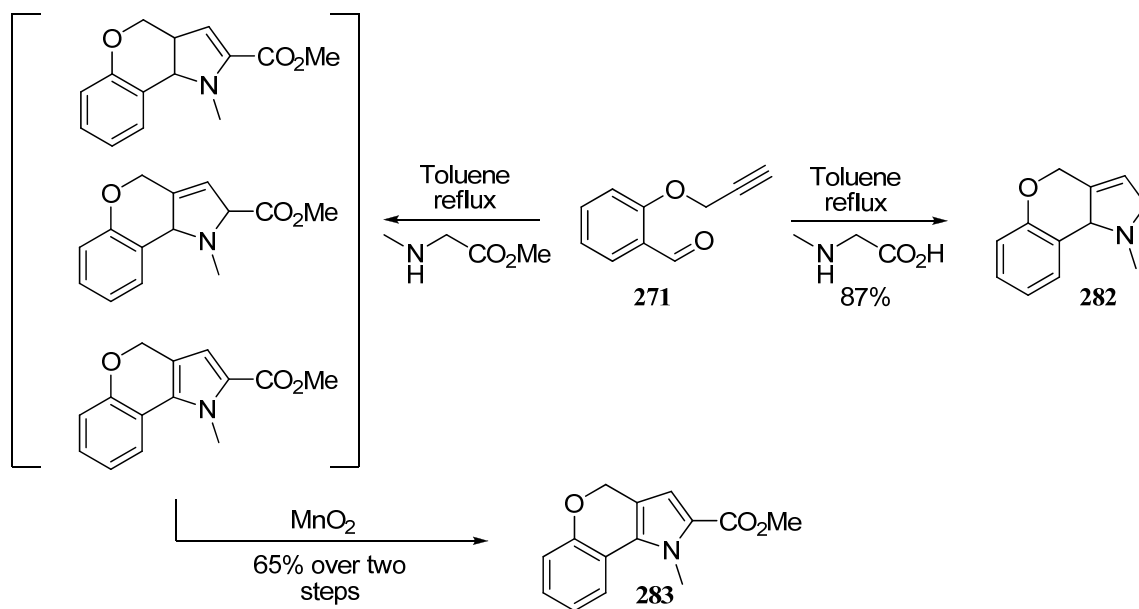
less reactive dipolarophiles are used as trapping agents and (ii) sufficient conjugating substituents are present on the azomethine ylide to lower the bond order in the central C-N-C moiety.<sup>116,117</sup>

Scheme 3.9.



Acyclic  $\alpha$ -amino acids and  $\alpha$ -amino esters have also been observed to provide azomethine ylides in the presence of aldehydes. For example, the reaction of *O*-propargylic salisaldehyde **271** (Scheme 3.10) with sarcosine provided dihydropyrrole **282** in 87% yield.

Scheme 3.10.

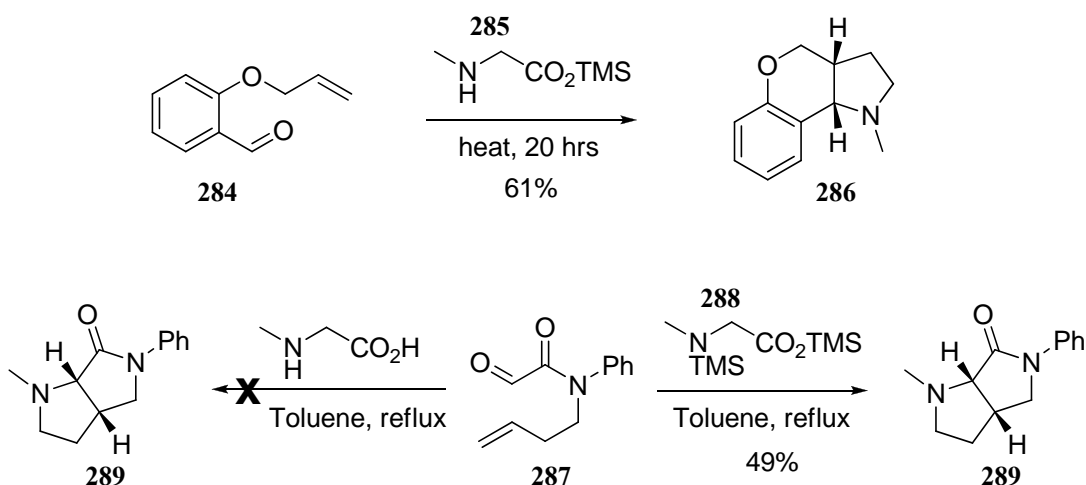


Furthermore, when the same tethered alkynyl aldehyde **271** (Scheme 3.10) is treated with sarcosine methyl ester, the reaction provides a mixture of cycloadducts, which were further oxidized in the presence of manganese dioxide to afford tricyclic pyrrole **283** in 65% yield.<sup>118</sup>

The intramolecular dipolar cycloaddition reaction to give a pyrrolidine product from an  $\alpha$ -amino acid was also reported by Confalone and Huie.<sup>119</sup> Treating aldehyde **284** (Scheme 3.11) with the trimethylsilyl ester of N-methyl-glycine (**285**) gave the

desired product **286** in 61% yield. Although this reaction involves the addition of an azomethine ylide to an alkene dipolarophile, it is important to note because it highlights the use of silylated  $\alpha$ -amino acid derivatives in dipolar cycloadditions.

Scheme 3.11.

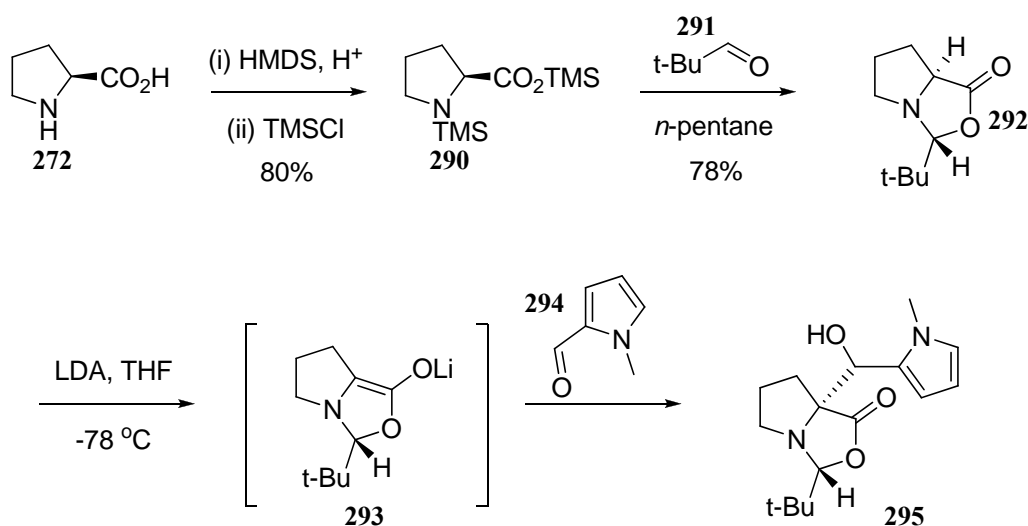


Furthermore, bis-trimethylsilyl sarcosine **288** (Scheme 3.11) was also reported to participate in reactions with aldehydes to provide pyrrolidine lactams (e.g. **289**) via dipolar cycloaddition reaction of azomethine ylides generated by decarboxylation. The silyl derivative **288** was employed in this reaction because the free amino acid's low solubility in the reaction solvent prevented formation of pyrrolidine **289**.<sup>120</sup>

Unrelated to dipolar cycloadditions, but relevant to the reactivity of bis-silyl amino acids with aldehydes to form oxazolidine-5-ones, is the reaction reported by Sisti<sup>121</sup> and co-workers (Scheme 3.12). On addition of pivalaldehyde (**291**) to a *n*-pentane solution of trimethylsilyl ester of N-trimethylsilyl proline **290**, an exothermic reaction took place and oxazolidine-5-one **292** was obtained in 78% yield after vacuum distillation. This species was also shown to react further in the presence of lithium

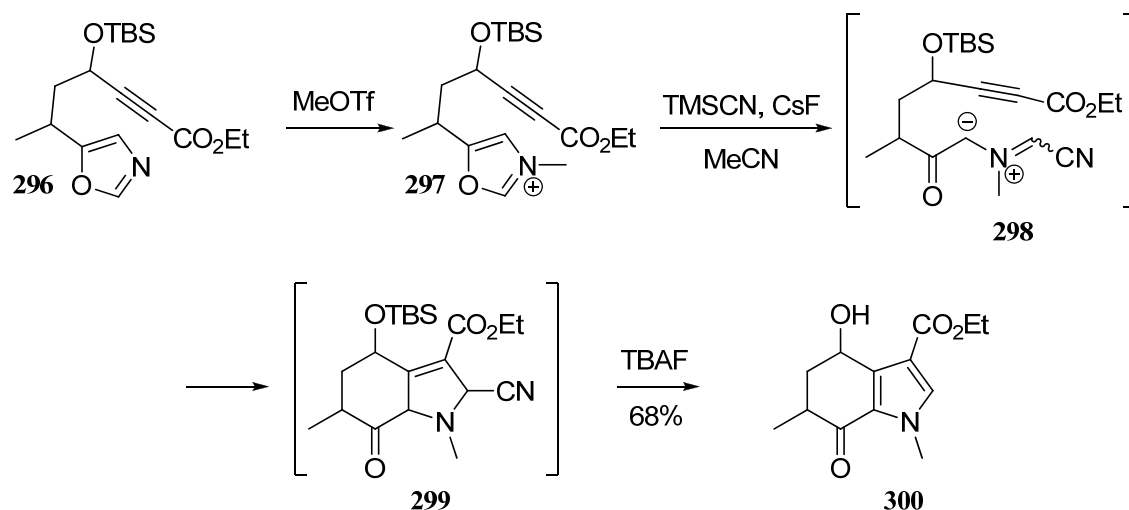
diisopropyl amide (LDA) to provide the corresponding chiral enolate **293**, which in turn traps the aldehyde **294** and yields the desired condensation product **295** as a single diastereomer.<sup>122</sup> This particular example highlights one of the few available methods for the efficient synthesis and isolation of **290** from L-proline (**272**).

Scheme 3.12.



Of particular significance to my work, ynoates have been shown to be competent dipolarophiles and react intramolecularly with azomethine ylides to afford various cycloadducts. For example, Vedejs<sup>123</sup> and co-workers reported the preparation of bicyclic pyrrole **300** (Scheme 3.13) by first treating oxazole **296** with methyl triflate (MeOTf) to provide oxazolinium intermediate **297** which further reacts with an excess of trimethylsilyl cyanide to afford the desired ylide **298**. Subsequent intramolecular cycloaddition with the pendant ynoate gives dihydropyrrole **299** which upon aromatization through expulsion of hydrogen cyanide, followed by silyl ether cleavage results in the formation of the tetrahydroindolone **300** in 68% overall yield.

Scheme 3.13.



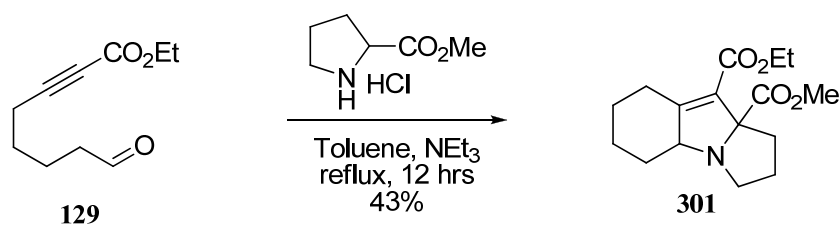
The reaction highlighted in Scheme 3.13 is one of the few examples in which the ynoate functional group has been shown to participate in intramolecular dipolar cycloadditions. It is also important to note that in this case the reactive azomethine ylide originates from the oxazole moiety via a different mechanism than that encountered with  $\alpha$ -amino esters and  $\alpha$ -amino acids. To the best of our knowledge, there are no reported instances of intramolecular [1,3]-dipolar cycloadditions of azomethine ylides generated from  $\alpha$ -amino acids and  $\alpha$ -amino esters which involve tethered aldehyde ynoates. We believe that the development of such reactions would be a significant advancement as it would allow for efficient assembly of complex polycyclic heterocycles from readily available starting materials using very few synthetic manipulations.

## 3.2. Intramolecular [1,3]-dipolarcycloadditions of tethered aldehyde ynoates with stabilized and unstabilized azomethine ylides

### 3.2.1. Intramolecular reactions with stabilized azomethine ylides

Our focus was initially directed towards exploring the reactivity of ethyl 8-oxooct-2-ynoate (**129**, Scheme 3.14) with secondary  $\alpha$ -amino esters which we expected to provide tricyclic diester **301**. As anticipated, preliminary studies showed that reacting aldehyde ynoate **129** with readily available methyl proline hydrochloride in refluxing toluene in the presence of triethyl amine provided the desired cycloadduct **301** in 43% yield.

Scheme 3.14.

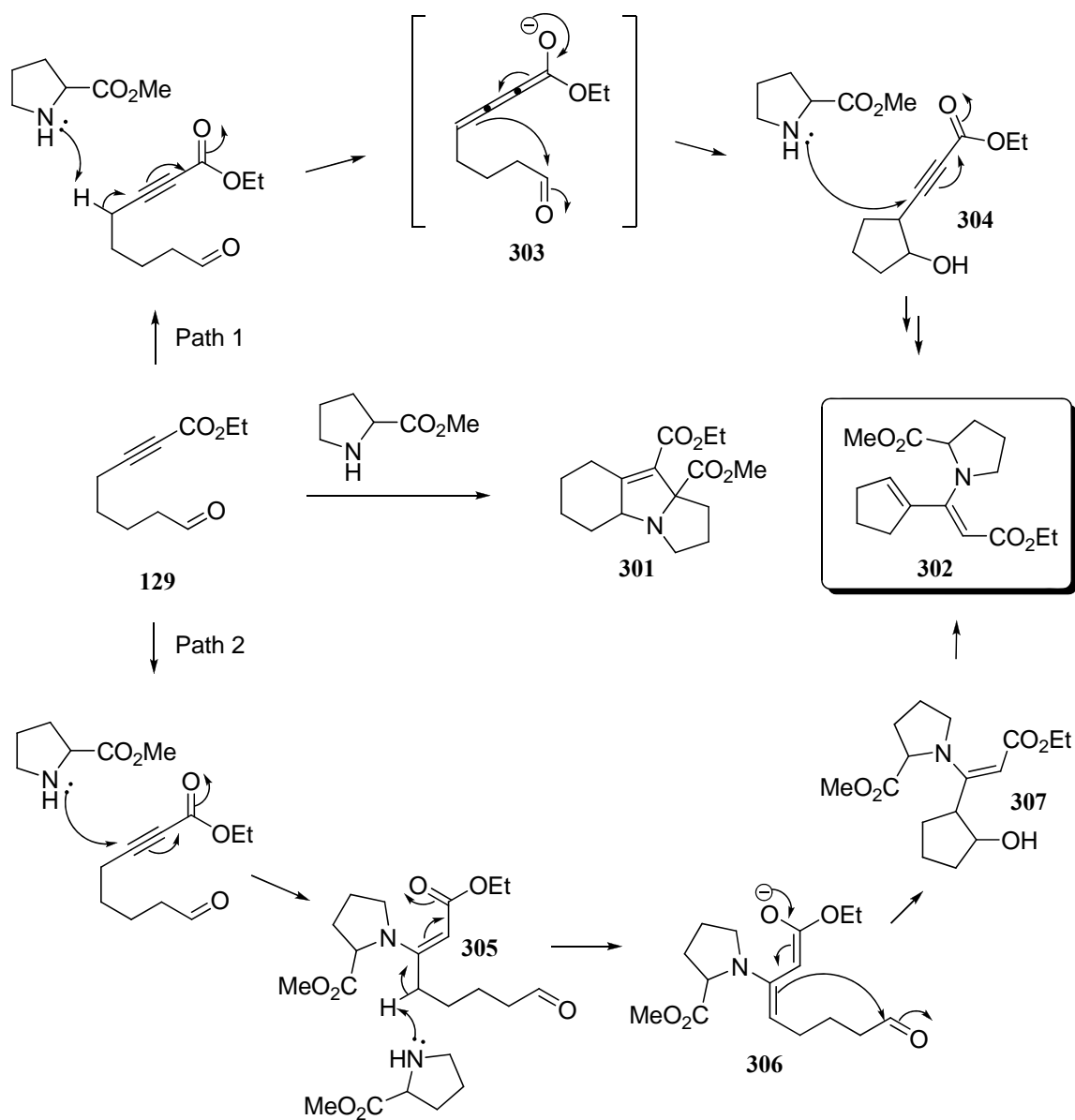


This result pleased us because it clearly demonstrated the ability of tethered aldehyde ynoate **129** to participate in azomethine ylide formation and a subsequent intramolecular dipolarcycloaddition reaction. The low yield, however, prompted us to conduct a screen of the reaction conditions. While conducting these studies, I observed that the reaction consistently provided a side product that was eventually identified through 2D NMR as the enamine ester **302** (Scheme 3.15).

The formation of **302** can be envisioned to occur via two mechanistically different pathways (Scheme 3.15). The first path assumes the deprotonation of ynoate

**129** to provide enolate **303**, which can undergo a 5-*exo*-trig cyclization to provide ynoate **304**. Subsequent 1,4-addition of methyl proline to the ynoate functional group and tautomerization of the ensuing enolate affords the observed enamine **302**.

**Scheme 3.15.**



Alternatively, ynoate **129** could act as a Michael acceptor to provide enamine **305**, which upon deprotonation yields reactive enamine enolate **306**. Intramolecular trapping of the aldehyde moiety by the enamine would then provide cyclic alcohol **307** which is a dehydration step away from enamine ester **302**. At this point it is unclear which, if either, of these paths is operative.

The results of my studies which aimed to optimize the reaction conditions in favor of tricycle **301** are shown in Table 3.1. In the end, I discovered that the best results were obtained when a mixture of methyl proline (308) and ynoate **129** were initially stirred for 30 minutes in toluene at 0 °C in the presence of 4 Å molecular sieves and then heated at reflux for one hour. This protocol provided the desired cycloadduct **301** in 65% yield along with undesired enamine ester **302** which was isolated in only 15 % yield (Entry 2). When the reaction was performed in the absence of molecular sieves the products were isolated in lower yields (Entry 1) and the addition of methyl proline (308) to the reaction mixture at room temperature, followed by immediate heating to reflux was accompanied by a small decrease in yields (Entry 3). Attempting to buffer the reaction in the presence of potassium carbonate resulted in even further decrease in yield (Entry 4). Furthermore, when the temperature of the reaction was slowly increased starting from room temperature and reaching reflux, enamine ester **302** was isolated exclusively in 38% yield (Entry 5), while introducing the methyl proline (308) at reflux temperature provided a mixture of **301** and **302** which were isolated in 51% and 17% yield respectively.



In summary, we believe that premixing the aldehyde ynoate **129** with methyl proline (308) at 0 °C is important for improved yields of tricycle **301** because it allows for a more efficient condensation to take place between the aldehyde moiety and the amino ester which is critical for the formation of stabilized azomethine ylides (see Scheme 3.8). Concomitantly, the premixing period at low temperature is also presumed to minimize the occurrence of the side reactions which lead to the formation of undesired enamine ester **302** (Scheme 3.15). Slowly raising the temperature of the premixing period improves efficiency of the side reactions which preclude azomethine ylide formation and ultimately leads to exclusive isolation of enamine ester **302**.

**Table 3.1. Optimization of reaction conditions**

<p>Reaction scheme: Aldehyde ynoate <b>129</b> (a 6-carbon chain with an aldehyde at one end and an ethyl ester at the other, with a triple bond at the 4-position) reacts with methyl proline <b>308</b> (a five-membered ring with an NH group and a methyl ester group) in Toluene Conditions to produce tricycle <b>301</b> (a complex polycyclic structure with two ester groups) and enamine ester <b>302</b> (a structure with a cyclopentene ring, an enamine group, and two ester groups).</p>					
Entry	$\alpha$ -Amino ester <sup>a</sup> / (eq)	Temp. (°C) / Time (hrs)	Additional conditions	<b>301</b> (% yield) <sup>b</sup>	<b>302</b> (% yield) <sup>b</sup>
1	<b>308</b> (1.1)	0 / .5 to 120 / 1	—	57	13
2	<b>308</b> (1.1)	0 / .5 to 120 / 1	4 Å MS <sup>c</sup>	65	15
3	<b>308</b> (1.1)	rt / 0 to 120 / 1	4 Å MS <sup>c</sup>	62	21
4	<b>308</b> (1.1)	rt / 0 to 120 / 1	4 Å MS <sup>c</sup> / K <sub>2</sub> CO <sub>3</sub>	48	26
5	<b>308</b> (1.1)	rt / .2 to 60 / 1 to 80 / 1.5 to 110 / 1	4 Å MS <sup>c</sup>	0	38
6	<b>308</b> (1.1)	120 / 1	4 Å MS <sup>c</sup> / <b>308</b> added @ reflux	51	17

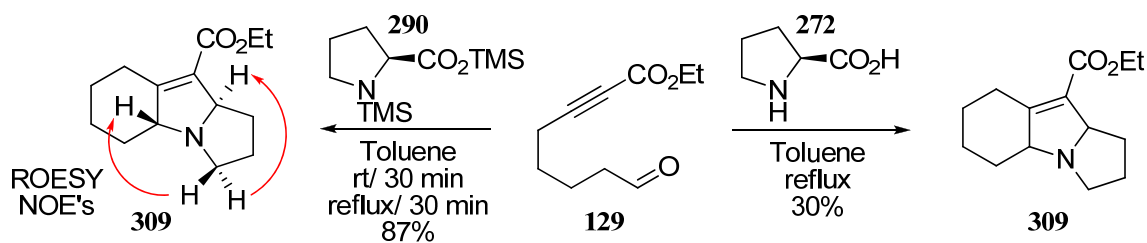
Note: <sup>a</sup>  $\alpha$ -amino ester was freebased prior to use. <sup>b</sup> yields reported after chromatography.

<sup>c</sup> molecular sieves were preactivated by heating under high vacuum.

### 3.2.2. Intramolecular reactions with unstabilized azomethine ylides

In order to test the ability of tethered aldehyde ynoates to undergo intramolecular [1,3]-dipolarcycloadditions with unstabilized azomethine ylides we decided to first employ readily available (L)-proline (**272**, Scheme 3.16) and our initial studies showed that refluxing a mixture of aldehyde ynoate **129** and (L)-proline (**272**) in toluene provided the desired dihydropyrrole **309** in 30% yield. We believed that the low solubility of (L)-proline (**272**) in organic solvents such as toluene was the main reason why the reaction occurred in low yield. However, changing solvent systems from toluene to dimethylformamide (DMF) did not have a positive impact on the outcome of the reaction.

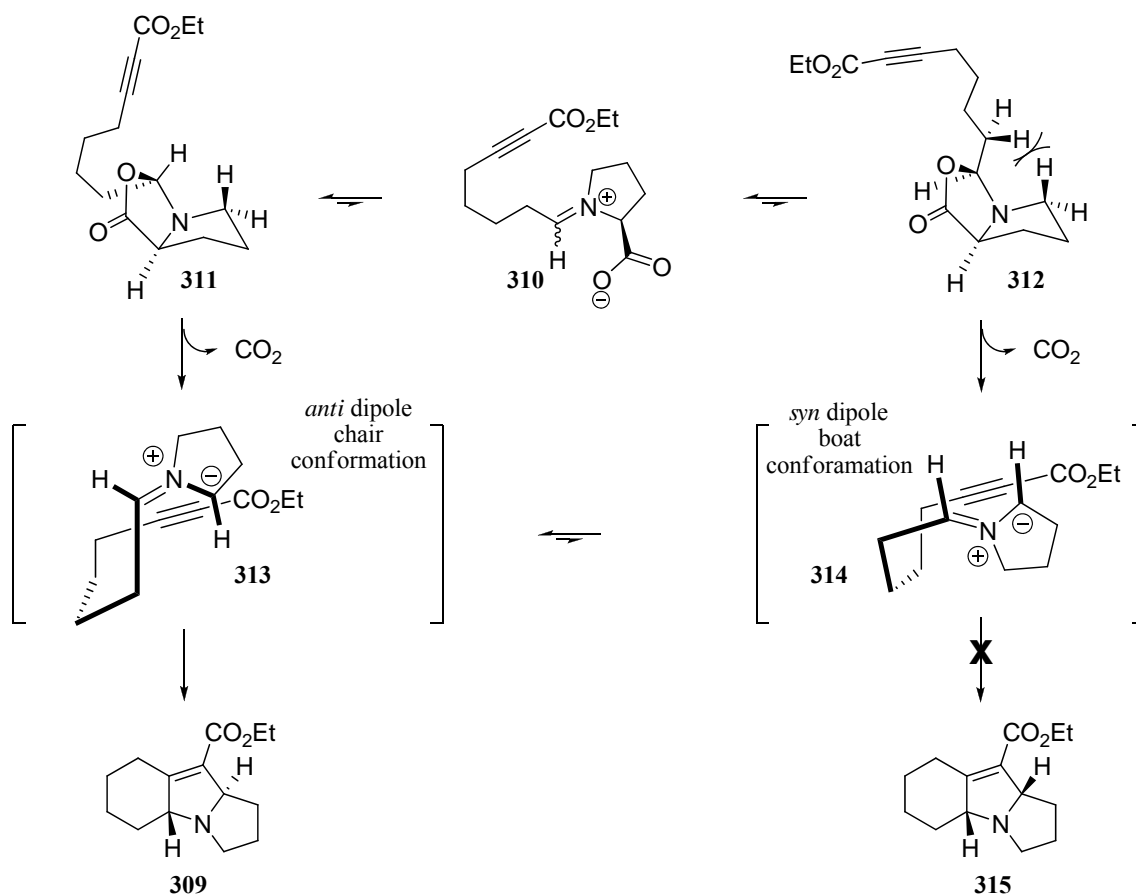
Scheme 3.16.



We turned our attention towards the use of bissilyl amino acid derivatives (e.g. **290**, Scheme 3.16) which are highly soluble in organic solvents. As trimethylsilyl 1-(trimethylsilyl)-pyrrolidine-2-carboxylate (**290**) had already been prepared and shown to efficiently react with aldehydes to form the oxazolidine-5-ones (see Section 3.1.3), we decided to begin by studying the reaction of aldehyde ynoate **129** with this reagent. Gratifyingly, the reaction provided the desired dihydropyrrole **309** as a single diastereomer in 87% isolated yield. The relative stereochemistry of **309** was determined

through 2D NMR experiments and the relevant ROESY NOE's are shown in Scheme 3.16.

Scheme 3.17.



The stereochemical outcome of the dipolar cycloaddition reaction highlighted in Scheme 3.16 can be explained by the following rationale. Formation of isomeric oxazolidine-5-ones **311** and **312** (known intermediates in this transformation, Scheme 3.17) from imminium ion **310** is a thermodynamically controlled process and therefore is expected to provide diastereomer **311** as the predominant species due to the unfavorable steric interactions encountered in diastereomer **312**. Provided that [1,3]-

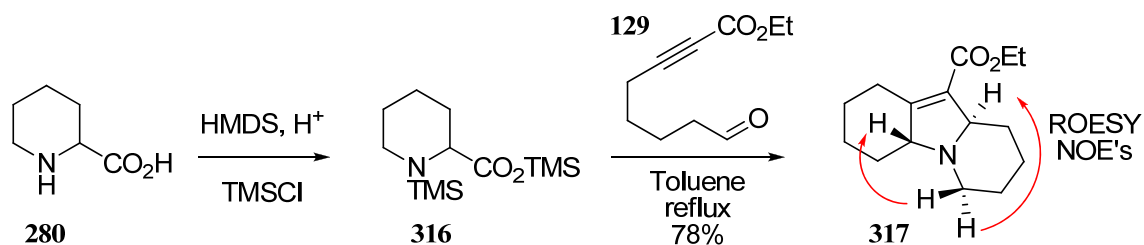
dipolar cycloreversions occur stereospecifically,<sup>110</sup> then the stereochemistry of the oxazolidine-5-ones is the only factor which determines the stereochemistry of the kinetically formed azomethine ylides. Thus, **311** would exclusively form the *anti* dipole **313**, while **312** would lead solely to the formation of *syn* dipole **314**.

The fact that none of the *syn* cycloadduct **315** (Scheme 3.17) was detected in the reaction mixtures suggests that the cycloaddition occurs exclusively via the *anti* azomethine ylide **313**. We believe that this is due to the proper orbital overlap that the *anti* dipole **313** achieves with the alkyne dipolarophile via a lower energy chair like conformation (e.g. **313**), while only a higher energy boat like conformation (e.g. **314**) would allow for favorable orbital overlap in the case of the *syn* azomethine ylide **314**. If indeed both azomethine ylides **313** and **314** are formed during the reaction then it is possible that stereomutation of the *syn* dipole to the *anti* dipole precedes cycloaddition via the high energy boat like conformation, thus leading to exclusive formation of dihydropyrrole **309**.

Pleased with the outcome of the reaction of tethered aldehyde ynoate **129** with bissilyl proline **290** which yielded cycloadduct **309** in high yield as a single diastereomer, we decided to further investigate this reactivity and determine whether similar results could be obtained if other bissilylated  $\alpha$ -amino acids were employed. Trimethylsilyl 1-(trimethylsilyl)piperidine-2-carboxylate (**316**, Scheme 3.18) emerged as our first choice for a test substrate and was prepared from readily available (D,L)-pipecolinic acid (**280**) using the same protocol as the one previously developed for the synthesis of bissilyl proline derivative **290**<sup>121</sup> (see Scheme 3.16). To our satisfaction,

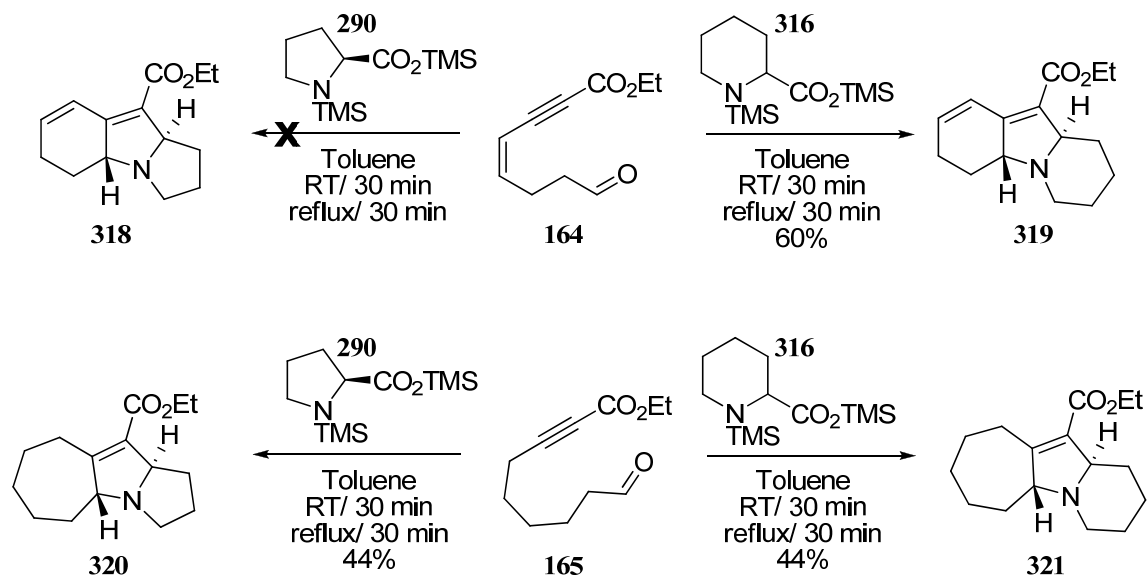
the reaction of aldehyde ynoate **129** with piperidine **316** provided the desired dihydropyrrole **317** in 78% isolated yield as a single diastereomer. The relative stereochemistry of **317** was determined through 2D NMR experiments and the relevant ROESY NOE's are shown in Scheme 3.18.

Scheme 3.18.



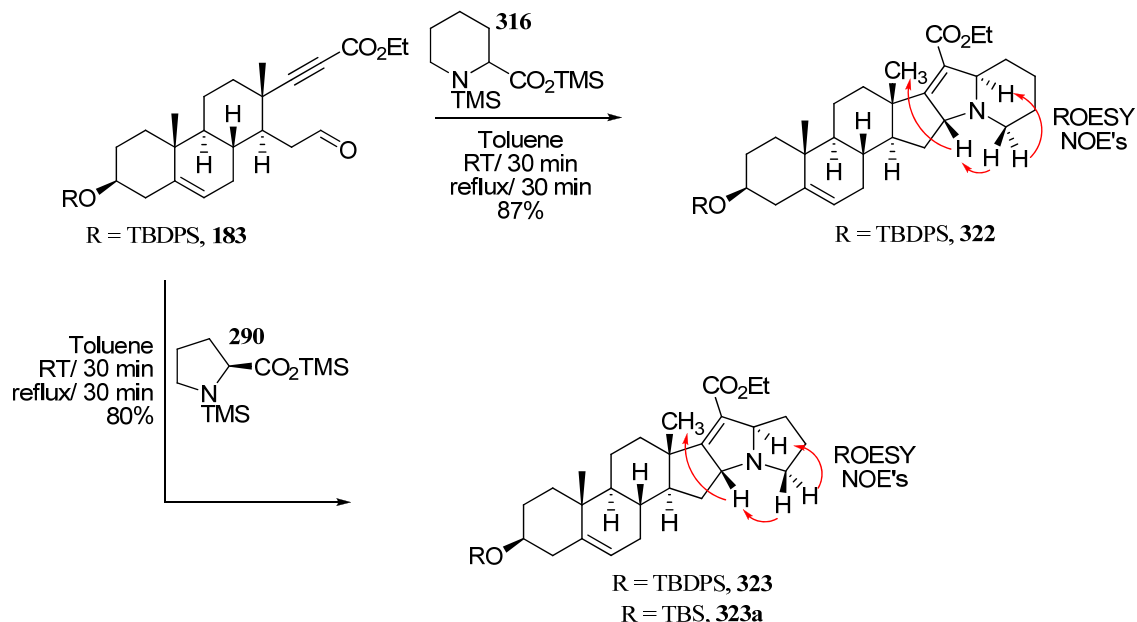
At this point I focused my efforts on assessing the general scope of the reaction with respect to whether other tethered aldehyde ynoates could undergo similar intramolecular dipolar cycloaddition reactions. In the end, I found that highly conjugated (Z)-ethyl 8-oxooct-4-en-2-ynoate (**164**, Scheme 3.19) provided the desired cycloadduct **319** in 60% isolated yield when treated with bisilylated pipercolinc acid **316**. Surprisingly, none of the desired dihydropyrrole **318** was isolated when bisilyl proline derivative **290** was employed. At this time we have no plausible explanation for this unexpected result. Furthermore, when ethyl 9-oxonon-2-ynoate (**165**, Scheme 3.19) was treated with either **290** or **316** the desired dihydropyrroles **320** and **321** respectively, were isolated in identical 44% yields. These results are notable as they highlight the ability of the intramolecular dipolar cycloaddition reaction to assemble frameworks which contain seven member rings, a task which has often proven to be synthetically challenging.

Scheme 3.19.



Structurally complex steroid derived tethered aldehyde ynoate **183** (Scheme 3.20) was also found to undergo efficient intramolecular cycloaddition in the presence of either **316** or **290** and the expected cycloadducts **322** and **323** were isolated from the reaction mixtures in excellent yields as a single diastereomer (relevant ROESY NOE's are shown in Scheme 3.20). Formation of cycloadduct **322** was a particularly gratifying result because it serves as a key step in our model studies towards the synthesis of steroidal alkaloid solanidine (a detailed account of this work is presented in Section 3.3).

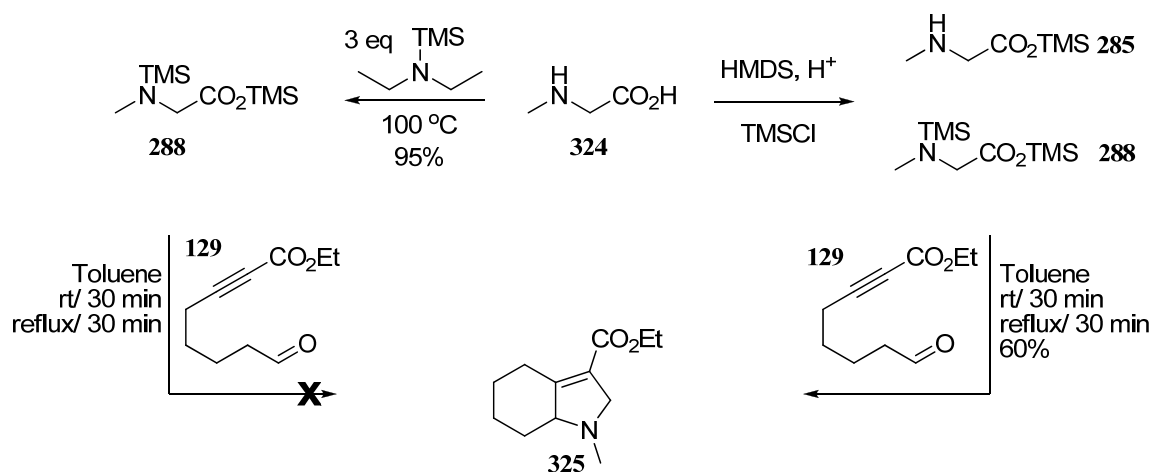
Scheme 3.20.



Pleased with the results obtained with the cyclic bissilated  $\alpha$ -amino acids, we decided to expand the applicable scope of this methodology to the use of acyclic secondary  $\alpha$ -amino acid derivatives. Readily available sarcosine (**324**, Scheme 3.21) was chosen as the requisite precursor to our first test substrate (e.g. **288**) and was submitted to bissilylation using the same protocol as previously employed. This reaction, however, provided a mixture of mono- and bissilyl sarcosine derivatives **285** and **288** after high vacuum distillation. Nonetheless, treatment of aldehyde ynoate **129** with the mixture of mono and bissilylated  $\alpha$ -amino acids afforded the desired bicyclic dihydropyrrole **325** in 60% isolated yield. We believed that the outcome of the intramolecular dipolar cycloaddition reaction would be greatly improved if clean bissilyl sarcosine derivative **288** were to be employed. Thus, pure **288** was prepared

using a variation of the protocol developed by Smith and Shewbart,<sup>124</sup> and subsequently isolated via high vacuum distillation (to maintain the integrity of the product it was important to use silanized glassware during the preparation and distillation sequence). Surprisingly, when aldehyde ynoate **129** was allowed to react with freshly prepared **288** absolutely none of the desired cycloadduct was detected.

Scheme 3.21.



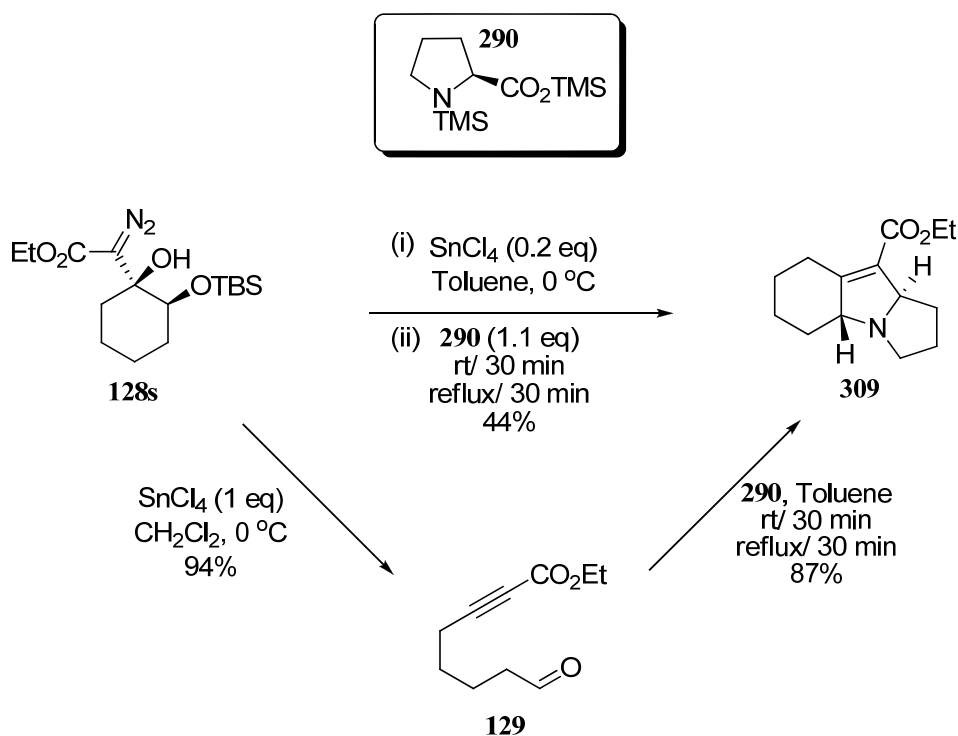
This conflicting result raises the question of whether the mono- or bis-silyl  $\alpha$ -amino acids are the reactive species in this transformation. Future studies should include the preparation of pure monosilylated sarcosine derivative **285** and the subsequent testing of its ability to promote intramolecular dipolar cycloaddition. If the monosilylated species is shown to undergo efficient cycloaddition, then additional studies should be aimed towards elucidating whether the same behavior is exhibited by the cyclic systems derived from (L)-proline and (D,L)-pipecolic acid.



### 3.2.3. Development of a one pot ring fragmentation / [1,3]-dipolar cycloaddition reaction protocol

The efficiency with which the newly developed ring fragmentation reaction (**128s** → **129**, Scheme 3.22) provides tethered aldehyde ynoates (e.g. **129**), and the ability of these fragmentation products to undergo facile intramolecular dipolar cycloadditions (**129** → **309**) with bisilylated (or perhaps monosilylated)  $\alpha$ -amino acids (e.g. **290**) to quickly assemble polycyclic *N*-containing cycloadducts (e.g. **309**), encouraged us to begin exploring the possibility of developing a one pot protocol that would allow for direct access to dihydropyrrole **309** from diazo ester **128s**.

Scheme 3.22.



In my initial studies, I attempted to induce formation of dihydropyrrole **309** from  $\gamma$ -silyloxy- $\beta$ -hydroxy- $\alpha$ -diazoester **128s** by using an equivalent amount of tin tetrachloride to promote the fragmentation. Unfortunately, this approach failed as none of the desired cycloadduct was ever detected. Better results were obtained when the Lewis acid was used in substoichiometric quantity. Thus, initial treatment of diazo ester **128s** with 20 mol% of tin tetrachloride at 0 °C, followed by the addition of bisilyl proline derivative **290** to the resulting reaction mixture and subsequent heating at reflux temperature provided dihydropyrrole **309** in 44% isolated yield.

We believe that the challenge in optimizing the yield of the one pot protocol is finding the appropriate conditions under which the Lewis acidity of tin tetrachloride is quenched post fragmentation but the [1,3]-dipolar cycloaddition can still efficiently occur. Unfortunately, this is not a straight forward endeavor and all attempts to optimize the reaction conditions such as: (i) employing the use of excess bisilylated  $\alpha$ -amino acid, (ii) adding tin chelating agents or (iii) switching reaction solvents have thus far failed.

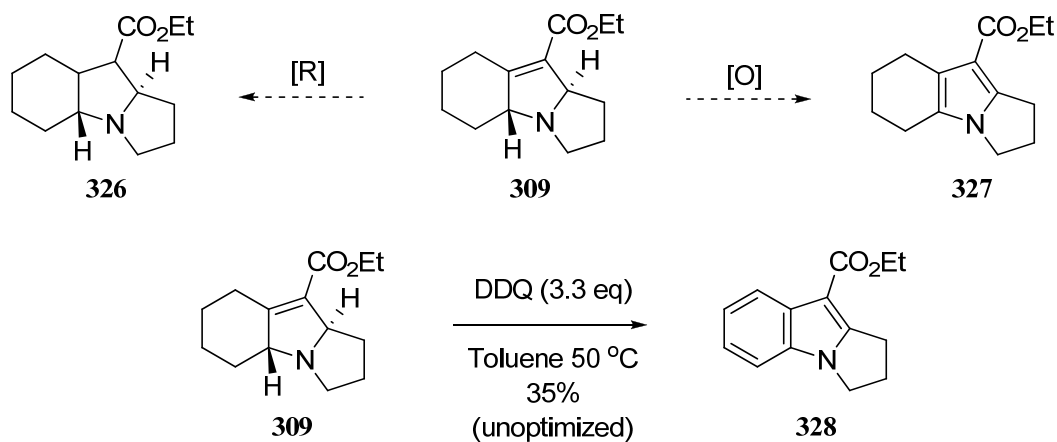
### 3.2.4. Conclusions and future perspective

My work has shown that tethered aldehyde ynoates are excellent substrates for intramolecular [1,3]-dipolar cycloaddition reactions with azomethine ylides generated from  $\alpha$ -amino acids and  $\alpha$ -amino esters, and can provide access to a variety of N-containing heterocyclic scaffolds as single diastereomers.

The dihydropyrroles (e.g. **309**, Scheme 3.23) formed through the intramolecular dipolar cycloaddition reaction are synthetically useful because they lay at an

intermediary oxidation state. That is, they can either be reduced to provide pyrrolidines (e.g. **326**, Scheme 3.23) or oxidized to afford pyrroles (e.g. **327**).

Scheme 3.23.



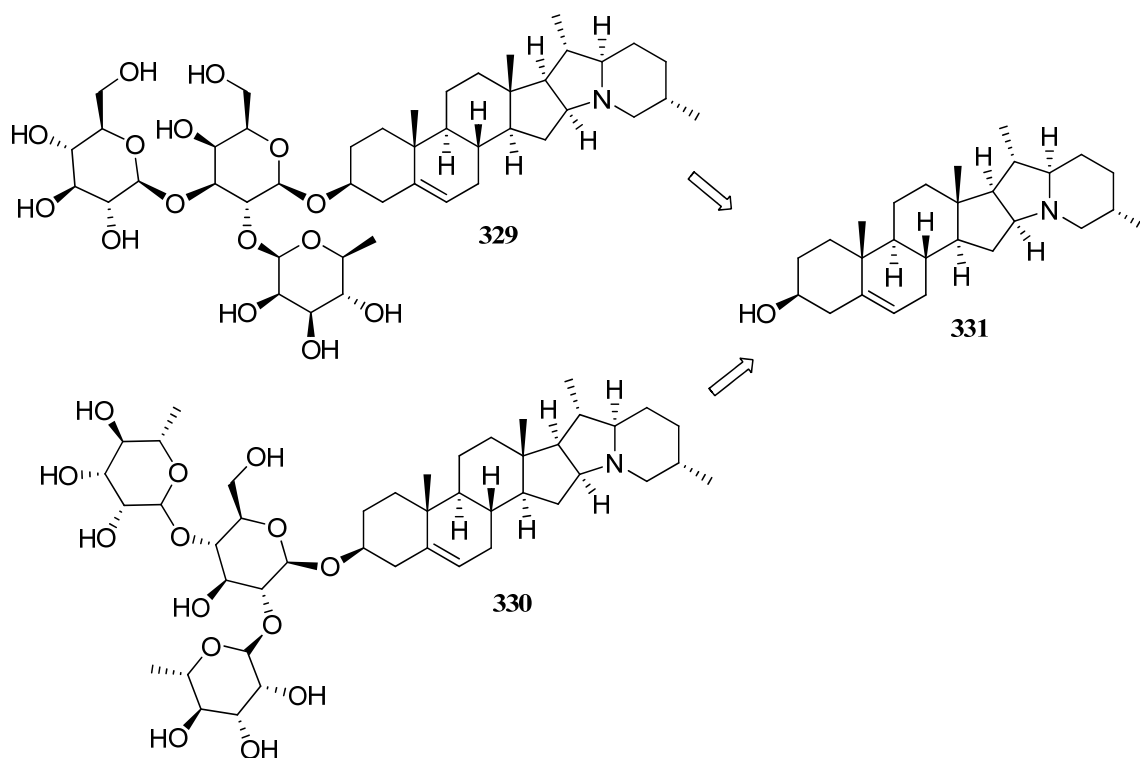
Furthermore, I have generated preliminary results which show that dihydropyrrole **309** is oxidized to indole **328** when treated with 2,3-dichloro-5,6-dicyanobenzoquinone (DDQ). This unoptimized result is highly gratifying because indoles are commonly found in biologically active natural products and synthetic drugs, and while there are a variety of methods which allow for functionalization at the  $\text{C}_2$  and  $\text{C}_3$  positions, introducing functional groups at the  $\text{C}_4$ ,  $\text{C}_5$ ,  $\text{C}_6$  and  $\text{C}_7$  positions it is not straight forward. Future studies should be aimed towards the development of appropriate conditions which would allow for the synthesis of functionalized indoles otherwise difficult to prepare by traditional methods.

### 3.3. Applications towards the synthesis of steroidal alkaloid solanidine

#### 3.3.1. Background

Steroidal glycoalkaloids (SGAs) are present in numerous poisonous and edible species of the *Solanum* genus (family Solanaceae) such as: *S. lycopersicum* (tomato), *S. melongena* (eggplant), *S. dulcamara* (woody nightshade), and *S. tuberosum* (potato).  $\alpha$ -Solanine (**329**, Scheme 3.24) and  $\alpha$ -chaconine (**330**), comprising 95% of all potato SGAs, are both glycosylated (trisaccharide) derivatives of the aglycone solanidine (**331**),<sup>125</sup> and are found to accumulate in high concentrations in tubers and leaves.<sup>126</sup>

Scheme 3.24.



Produced in the bioactive parts of the plant, these substances protect the plant against fungi, insect pests, and herbivores.<sup>126</sup> The accumulation of SGAs can influence

the quality of tubers in fresh and processed potatoes by introducing a bitter flavor. SGAs are also potential food safety hazards as these compounds are toxic and can inhibit acetylcholinesterase and disrupt cell membranes.<sup>127</sup> Death from consumption of Solanaceae was reported as early as 1859 in a 14-year-old girl who ate unripe “potatoe [sic] berries.”<sup>128</sup>

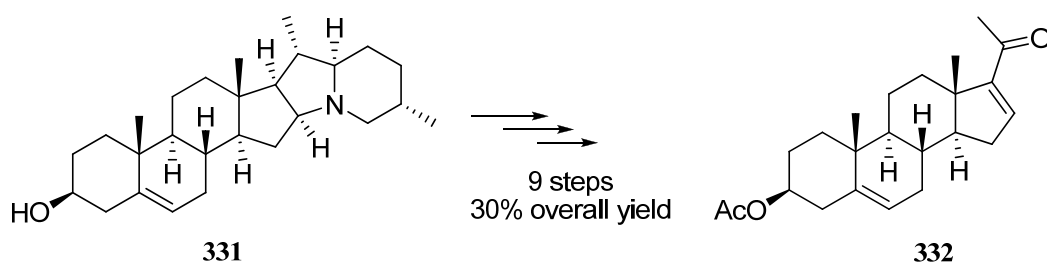
Recent studies report that potato glycoalkaloids can be toxic in humans at doses greater than 2mg of total SGAs  $\text{kg}^{-1}$  body weight,<sup>129</sup> causing gastrointestinal disturbances including vomiting, diarrhea, and abdominal pain. Cases of lethal poisoning have also been reported and are estimated to occur at doses greater than 3 mg total SGAs  $\text{kg}^{-1}$  body weight.<sup>129</sup> The total concentration of SGAs in consumption potatoes varies, but the average amount is less than 100 mg  $\text{kg}^{-1}$  fresh potato weight. Generally, 200 mg SGAs  $\text{kg}^{-1}$  fresh potato weight is the accepted upper safety limit.<sup>130</sup> Although the glycoalkaloid concentration of most commercial potatoes is well below the suggested upper limit, it can increase substantially on exposure of potatoes to light or as a result of mechanical injury.<sup>131</sup> Notably, home cooking, such as frying, baking and microwaving will *not* destroy SGAs as they are characterized by fairly high thermal stability.

Glycoalkaloids and aglycones also have beneficial effects, and have been reported to inactivate the *Herpes simplex*, *Herpes zoster*, and *Herpes genitalis* viruses in humans,<sup>132</sup> to protect mice against infection by *Salmonella typhimurium*,<sup>133</sup> to enhance the duration of action of anesthetics which act by inhibiting acetylcholinesterase,<sup>134</sup> and to potentiate the immune response for vaccines in mice.<sup>135</sup>

Solanidine (**331**) in particular has been shown to be a potent inhibitor of human colon and liver carcinoma cells.<sup>136</sup>

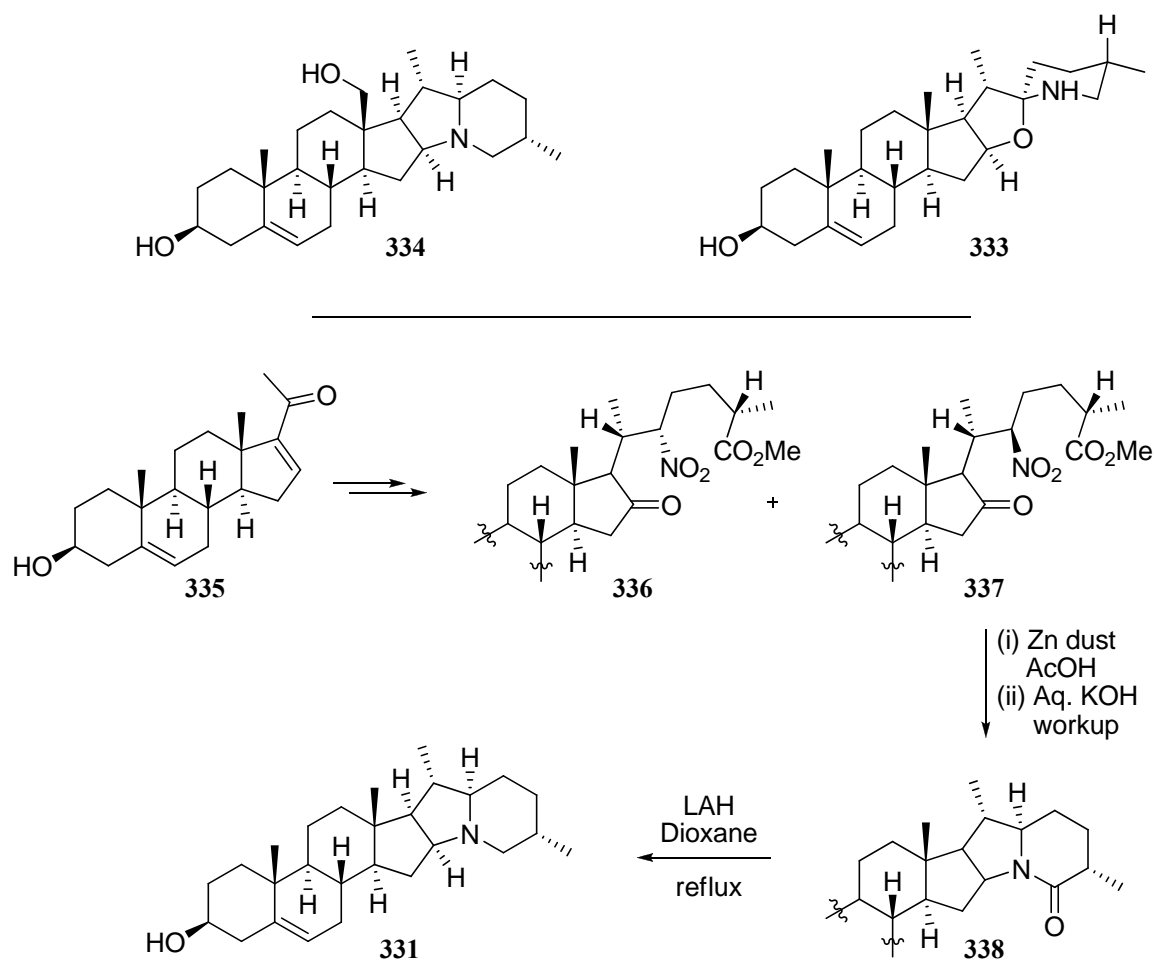
Aglycone solanidine (**331**) has also been shown to be a valuable starting material for the production of dehydropregnenolone acetate (**332**, Scheme 3.25), a key intermediate in the industrial synthesis of progesterone and cortisone derivatives.<sup>125</sup> This process was stimulated by the possibility of isolating large amounts (ton scale) of potato glycoalkaloids ( $\alpha$ -solanine and  $\alpha$ -chaconine) from a waste stream of the potato starch production.

Scheme 3.25.



The fact that solanidine can be easily attained in large quantities from potatoes probably explains why there are very few reported synthetic preparations of this steroidal alkaloid. So far, the general approach towards the preparation of solanidine has been to utilize structurally similar natural products as starting materials. For example, Schreiber<sup>137</sup> and co-workers converted the related steroidal alkaloid tomatidine (**333**, Scheme 3.26) to prepare solanidine (**331**) in five synthetic steps, while Pelletier<sup>138</sup> reported the conversion of isorubijervine (**334**) to solanidine in 2 steps.

Scheme 3.26

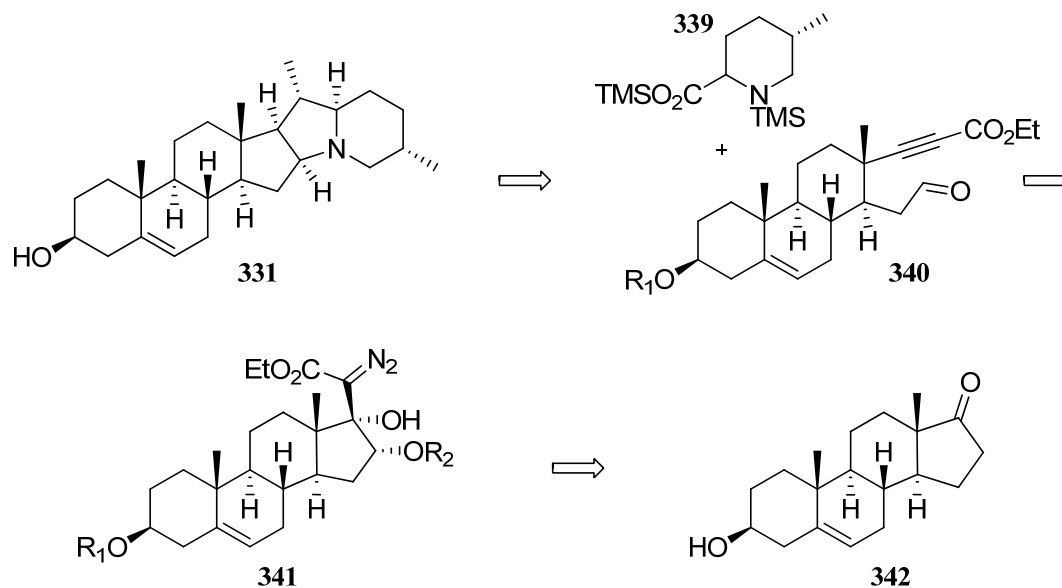


To date, there is only one account which reports the synthesis of solanidine (**331**) from intermediates other than natural products, and requires the use of dehydropregnenolone (**335**, Scheme 3.26) as a starting material.<sup>139</sup> The key step in the sequence was the reduction of chiral nitro ester **337** to a secondary amine which undergoes reductive amination and cyclization to afford amide **338**. A subsequent reduction of the amide with lithium aluminum hydride (LAH) then affords the desired solanidine (**331**).

### 3.3.2. Application of fragmentation / [1,3] – dipolarcycloaddition protocol towards the synthesis of solanidine

In our approach towards the synthesis of solanidine (**331**, Scheme 3.27) we intended to utilize both the newly developed fragmentation reaction and the intramolecular [1,3]-dipolar cycloaddition protocol as key steps. In effect, we envisioned that the N-containing carboskeletal core of solanidine (**331**) could be accessed via the stereoselective intramolecular dipolar cycloaddition of the azomethine ylide generated from the requisite bisilylated amino acid **339** and tethered aldehydoate **340**, which, in turn, could be prepared by the tin mediated fragmentation of the *syn*  $\gamma$ -silyloxy- $\beta$ -hydroxy- $\alpha$ -diazo ester **341**. Finally, commercial dehydroepiandrosterone (**342**) would serve as starting point towards the synthesis of requisite diazo ester (**341**).

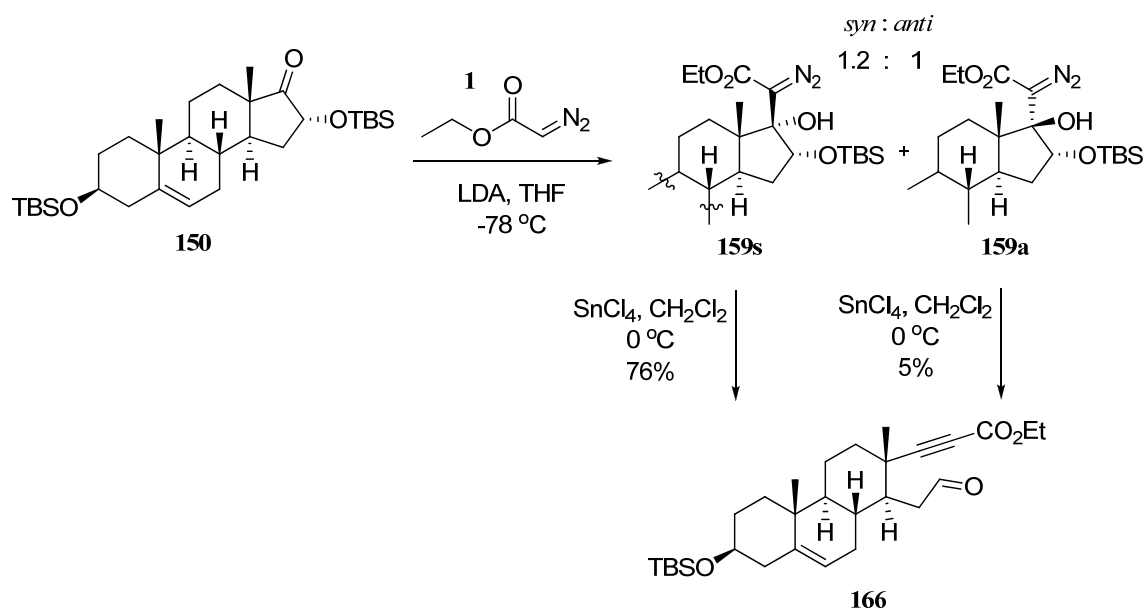
Scheme 3.27.





Preliminary analysis of the proposed synthetic route revealed that the ability to only efficiently fragment the *syn* diastereomer **159s** (Scheme 3.28) in good yields, would effectively obligate us to discard approximately half of our synthetic material at premature stage of our synthesis. The reason being that the ethyl lithio-diazo acetate addition to the requisite  $\alpha$ -tert-butyldimethylsilyloxy ketone **150** (Scheme 3.28) only provides a 1.2 : 1 (*syn* : *anti*) mixture of diastereomers.

Scheme 3.28.



Thus, my primary objective became studying the factors which could bias the diastereoselectivity of the ethyl lithio-diazoacetate addition to  $\alpha$ -silyloxy ketones in favor of the desired *syn* diastereomer. In considering the steric environment around the ketone it seemed likely that the axial methyl would hinder approach to the top face of the ketone (Figure 3.2) while the bulky silyl group would hinder the approach from the

bottom face of the ketone. We thought it might be possible to take advantage of the steric shielding interactions to influence the outcome of the reaction by directing the incoming nucleophile to approach from the less obstructed face. Attack from the *si* face affords the desired *syn* diastereomer, while the undesired *anti* diastereomer is the product of the nucleophilic attack from the *re* face. Based on this rational we hypothesized that if the steric bulk of the silyl group were to be increased we would induce effective obstruction of the bottom face and force the nucleophile to preferentially add from the less hindered top face, ultimately biasing the reaction in the favor of *syn* diastereomer formation.

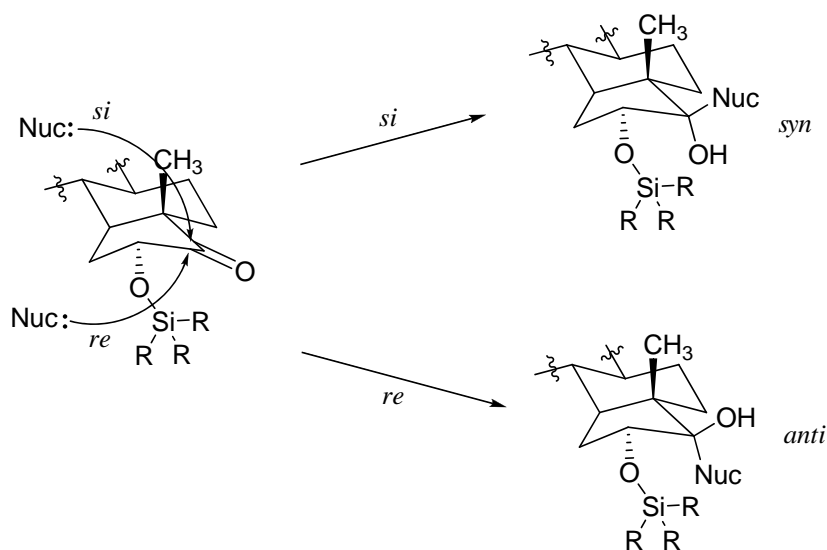
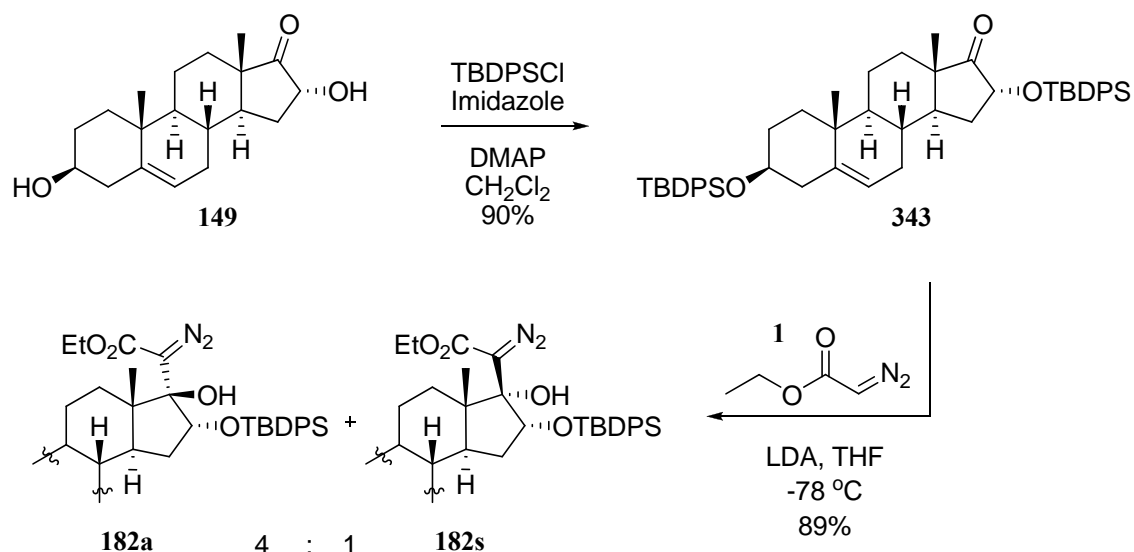


**Figure 3.2. Proposed steric effect of the neighboring groups on the stereoselectivity of ethyl lithio-diazoacetate addition**

In order to test the hypothesis, we prepared the bis-*tert*-butyldiphenylsilyl derivative **343** (Scheme 3.29) starting from the dehydroepiandrosterone derived secondary alcohol **149** (for the preparation of **149** see Section 2.5.1, Scheme 2.14). We

were surprised to observe that submitting **343** to ethyl lithio-diazoacetate addition provided a 4:1 mixture of isomers in favor of the undesired *anti* diastereomer **182a**. It appears that the larger tert-butyldimethylsilyl group effectively increased the steric bulk around the *re* face of the electrophile and forced the nucleophile to approach from the bottom face.

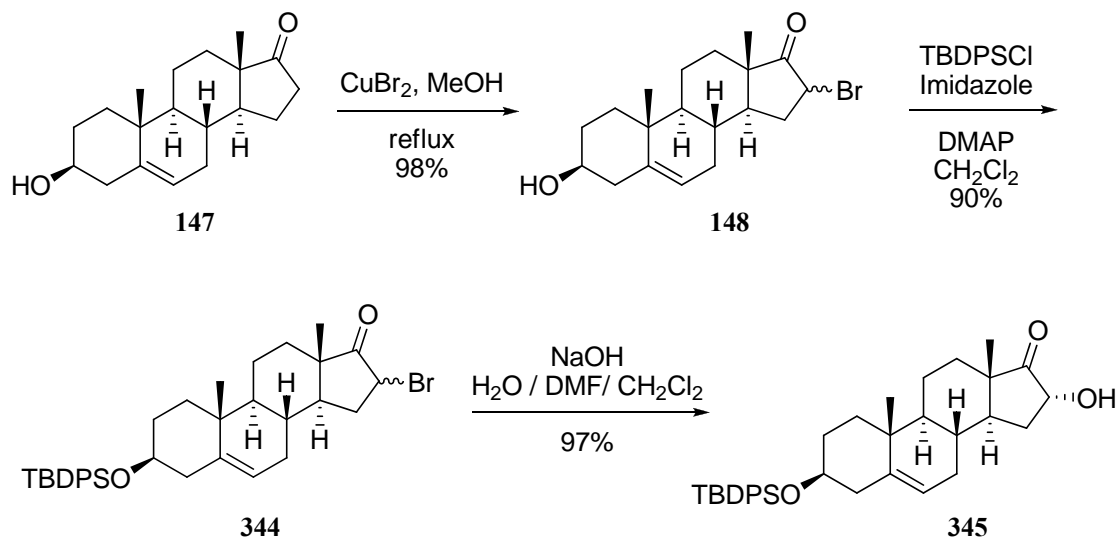
Scheme 3.29.



Although this was an unexpected result, it became clear that altering the steric bulk of the  $\alpha$ -silyloxy moiety did have an effect on the distereoselectivity of the reaction. Given that increasing the size of the protecting group produced the undesired response, I decided to use a smaller protecting group to gauge the outcome of the reaction. Thus, I prepared the requisite  $\alpha$ -silyloxy ketones by employing a variation of the previously used protocol (see Section 2.5.1, Scheme 2.14) which allowed for differential protection of the two secondary alcohols of diol **149** (Scheme 3.29).

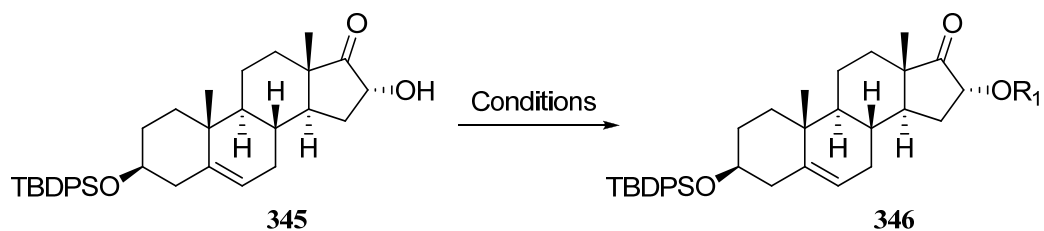
Treatment of dehydroepiandrosterone (**147**, Scheme 3.30) with  $\text{CuBr}_2$  in refluxing methanol<sup>84</sup> afforded epimeric  $\alpha$ -bromo ketone **148** and subsequent protection of the secondary alcohol with tertbutyldimethylsilyl chloride (TBDPSCI) afforded  $\alpha$ -bromo ketone **344**. Treating bromide **344** with hydroxide results in epimerization of the bromide and subsequent selective  $\text{S}_{\text{N}}2$  displacement of the  $16\beta$ -isomer stereoselectively provides the  $\alpha$ -hydroxyl ketone **345** in 97% yield.

Scheme 3.30.



The synthesis of the differentially protected  $\alpha$ -silyloxy and  $\alpha$ -alkoxy ketones was achieved starting from **345**, using standard conditions for the protection of alcohols, and the results are presented in Table 3.2.

**Table 3.2. Synthesis of  $\alpha$ -silyloxy and  $\alpha$ -alkoxy ketones **346a**, **346b**, **346c****

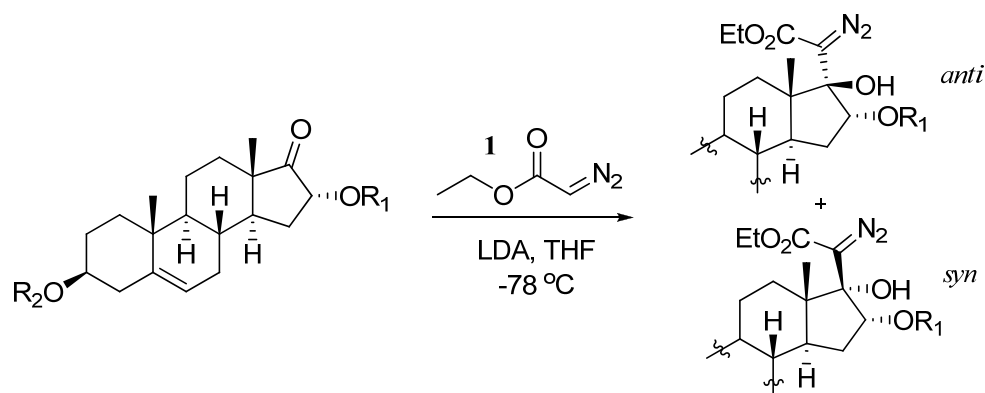


Entry	R1	Conditions	Compound #	Yield <sup>a</sup> (%)
1	TES	TESCl, Imidazole DMAP, CH <sub>2</sub> Cl <sub>2</sub>	<b>346a</b>	97
2	MOM	MOMCl, (iPr) <sub>2</sub> NEt CH <sub>2</sub> Cl <sub>2</sub> , Reflux	<b>346b</b>	87
3	Bn	BnBr, Ag <sub>2</sub> O CH <sub>2</sub> Cl <sub>2</sub> , rt.	<b>346c</b>	42

Note: <sup>a</sup> yield reported after chromatography

At this point, I was ready to investigate the effect of the less sterically encumbering protecting groups on the diastereoselectivity of the ethyl lithio-diazoacetate addition reaction. All reactions were run under the same conditions unless otherwise specified, and the results are summarized in Table 3.3. In the end, I was pleased to find that decreasing the steric bulk of the protecting group did in fact favor the formation of the desired *syn* diastereomer. Thus, switching from the TBS to TES improved the *syn* : *anti* ratio to 3.7 : 1, and the two diastereomers could be easily separated by chromatography (Entry 3). Furthermore, when the addition precursors **346b** and **346c** bearing alkoxy protecting groups (MOM, Entry 5 and Bn, Entry 6) were employed the *syn* : *anti* ratios were also found to favor the desired *syn* diastereomer, but the mixture of isomers was inseparable by chromatography.

**Table 3.2.** Ethyl lithio-diazoacetate addition to steroid derived differentially protected  $\alpha$ -silyloxy and  $\alpha$ -alkoxy ketones.



Entry	$\alpha$ -OR <sub>1</sub> ketone	R <sub>1</sub>	R <sub>2</sub>	Yield <sup>a</sup> (%)	Compound # <i>syn</i> : <i>anti</i> <sup>b</sup>
1	<b>343</b>	TBDPS	TBDPS	89%	<b>182s : 182a</b> 1 : 4
2	<b>150</b>	TBS	TBS	84%	<b>159s : 159a</b> 1.2 : 1
3	<b>346a</b>	TES	TBDPS	83%	<b>181s : 181a</b> 3.7 : 1
4 <sup>c</sup>	<b>347</b>	H	TBS	41% <sup>d</sup>	<b>348s : 348a</b> 10:1 <sup>e</sup>
5	<b>346b</b>	MOM	TBDPS	N.A.	<b>349s : 349a</b> 5 : 1 <sup>e</sup>
6	<b>346c</b>	Bn	TBDPS	N.A.	<b>350s : 350a</b> 5 : 1 <sup>e</sup>

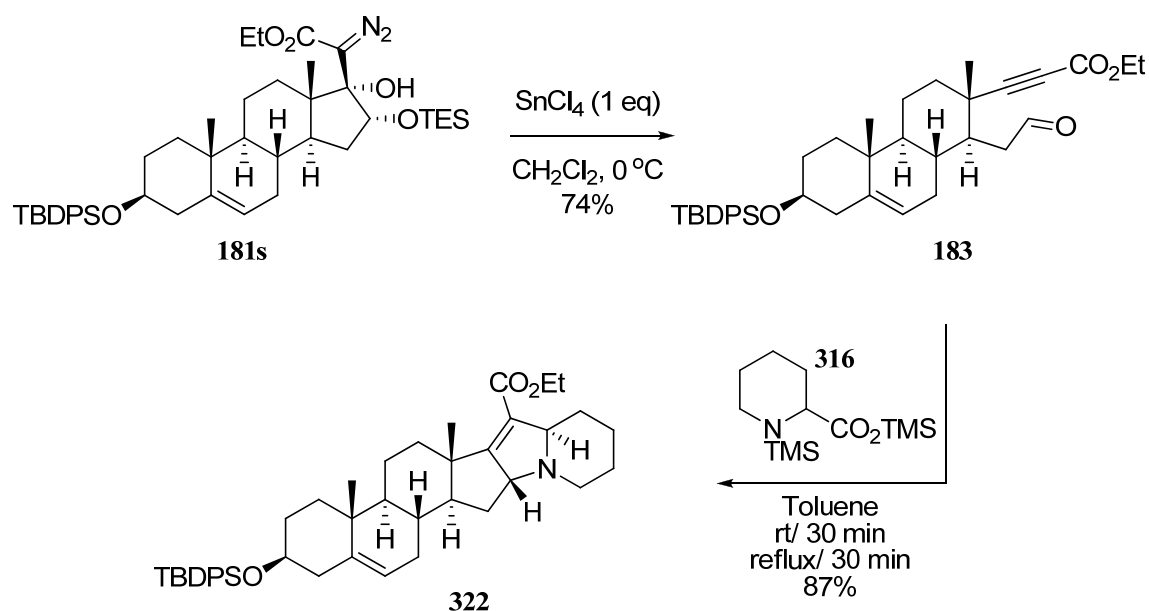
Note: <sup>a</sup> Isolated yield after purification by column chromatography. <sup>b</sup> ratios determined after isolation by chromatography unless otherwise specified. <sup>c</sup> reaction performed with excess ethyl lithio-diazoacetate but full conversion was not achieved. <sup>d</sup> only one isomer isolated and tentatively assigned as the *syn* diastereomer. <sup>e</sup> ratio determined by <sup>1</sup>H NMR analysis of the crude reaction mixture.

Lastly, the reaction of unprotected  $\alpha$ -hydroxy ketone **347** with excess ethyl lithio-diazoacetate (Entry 4) provided a single diastereomer which is tentatively assigned as the *syn* isomer based on the <sup>1</sup>H NMR spectra (see Section 2.5.3). Unfortunately, in

this case the reaction only proceeded to approximately 50% conversion even in the presence of excess reagents and the remainder of the material is recovered as starting material. At this time it is unclear why the reaction stops at 50% conversion. We believe that the observed increased stereoselectivity in favor of the *syn* diastereomer is due to conformational change of the five member ring imparted by the less sterically bulky protection groups so that approach from the *re* face of the ketone is favored.

Having found the appropriate conditions under which we can increase the diastereoselectivity meant we could switch our focus towards the next steps of our proposed synthetic plan.

Scheme 3.31.



Because *syn*  $\gamma$ -triethylsilyloxy- $\beta$ -hydroxy- $\alpha$ -diazoester **181s** (Table 3.2, Entry 3) could be efficiently isolated in good yields as the major diastereomer, we decided to further utilize this substrate and subject it to the newly developed tin mediated ring

fragmentation reaction (Scheme 3.31), which provided the desired aldehyde ynoate **183** in 74% isolated yield. The next step in our strategy was to utilize the intramolecular [1,3]-dipolarcycloaddition protocol to install the N-containing heterocyclic core of solanidine (**331**). I was pleased to observe that treatment of tethered aldehyde ynoate **183** bissilylated pipecolic acid **316** to afford the desired dihydropyrrole cycloadduct in 87% yield as a single diastereomer.

At this point we have successfully assembled the carboskeletal core of solanidine. However, completing the synthesis of solanidine would require (Figure 3.3): (i) installing the missing methyl, (ii) addressing the oxidation state of the dihydropyrrole moiety and (iii) setting the correct stereochemistry of the highlighted centers.

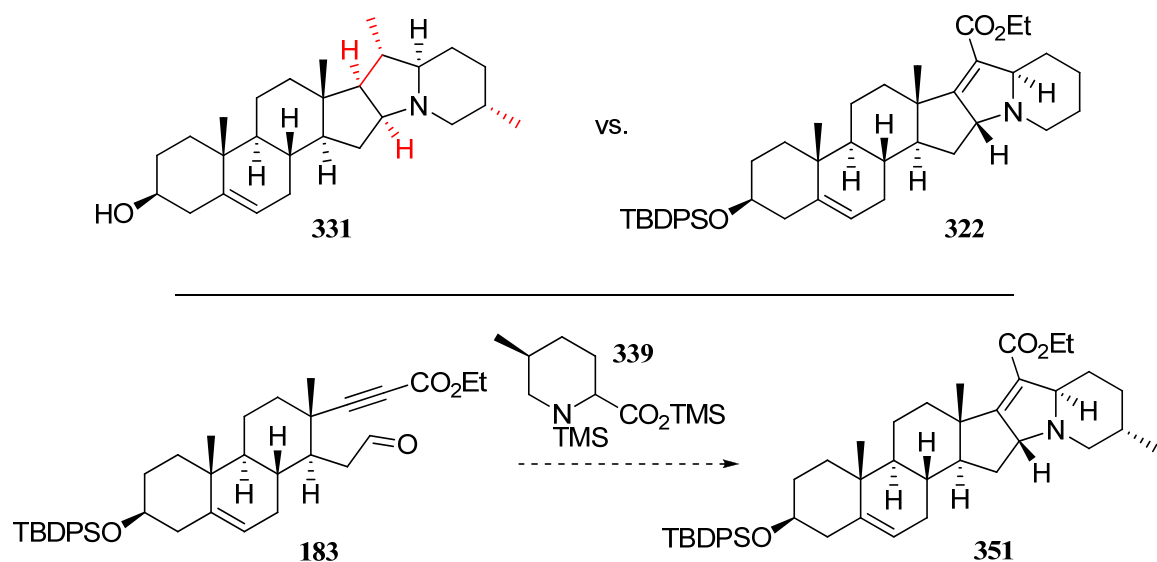
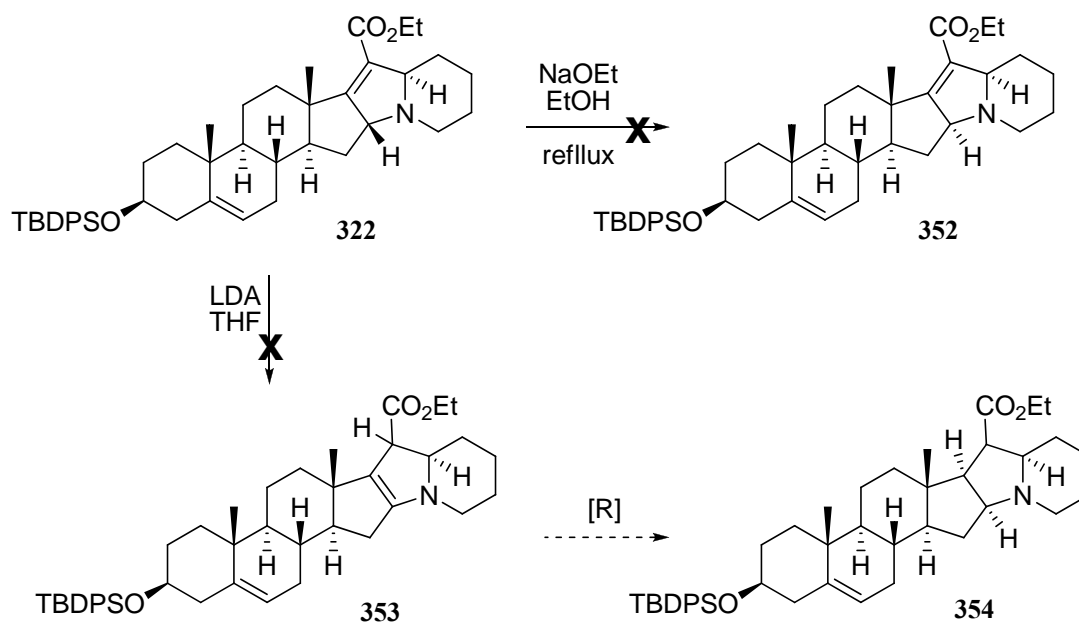


Figure 3.3. Remaining challenges in the synthesis of solanidine.



We believe that the missing methyl group will be most effectively introduced by incorporating it into the appropriate  $\alpha$ -amino acid dipolar cycloaddition precursor (e.g. **339**, Figure 3.3). Since the preparation of **339** in a stereoselective fashion is not straight forward, we felt our time would be better served if we addressed the oxidation state and stereochemical issues using dihydropyrrole **322** as a model system.

Scheme 3.32.

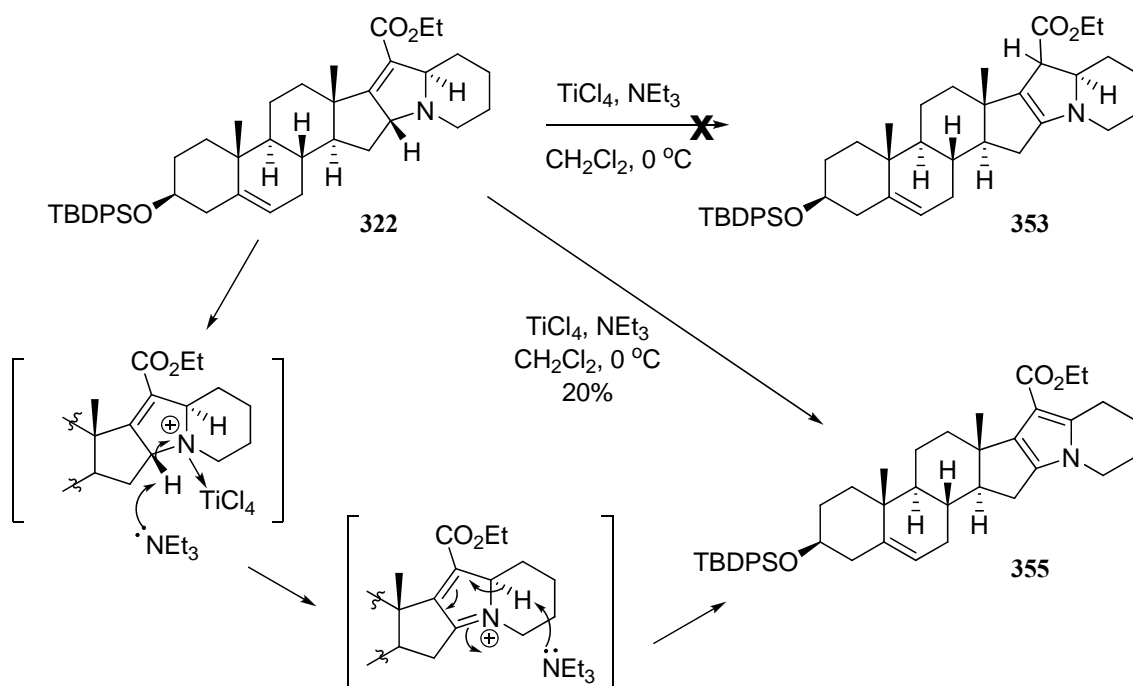


The initial strategy in addressing the stereochemistry was to promote the epimerization (**322**  $\rightarrow$  **352**, Scheme 3.32) of the inverted stereocenter under thermodynamic conditions. Unfortunately, treating dihydropyrrole **322** with sodium ethoxide (NaOEt) in ethanol did not provide the desired epimer, dihydropyrrole **352**, and only starting material was isolated from the reaction mixture. Empirical calculations at the AM1 level of theory on **322** and **352** showed that **352** is more stable

by approximately 6 Kcal mol<sup>-1</sup>, which explains the lack of success in the thermodynamic epimerization approach.

In an alternative approach, enamine **353** (Scheme 3.32) could serve as an intermediate that could undergo stereoselective reduction controlled by the axial methyl group to set two of the desired stereocenters as shown in pyrrolidine **354**. Attempts to induce formation of enamine **353** from dihydropyrrole **322** in the presence of lithium diisopropyl amide (LDA) were unsuccessful and so, I tried to promote the same transformation using a Lewis acid (Scheme 3.33).

Scheme 3.33.

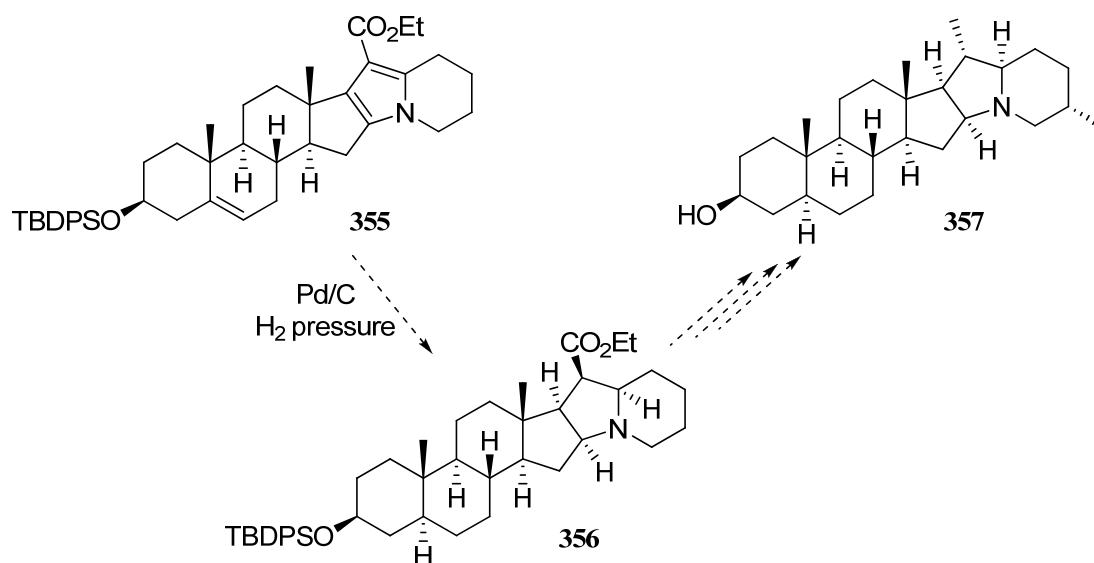


Unfortunately, treatment of dihydropyrrole **322** (Scheme 3.33) with titanium tetrachloride and triethyl amine did not provide the desired enamine **353**, but instead returned pyrrole **355** in 20% yield along with unreacted starting material. This result

can be explained by coordination of the nitrogen to the Lewis acid which, following the sequence highlighted in Scheme 3.33, ultimately leads to the formation of pyrrole **355**.

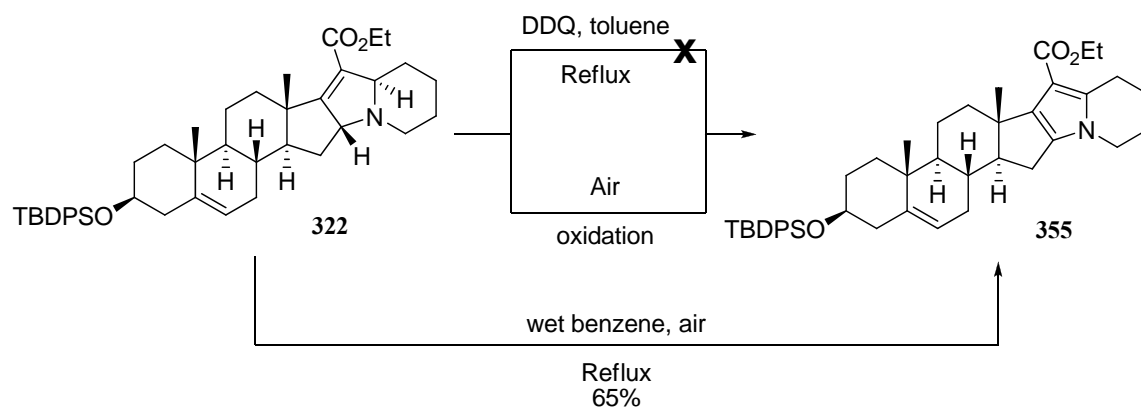
Thus far, all my efforts directed towards addressing the stereochemical and oxidation issues (see Figure 3.3) have been unsuccessful. However, we believe that the oxidation of the dihydropyrrole **322** to the pyrrole **355**, could prove to be a useful avenue towards the synthesis of demisidine (**357**, Scheme 3.34), another natural product which can be best described as the fully saturated version of solanidine. As a key step in our strategy towards the synthesis of demisidine (**357**), we envision a stereoselective reduction of the pyrrole moiety directed by the axial methyl group. In effect, we hope that the proximity of the methyl group to the reacting center will direct the palladium catalyst to approach from the opposite face thus forcing the reduction to install the desired correct stereocenters.

Scheme 3.34.



Recent efforts aimed towards the preparation of pyrrole **355** (Scheme 3.35) revealed that oxidation of dihydropyrrole **322** with 2,3-dichloro-5,6-dicyano-benzoquinone (DDQ) was unsuccessful even while refluxing in toluene, which was somewhat surprising given that dihydropyrrole **322** oxidizes when exposed to air for longer periods of time. This suggested a different approach, in which **322** was refluxed in wet benzene under atmospheric pressure. To our satisfaction these conditions, although at this point unoptimized, induced desired oxidation and allowed for the isolation of pyrrole **355** in 65% yield.

Scheme 3.35.



In summary, in my studies towards the total synthesis of steroidal alkaloids solanidine and demisidine I was able to enhance the diastereoselectivity of the ethyl lithio-diazoacetate addition reaction and then successfully implement the newly developed ring fragmentation and intramolecular [1,3]-dipolarcycloaddition reaction to efficiently prepare key intermediate dihydropyrrole **322**. Although my efforts aimed

towards further synthetically modifying **322** to achieve the desired natural product were unsuccessful, dihydropyrrole **322** will serve as a good model for future studies.

### **3.4. Conclusions**

I have successfully developed an efficient intramolecular [1,3]-dipolar cycloaddition of azomethine ylides generated from  $\alpha$ -amino acids and  $\alpha$ -amino esters which involves tethered aldehyde ynoates. We believe that the development of this protocol is a significant advancement as it allows for the efficient assembly of complex polycyclic heterocycles from readily available starting materials using very few synthetic manipulations. Thus far this methodology has been successfully implemented in the assembly of bi- and tricyclic dihydropyrroles and the N-containing core of steroidal alkaloids solanidine and demisidine.

## 4. CHAPTER 4: RADICAL ADDITION APPROACH TO ASYMMETRIC AMINE SYNTHESIS

### AMINE SYNTHESIS

#### 4.1. Background

Chiral  $\alpha$ -branched amines (e.g. **357**, Figure 4.1) are common substructures of bioactive synthetic targets. Direct asymmetric amine synthesis by addition to the C=N bond of carbonyl imino derivatives<sup>140-143</sup> (e.g. **356**) holds promise for improved efficiency by introducing the stereogenic center and a C–C bond in one step under mild, non-basic conditions.

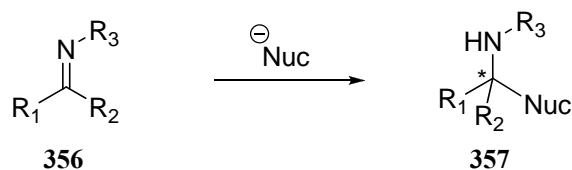
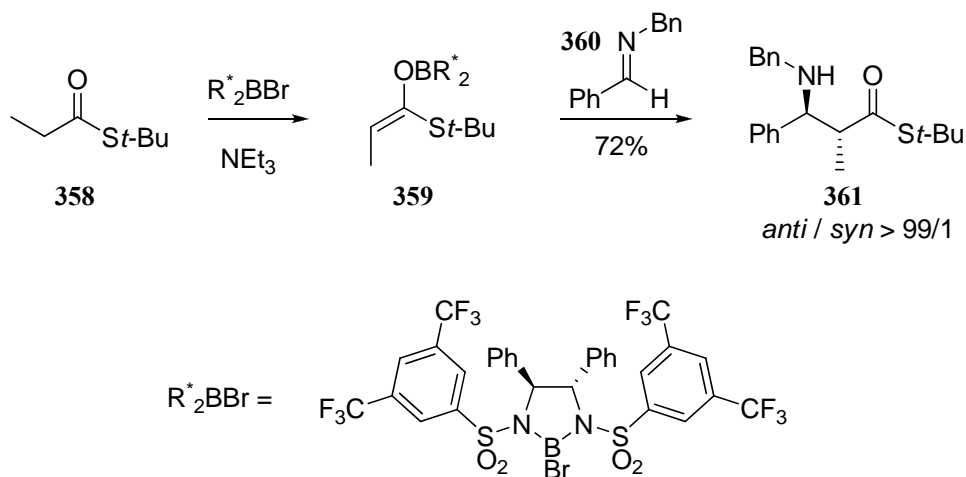


Figure 4.1. Nucleophilic addition to C=N bonds.

As an example, consider asymmetric Mannich-type reactions which provide useful routes for the synthesis of optically active  $\alpha$ -branched amines. In 1991, Corey<sup>144</sup> and co-workers reported the first enantioselective Mannich-type reaction to prepare chiral  $\beta$ -amino acid ester **361** (Scheme 4.1). Treatment of (E)-N-benzylidene-1-phenylmethanamine **360** with chiral boron enolate **359** afforded the  $\alpha$ -chiral branched amine **361** in good yield and 95% enantioselectivity.

Scheme 4.1.



New methods for the stereocontrolled construction of C–C bonds would broaden the scope of the direct asymmetric amine synthesis strategy for access to chiral amines (e.g. **363**, Figure 4.2). An ongoing search for more versatile methods for addition to C=N bonds under mild conditions has led to several promising developments, including intermolecular radical addition to imino compounds (e.g. **362**, Figure 4.2).<sup>145,146</sup>

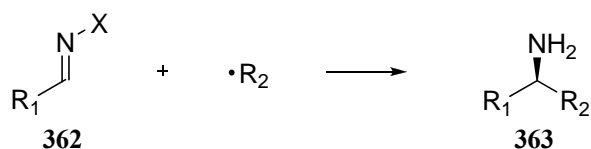


Figure 4.2. Radical addition to C=N bonds.

The radical addition approach to chiral amines (Figure 4.2) offers the potential for practical advantages in chemoselectivity and versatility typical of radical reactions.<sup>147,148</sup> For example, compare the radical approach with related additions of basic organometallic reagents to imines. These later reactions often suffer from

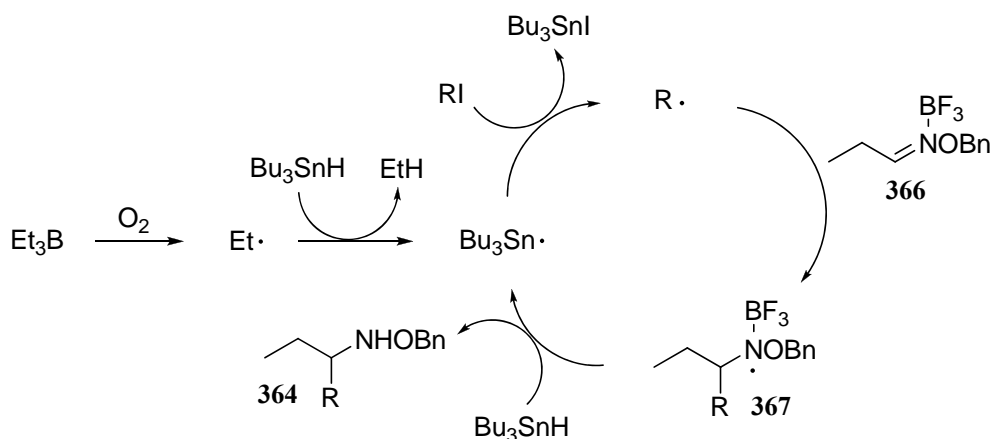
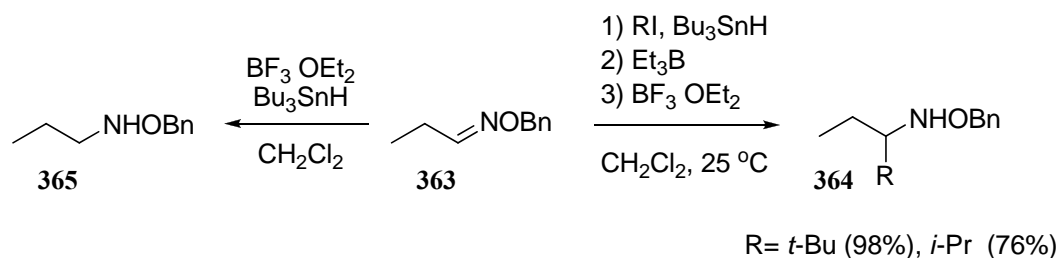
competing aza-enolization and lack generality and functional group tolerance. For example, branched organometallic reagents, such as *i*-PrMgBr, can competitively reduce the C=N bond via hydride transfer.<sup>149</sup> Hindered reagents such as *t*-BuMgBr or *t*-BuLi often fail to give addition products,<sup>150</sup> whereas *tert*-butyl radical addition is quite capable of constructing hindered C–C bonds. The high basicity associated with these organometallic nucleophiles is complemented by the milder conditions inherent to Strecker,<sup>151</sup> Mannich,<sup>152</sup> and allylsilane additions,<sup>153</sup> along with other recently developed addition reactions.<sup>154-156</sup> Still, these place significant restrictions on the identity of the incoming nucleophile destined to become R<sub>2</sub> of the chiral amine (Figure 4.2). On the other hand, radical reactions can accommodate a broad range of functionality within the radical itself. This suggests great potential scope in their future application in asymmetric amine synthesis, pending development of versatile imino acceptors capable of effective stereocontrol.

Previous intermolecular radical additions developed by Naito<sup>157</sup> showed that imino acceptors were effective substrates for additions of radicals derived from secondary and tertiary alkyl iodides. For example, treatment of oxime ether **363** (Scheme 4.2) with alkyl iodides, tributyltin hydride (Bu<sub>3</sub>SnH) and triethylborane (Et<sub>3</sub>B) followed by addition of BF<sub>3</sub>·OEt<sub>2</sub> gave the desired C-alkylated product **364**. Bulky tertiary alkyl radicals also worked well. In all cases the addition of BF<sub>3</sub>·OEt<sub>2</sub> as a final reagent was crucial for the successful radical reaction. In the presence of BF<sub>3</sub>·OEt<sub>2</sub>, the Bu<sub>3</sub>SnH mediated reduction of oxime ether **363** proceeded to give benzyloxyamine **365**. The radical reaction was described to proceed as follows (Scheme 4.2): (i) the



stannyl radical, generated from Et<sub>3</sub>B and Bu<sub>3</sub>SnH, reacts with the secondary or tertiary alkyl iodide to give the alkyl radical; (ii) the alkyl radical then attacks the BF<sub>3</sub>-activated oxime ether **366** to afford the intermediate aminyl radical **367** which is then converted to **364**.

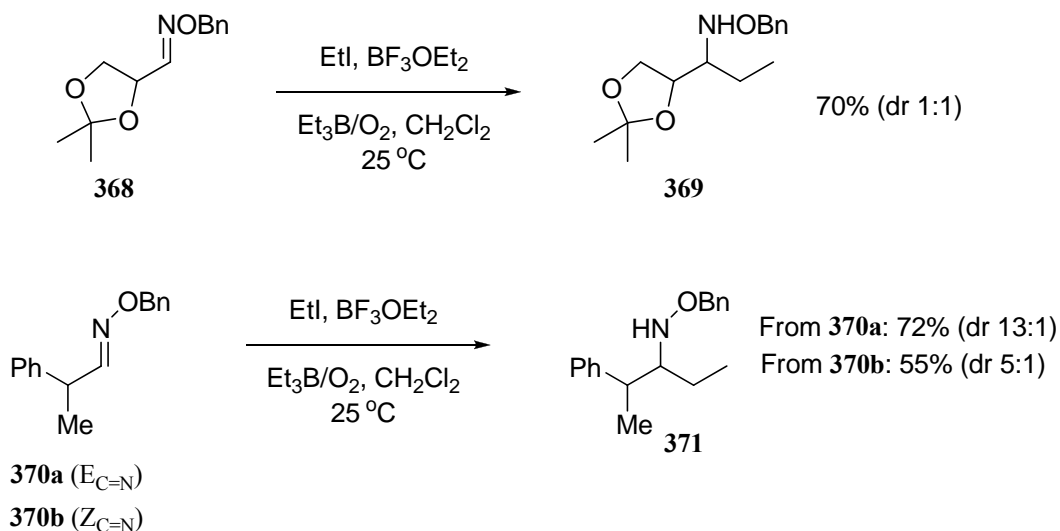
Scheme 4.2.



Diastereoselective intermolecular radical additions to C=N bonds have also been observed. For example, Naito<sup>158</sup> and co-workers reported radical additions to chiral oxime ethers (e.g. **368**, Scheme 4.3) with  $\alpha$ -substituents. Glyceraldoxime acetone **368** gave no stereocontrol, while oximes **370a** and **370b** gave the same

product **371** with 13:1 and 5:1 diastereomer ratios, respectively (configurations not reported), showing an interesting dependence on C=N isomerism.

Scheme 4.3.

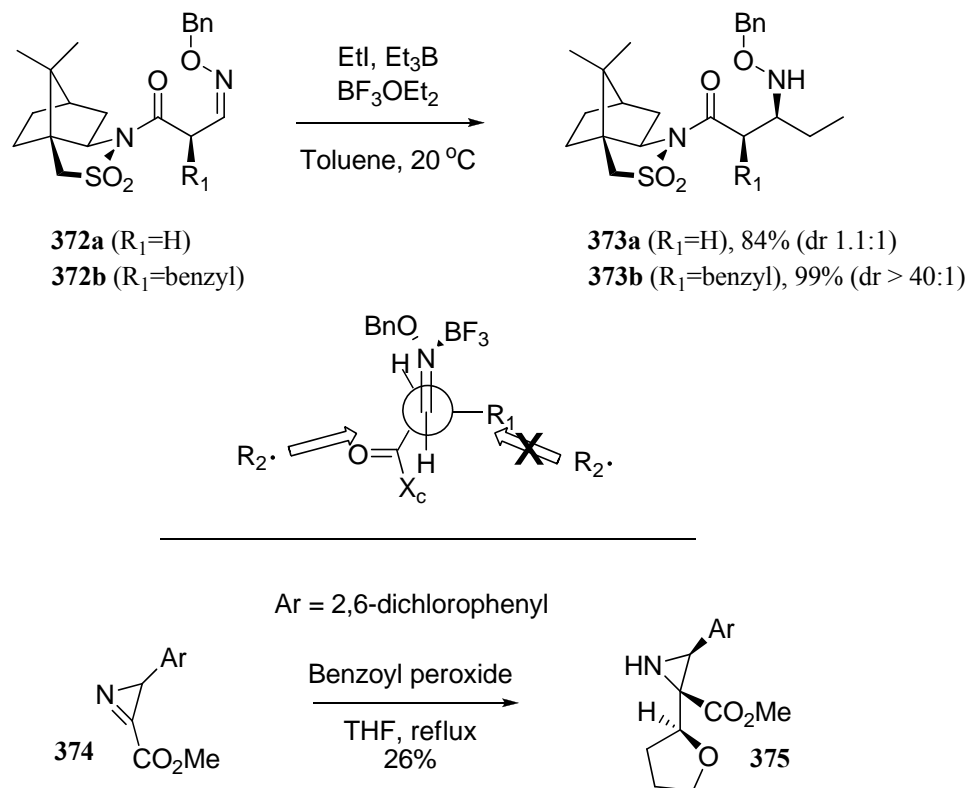


More recently, Naito exploited malonate-derived substrates **372** (Scheme 4.4), prepared by stereoselective alkylation of the chiral camphorsultams, for 1,2-asymmetric induction in radical addition.<sup>159</sup> For oxime acceptor **372b** diastereoselectivity was extremely high (dr > 40:1) in ethyl radical addition utilizing  $\text{BF}_3\cdot\text{OEt}_2$  and  $\text{Et}_3\text{B}$ . The camphorsultam itself was not the major stereocontrol element as **372a** led to essentially no stereocontrol, consistent with precedent involving radical addition to acrylamides using this auxiliary.<sup>148</sup> It is believed that minimization of allylic strain favors the reactive conformation shown in Scheme 4.4, wherein the  $\alpha$ -substituent  $\text{R}_1$  blocks one face of the C=N acceptor.

In isolated cases, prochiral radicals have also been observed to induce stereoselectivity in intramolecular radical additions to C=N acceptors. For example,

Gilchrist<sup>160</sup> and co-workers fortuitously found high diastereoselectivity in a radical addition of tetrahydrofuran (THF) to an azirine (e.g. **374**, Scheme 4.4).

Scheme 4.4.

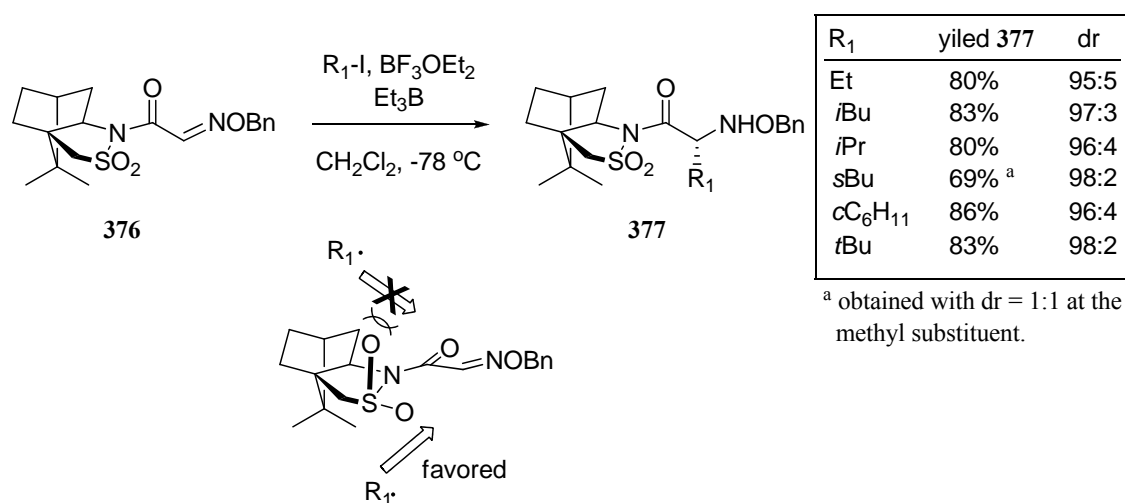


After the adduct was first obtained as an unexpected side product in an attempted malonate addition to the azirine **374**, a subsequent intentional preparation using benzoyl peroxide in refluxing THF also gave the same aziridine product **375** in modest yield. Only a single diastereomer was detected, indicating that the aryl group controlled the face of attack on the azirine **374**. More surprisingly, the configuration generated at the prochiral radical center was also controlled in this reaction.

In some cases, intramolecular radical additions have been rendered stereoselective by employing a chiral auxiliary attached either to the carbon or nitrogen

of the C=N bond. Naito and coworkers first reported intermolecular stereoselective radical addition to C=N bonds in 1997.<sup>161</sup> In this seminal paper, Oppolzer's camphorsultam auxiliary (Scheme 4.5) was linked through an amide bond to the *O*-benzyloxime derivative of glyoxylic acid.

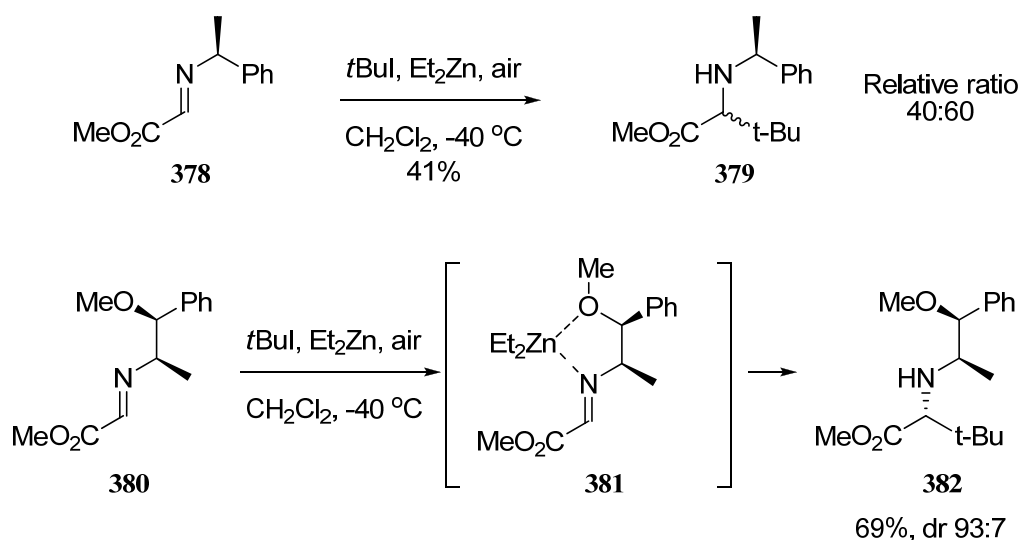
Scheme 4.5.



Substrate **376** was submitted to radical addition conditions using a variety of Lewis acid promoters and alkyl iodides along with triethyl borane initiation. Optimal yields and selectivities were obtained using BF<sub>3</sub>·OEt<sub>2</sub> and CH<sub>2</sub>Cl<sub>2</sub>; under these conditions addition of ethyl, isopropyl, cyclohexyl and *tert*-butyl radicals gave amino acid derivatives **377** in 80-86% yields with very high stereoselectivity. A stereocontrol model consistent with the observed product configuration was proposed, suggesting that the sulfonamide oxygen was critical for blocking one of the approach trajectories (see Scheme 4.5).

More recently, Bertrand<sup>162</sup> et al. described the use of diethyl zinc to promote radical addition to chiral imines (e.g. **380**, Scheme 4.6). Stereoselectivity was poor in additions to phenethylamine derivative **378**, but the use of imines capable of an additional binding interaction with Lewis acidic Zn(II), such as norephedrine-derived imine **380** led to improved diastereomer ratios in *tert*-butyl radical adduct **382**, presumably via a chelated acceptor **381**.

Scheme 4.6.



These seminal precedents established that stereochemical information can be transferred during radical additions to imines through the carbon branch or nitrogen substituent of the imine (Figure 4.3, (a)). However, in each case, a second independent activating substituent was employed, and thus, the imino acceptors required modifications to both nitrogen and carbon substituents of the imine. A potentially more versatile approach to stereocontrolled radical addition to imines would achieve both activation and stereocontrol from a single modification to the nitrogen substituent of the

imino acceptor (Figure 4.3, **(b)**). Successful addition would then be independent of the identity of the aldehyde precursor to the imine, which would potentially broaden the scope of the reaction. Toward this end, the Friestad group conceived a nitrogen-linked chiral auxiliary approach incorporating Lewis acid activation and restriction of rotamer populations as key design elements.

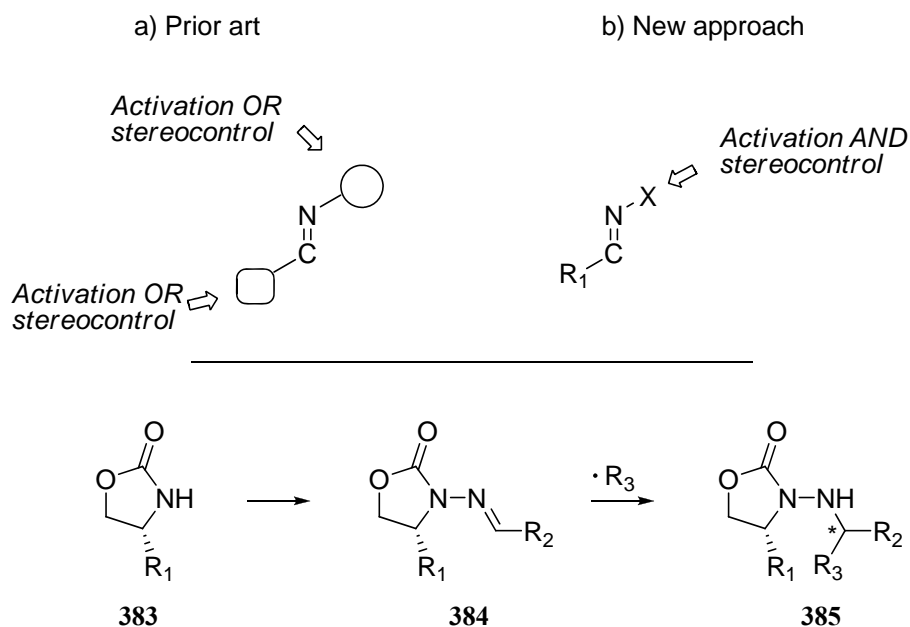


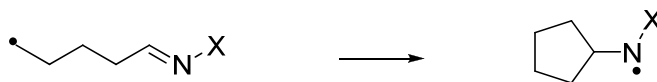
**Figure 4.3. Approaches to stereocontrol for radical addition to C=N bonds.**

In the following sections I will present details about the design and preparation of chiral *N*-acylhydrazones (e.g. **384**, Figure 4.3) from 2-oxazolidinones (e.g. **383**) and their implementation for highly stereoselective intermolecular radical addition reactions as developed by previous members in the Friestad group, along with my contributions in the area.

## 4.2. Design and synthesis of chiral *N*-acylhydrazones

Early in the design phase, the hydrazone functional group emerged as a desirable starting point for a new chiral radical acceptor; some basic aspects of hydrazone structure and reactivity supported this notion. Although formation of *E/Z* mixtures frequently complicates the use of oxime ethers, aldehyde hydrazones generally adopt C=N *E*-geometry. In hydrazones, the nitrogen external to the C=N offers two valences from which to build a stereocontrol element, a further advantage over oxime ethers. Spectroscopic methods have shown *N,N*-dialkylhydrazones to have a predominant conformer with the *N*-alkyl bond nearly coplanar with C=N bond.<sup>163</sup> Hydrazones are more effective than imines as radical acceptors for nucleophilic alkyl radicals. Rate constants for 6-*aza*-5-hexenyl radical cyclizations (Scheme 4.7) of *N*-benzylimine, *O*-benzyloxime, and *N,N*-diphenylhydrazone are  $6.0 \times 10^6 \text{ s}^{-1}$ ,  $2.4 \times 10^7 \text{ s}^{-1}$ , and  $1.6 \times 10^8 \text{ s}^{-1}$  (80 °C), respectively.<sup>145</sup> This trend may be attributed to beneficial effects of the heteroatom substituent X (Scheme 4.7) of the C=N–X system, combining inductive activation of the acceptor toward nucleophilic radicals and stabilization of the adduct aminyl radical by the adjacent non-bonding electrons.

Scheme 4.7.



The exothermicity of 6-*aza*-5-hexenyl cyclization of a dimethylhydrazone (Scheme 4.7, X = NMe<sub>2</sub>;  $\Delta H = -11.6 \text{ kcal mol}^{-1}$ ) suggests an early transition state for the addition step.<sup>145</sup> This assumption simplifies the design of a stereocontrol model

because it enables the ground-state structure to serve as a reasonable approximation of the transition state geometry for radical addition to the hydrazones. Together, these factors prompted the choice of hydrazones as a platform for auxiliary design. It was therefore hypothesized that steric blocking of one of the diastereotopic approach trajectories by a substituent above or below the plane of the hydrazone should lead to a diastereoselective process.

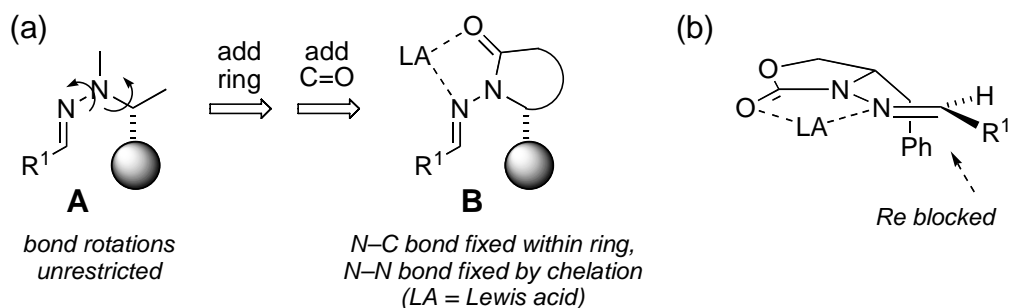


**Figure 4.4. (a) Design of a hypothetical N-linked auxiliary approach for stereocontrolled radical addition to C=N bonds, with Lewis acid (LA) chelation inducing a rigid, electronically activated radical acceptor. (b) Implementation with N-acylhydrazones derived from 4-benzyl-2-oxazolidinone.**

The design process next focused on incorporating specific features desirable for stereocontrol, namely *restricted rotamer populations* and *Lewis acid activation*, beginning with a hydrazone bearing a proximal stereogenic center (**A**, Figure 4.4). Constraining the C–N bond within a ring and including a carbonyl group would enable two-point binding of a Lewis acid to afford a rigid chelate structure (**B**) with the stereocontrol element localized over one face of the hydrazone. The Lewis acid would also increase reactivity toward nucleophilic radicals by lowering the LUMO energy of the C=N bond.<sup>164</sup> Finally, the facility of reductive cleavage of N–N bonds was



noted,<sup>165-167</sup> whereby an *N*-linked auxiliary could be released for reuse after stereoisomer purification. Oxazolidinones (e.g. **384**, Figure 4.3),<sup>168</sup> which had been previously used for stereocontrolled radical addition to alkenes,<sup>169,170</sup> emerged as obvious initial candidates to test the hypothesis.

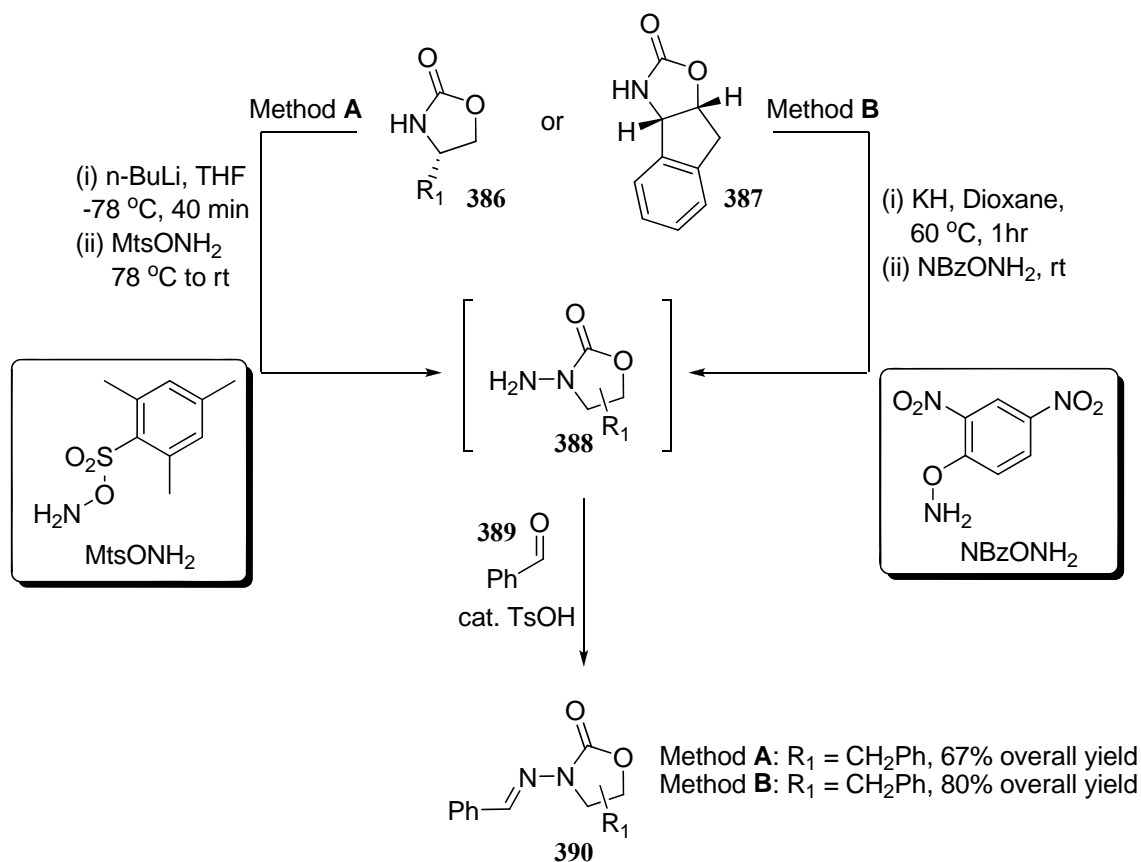
#### 4.2.1. Synthesis of chiral *N*-acylhydrazones

Experimental evaluation of the design hypothesis began with preparation of the requisite hydrazones (e.g. **390**, Scheme 4.8) and previous members of the Friestad group had developed two different methods for their preparation.<sup>171</sup> For example, sequential treatment of commercially available (*S*)-4-benzyl-2-oxazolidinone (**386**, R<sub>2</sub>=CH<sub>2</sub>Ph, Scheme 4.8, Method **A**) with *n*-butyllithium and *O*-(mesitylenesulfonyl)-hydroxylamine (MtsONH<sub>2</sub>) gives intermediate *N*-aminooxazolidinone **388** (R<sub>2</sub>=CH<sub>2</sub>Ph) which upon subsequent condensation with benzaldehyde (**389**) affords chiral *N*-acylhydrazone **390** (R<sub>2</sub>=CH<sub>2</sub>Ph) in 67% overall yield.

Alternatively, *N*-acylhydrazone **390** (R<sub>2</sub>=CH<sub>2</sub>Ph) can be prepared employing *O*-(*p*-nitrobenzoyl)hydroxylamine (NbzONH<sub>2</sub>, Scheme 4.8, Method **B**). This electrophilic ammonia equivalent is more easily prepared, handled, and stored than MtsONH<sub>2</sub>; the latter has a tendency toward exothermic decomposition. The optimized procedure for *N*-amination using NbzONH<sub>2</sub> involves heating the oxazolidinone **386** (R<sub>2</sub>=CH<sub>2</sub>Ph) with KH in dioxane, followed by introduction of NbzONH<sub>2</sub> as a solid at ambient temperature which affords *N*-aminooxazolidinone **388** (R<sub>2</sub>=CH<sub>2</sub>Ph). Subsequent condensation with benzaldehyde (**389**) provides chiral *N*-acylhydrazone **390** (R<sub>2</sub>=CH<sub>2</sub>Ph) with an improved 80% overall yield. Employing the optimized procedures

described above, a series of chiral *N*-acylhydrazones (e.g. **390**, Scheme 4.8) bearing different substituents on the oxazolidinone were prepared starting from commercially available chiral oxazolidinones and various aldehydes such as propionaldehyde, isobutyraldehyde, pivalaldehyde, ethyl 2-oxoacetate and benzaldehyde.

**Scheme 4.8.**

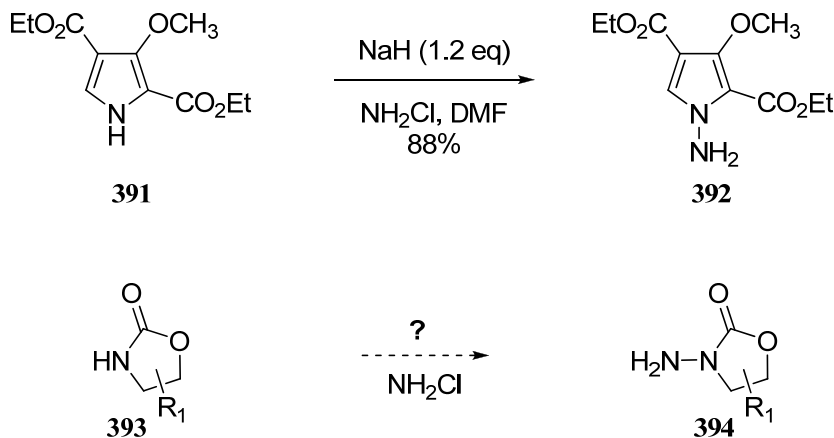


#### 4.2.1.1. *N*-amination of 4-alkyl-2-oxazolidinones with Monochloramine

Following Friestad's communication of the *N*-amination of 4-alkyl-2-oxazolidinones,<sup>171</sup> Hynes<sup>172</sup> et al. reported a simple, scalable method for *N*-amination of heterocyclic amines (e.g. **391**, Scheme 4.9) with monochloramine ( $\text{NH}_2\text{Cl}$ ). For

example, treating of 3-methoxypyrrole-2,4-dicarboxylate **391** with sodium hydride (NaH) followed by addition anhydrous ethereal  $\text{NH}_2\text{Cl}$  (1.2eq) produces hydrazine **392** in 88% yield. Ethereal  $\text{NH}_2\text{Cl}$  is readily prepared from  $\text{NH}_4\text{Cl}$ ,  $\text{NH}_4\text{OH}$ , and bleach, and the reaction byproducts are environmentally benign. Ease of reagent preparation, shorter reaction times and the possibility of using less harmful solvents prompted my investigation of  $\text{NH}_2\text{Cl}$  as an alternate  $\text{NH}_2^+$  source in the preparation of *N*-aminooxazolidonones (e.g. **394**, Scheme 4.9).

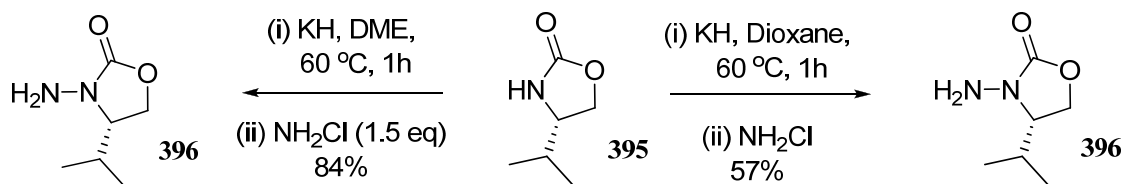
Scheme 4.9.



Preliminary studies revealed that  $\text{NH}_2\text{Cl}$  was able to induce *N*-amination of chiral oxazolidinone **395** (Scheme 4.10) in the presence of potassium hydride and dioxane to provide (S)-3-amino-4-isopropylloxazolidin-2-one **396**, although in a modest 57% yield. Optimization of reaction conditions showed that switching solvent systems from dioxane to dimethoxy ethane (DME) as well as using a freshly prepared solution of monochloramine in methyltertbutyl ether (MTBE) had a beneficial effect on the reaction outcome. Additionally, determining the concentration of monochloramine in

MTBE (achieved by iodometric titrations) prior to use, proved to be critical because hydrazines (e.g. **396**) can react with excess  $\text{NH}_2\text{Cl}$  to give oxidation products.<sup>172</sup> Thus, the optimized procedure for *N*-amination using  $\text{NH}_2\text{Cl}$  involves heating oxazolidinone **395** (Scheme 4.10) with potassium hydride in DME, followed by introduction of the  $\text{NH}_2\text{Cl}$  solution at ambient temperature which yields the desired *N*-amino-oxazolidinone **396** in 84% yield.

Scheme 4.10.

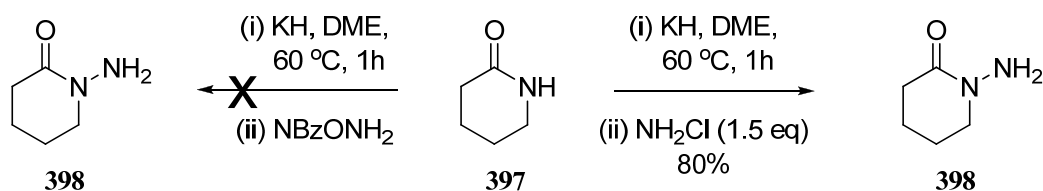


This result was satisfying because: (i) previously developed methods for *N*-amination of **395** sometimes, for reasons that have yet to be determined, lead to lower yields of **396** as a result of poor conversion in the amination step, a trend which was not observed when  $\text{NH}_2\text{Cl}$  was employed; (ii) the amination occurred at faster rates compared to the previous methods and complete conversions were observed within 30 minutes from the addition of the reagent; (iii) less toxic solvents could be used and (iv) the reaction byproducts are nontoxic (*N*-amination with  $\text{NBzONH}_2$  produces as a byproduct highly toxic 2,4-dinitrophenol with rat oral  $\text{LD}_{50} = 30 \text{ mg kg}^{-1}$ ).

The new protocol developed for *N*-amination of oxazolidinones was also applied to the preparation of 1-aminopiperidin-2-one (**398**, Scheme 4.11). Sequential treatment of  $\delta$ -valerolactam (**397**) with potassium hydride (KH) and  $\text{NH}_2\text{Cl}$  afforded

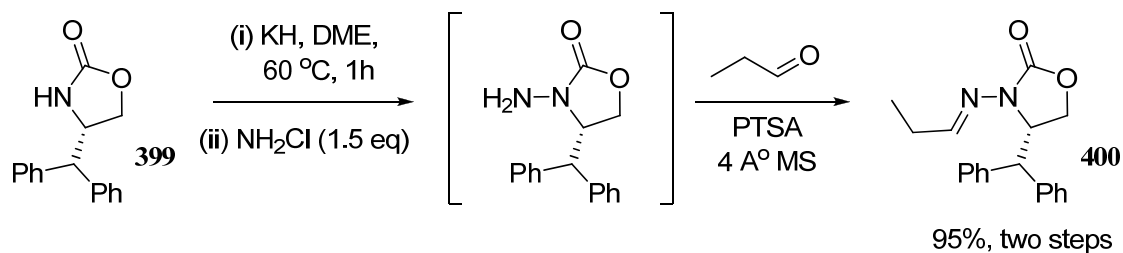
the desired acylhydrazine **398** in 80% yield. This result is notable because previous attempts made to promote the same transformation with NBzONH<sub>2</sub> and MtsONH<sub>2</sub> had always failed.

Scheme 4.11.



Introduction of activated 4 Å molecular sieves and propionaldehyde directly to the amination reaction mixture of (S)-4-benzhydryloxazolidin-2-one (**399**, Scheme 4.12) provided *N*-acylhydrazone **400** in 95% yield via a convenient one-pot protocol.

Scheme 4.12

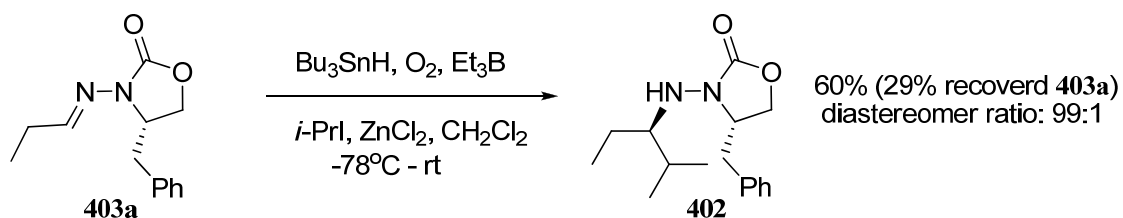


These preliminary results show that monochloramine is an efficient *N*-aminating agent for chiral oxazolidinones. However, further investigations are required in order to assess the full synthetic scope of this reaction.

#### 4.2.2. Effect of varying the stereocontrol element in radical additions to *N*-acylhydrazones

Previous work in the Friestad group showed that the addition of isopropyl iodide to propionaldehyde hydrazones (**403a**, Scheme 4.13) under tin hydride radical chain conditions in the presence of ZnCl<sub>2</sub> gave *N*-acylhydrazine adduct **402** in 60 % yield with a diastereomeric ratio of 99:1.<sup>173</sup>

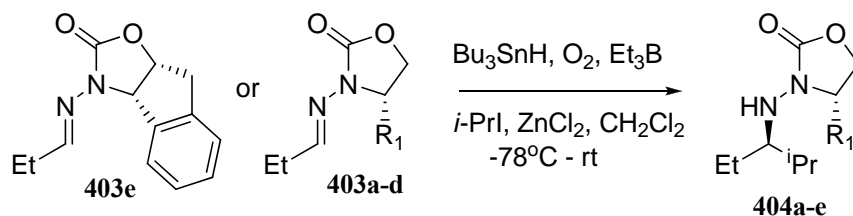
Scheme 4.13.



During my studies in the Friestad group, I investigated the effects of varying the stereocontrol element substituents on the oxazolidinone moiety, with the main goal to examine the change in diastereoselectivity. Isopropyl radical additions to several *N*-acylhydrazones **403a–e** are compared in Table 4.1. Although the yields given for reactions of **403b–e** (Entries 2–5) were inferior to the previous addition to **403a** (see Scheme 4.13), they were not optimized for yield and there was no attempt to achieve complete conversion. In the end I determined that all of the auxiliaries gave very high diastereoselectivity in the addition reactions, using the specific case of addition of isopropyl radical to propionaldehyde hydrazone. The benzyl (dr 99:1 by HPLC) and diphenylmethyl (dr >98:2 by <sup>1</sup>H NMR) blocking groups gave the most effective stereocontrol (Entries 1 & 2) and with diphenylmethyl (Entry 2), none of the minor

diastereomer could be detected by  $^1\text{H}$  NMR. The reason for decreased stereoselectivity in additions to **403d** and **403e** is unclear, but it might be speculated that increased rigidity of the blocking group on the oxazolidinone prevents the aromatic pi-system from effectively blocking the face of the C=N bond.

**Table 4.1. Diastereoselectivity in tin-mediated radical additions of isopropyl iodide with propionaldehyde hydrazone.**



Entry	hydrazone	R <sub>1</sub>	product, diastereomer ratio <sup>b</sup>
1	<b>403a</b>	CH <sub>2</sub> Ph	<b>404a</b> (60%) <sup>a</sup> , 99:1
2	<b>403b</b>	CHPh <sub>2</sub>	<b>404b</b> (15%) <sup>a</sup> , 98:2
3	<b>403c</b>	CHMe <sub>2</sub>	<b>404c</b> (16%) <sup>a</sup> , ---- <sup>c</sup>
4	<b>403d</b>	Ph	<b>404d</b> (35%) <sup>a</sup> , 94:6
5	<b>403e</b>	----	<b>404e</b> (50%) <sup>a</sup> , 95:5

Note: <sup>a</sup> Isolated Yield. <sup>b</sup> Ratios by HPLC (**404a**, **404e**) or  $^1\text{H}$  NMR integration (**404b**, **404d**) versus authentic mixtures. <sup>c</sup> Ratio not available; no method was found to resolve the diastereomers **404c**.

### 4.3. Conclusions

In summary, during my studies in the Friestad group, I investigated the use of monochloramine ( $\text{NH}_2\text{Cl}$ ) as an alternative reagent for the *N*-amination of oxazolidinones under milder conditions. Preliminary results show that this is a viable method for the preparation of chiral oxazolidinone hydrazines and acylhydrazines but further studies are necessary to establish the general synthetic scope of this reaction. I also studied intermolecular isopropyl radical additions to a series of propionaldehyde

*N*-acylhydrazones bearing different substituents on the oxazolidinone moiety, which revealed that benzyl and diphenylmethyl were the most effective stereocontrol elements. However, only slight differences were noted between the stereocontrol elements, which are insignificant from a synthetic standpoint.



## 5. CHAPTER 5: EXPERIMENTAL PROCEDURES

### 5.1. General

All reactions were carried out under an atmosphere of argon using flame-dried glassware. A Büchi rotary evaporator equipped with a water condenser and attached to a Welch Model 2026 self-cleaning dry vacuum system was used to concentrate *in vacuo*. Samples were further dried under reduced pressure on a high vacuum line.

Tetrahydrofuran (THF), dichloromethane ( $\text{CH}_2\text{Cl}_2$ ), and diethyl ether ( $\text{Et}_2\text{O}$ ) were dried via a Glass Contour solvent dispensing system. Commercially available  $\text{SnCl}_4$  was distilled twice from  $\text{P}_2\text{O}_5$  under inert atmosphere conditions and stored in sealed tubes under an atmosphere of nitrogen as a 1 M solution in  $\text{CH}_2\text{Cl}_2$ . Triethyl amine and diisopropyl amine were dried over  $\text{CaH}_2$  and subsequently distilled under nitrogen and stored in a septum sealed bottle over solid KOH. All other commercial reagents were purchased from Acros Organics or VWR International.

Radial chromatography refers to centrifugally accelerated thin-layer chromatography performed using a Chromatotron (Harrison Research, Palo Alto, CA) with precast rotors supplied by Analtech (Newark, DE). Infrared spectra were recorded with a Perkin-Elmer 2000 FT-IR spectrophotometer. Optical rotations were determined using a Rudolph Research Autopol IV polarimeter.

Reactions were cooled to  $-78\text{ }^\circ\text{C}$  via dry ice-acetone baths. Flash column chromatography was performed using Merck grade 60 silica gel (230-400 mesh) and TLC analysis was carried out using Merck 60F-254 silica on glass plates. Visualization

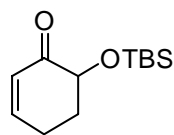
of TLC plates was achieved using ultraviolet light, polyphosphomolybdic acid and cerium sulfate in EtOH with H<sub>2</sub>SO<sub>4</sub>, ceric ammonium molybdate, or iodine.

<sup>1</sup>H and <sup>13</sup>C NMR spectra were recorded on a Bruker ARX 500 or a Varian Unity Inova 500 spectrometer in CDCl<sub>3</sub> at ambient temperature unless otherwise noted. <sup>1</sup>H chemical shifts in CDCl<sub>3</sub> were reported in ppm (δ units) downfield from tetramethylsilane. Solvent peaks were used as internal references for all <sup>13</sup>C NMR. Mass spectra were recorded on a LCT Premier (Waters) operated in positive ion electrospray mode by John Greaves at the University of California-Irvine.

Chromatographic diastereomer ratio analyses employed a Hewlett Packard 5988 GCMS with 15 mL x 0.25 mm I.D X 0.25 μ F.T 5%-phenyl-95%-dimethylsiloxane column and helium as mobile phase or Rainin Dynamax SD-200 HPLC system with Microsorb-MV Si 8um 100A column or Chiralcel OD 0.46 cm I. D. X 25 cm column and 2-propanol/hexane as mobile phase.

## 5.2. Experimental procedures for the preparation of new α-silyloxy and α-alkoxy ketones

### 6-(*tert*-butyldimethylsilyloxy)cyclohex-2-enone (137):

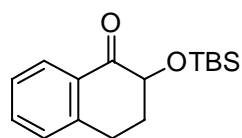


*tert*-Butyldimethylsilyl triflate (3.39 mL, 14.7 mmol) was added in a dropwise manner to a 0 °C solution of cyclohexenone (1.00 mL, 9.84 mmol) and anhydrous triethylamine (2.75 mL, 19.68 mmol) in CH<sub>2</sub>Cl<sub>2</sub> (50 mL) under an atmosphere of N<sub>2</sub>. The cold bath was removed and upon completion of the reaction

(determined by TLC; ~1h) the mixture was poured into a cold solution of aqueous saturated NaHCO<sub>3</sub>. The aqueous layer was extracted three times with hexanes, the organics were combined, washed with brine, and dried over anhydrous MgSO<sub>4</sub>. The solvents were removed *in vacuo* to provide the crude silylenolether, which was used without further purification.

The crude silylenolether (2.06 g) was dissolved in CH<sub>2</sub>Cl<sub>2</sub> (100 mL) and the mixture was cooled to 0 °C. Solid *m*-CPBA (70-75%, 2.90 g, 12.6 mmol) was added portion wise over a period of 30 min at which point the cold bath was removed. Upon completion of the reaction (as determined by TLC; ~1.5h) the mixture was washed with saturated aqueous Na<sub>2</sub>SO<sub>3</sub> solution, 10% aqueous Na<sub>2</sub>CO<sub>3</sub>, brine and dried (MgSO<sub>4</sub>). The solvents were removed *in vacuo* and the residue was purified by flash silica gel chromatography (hexane:EtOAc = 10:1) to afford pure title compound (0.986 g, 44% over two steps): <sup>1</sup>H NMR (500 MHz, CDCl<sub>3</sub>) δ 6.86-6.92 (m, 1H), 5.98 (ddd, *J* = 10.0, 2.4, 1.0 Hz, 1H), 4.17 (dd, *J* = 11.1, 4.5 Hz, 1H), 2.50 (dq, *J* = 19.1, 4.5 Hz, 1H), 2.37-2.46 (m, 1H), 2.13-2.20 (m, 1H), 2.00-2.10 (m, 1H), 0.91 (s, 9H), 0.16 (s, 3H), 0.08 (s, 3H); <sup>13</sup>C NMR (125 MHz, CDCl<sub>3</sub>) δ 198.7, 149.6, 128.6, 74.3, 32.6, 25.9, 25.4, 18.6, -4.3, -5.3; MS (ESI): Calculated for [C<sub>12</sub>H<sub>22</sub>O<sub>2</sub>SiNa]<sup>+</sup>: 249.1287. Found: 249.1283

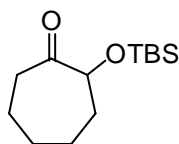
**2-(*tert*-butyldimethylsilyloxy)-3,4-dihydronaphthalen-1(2H)-one (139):**



Following the protocol described for the preparation of 6-(*tert*-butyldimethylsilyloxy)cyclohex-2-enone (**137**), title compound

was synthesized in 70% yield starting from  $\alpha$ -tetralone. Characterization data matched previously reported values.<sup>174</sup>

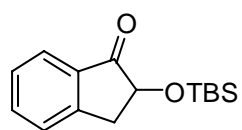
**2-(tert-butyldimethylsilyloxy)cycloheptanone (141):**



Following the protocol described for the preparation of 6-(*tert*-butyldimethylsilyloxy)cyclohex-2-enone (**137**), title compound was synthesized in 73% yield starting from cycloheptanone.

Characterization data matched previously reported values.<sup>175</sup>

**2-(tert-butyldimethylsilyloxy)-2,3-dihydro-1H-inden-1-one (144):**

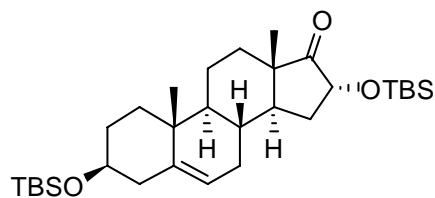


(1*H*-inden-3-yloxy)(*tert*-butyl)dimethylsilane<sup>176</sup> (1.865 g, 7.57 mmol) was added in a dropwise manner to a 0 °C solution of AD-mix- $\alpha$  (10.6 g), *t*-BuOH/H<sub>2</sub>O (36ml/36ml) and methylsulfonamide (716 mg, 7.57 mmol) under atmospheric pressure. The cold bath was removed and upon completion of the reaction (determined by TLC) the mixture was quenched with sodium sulfite and stirred at room temperature for 1 hour. The resulting mixture was extracted with 30 ml of CH<sub>2</sub>Cl<sub>2</sub> (three times), and combined organic extracts washed with 5% KOH and dried of anhydrous Na<sub>2</sub>SO<sub>4</sub>. The solvents were removed *in vacuo* to provide a crude mixture of title compound **144** and 2-hydroxy-2,3-dihydro-1*H*-inden-1-one which was submitted to subsequent *tert*butyldimethylsilyl protection.

*Tert*-butyldimethylsilyl chloride (335 mg, 2.25 mmol), imidazole (204 mg, 3 mmol) and dimethylamino pyridine (catalytic) were sequentially added to a stirring

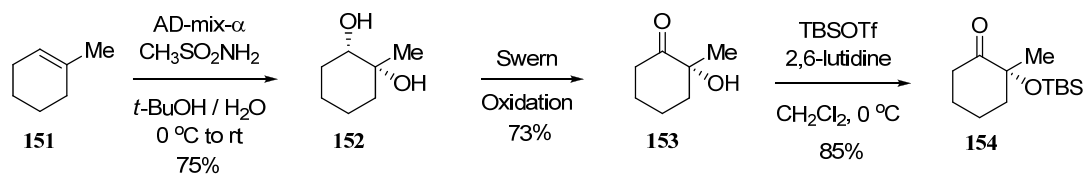
solution of crude **144** and 2-hydroxy-2,3-dihydro-1H-inden-1-one (~100 mg, 0.75 mmol by  $^1\text{H}$  NMR of crude) in anhydrous  $\text{CH}_2\text{Cl}_2$  at room temperature. Upon completion of the reaction (determined by TLC, ~ 2h) the mixture was quenched with saturated ammonium chloride solution, aqueous layer extracted with  $\text{CH}_2\text{Cl}_2$  (three times) and combined organic layers washed with brine and dried ( $\text{MgSO}_4$ ). The solvents were removed *in vacuo* and the residue was purified by flash silica gel chromatography (hexane:EtOAc = 20:1) to afford pure title compound (0.340 g, 20% over two steps). Characterization data matched previously reported values.<sup>177</sup>

### 3,16-bis(*tert*-butyldimethylsilyloxy)dehydroisoandrosterone (**150**):



*tert*-Butyldimethylsilyl chloride (6.93 g, 46 mmol) was added to a 0 °C solution of imidazole (4.70 g, 69 mmol), 4-*N,N*-dimethylaminopyridine (0.07 g, 0.58 mmol) and 16-hydroxydehydroisoandrosterone<sup>85</sup> (11.5 mmol, 3.5 g) in  $\text{CH}_2\text{Cl}_2$  (100 mL). The cold bath was removed, the mixture stood at room temperature for 12 h and was then poured into aqueous 1% HCl (100 mL), the aqueous layer was extracted twice with EtOAc (200 mL) and the combined organics were washed with aqueous saturated  $\text{NaHCO}_3$ , water, brine, dried ( $\text{MgSO}_4$ ) and concentrated to an off white solid which was purified by chromatography (90/10 Hexane/EtOAc) to provide 5.42 g (10.2 mmol, 89% yield) of the titled product:  $^1\text{H}$  NMR (500 MHz,  $\text{CDCl}_3$ )  $\delta$  5.31-5.37 (m, 1H), 4.33 (d,  $J$  = 7.9 Hz, 1H), 3.44-3.53 (m, 1H), 2.23-2.31 (m, 1H), 2.19 (ddd,  $J$  = 13.3, 5.0, 2.1 Hz, 1H), 2.01-2.09 (m, 1H), 1.87-1.96 (m, 1H), 1.32-1.85 (m, 11H), 0.98-

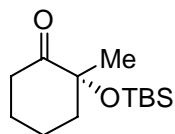
1.12 (m, 2H), 1.02 (s, 3H), 0.91 (s, 3H), 0.89 (s, 18H), 0.12 (s, 3H), 0.10 (s, 3H), 0.06 (s, 6H);  $^{13}\text{C}$  NMR (125 MHz,  $\text{CDCl}_3$ )  $\delta$  217.8, 141.7, 120.4, 72.4, 72.2, 50.2, 48.6, 47.0, 42.7, 37.2, 36.7, 32.8, 32.0, 31.4, 31.3, 30.5, 25.9, 25.8, 20.0, 19.4, 18.4, 18.2, 14.3, -4.6, -4.5, -5.2; MS (ESI): Calculated for  $[\text{C}_{31}\text{H}_{56}\text{O}_3\text{Si}_2\text{Na}]^+$ : 555.3666. Found: 555.3669.



**(R)-2-hydroxy-2-methylcyclohexanone (153):**

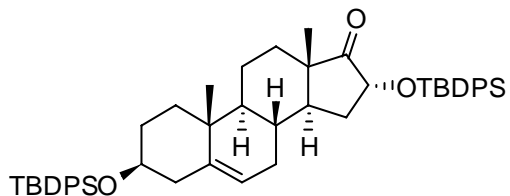
To a solution of DMSO (2.18 ml, 27.98 mmol) in  $\text{CH}_2\text{Cl}_2$  at  $-78\text{ }^\circ\text{C}$  (COCl) $_2$  (1.093 ml, 11.75 mmol) was added dropwise via syringe. The mixture was stirred for 10 min at  $-78\text{ }^\circ\text{C}$ , then a solution of diol **152**<sup>178</sup> (1.457 g, 11.19 mmol) in  $\text{CH}_2\text{Cl}_2$  was added via cannula. The resulting cloudy mixture was stirred at  $-78\text{ }^\circ\text{C}$  for 1h and  $\text{NEt}_3$  (7.8 ml, 55.95 mmol) was added. The mixture was then warmed to room temperature, extracted with  $\text{Et}_2\text{O}$ , and the organic extracts were dried ( $\text{MgSO}_4$ ), filtered, and concentrated *in vacuo*. Purification of the residue via flash chromatography (pentane: $\text{Et}_2\text{O}$  = 4:1) provided 1.044 g (73%) of title compound. Characterization data matched previously reported values.<sup>179</sup>

**(R)-2-(tert-butyldimethylsilyloxy)-2-methylcyclohexanone (154):**



*tert*-Butyldimethylsilyl triflate (2.81 mL, 12.2 mmol) was added to a 0 °C solution of (R)-2-hydroxy-2-methylcyclohexanone (**153**) (1.04 g, 8.1 mmol) and 2,6-lutidine (1.87 mL, 16.2 mmol) in CH<sub>2</sub>Cl<sub>2</sub> (40 mL). The mixture stood at 0 °C for 2 h and was then poured into saturated aqueous NaHCO<sub>3</sub>. The organics were separated, washed with aqueous 10% HCl, saturated NaHCO<sub>3</sub>, brine, dried (MgSO<sub>4</sub>) and concentrated in vacuo. The oily residue was purified by flash silica gel chromatography (20:1 hexane/EtOAc) to provide 1.67 g (85%) of the title compound: <sup>1</sup>H NMR (500 MHz, CDCl<sub>3</sub>) δ 2.81 (ddd, *J* = 13.1, 11.4, 5.7 Hz, 1H), 2.25 (dt, *J* = 13.3, 4.9 Hz, 1H), 1.88-2.02 (m, 3H), 1.61-1.72 (m, 1H), 1.51-1.61 (m, 2H), 1.31 (s, 3H), 0.90 (s, 9H), 0.12 (s, 3H), 0.03 (s, 3H); <sup>13</sup>C NMR (125 MHz, CDCl<sub>3</sub>) δ 212.0, 78.5, 43.2, 38.4, 27.9, 25.9, 24.4, 21.3, 18.3, -2.1, -3.0; MS (ESI): Calculated for [C<sub>13</sub>H<sub>26</sub>O<sub>2</sub>SiNa]<sup>+</sup>: 265.1600. Found: 265.1593.

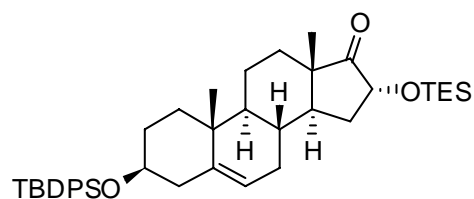
**3,16-bis(tert-butyldiphenylsilyloxy)dehydroisoandrosterone (343):**



*tert*-Butyldiphenylsilyl chloride (12.64g, 46 mmol) was added to a 0 °C solution of imidazole (4.70 g, 69 mmol), 4-*N,N*-dimethylaminopyridine (0.07 g, 0.58 mmol) and 16-hydroxydehydroisoandrosterone<sup>85</sup> (3.5 g, 11.5 mmol) in CH<sub>2</sub>Cl<sub>2</sub> (100 mL). The cold bath was removed, the mixture stood at room temperature for 12h and was then poured into aqueous 1% HCl (100 mL), the aqueous layer was extracted twice with

EtOAc (200 mL) and the combined organics were washed with aqueous saturated NaHCO<sub>3</sub>, water, brine, dried (MgSO<sub>4</sub>) and concentrated to an off white solid which was purified by chromatography (90:10 = Hexane:EtOAc) to provide 8.09 g (10.35 mmol, 90 % yield) of the titled product: <sup>1</sup>H NMR (500 MHz, CDCl<sub>3</sub>) δ 7.75 (m, 3H), 7.65-7.68 (m, 8H), 7.34-7.41 (m, 10H), 5.12 (m, 1H), 4.33 (d, *J* = 7.61 Hz, 1H), 3.49-3.56 (m, 1H), 2.32 (m, 1H), 2.14 (ddd, *J* = 13.3, 4.59, 2.1 Hz, 1H); 1.85-1.95 (m, 1H), 1.24-1.80 (m, 11H), 1.06 (s, 18H), 0.97 (s, 3H), 0.81-0.94 (m, 3H), 0.77 (s, 3H); <sup>13</sup>C NMR (125 MHz, CDCl<sub>3</sub>) δ 217.2, 141.4, 135.8, 135.75, 135.73, 134.73, 134.71, 134.05, 133.23, 129.65, 129.45, 127.57, 127.52, 127.46, 127.44, 120.30, 73.07, 72.76, 50.07, 48.63, 47.00, 42.43, 37.06, 36.57, 31.48, 31.24, 30.47, 26.99, 26.85, 19.97, 19.40, 19.27, 19.12, 14.20; MS (ESI): Calculated for [C<sub>51</sub>H<sub>64</sub>O<sub>3</sub>Si<sub>2</sub>Na]<sup>+</sup>: 803.4292. Found: 803.4285.

**3-(*tert*-butyldiphenylsilyloxy)-16-(triethylsilyloxy)dehydroisoandrosterone (346a):**



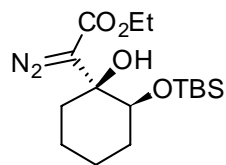
Triethylsilyl chloride (139 μL, 0.828 mmol) was added to a 0 °C solution of imidazole (75 mg, 1.10 mmol), 4-*N,N*-dimethylaminopyridine (2 mg, 0.0828 mmol) and 3-(*tert*-butyldiphenylsilyloxy)-16-hydroxydehydroisoandrosterone<sup>85</sup> (300 mg, 0.552 mmol) in CH<sub>2</sub>Cl<sub>2</sub> (6 mL). The cold bath was removed, the mixture stood at room temperature for 3h and was then poured into aqueous ammonium chloride, the aqueous layer was extracted twice with CH<sub>2</sub>Cl<sub>2</sub> and the combined organics were washed with, water,



brine, dried (MgSO<sub>4</sub>) and concentrated to an off white solid which was purified by chromatography (25:1 = Hexane:EtOAc) to provide 354 mg (90 % yield) of the titled product: <sup>1</sup>H NMR (500 MHz, CDCl<sub>3</sub>) δ 7.65-7.69 (m, 4H), 7.32-7.44 (m, 6H), 5.13 (m, 1H), 4.34 (d, *J* = 7.66 Hz, 1H), 3.50-3.56 (m, 1H), 2.29-2.36 (m, 1H), 2.11-2.18 (m, 1H), 1.82-2.00 (m, 2H), 1.64-1.82 (m, 4H), 1.49-1.64 (m, 6H), 1.22-1.48 (m, 3H), 1.08 (s, 9H), 1.03 (s, 3H), 0.98 (t, *J* = 8.0 Hz, 9 H), 0.88 (s, 3H), 0.56-0.67 (m, 6H); <sup>13</sup>C NMR (125 MHz, CDCl<sub>3</sub>) δ 217.80, 141.39, 134.69, 127.44, 127.42, 120.36, 73.04, 71.90, 50.03, 48.62, 47.04, 42.42, 36.57, 30.46, 26.98, 19.41, 19.10, 14.29, 6.67, 4.73; MS (ESI): Calculated for [C<sub>41</sub>H<sub>60</sub>O<sub>3</sub>Si<sub>2</sub>Na]<sup>+</sup>: 679.3979. Found: 679.3989.

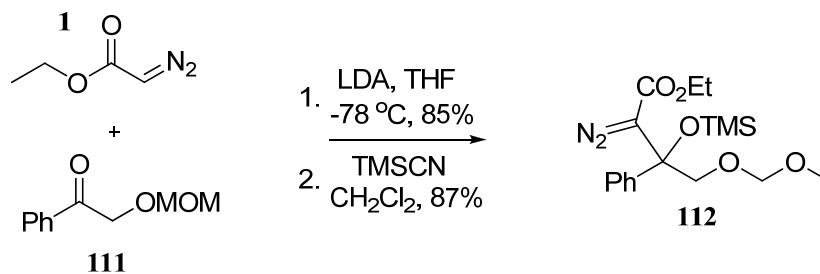
### 5.3. Experimental procedures for the preparation $\gamma$ -hydroxy- $\beta$ -silyloxy- $\alpha$ -diazoesters and $\gamma$ -hydroxy- $\beta$ -alkoxy- $\alpha$ -diazoesters

#### Ethyl 2-(2-(*tert*-butyldimethylsilyloxy)-1-hydroxycyclohexyl)-2-diazoacetate (**128s**)

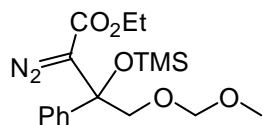


A cold (-78 °C) solution of lithium diisopropylamide [prepared by the addition of *n*-butyllithium in hexanes (5.26 mL of a 2.5 M solution) to a solution of diisopropylamine (2.12 mL, 14.89 mmol) in THF (10 mL)] was added via cannula over a period of 30 min to a stirred -78 °C solution of 2-(*tert*-butyldimethylsilyloxy)cyclohexanone (**127**)<sup>180</sup> (2.00 g, 8.76 mmol) and ethyl diazoacetate (1.48 mL, 14.02 mmol) in THF (80 mL). The mixture was maintained at -78 °C until complete conversion was achieved as monitored by TLC (~ 30 min). Saturated aqueous NH<sub>4</sub>Cl solution (10 mL) was added to the cold reaction

mixture and upon reaching room temperature the mixture was diluted further with saturated aqueous  $\text{NH}_4\text{Cl}$ . The aqueous layer was extracted three times with EtOAc, the combined organic extracts were washed with brine, dried ( $\text{MgSO}_4$ ), and concentrated under reduced pressure. The residue was subjected to flash silica gel chromatography (Hexane:Et<sub>2</sub>O = 20:1; R<sub>f</sub> : 0.25) to afford  $\beta$ -hydroxy- $\gamma$ -silyloxy- $\alpha$ -diazoester **128s** (2.67 g, 89%): <sup>1</sup>H NMR (500 MHz, CDCl<sub>3</sub>)  $\delta$  4.22 (dq,  $J$  = 10.8, 7.1 Hz, 1H), 4.16 (dq,  $J$  = 10.8, 7.1 Hz, 1H), 4.09 (dd,  $J$  = 10.9, 5.2 Hz, 1H), 3.11 (d,  $J$  = 2.4 Hz, 1H), 2.03 (tdd,  $J$  = 13.9, 4.6, 2.4 Hz, 1H), 1.89 (dq,  $J$  = 13.8, 3.1 Hz, 1H), 1.70-1.77 (m, 1H), 1.62-1.69 (m, 1H), 1.45-1.63 (m, 4H), 1.27 (t,  $J$  = 7.1 Hz, 3H), 0.88 (s, 9H), 0.06 (s, 3H), 0.01 (s, 3H); <sup>13</sup>C NMR (125 MHz, CDCl<sub>3</sub>)  $\delta$  166.0, 71.9, 71.5, 64.1, 60.3, 34.1, 31.3, 25.8, 23.7, 21.0, 17.9, 14.7, -4.3, -5.2; IR (film) 3487, 2936, 2860, 2094, 1685, 1299, 1252, 1093, 837 cm<sup>-1</sup>; MS (ESI): Calculated for [C<sub>16</sub>H<sub>30</sub>N<sub>2</sub>O<sub>4</sub>SiNa]<sup>+</sup>: 365.1873. Found: 365.1867.



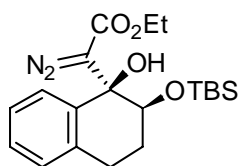
**Ethyl 2-diazo-4-(methoxymethoxy)-3-phenyl-3-(trimethylsilyloxy)butanoate (112):**



Ethyl lithio-diazoacetate addition was performed according to the protocol described for the preparation of **128s** and the resulting free tertiary alcohol was protected by the following protocol. TMSCN (2.56 ml, 19.1 mmol) and free tertiary alcohol (0.562 g, 1.91 mmol)

were heated neat at 80 °C and allowed to react overnight. Upon completion the resulting crude oil was subjected to flash silica gel chromatography (Hexane:Et<sub>2</sub>O = 5:1; R<sub>f</sub>: 0.25) to afford title compound (0.556 g, 87%); <sup>1</sup>H NMR (500 MHz, CDCl<sub>3</sub>) δ 7.53 – 7.48 (m, 2H), 7.33 (t, *J* = 7.5, 2H), 4.59 (d, *J* = 1.3, 2H), 4.13 (q, *J* = 7.1, 2H), 4.02 (dd, *J* = 25.0, 10.2, 2H), 3.26 (s, 3H), 1.17 (t, *J* = 7.1, 3H), 0.15 (s, 9H).

**Ethyl 2-(2-(tert-butyldimethylsilyloxy)-1-hydroxy-1,2,3,4-tetrahydronaphthalen-1-yl)-2-diazoacetate (155): Obtained as a 11:1 ratio of diastereomers**

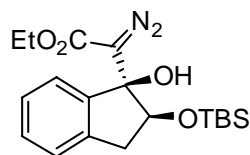


Chromatography eluent (20:1 Hexane:EtOAc; R<sub>f</sub>: 0.32); Isolated yield: 91%; <sup>1</sup>H NMR (500 MHz, CDCl<sub>3</sub>) δ 7.52 (m, 1H), 7.21 (m, 2H), 7.08 (m, 1H), 4.44 (dd, *J* = 11.09, 3.68 Hz, 1H), 4.10-4.18

(m, 1H), 4.04 (dq, *J* = 10.77, 7.14 Hz, 1H), 3.82 (s, 1H), 2.83-2.93 (m, 2H), 2.00-2.09 (m, 1H), 1.88-1.94 (m, 1H), 1.15 (t, *J* = 6.74 Hz, 3H), 0.93 (s, 9H), 0.14 (s, 3H), 0.10 (s, 3H); <sup>13</sup>C NMR (125 MHz, CDCl<sub>3</sub>) δ 165.4, 137.7, 136.5, 128.3, 128.2, 128.1, 126.5, 72.3, 71.5, 65.1, 60.3, 27.9, 27.8, 25.7, 17.8, 14.4, -4.5, -5.3; MS (ESI): Calculated for [C<sub>20</sub>H<sub>30</sub>O<sub>4</sub>N<sub>2</sub>SiNa]<sup>+</sup>: 413.1873. Found: 413.1870.

Observable Resonances from Minor Diastereomer: <sup>1</sup>H NMR (500 MHz, CDCl<sub>3</sub>) δ 7.60-7.63 (m, 1H), 4.24-4.32 (m, 2H), 2.98-3.07 (m, 1H), 2.69 (dt, *J* = 16.5, 5.2 Hz, 1H), 2.15-2.23 (m, 1H), 0.87 (s, 9H), 0.11 (s, 3H), 0.08 (s, 3H).

**Ethyl 2-(2-(tert-butyldimethylsilyloxy)-1-hydroxy-2,3-dihydro-1*H*-inden-1-yl)-2-diazoacetate (156): Obtained as a 11:1 ratio of diastereomers**



Chromatography eluent (20:1 Hexane:EtOAc; Rf: 0.20); Isolated

yield: 87%; Major Diastereomer:  $^1\text{H}$  NMR (500 MHz,  $\text{CDCl}_3$ )  $\delta$

7.35 (d,  $J = 6.6$  Hz, 1H), 7.23-7.29 (m, 2H), 7.19 (d,  $J = 7.0$  Hz,

1H), 4.84 (t,  $J = 6.9$  Hz, 1H), 4.05-4.25 (m, 2H), 4.02 (s, 1H), 3.18 (dd,  $J = 15.4$ , 7.1

Hz, 1H), 2.91 (dd,  $J = 15.3$ , 6.8 Hz, 1H), 1.19 (t,  $J = 7.0$  Hz, 3H), 0.94 (s, 9H), 0.15 (s,

3H), 0.14 (s, 3H);  $^{13}\text{C}$  NMR (125 MHz,  $\text{CDCl}_3$ )  $\delta$  165.3, 141.8, 139.8, 129.3, 127.2,

125.1, 124.2, 77.1, 76.5, 62.2, 60.4, 38.2, 25.7, 18.0, 14.4, -4.7, -5.0; MS (ESI):

Calculated for  $[\text{C}_{19}\text{H}_{28}\text{N}_2\text{O}_4\text{SiNa}]^+$ : 399.1716. Found: 399.1709.

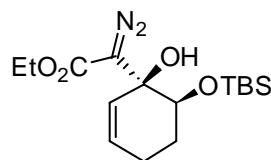
Observable Resonances from Minor Diastereomer:  $^1\text{H}$  NMR (500 MHz,  $\text{CDCl}_3$ )  $\delta$  7.46

(d,  $J = 6.6$  Hz, 1H), 4.53 (t,  $J = 5.6$  Hz, 1H), 4.28 (q,  $J = 7.2$  Hz, 2H), 3.25 (dd,  $J =$

15.9, 6.0 Hz, 1H), 2.73 (dd,  $J = 15.8$ , 5.4 Hz, 1H), 0.88 (s, 9H), 0.12 (s, 3H), 0.11 (s,

3H).

**Ethyl 2-(6-(tert-butyldimethylsilyloxy)-1-hydroxycyclohex-2-enyl)-2-diazoacetate (157s):**



Chromatography eluent (20:1Hexane:EtOAc; Rf : 0.25); Isolated

yield: 91% of a 5:1 mixture of diastereomers; Selective

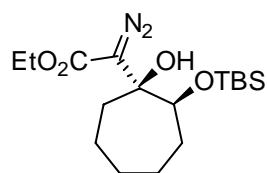
crystallization of the major diastereomer (67% return) was

achieved by dissolving 1.04 g of sample in methanol (5 mL) and allowing the solution

to stand overnight at  $-20\text{ }^\circ\text{C}$ ;  $^1\text{H}$  NMR (500 MHz,  $\text{CDCl}_3$ )  $\delta$  5.93-5.98 (m, 1H), 5.67

(ddd,  $J = 9.9, 2.4, 1.7$  Hz, 1H), 4.11-4.28 (m, 3H), 3.65 (s, 1H), 2.09-2.25 (m, 2H), 1.79-1.90 (m, 1H), 1.68-1.76 (m, 1H), 1.26 (t,  $J = 7.3$  Hz, 3H), 0.91 (s, 9H), 0.1 (s, 3H), 0.07 (s, 3H);  $^{13}\text{C}$  NMR (125 MHz,  $\text{CDCl}_3$ )  $\delta$  165.5, 131.9, 128.5, 71.1, 68.4, 63.5, 60.3, 27.2, 25.6, 24.1, 17.8, 14.5, -4.6, -5.3; MS (ESI): Calculated for  $[\text{C}_{16}\text{H}_{28}\text{N}_2\text{O}_4\text{SiNa}]^+$ : 363.1716. Found: 363.1721.

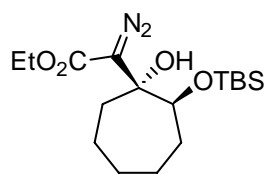
**Ethyl 2-(*cis*-2-(tert-butyldimethylsilyloxy)-1-hydroxycycloheptyl)-2-diazoacetate (158s):**



Chromatography eluent (20:1 Pentane: $\text{Et}_2\text{O}$ ; Rf: 0.25); Isolated yield: 23%;  $^1\text{H}$  NMR (500 MHz,  $\text{CDCl}_3$ )  $\delta$  4.21 (dq,  $J = 10.8, 7.1$  Hz, 1H), 4.16 (dq,  $J = 10.8, 7.1$  Hz, 1H), 4.11 (dd,  $J = 10.4,$

3.1 Hz, 1H), 3.60 (d,  $J = 1.7$  Hz, 1H), 2.14-2.22 (m, 1H), 1.67-1.95 (m, 4H), 1.40-1.59 (m, 5H), 1.26 (t,  $J = 7.1$  Hz, 3H), 0.88 (s, 9H), 0.07 (s, 3H), 0.01 (s, 3H);  $^{13}\text{C}$  NMR (125 MHz,  $\text{CDCl}_3$ )  $\delta$  166.1, 73.1, 66.2, 60.1, 35.0, 30.4, 26.3, 25.7, 21.3, 18.9, 17.7, 14.5, -4.6, -5.4; MS (ESI): Calculated for  $[\text{C}_{17}\text{H}_{32}\text{O}_4\text{N}_2\text{SiNa}]^+$ : 379.2029. Found: 379.2029.

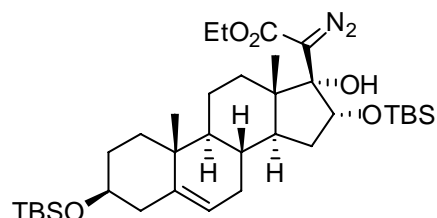
**Ethyl 2-(*trans*-2-(tert-butyldimethylsilyloxy)-1-hydroxycycloheptyl)-2-diazoacetate (158a):**



Chromatography eluent (20:1 Pentane: $\text{Et}_2\text{O}$ ; Rf: 0.20); Isolated yield: 65%;  $^1\text{H}$  NMR (500 MHz,  $\text{CDCl}_3$ )  $\delta$  4.46 (s, 1H), 4.26 (dq,

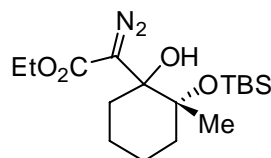
$J = 10.7, 7.1$  Hz, 1H), 4.21 (dq,  $J = 10.7, 7.1$  Hz, 1H), 3.97 (d,  $J = 6.9$  Hz, 1H), 1.96 (dddd,  $J = 14.8, 11.3, 3.4, 1.4$  Hz, 1H), 1.73-1.87 (m, 4H), 1.48-1.68 (m, 4H), 1.40-1.48 (m, 1H), 1.28 (t,  $J = 7.0$  Hz, 3H), 0.90 (s, 9H), ) 0.04 (s, 3H), -0.01 (s, 3H);  $^{13}\text{C}$  NMR (125 MHz,  $\text{CDCl}_3$ )  $\delta$  168.3, 76.2, 75.5, 62.1, 60.7, 33.3, 28.6, 26.5, 25.8, 19.6, 19.2, 17.9, 14.5, -4.7, -5.6; MS (ESI): Calculated for  $[\text{C}_{17}\text{H}_{32}\text{O}_4\text{N}_2\text{SiNa}]^+$ : 379.2029. Found: 379.2022.

**Ethyl 2-((3S,10R,13S,16R,17R)-3,16-bis(tert-butyldimethylsilyloxy)-17-hydroxy-10,13-dimethyl-2,3,4,7,8,9,10,11,12,13,14,15,16,17-tetradecahydro-1H-cyclopenta[a]phenanthren-17-yl)-2-diazoacetate (159s):**



Chromatography eluent (98:2 Hexane: $\text{Et}_2\text{O}$ ; Rf: 0.22); Isolated yield: 46%;  $^1\text{H}$  NMR (500 MHz,  $\text{CDCl}_3$ )  $\delta$  5.36 (dd,  $J = 9.0, 1.7$  Hz, 1H), 5.27-5.31 (m, 1H), 4.20 (dq,  $J = 10.8, 7.3$  Hz, 1H), 4.13 (dq,  $J = 10.8, 7.3$  Hz, 1H), 4.02 (s, 1H), 3.43-3.52 (m, 1H), 2.21-2.30 (m, 1H), 2.16 (ddd,  $J = 13.2, 4.9, 2.1$  Hz, 1H), 1.88-1.98 (m, 2H), 1.65-1.83 (m, 4H), 1.35-1.64 (m, 7H), 1.26 (t,  $J = 7.3$  Hz, 3H), 0.94-1.08 (m, 2H), 1.00 (s, 3H), 0.89 (s, 9H), 0.88 (s, 9H), 0.77 (s, 3H), 0.09 (s, 3H), 0.06 (s, 6H), 0.05 (s, 3H);  $^{13}\text{C}$  NMR (125 MHz,  $\text{CDCl}_3$ )  $\delta$  165.9, 141.6, 120.7, 79.1, 72.5, 71.6, 60.8, 60.1, 50.0, 49.9, 47.9, 42.8, 37.2, 36.6, 34.4, 32.0, 31.8, 30.3, 25.9, 25.7, 19.8, 19.4, 18.2, 17.9, 15.1, 14.5, -4.5, -4.6, -5.0; MS (ESI): Calculated for  $[\text{C}_{35}\text{H}_{62}\text{O}_5\text{N}_2\text{Si}_2\text{Na}]^+$ : 669.4095. Found: 669.4096.

**Ethyl 2-(2-(tert-butyldimethylsilyloxy)-1-hydroxy-2-methylcyclohexyl)-2-diazoacetate (160):**



Chromatography eluent (20:1 Hexane:EtOAc; Rf: 0.25); Isolated

yield: 95%;  $^1\text{H}$  NMR (500 MHz,  $\text{CDCl}_3$ )  $\delta$  4.18 (qd,  $J = 6.9, 2.1$

Hz, 2H), 3.99 (d,  $J = 2.8$  Hz, 1H), 2.29 (tdd,  $J = 13.9, 4.5, 2.4$

Hz, 1H), 1.80-1.91 (m, 2H), 1.72 (qt,  $J = 13.2, 4.2$  Hz, 1H), 1.59-1.66 (m, 2H), 1.46-

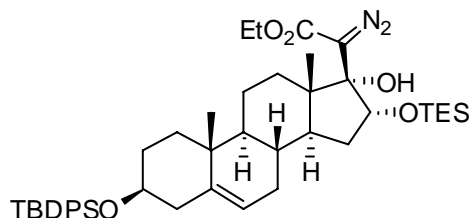
1.53 (m, 1H), 1.35 (s, 3H), 1.28-1.34 (m, 1H), 1.26 (t,  $J = 6.9$  Hz, 3H), 0.88 (s, 9H),

0.14 (s, 3H), 0.12 (s, 3H);  $^{13}\text{C}$  NMR (125 MHz,  $\text{CDCl}_3$ )  $\delta$  166.4, 81.0, 74.9, 62.5, 60.1,

37.8, 31.8, 25.9, 23.5, 23.1, 20.3, 18.0, 14.4, -1.9, -2.1; MS (ESI): Calculated for

$[\text{C}_{17}\text{H}_{32}\text{O}_4\text{N}_2\text{SiNa}]^+$ : 379.2029. Found: 379.2018.

**Ethyl 2-((3S,8R,9S,10R,13S,14S,16R,17R)-3-(tert-butyldiphenylsilyloxy)-17-hydroxy-10,13-dimethyl-16-(triethylsilyl)-2,3,4,7,8,9,10,11,12,13,14,15,16,17-tetradecahydro-1H-cyclopenta[a]phenanthren-17-yl)-2-diazoacetate (181s):**



Chromatography eluent (98:2 Hexane:Et<sub>2</sub>O; Rf:

0.25); Isolated yield: 65.3%;  $^1\text{H}$  NMR (500

MHz,  $\text{CDCl}_3$ )  $\delta$  7.65-7.70 (m, 4H), 7.34-7.44 (m,

6H), 5.34 (dd,  $J = 8.86, 1.61$  Hz, 1H), 5.14 (m.

1H), 4.21 (dq,  $J = 10.8, 7.12$  Hz, 1H), 4.13 (dq,  $J = 10.8, 7.12$  Hz, 1H), 4.09 (s, 1H),

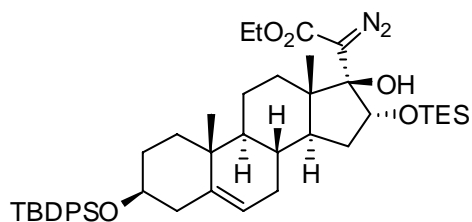
3.54 (m, 1H), 2.32 (m, 1H), 2.14 (ddd,  $J = 13.21, 5.4, 1.8$  Hz, 1H), 1.81-1.91 (m, 1H),

1.29-1.77 (m, 13 H), 1.26 (t,  $J = 7.10$  Hz, 3H), 1.06 (s, 9H), 1.02 (s, 3H), 0.93 (t,  $J =$

7.94 Hz, 9H), 0.77 (s, 3H), 0.66 (q,  $J = 7.94$  Hz, 6H);  $^{13}\text{C}$  NMR (125 MHz,  $\text{CDCl}_3$ )  $\delta$

165.97, 141.27, 135.72, 134.76, 129.40, 127.42, 120.73, 78.99, 73.12, 71.20, 60.85, 60.04, 50.00, 49.75, 47.80, 42.44, 37.05, 36.53, 34.67, 31.93, 31.80, 31.71, 30.21, 26.98, 19.75, 19.38, 19.09, 15.06, 14.48, 6.56, 4.61. MS (ESI): Calculated for  $[C_{45}H_{66}N_2O_4Si_2Na]^+$ : 793.4408. Found: 793.4406.

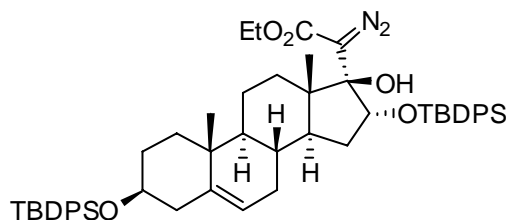
**Ethyl 2-((3S,8R,9S,10R,13S,14S,16R,17S)-3-(tert-butyldiphenylsilyloxy)-17-hydroxy-10,13-dimethyl-16-(triethylsilyl)-2,3,4,7,8,9,10,11,12,13,14,15,16,17-tetradecahydro-1H-cyclopenta[a]phenanthren-17-yl)-2-diazoacetate (181a):**



Chromatography eluent (98:2 Hexane:Et<sub>2</sub>O; R<sub>f</sub>: 0.22); Isolated yield: 17.6%; <sup>1</sup>H NMR (500 MHz, CDCl<sub>3</sub>) δ 7.65-7.70 (m, 4H), 7.32-7.42 (m, 6H), 5.10 (d, *J* = 4.81 Hz, 1H), 5.03 (br s, 1H), 4.50 (dd, *J* = 10.5, 4.0 Hz, 1H), 4.22 (dq, *J* = 7.09, 2.96 Hz, 2H), 3.49 (m, 1H), 2.32 (m, 1H), 2.13 (m, 1H), 1.75-1.95 (m, 2H), 1.31-1.75 (m, 10H), 1.30 (t, *J* = 7.11 Hz, 3H), 1.08-1.22 (m, 3H), 1.05 (s, 9H), 1.00 (s, 3H), 0.94 (t, *J* = 7.95 Hz, 9H), 0.89 (s, 3H), 0.56-0.67 (m, 6H); <sup>13</sup>C NMR (125 MHz, CDCl<sub>3</sub>) δ 169.90, 141.40, 135.74, 134.75, 134.72, 129.44, 127.44, 120.50, 87.28, 79.39, 73.20, 60.83, 56.90, 50.08, 49.71, 49.10, 42.44, 37.06, 36.48, 34.15, 33.26, 32.30, 31.80, 31.68, 26.98, 20.13, 19.36, 19.11, 14.89, 14.39, 6.62, 4.65. MS (ESI): Calculated for  $[C_{45}H_{66}N_2O_4Si_2Na]^+$ : 793.4408. Found: 793.4409.



**Ethyl 2-((3S,8R,9S,10R,13S,14S,16R,17S)-3,16-bis(tert-butyldiphenylsilyloxy)-17-hydroxy-10,13-dimethyl-2,3,4,7,8,9,10,11,12,13,14,15,16,17-tetradecahydro-1H-cyclopenta[a]phenanthren-17-yl)-2-diazoacetate (182a):**



Chromatography eluent (98:2 Hexane:Et<sub>2</sub>O;

R<sub>f</sub>: 0.22); Isolated yield: 71.6 %: <sup>1</sup>H NMR

(500 MHz, CDCl<sub>3</sub>) δ 7.73 (m, 2H), 7.62-7.68

(m, 6H), 7.32-7.43 (m, 12H), 5.05 (m, 1H),

5.03 (br s, 1H), 4.54 (dd, *J* = 10.4, 4.46 Hz, 1H), 4.26 (m, 2H), 3.48 (m, 1H), 2.28 (m,

1H), 2.11 (ddd, *J* = 13.31, 4.23, 1.74 Hz, 1H), 1.73-1.82 (m, 1H), 1.61-1.69 (m, 2H),

1.22-1.50 (m, 9H), 1.09-1.19 (m, 3H), 1.05 (s, 9H), 0.92 (s, 3H), 0.75-0.87 (m, 3H),

0.70 (s, 3H); <sup>13</sup>C NMR (125 MHz, CDCl<sub>3</sub>) δ 169.79, 141.43, 136.14, 135.91, 135.75,

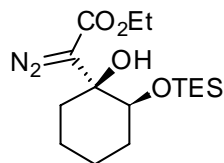
134.76, 134.03, 133.13, 129.63, 129.57, 129.44, 127.50, 127.45, 127.38, 120.41, 87.26,

80.31, 73.19, 60.98, 56.79, 49.97, 49.69, 48.90, 42.41, 37.04, 36.48, 33.70, 33.12,

32.17, 31.79, 31.67, 26.99, 26.91, 20.05, 19.32, 19.23, 19.12, 14.81, 14.43. MS (ESI):

Calculated for [C<sub>55</sub>H<sub>70</sub>N<sub>2</sub>O<sub>5</sub>Si<sub>2</sub>Na]<sup>+</sup>: 917.4721. Found: 917.4720.

**Ethyl 2-(2-(triethylsilyloxy)-1-hydroxycyclohexyl)-2-diazoacetate (190a):**



Prepared from **193a**.<sup>181</sup> Chromatography eluent (20:1

Hexane:EtOAc; R<sub>f</sub>: 0.2); Isolated yield: 94 %: <sup>1</sup>H NMR (500 MHz,

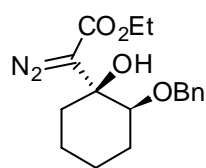
CDCl<sub>3</sub>) δ 4.23 (dq, *J* = 10.76, 7.12 Hz, 1H), 4.15 (dq, *J* = 10.76,

7.12 Hz, 1H), 4.08 (dd, *J* = 10.89, 5.15 Hz, 1H), 3.18 (d, *J* = 2.2 Hz, 1H), 2.02 (tdd, *J*

= 13.57, 4.52, 2.23 Hz, 1H), 1.89 (ddd, *J* = 14.15, 5.79, 2.95 Hz, 1H), 1.70-1.78 (m,

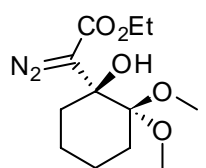
1H), 1.66 (ddd,  $J = 12.97, 5.84, 3.15$  Hz, 1H), 1.51-1.62 (m, 2H), 1.41-1.49 (m, 1H), 1.27 (t,  $J = 7.10$  Hz, 3H), 0.93 (t,  $J = 7.95$  Hz, 9H), 0.51-0.63 (m, 6H);  $^{13}\text{C}$  NMR (125 MHz,  $\text{CDCl}_3$ )  $\delta$  165.74, 71.66, 71.28, 63.90, 60.00, 33.88, 31.15, 23.52, 20.72, 14.39, 6.51, 4.71. MS (ESI): Calculated for  $[\text{C}_{16}\text{H}_{30}\text{N}_2\text{O}_4\text{SiNa}]^+$ : 365.1873. Found: 365.1877.

**Ethyl 2-(2-(triethylsilyloxy)-1-hydroxycyclohexyl)-2-diazoacetate (190b):**



Prepared from **193b**.<sup>182</sup> Chromatography eluent (20:1 Hexane:EtOAc; Rf: 0.2); Isolated yield: 92 %;  $^1\text{H}$  NMR (500 MHz,  $\text{CDCl}_3$ )  $\delta$  7.26-7.38 (m, 5H), 4.56 (dd,  $J = 86.81$  Hz, 11.62 Hz, 2H), 4.14 (q,  $J = 7.14$  Hz, 2H), 3.86 (dd,  $J = 10.86, 4.76$  Hz, 1H), 1.83-2.00 (m, 4H), 1.68-1.78 (m, 1H), 1.62 (ddd,  $J = 24.07, 12.71, 3.71$  Hz, 2H), 1.41-1.51 (m, 1H), 1.25 (t,  $J = 7.11$  Hz, 3H);  $^{13}\text{C}$  NMR (125 MHz,  $\text{CDCl}_3$ )  $\delta$  165.77, 138.11, 128.15, 127.62, 127.50, 77.57, 71.37, 71.20, 63.48, 60.09, 34.70, 26.82, 23.25, 20.80, 14.25. MS (ESI): Calculated for  $[\text{C}_{17}\text{H}_{22}\text{N}_2\text{O}_4\text{Na}]^+$ : 341.1477. Found: 341.1466.

**(S)-Ethyl 2-diazo-2-(1-hydroxy-2,2-dimethoxycyclohexyl)acetate (199):**

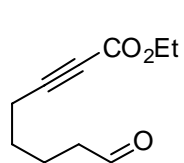


Prepared from **198b**.<sup>183</sup> Chromatography eluent (10:1 Hexane:EtOAc; Rf: 0.2); Isolated yield: 86 %;  $^1\text{H}$  NMR (500 MHz,  $\text{CDCl}_3$ )  $\delta$  5.25 (br s, 1H), 4.23 (dq,  $J = 11.26, 7.11$  Hz, 2H), 3.45 (s, 3H), 3.26 (s, 3H), 1.84-1.97 (m, 5H), 1.66-1.76 (m, 1H), 1.56-1.64 (m, 1H), 1.45-1.52 (m, 1H), 1.36 (qt,  $J = 12.95, 4.10$  Hz, 1H), 1.29 (t,  $J = 7.12$ , 3H);  $^{13}\text{C}$  NMR (125 MHz,  $\text{CDCl}_3$ )  $\delta$  168.57,

103.38, 74.82, 60.61, 59.18, 51.86, 48.60, 34.65, 26.10, 21.82, 20.05, 14.32. MS (ESI):  
Calculated for  $[C_{12}H_{20}N_2O_5Na]^+$ : 295.1270. Found: 295.1267.

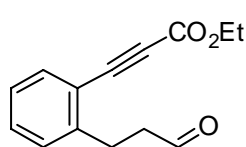
#### 5.4. Experimental procedures for the preparation of fragmentation products

##### Ethyl 8-oxooct-2-ynoate (**129**):



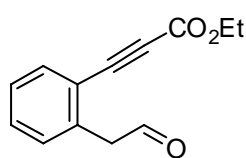
$SnCl_4$  (0.292 mL of a 1M solution in  $CH_2Cl_2$ , 0.292 mmol) was added in a steady stream to a 0 °C solution of  $\beta$ -hydroxy- $\gamma$ -silyloxy- $\alpha$ -diazoester **128s** (0.100 g, 0.292 mmol) in  $CH_2Cl_2$  (6 mL) at which point the yellow solution turned colorless and gas evolution was observed. After 15 minutes, saturated aqueous  $NaHCO_3$  (10 mL) was added and the reaction mixture was transferred with the aid of pentane (10 mL) into a separatory funnel containing saturated aqueous  $NaHCO_3$  (20 mL). The layers were separated, the aqueous layer was extracted with three portions of ethyl acetate, the organics were combined, washed with water, brine and dried over anhydrous  $MgSO_4$ . The solvents were removed *in vacuo* and the residue was subjected to flash silica gel chromatography (Hexane:EtOAc = 4:1; Rf: 0.22) to afford pure aldehyde **5** (50 mg, 94 %):  $^1H$  NMR (500 MHz,  $CDCl_3$ )  $\delta$  9.78 (t,  $J$  = 1.5 Hz, 1H), 4.22 (q,  $J$  = 7.1 Hz, 2H), 2.49 (td,  $J$  = 7.2, 1.5 Hz, 2H), 2.38 (t,  $J$  = 7 Hz, 2H), 1.73-1.79 (m,  $J$  = 2H), 1.60-1.66 (m, 2H), 1.31 (t,  $J$  = 7.1 Hz, 3H);  $^{13}C$  NMR (125 MHz,  $CDCl_3$ )  $\delta$  201.7, 153.7, 88.3, 73.6, 61.8, 43.1, 26.9, 21.2, 18.5, 14.0; MS (ESI):  
Calculated for  $[C_{10}H_{14}O_3Na]^+$ : 205.0841. Found: 205.0840.

**Ethyl 3-(2-(3-oxopropyl)phenyl)propiolate (162):**



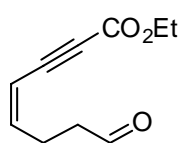
Chromatography eluent (Hexane:EtOAc = 4:1; Rf: 0.30); Isolated yield: 90%;  $^1\text{H}$  NMR (500 MHz,  $\text{CDCl}_3$ )  $\delta$  9.83 (t,  $J$  = 1.3 Hz, 1H), 7.57 (d,  $J$  = 7.7 Hz, 1H), 7.38 (t,  $J$  = 7.7 Hz, 1H), 7.27 (d,  $J$  = 7.7 Hz, 1H), 7.23 (t,  $J$  = 7.7 Hz, 1H), 4.30 (q,  $J$  = 7.2 Hz, 2H), 3.15 (t,  $J$  = 7.4 Hz, 2H), 2.84 (td,  $J$  = 7.4, 1.3 Hz, 2H), 1.36 (t,  $J$  = 7.2 Hz, 3H);  $^{13}\text{C}$  NMR (125 MHz,  $\text{CDCl}_3$ )  $\delta$  201.0, 153.9, 144.4, 133.8, 130.9, 129.2, 126.6, 119.0, 84.7, 84.2, 62.1, 44.2, 26.9, 14.0; MS (ESI): Calculated for  $[\text{C}_{14}\text{H}_{14}\text{O}_3\text{Na}]^+$ : 253.0841. Found: 253.0843.

**Ethyl 3-(2-(2-oxoethyl)phenyl)propiolate (163):**



Chromatography eluent (Hexane:EtOAc = 5:1; Rf: 0.20); Isolated yield: 71%;  $^1\text{H}$  NMR (500 MHz,  $\text{CDCl}_3$ )  $\delta$  9.80 (t,  $J$  = 1.5 Hz, 1H), 7.65 (d,  $J$  = 7.54 Hz, 1H), 7.45 (t,  $J$  = 7.54 Hz, 1H), 7.33 (t,  $J$  = 7.54 Hz, 1H), 7.26 (d,  $J$  = 7.54 Hz, 1H), 4.30 (q,  $J$  = 7.1 Hz, 2H), 3.95 (d,  $J$  = 1.5 Hz, 2H), 1.35 (t,  $J$  = 7.1 Hz, 3H);  $^{13}\text{C}$  NMR (125 MHz,  $\text{CDCl}_3$ )  $\delta$  197.9, 153.7, 136.2, 134.0, 131.1, 130.4, 127.7, 120.2, 84.9, 83.8, 62.2, 48.9, 14.1; MS (ESI): Calculated for  $[\text{C}_{13}\text{H}_{12}\text{O}_3\text{Na}]^+$ : 239.0684. Found: 239.0689.

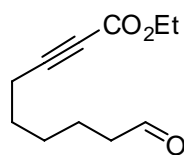
**(Z)-Ethyl 8-oxooct-4-en-2-ynoate (164):**



Chromatography eluent (Hexane:EtOAc = 5:1; Rf: 0.20); Isolated yield: 97%;  $^1\text{H}$  NMR (500 MHz,  $\text{CDCl}_3$ )  $\delta$  9.80 (t,  $J$  = 1.0 Hz, 1H), 6.26 (dt,  $J$

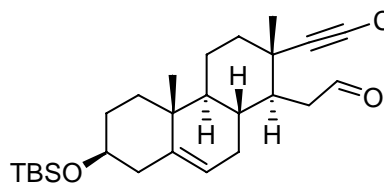
= 10.7, 7.4 Hz, 1H), 5.62 (dt,  $J = 10.8, 1.3$  Hz, 1H), 4.26 (q,  $J = 7.2$  Hz, 2H), 2.70 (qt,  $J = 7.1, 1.3$  Hz, 2H), 2.62 (tt,  $J = 7.1, 1.3$  Hz, 2H), 1.33 (t,  $J = 7.2$  Hz, 3H);  $^{13}\text{C}$  NMR (125 MHz,  $\text{CDCl}_3$ )  $\delta$  200.6, 153.8, 148.0, 108.0, 85.6, 82.1, 62.0, 42.4, 23.4, 14.0; MS (ESI): Calculated for  $[\text{C}_{10}\text{H}_{12}\text{O}_3\text{Na}]^+$ : 203.0684. Found: 203.0675.

**Ethyl 9-oxonon-2-ynoate (165):**



Chromatography eluent (Hexane:EtOAc = 5:1; Rf: 0.30); Isolated yield: 80%;  $^1\text{H}$  NMR (500 MHz,  $\text{CDCl}_3$ )  $\delta$  9.78 (t,  $J = 1.6$  Hz, 1H), 4.22 (q,  $J = 7.1$  Hz, 2H), 2.46 (td, 7.2, 1.6 Hz, 2H), 2.35 (t,  $J = 7.0$  Hz, 2H), 1.66 (p,  $J = 7.6$  Hz, 2H), 1.61 (p,  $J = 7.2$  Hz, 2H), 1.41-1.50 (m, 2H), 1.31 (t,  $J = 7.1$  Hz, 3H);  $^{13}\text{C}$  NMR (125 MHz,  $\text{CDCl}_3$ )  $\delta$  202.2, 153.7, 88.7, 73.4, 61.8, 43.6, 28.2, 27.2, 21.4, 18.4, 14.0; MS (ESI): Calculated for  $[\text{C}_{11}\text{H}_{16}\text{O}_3\text{Na}]^+$ : 219.0997. Found: 219.0993.

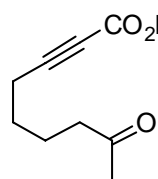
**Ethyl 3-((2S,4bR,7S)-7-(tert-butyldimethylsilyloxy)-2,4b-dimethyl-1-(2-oxoethyl)-1,2,3,4,4a,4b,5,6,7,8,10,10a-dodecahydrophenanthren-2-yl)propiolate (166):**



Chromatography eluent (Hexane:EtOAc = 10:1; Rf: 0.25); Isolated yield: 76%;  $^1\text{H}$  NMR (500 MHz,  $\text{CDCl}_3$ )  $\delta$  9.81 (dd,  $J = 2.8, 1.0$  Hz, 1H), 5.23-5.27 (m, 1H), 4.20 (q,  $J = 7.3$  Hz, 2H), 3.43-3.52 (m, 1H), 2.70 (dd,  $J = 17.0, 3.1$  Hz, 1H), 2.41 (ddd,  $J = 17.0, 6.9, 3.1$  Hz, 1H), 2.12-2.27 (m, 2H), 2.06-2.12 (m, 1H), 1.87-1.97 (m, 2H), 1.76-1.85 (m, 2H), 1.69-1.76 (m, 1H), 1.58-1.65 (m, 1H), 1.30-1.57

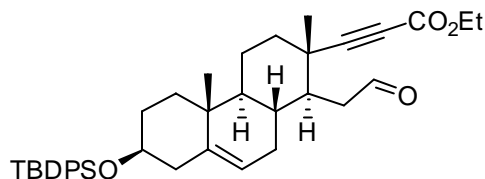
(m, 4H), 1.29 (t,  $J = 7.3$  Hz, 3H), 1.19 (s, 3H), 1.00-1.14 (m, 2H), 0.96 (s, 3H), 0.88 (s, 9H), 0.05 (s, 6H);  $^{13}\text{C}$  NMR (125 MHz,  $\text{CDCl}_3$ )  $\delta$  201.5, 153.7, 141.0, 120.0, 95.1, 73.8, 72.2, 61.8, 48.9, 46.5, 44.7, 42.4, 38.1, 37.0, 36.7, 35.5, 33.3, 32.0, 31.9, 25.9, 19.3, 19.2, 18.5, 18.2, 14.0, -4.6; MS (ESI): Calculated for  $[\text{C}_{29}\text{H}_{46}\text{O}_4\text{SiNa}]^+$ : 509.3063. Found: 509.3047.

**Ethyl 8-oxonon-2-ynoate (167):**



Chromatography eluent (Hexane:EtOAc = 5:1; Rf: 0.30); Isolated yield: 27%;  $^1\text{H}$  NMR (500 MHz,  $\text{CDCl}_3$ )  $\delta$  4.21 (q,  $J = 6.9$  Hz, 2H), 2.47 (t,  $J = 6.9$  Hz, 2H), 2.35 (t,  $J = 6.9$  Hz, 2H), 2.15 (s, 3H), 1.65-1.73 (m, 2H), 1.55-1.62 (m, 2H), 1.31 (t,  $J = 6.9$  Hz, 3H);  $^{13}\text{C}$  NMR (125 MHz,  $\text{CDCl}_3$ )  $\delta$  208.2, 153.7, 88.6, 73.5, 61.8, 42.9, 29.9, 26.9, 22.8, 18.5, 14.0; MS (ESI): Calculated for  $[\text{C}_{11}\text{H}_{16}\text{O}_3\text{Na}]^+$ : 219.0997. Found: 219.0998.

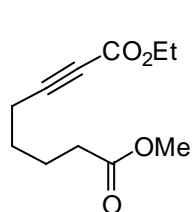
**Ethyl 3-((1S,2S,4aS,4bR,7S,10aR)-7-(tert-butyldiphenylsilyloxy)-2,4b-dimethyl-1-(2-oxoethyl)-1,2,3,4,4a,4b,5,6,7,8,10,10a-dodecahydrophenanthren-2-yl)propiolate (183):**



Chromatography eluent (Hexane:EtOAc = 12:1, 1%  $\text{NEt}_3$ ) ; Rf: 0.18); Isolated yield: 74%;  $^1\text{H}$  NMR (500 MHz,  $\text{CDCl}_3$ )  $\delta$  9.77 (d,  $J = 3.06$  Hz, 1H), 7.63-7.70 (m, 4H), 7.33-7.45 (m, 6H), 5.05 (d,  $J = 5.10$  Hz, 1H), 4.18 (q,  $J = 7.12$  Hz, 2H), 3.47-3.56 (m, 1H), 2.67 (dd,  $J = 17.12, 3.26$  Hz, 1H), 2.37 (ddd,  $J =$

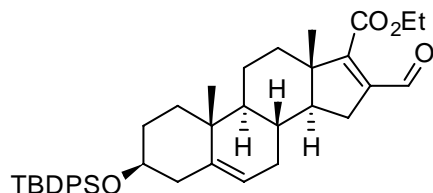
17.10, 7.10, 3.11 Hz, 1H), 2.23-2.32 (m, 1H), 2.10 (ddd,  $J = 13.41, 4.66, 1.81$  Hz, 1H), 1.99-2.06 (m, 1H), 1.91 (dt,  $J = 13.20, 3.28$  Hz, 1H), 1.79-1.87 (m, 1H), 1.75 (dd,  $J = 13.61, 3.58$  Hz, 1H), 1.64-1.73 (m, 2H), 1.5-1.63 (m, 1H), 1.30-1.44 (m, 2H), 1.28 (t,  $J = 7.12$  Hz, 3H), 1.16 (s, 3H), 1.05 (s, 9H), 0.95-1.02 (m, 2H), 0.94 (s, 3H), 0.79-0.91 (m, 2H);  $^{13}\text{C}$  NMR (125 MHz,  $\text{CDCl}_3$ )  $\delta$  201.46, 153.64, 140.69, 135.67, 135.66, 134.61, 134.57, 129.46, 129.42, 127.44, 127.41, 119.96, 95.04, 73.73, 72.87, 61.79, 48.73, 46.43, 44.66, 42.03, 37.98, 36.77, 36.58, 35.45, 33.23, 31.92, 31.60, 26.94, 19.25, 19.06, 18.40, 13.97, 6.56, 5.77; MS (ESI): Calculated for  $[\text{C}_{39}\text{H}_{50}\text{O}_4\text{Si Na}]^+$ : 633.3376. Found: 633.3391.

**1-Ethyl 8-methyl oct-2-ynedioate (202):**



Chromatography eluent (Hexane:EtOAc = 10:1; Rf: 0.22); Isolated yield: 45%;  $^1\text{H}$  NMR (500 MHz,  $\text{CDCl}_3$ )  $\delta$  4.21 (q,  $J = 7.13$  Hz, 2 H), 3.67 (s, 3H), 2.31-2.39 (m, 4H), 1.71-1.79 (m, 2H), 1.57-1.67 (m, 2H), 1.33 (t,  $J = 7.12$  Hz, 3H);  $^{13}\text{C}$  NMR (125 MHz,  $\text{CDCl}_3$ )  $\delta$  173.51, 153.68, 88.41, 73.46, 61.75, 51.52, 33.33, 26.90, 24.00, 18.37, 13.98.

**(3S,8R,9S,10R,13S,14S)-Ethyl 3-(tert-butyldiphenylsilyloxy)-16-formyl-10,13-dimethyl-2,3,4,7,8,9,10,11,12,13,14,15-dodecahydro-1H-cyclopenta[a]phenanthrene-17-carboxylate (184):**



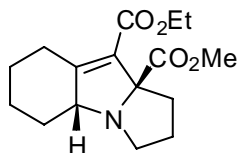
Chromatography eluent (Hexane:EtOAc = 12:1; Rf: 0.35); Isolated yield: 18 % starting with **181s** and 51% starting from **182a**; <sup>1</sup>H NMR (500 MHz,

CDCl<sub>3</sub>) δ 10.31 (s, 1H), 7.65-7.72 (m, 4H), 7.34-7.46 (m, 6H), 5.15 (d, *J* = 5.12 Hz, 1H), 4.31 (dq, *J* = 10.86, 7.13 Hz, 2H), 3.50-3.58 (m, 1H), 2.62 (dd, *J* = 16.54, 6.58 Hz, 1H), 2.30-2.39 (m, 1H), 2.05-2.19 (m, 3H), 1.94-2.02 (m, 1H), 1.50-1.76 (m, 7H), 1.35-1.50 (m, 2H), 1.35 (t, *J* = 7.14 Hz, 3H), 1.07 (s, 9H), 1.06 (s, 3H), 1.04 (s, 3H), 0.83-1.00 (m, 2H); <sup>13</sup>C NMR (125 MHz, CDCl<sub>3</sub>) δ 190.98, 164.12, 157.00, 149.11, 141.55, 135.74, 134.74, 134.69, 129.46, 129.42, 127.46, 127.42, 120.44, 73.07, 61.10, 54.40, 50.09, 49.69, 42.41, 37.03, 36.60, 33.93, 31.78, 31.18, 30.18, 30.11, 26.98, 20.50, 19.30, 19.11, 15.84, 15.26, 14.22. MS (ESI): Calculated for [C<sub>39</sub>H<sub>50</sub>O<sub>4</sub>SiNa]<sup>+</sup>: 633.3376. Found: 633.3374.



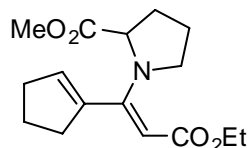
## 5.5. Procedures for the preparation of *N*-containing heterocycles via [1,3]-dipolar cycloaddition reactions

### 9-Ethyl 9a-methyl 2,3,4a,5,6,7,8,9a-octahydro-1*H*-pyrrolo[1,2-*a*]indole-9,9a-dicarboxylate (301):



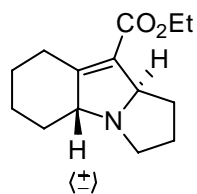
A solution of methyl prolinatate (0.164 mmol) in toluene (0.164 ml) was added dropwise to a 0 °C stirring solution of aldehyde ynoate **129** (25 mg, 0.137 mmol) and preactivated 4 Å MS (~120 mg) in toluene (1.5 ml). After stirring at 0 °C for 30 min the reaction flask was fitted with a dry condenser and placed in a preheated oil bath at 120 °C. Mixture was refluxed and monitored by TLC. Upon completion (~ 1h) reaction mixture was cooled, filtered through a pad of Celite. The solvents were removed *in vacuo* and the residue was subjected to flash silica gel chromatography (Hexane:EtOAc = 10:1 to 5:1 to 1:1) to afford title compound (25mg, 65 %); <sup>1</sup>H NMR (500 MHz, CDCl<sub>3</sub>) δ 4.19 (q, *J* = 7.10 Hz, 2H), 3.95 (dd, *J* = 12.03, 5.76 Hz, 1H), 3.70 (s, 3H), 3.59 (m, 1H), 2.85-2.96 (m, 2H), 2.75 (dd, *J* = 9.57, 7.21 Hz, 1H), 2.14-2.21 (m, 1H), 2.03-2.13 (m, 1H), 1.84-2.01 (m, 3H), 1.70-1.80 (m, 2H), 1.32-1.53 (m, 3H), 1.28 (t, *J* = 7.11 Hz, 3H); <sup>13</sup>C NMR (125 MHz, CDCl<sub>3</sub>) δ 174.22, 164.38, 158.38, 125.39, 82.05, 68.57, 59.91, 52.26, 48.62, 34.26, 29.67, 29.16, 26.64, 26.60, 25.55, 24.12, 14.15.

**(Z)-Methyl 1-(1-cyclopentenyl-3-ethoxy-3-oxoprop-1-enyl)pyrrolidine-2-carboxylate (302):**



Isolated as a byproduct during the preparation of **301** in 15% yield.  $^1\text{H}$  NMR (500 MHz,  $\text{CDCl}_3$ )  $\delta$  7.47 (s, 1H), 5.38-5.40 (m, 1H), 4.26 (dd,  $J = 8.53, 3.34$  Hz, 1H), 3.72 (s, 3H), 3.43-3.54 (m, 1H), 3.19-3.31 (m, 1H), 2.49-2.62 (m, 1H), 2.24-2.47 (m, 3H), 2.24 (ddd,  $J = 16.68, 12.78, 8.57$  Hz, 1H), 1.98-2.07 (m, 1H), 1.80-1.97 (m, 4H), 1.25 (t,  $J = 7.11$  Hz, 3);  $^{13}\text{C}$  NMR (125 MHz,  $\text{CDCl}_3$ )  $\delta$  172.83, 169.46, 144.35, 138.27, 131.09, 98.50, 59.40, 52.13, 51.58, 37.72, 32.46, 30.25, 23.80, 23.42, 14.46.

**Ethyl 2,3,4a,5,6,7,8,9a-octahydro-1H-pyrrolo[1,2-a]indole-9-carboxylate (309):**

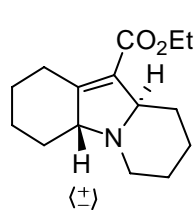


One pot protocol:  $\text{SnCl}_4$  (0.030 mL of a 1M solution in  $\text{CH}_2\text{Cl}_2$ , 0.029 mmol) was added in a continuous stream to a solution of  $\gamma$ -silyloxy- $\beta$ -hydroxy- $\alpha$ -diazoester **128s** (0.100 g, 0.292 mmol) in toluene (3 mL) at which point the yellow solution turned colorless and gas evolution was observed. After 15 minutes *N*-(trimethylsilyl)prolin-trimethylsilylester (0.092 mL, 0.321 mmol) was added dropwise and the solution became pale green and a white precipitate formed. After 30 minutes the reaction flask was fitted with a dry condenser and transferred to an oil bath preheated to 120 °C. The solution was heated at reflux for 15 minutes and then cooled to room temperature, at which point aqueous KOH (1.5 mL of a 1N solution) was added with vigorous stirring. After one minute the mixture was transferred to a separatory funnel with the aid of diethyl ether, the aqueous layer was

removed, the organic layer was dried (MgSO<sub>4</sub>), the solvents were removed *in vacuo* and the residue was subjected to flash silica gel chromatography (99:1 CH<sub>2</sub>Cl<sub>2</sub>:MeOH / 0.5 % NEt<sub>3</sub>) to provide 0.030g (44% yield) of the title product.

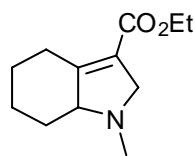
Two step protocol : *N*-(trimethylsilyl)prolin-trimethylsilylester<sup>121</sup> (0.086 ml, .301 mmol) was added dropwise to a stirring solution of ethyl 8-oxooct-2-ynoate **129** (0.050 g, 0.274 mmol) in dry toluene (2.7 ml). After 5 minutes a pale green solution and a white precipitate were observed. After 30 minutes the reaction flask was fitted with a dry condenser and transferred to an oil bath preheated to 120 °C. The solution was heated at reflux for 15 minutes and then cooled to room temperature. The solvents were removed *in vacuo* and the resulting yellow oil was subjected to flash silica gel chromatography (99:1 CH<sub>2</sub>Cl<sub>2</sub>:MeOH / 0.5 % NEt<sub>3</sub>) to provide 0.057g (88% yield) of the title product: (TLC eluent 92:8 CH<sub>2</sub>Cl<sub>2</sub>:MeOH; Rf: 0.3); <sup>1</sup>H NMR (500 MHz, CDCl<sub>3</sub>) δ 4.43 (q, *J* = 6.2 Hz, 1H), 4.23 (dq, *J* = 10.8, 7.2 Hz, 1H), 4.17 (dq, *J* = 10.8, 7.2 Hz, 1H), 3.47-3.53 (m, 1H), 3.30-3.60 (m, 1H), 3.11 (dt, *J* = 10.3, 5.8 Hz, 1H), 2.63 (dt, *J* = 10.2, 6.7 Hz, 1H), 2.04-2.17 (m, 2H), 1.93 (td, *J* = 13.3, 5.4 Hz, 1H), 1.70-1.88 (m, 4H), 1.50-1.61 (m, 1H), 1.17-1.44 (m, 3H), 1.30 (t, *J* = 7.2 Hz, 3H); <sup>13</sup>C NMR (125 MHz, CDCl<sub>3</sub>) δ 164.9, 156.6, 124.9, 75.9, 71.4, 59.8, 56.0, 37.1, 31.9, 27.2, 26.6, 25.5, 24.2, 14.3; MS (ESI): Calculated for [C<sub>14</sub>H<sub>22</sub>O<sub>2</sub>N]<sup>+</sup>: 236.1651. Found: 236.1650.

**Ethyl 1,2,3,4,4a,6,7,8,9,9a-decahydropyrido[1,2-a]indole-10-carboxylate (317):**



N-(trimethylsilyl)pipecolin-trimethylsilylester (**316**) (0.087 ml, 0.288 mmol) was added dropwise to a stirring solution of ethyl 8-oxooct-2-ynoate **129** (0.050 g, 0.274 mmol) in dry toluene (3 ml). After 5 minutes a hazy white solution and a precipitate were observed. After 30 minutes the reaction flask was fitted with a dry condenser and transferred to an oil bath preheated to 120 °C. The solution was heated at reflux for 15 minutes and then cooled to room temperature. The solvents were removed *in vacuo* and the resulting yellow oil was subjected to flash silica gel chromatography (99:1 CH<sub>2</sub>Cl<sub>2</sub>:MeOH / 0.5 % NEt<sub>3</sub>) to provide 0.054g (79% yield) of the title product: (TLC eluent 92:8 CH<sub>2</sub>Cl<sub>2</sub>:MeOH; R<sub>f</sub>: 0.3); <sup>1</sup>H NMR (500 MHz, CDCl<sub>3</sub>) δ 4.19 (dq, *J* = 7.11, 1.30 Hz, 2H), 3.91 (dt, *J* = 11.20, 3.57 Hz, 1H), 3.60-3.65 (m, 1H), 3.53-3.59 (m, 1H), 2.98-3.05 (m, 1H), 2.83 (dddd, *J* = 16.4, 14.75, 12.45, 3.01 Hz, 1H), 2.16-2.24 (m, 1H), 1.90-1.99 (m, 1H), 1.73-1.88 (m, 5H), 1.30-1.49 (m, 4H), 1.29 (t, *J* = 7.13 Hz, 3H), 1.03-1.24 (m, 2H); <sup>13</sup>C NMR (125 MHz, Toluene-*d*<sub>8</sub>) δ 164.9, 156.1, 137.4, 125.3, 65.0, 63.8, 59.5, 45.2, 33.0, 29.3, 27.2, 25.8, 23.9, 23.4, 21.6, 20.4, 14.3.

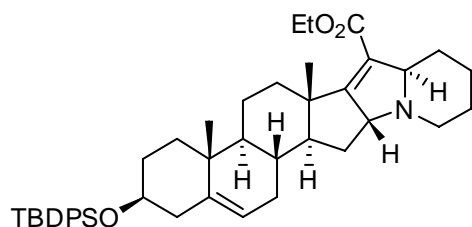
**ethyl 1-methyl-2,4,5,6,7,7a-hexahydro-1*H*-indole-3-carboxylate (325):**



A mixture of N-(trimethylsilyl)sarcosine-trimethylsilylester<sup>124</sup> (**288**) and sarcosine-trimethylsilylester (**285**) (0.050 ml, 0.190 mmol) was added dropwise to a stirring solution of ethyl 8-oxooct-2-ynoate **129** (0.033 g, 0.181 mmol) in dry toluene (2 ml). After 30 minutes the reaction flask was

fitted with a dry condenser and transferred to an oil bath preheated to 120 °C. The solution was heated at reflux for 30 minutes and then cooled to room temperature. The solvents were removed *in vacuo* and the resulting yellow oil was subjected to flash silica gel chromatography (99:1 CH<sub>2</sub>Cl<sub>2</sub>:MeOH / 0.5 % NEt<sub>3</sub>) to provide 0.022g (59% yield) of the title product: (TLC eluent 95:5 CH<sub>2</sub>Cl<sub>2</sub>:MeOH; Rf: 0.3); <sup>1</sup>H NMR (500 MHz, CDCl<sub>3</sub>) δ 4.18 (qd, *J* = 7.11, 3.85 Hz, 2H), 3.99 (ddd, *J* = 12.82, 4.08, 1.39 Hz, 1H), 3.52 (d, *J* = 15.21 Hz, 1H), 3.34 (ddd, *J* = 12.80, 4.97, 4.19 Hz, 1H), 3.11 (dt, *J* = 10.05, 4.96 Hz, 1H), 2.43 (s, 3H), 2.16 (ddd, *J* = 6.06, 5.11, 2.30 Hz, 1H), 1.87-1.97 (m, 1H), 1.78-1.90 (m, 2H), 1.28 (t, *J* = 7.12 Hz, 3H), 1.19-1.41 (m, 3H); <sup>13</sup>C NMR (125 MHz, CDCl<sub>3</sub>) δ 164.64, 156.40, 122.06, 72.86, 61.34, 59.79, 40.24, 33.72, 26.77, 25.38, 23.36, 14.30. Calculated for [C<sub>14</sub>H<sub>22</sub>O<sub>2</sub>NH]<sup>+</sup>: 210.1494. Found: 214.1488.

**Dehydroepiandrosterone derived 2,5-dihydropyrrole (322):**

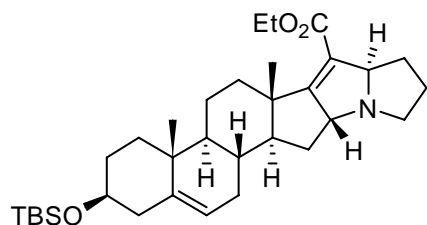


Employing the same protocol used for the preparation of **317**, title compound was isolated after flash silica gel chromatography (99:1 CH<sub>2</sub>Cl<sub>2</sub>:MeOH / 0.5 % NEt<sub>3</sub>) in 87% yield; <sup>1</sup>H

NMR (500 MHz, CDCl<sub>3</sub>) δ 7.65-7.71 (m, 4H), 7.34-7.44 (m, 6H), 5.12 (d, *J* = 5.21 Hz, 1H), 4.43 (d, *J* = 9.47 Hz, 1H), 4.18 (dq, *J* = 7.12, 1.85 Hz, 2H), 4.04 (dt, *J* = 10.63, 3.40 Hz, 1H), 3.50-3.61 (m, 1H), 2.90 (ddd, *J* = 22.15, 16.94, 8.55 Hz, 2H), 2.38 (m, 2H), 2.17 (ddd, *J* = 13.26, 4.71, 1.84 Hz, 1H), 1.93 (d, *J* = 15.74 Hz, 1H), 1.77-1.84

(m, 1H), 1.64-1.74 (m, 4H), 1.50-1.60 (m, 6H), 1.29-1.49 (m, 5H), 1.26 (t,  $J = 7.11$  Hz, 3H), 1.06 (s, 9H), 1.01 (s, 3H), 1.00 (s, 3H), 0.78-0.97 (m, 3H).

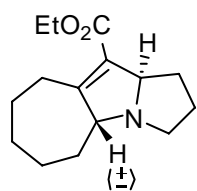
**Dehydroepiandrosterone derived 2,5-dihydropyrrole (323a):**



Employing the same protocol used for the preparation of **309**, title compound was isolated after flash silica gel chromatography (99:1  $\text{CH}_2\text{Cl}_2$ :MeOH / 0.5 %  $\text{NEt}_3$ ) in 70% yield;  $^1\text{H}$  NMR

(500 MHz,  $\text{CDCl}_3$ )  $\delta$  5.30 (d,  $J = 4.61$  Hz, 1H), 4.49 (dd,  $J = 11.22, 7.27$  Hz, 1H), 4.12-4.24 (m, 3H), 3.43-3.53 (m, 1H), 2.82-2.93 (m, 1H), 2.69-2.79 (m, 1H), 2.33 (d,  $J = 12.47$  Hz, 1H), 2.26 (t,  $J = 12.20$  Hz, 1H), 2.14-2.20 (m, 1H), 1.87-2.09 (m, 3H), 1.76-1.87 (m, 2H), 1.38-1.76 (m, 12H), 1.28 (t,  $J = 7.11$  Hz, 3H), 1.02-1.23 (m, 1H), 1.01 (s, 3H), 0.99 (s, 3H), 0.89 (s, 9H), 0.05 (s, 6H);  $^{13}\text{C}$  NMR (125 MHz, Toluene –  $d_8$ )  $\delta$  168.88, 163.99, 141.59, 123.17, 121.68, 77.18, 77.07, 73.08, 60.22, 56.83, 54.25, 50.46, 43.75, 43.54, 37.66, 37.06, 35.75, 32.93, 32.83, 31.86, 31.74, 30.80, 27.26, 26.46, 21.22, 19.74, 18.76, 16.12, 14.77, -4.10.

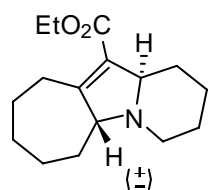
**Ethyl 1,2,3,4a,5,6,7,8,9,10a-decahydrocyclohepta[b]pyrrolizine-10-carboxylate (320):**



Employing the same protocol used for the preparation of **309**, title compound was isolated after flash silica gel chromatography (99:1  $\text{CH}_2\text{Cl}_2$ :MeOH / 0.5 %  $\text{NEt}_3$ ) in 44% yield;  $^1\text{H}$  NMR (500 MHz,

CDCl<sub>3</sub>)  $\delta$  4.35 (dd,  $J$  = 12.08, 6.83 Hz, 1H), 4.20-4.27 (m, 2H), 4.16 (ddd,  $J$  = 14.25, 10.89, 7.11 Hz, 1H), 3.65 (ddd,  $J$  = 8.39, 4.62, 3.62 Hz, 1H), 3.06 (dt,  $J$  = 10.58, 5.99 Hz, 1H), 2.78-2.88 (m, 1H), 2.57-2.70 (m, 2H), 2.29-2.37 (m, 1H), 2.08 (dt,  $J$  = 12.75, 7.19 Hz, 1H), 1.86-1.96 (m, 1H), 1.34-1.83 (m, 9H), 1.30 (t,  $J$  = 7.12 Hz, 3H).

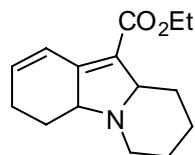
**Ethyl 2,3,4,5a,6,7,8,9,10,11a-decahydro-1H-cyclohepta[b]indolizine-11-carboxylate (321):**



Employing the same protocol used for the preparation of **317**, title compound was isolated after flash silica gel chromatography (99:1 CH<sub>2</sub>Cl<sub>2</sub>:MeOH / 0.5 % NEt<sub>3</sub>) in 43% yield; <sup>1</sup>H NMR (500 MHz,

CDCl<sub>3</sub>)  $\delta$  4.13-4.28 (m, 4H), 3.39 (m, 1H), 3.87 (m, 1H), 3.02 (d,  $J$  = 14.79 Hz, 1H), 2.74-2.88 (m, 2H), 2.70 (dd,  $J$  = 16.16, 7.52 Hz, 1H), 2.05-2.14 (m, 1H), 1.92-1.98 (m, 1H), 1.76-1.85 (m, 2H), 1.34-1.75 (m, 7H), 1.28 (t,  $J$  = 7.11 Hz, 3H), 1.09-1.19 (m, 1H); <sup>13</sup>C NMR (125 MHz, CDCl<sub>3</sub>)  $\delta$  164.74, 137.50, 129.51, 68.08, 63.57, 59.64, 44.98, 31.15, 30.14, 29.02, 28.59, 27.02, 26.18, 23.53, 21.29, 19.87, 14.24, 13.95.

**Ethyl 3,4,4a,6,7,8,9,9a-octahydropyrido[1,2-a]indole-10-carboxylate (319):**



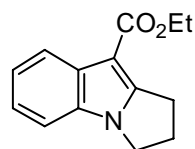
Employing the same protocol used for the preparation of **317**, title compound was isolated after flash silica gel chromatography (99:1 CH<sub>2</sub>Cl<sub>2</sub>:MeOH / 0.5 % NEt<sub>3</sub>) in 60% yield; <sup>1</sup>H NMR (500 MHz,

CDCl<sub>3</sub>)  $\delta$  7.05 (dd,  $J$  = 9.86, 2.70 Hz, 1H), 6.22 (dddd,  $J$  = 9.24, 8.27, 5.60, 2.51 Hz, 1H), 4.22 (q,  $J$  = 7.11 Hz, 2H), 4.03 (dt,  $J$  = 11.67, 3.44 Hz, 1H), 3.87 (dt,  $J$  = 12.11,

4.02 Hz, 1H), 2.37 (dt,  $J = 18.86, 5.16$  Hz, 1H), 2.23-2.33 (m, 1H), 2.15-2.22 (m, 1H), 1.77-1.88 (m, 2H), 1.35-1.56 (m, 3H), 1.30 (t,  $J = 7.11$  Hz, 3H), 1.09-1.27 (m, 2H).

## 5.6. Miscellaneous procedures

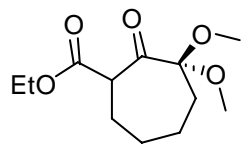
### Ethyl 2,3-dihydro-1*H*-pyrrolo[1,2-*a*]indole-9-carboxylate (**328**):



A solution of DDQ (0.142 g, 0.617 mmol) in toluene (1.4 ml) was added drop-wise to room temperature stirring solution of **309** (0.044 g, 0.187 mmol) in toluene (2.2 ml). Resulting dark solution was stirred at 50 °C for 6.5 h and reaction progress monitored by TLC. Upon completion reaction was cooled and poured over NaHCO<sub>3</sub>, aqueous layer extracted with Et<sub>2</sub>O (3x), combined organics washed with brine and dried over Mg<sub>2</sub>SO<sub>4</sub>. The solvents were removed *in vacuo* and the resulting oil was subjected to flash silica gel chromatography (10:1, Hexanes:EtOAc) to provide 0.015g (35% yield) of the title product: (TLC eluent 95:5 CH<sub>2</sub>Cl<sub>2</sub>:MeOH; R<sub>f</sub>: 0.8); <sup>1</sup>H NMR (500 MHz, CDCl<sub>3</sub>) δ 8.11 (d,  $J = 8.1$ , 1H), 7.22 (m, 4H), 4.36 (q,  $J = 7.1$ , 2H), 4.10 (t,  $J = 7.0$ , 2H), 3.29 (t,  $J = 7.4$ , 2H), 2.65 (p,  $J = 7.2$ , 2H), 1.41 (t,  $J = 7.1$ , 3H); <sup>13</sup>C NMR (125 MHz, CDCl<sub>3</sub>) δ 165.54, 152.80, 132.68, 130.93, 121.64, 121.54, 121.46, 109.76, 99.36, 59.24, 44.42, 26.61, 26.12, 14.66. MS (ESI): Calculated for [C<sub>14</sub>H<sub>15</sub>NO<sub>2</sub>Na]<sup>+</sup>: 252.1001. Found: 252.0994.

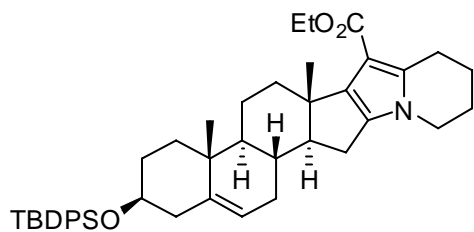


### Ethyl 3,3-dimethoxy-2-oxocycloheptanecarboxylate (**206**):



Methanesulphonyl chloride (0.045 ml, 0.551 mmol) and triethylamine (0.075 ml, 0.551 mmol), were added sequentially to a stirring solution of diazo ester **199** (0.100 g, 0.376 mmol) in  $\text{CH}_2\text{Cl}_2$  (4 ml). After overnight stirring the solution was poured over  $\text{NH}_4\text{Cl}$ , extracted with  $\text{CH}_2\text{Cl}_2$  (2x), combined organics washed with brine and dried over  $\text{Mg}_2\text{SO}_4$ . The solvents were removed *in vacuo* and the resulting oil was subjected to flash silica gel chromatography (10:1, Hexanes:EtOAc) to provide 0.045g (50% yield) of the title product: (TLC eluent Hexanes:EtOAc; Rf: 0.45);  $^1\text{H}$  NMR (500 MHz,  $\text{CDCl}_3$ )  $\delta$  4.21 (dq,  $J = 10.72, 7.12$  Hz, 1H), 4.16 (dq,  $J = 10.72, 7.12$  Hz, 1H), 3.66 (dd,  $J = 8.72, 7.47$  Hz, 1H), 3.26 (s, 3H), 3.24 (s, 3H), 2.06-2.15 (m, 1H), 1.94-2.03 (m, 2H), 1.74-1.82 (m, 1H), 1.56-1.71 (m, 2H), 1.27-1.45 (m, 2H), 1.24 (t,  $J = 7.14$  Hz, 3H);  $^{13}\text{C}$  NMR (125 MHz,  $\text{CDCl}_3$ )  $\delta$  203.49, 169.60, 105.35, 60.95, 55.32, 50.12, 48.73, 32.99, 26.50, 25.33, 24.02, 13.98.

### Dehydroepiandrosterone derived pyrrole (**355**):



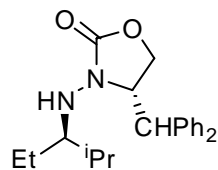
A mixture of **322** (0.037 g, 0.0546 mmol) in wet benzene (2 ml) was refluxed under atmospheric and reaction progress monitored by TLC (TLC eluent 95:5  $\text{CH}_2\text{Cl}_2$ :MeOH; Rf: 0.85). After overnight reflux solution cooled and concentrated *in vacuo* and resulting dark oil was subjected to flash silica gel chromatography (99:1,  $\text{CH}_2\text{Cl}_2$ :MeOH, 0.5%  $\text{NEt}_3$ ) to

provide 0.024 g (65% yield) of the title product:  $^1\text{H}$  NMR (500 MHz,  $\text{CDCl}_3$ )  $\delta$  7.70 (dd,  $J = 6.19, 4.77$  Hz, 4H), 7.35-7.46 (m, 6H), 5.17 (d,  $J = 4.79$  Hz, 1H), 4.24 (dq,  $J = 10.86, 7.14$  Hz, 2H), 3.77 (qt,  $J = 12.10, 5.40$  Hz, 1H), 3.51-3.60 (m, 1H), 3.07 (qt,  $J = 17.88, 6.24$  Hz, 1H), 2.51 (d,  $J = 12.21$  Hz, 1H), 2.46 (dd,  $J = 13.49, 5.35$  Hz, 1H), 2.32-2.42 (m, 1H), 2.12-2.24 (m, 2H), 1.68-2.04 (m, 10H), 1.46-1.67 (m, 6H), 1.32 (t,  $J = 7.13$  Hz, 3H), 1.08 (s, 9H), 1.07 (s, 3H), 0.94 (s, 3H), 0.80-0.90 (m, 2H).

### 5.7. Tin-Mediated Radical Addition to Hydrazones

**General Procedure:** To a solution of the hydrazone (**403a-e**) in  $\text{CH}_2\text{Cl}_2$  (ca. 0.25 M) was added  $\text{ZnCl}_2$  (1 M in  $\text{Et}_2\text{O}$ , 2 eq). After 1 h at room temperature, the mixture was cooled to  $-78^\circ\text{C}$ , followed by addition of  $\text{Et}_3\text{B}$  (10 eq) and the appropriate alkyl iodide (10 eq).  $\text{Bu}_3\text{SnH}$  (0.25 M in  $\text{CH}_2\text{Cl}_2$ , 5 eq) and  $\text{O}_2$  (ca. 7 mL/mmol hydrazone) were introduced by syringe pump over ca. 5 h. The reaction mixture was allowed to warm slowly to room temperature. After 2 d, stannanes were removed by dilution with  $\text{EtOAc}$ , stirring overnight with excess KF, and filtration through a short pad of silica gel. Concentration and radial chromatography (hexane/ $\text{EtOAc}$ ) afforded *N*-acylhydrazines **404a-e** as diastereomeric mixtures; no change in these diastereomer ratios occurred during radial chromatography.

**(4*S*,3'*R*)-3-(2'-Methyl-3'-pentylamino)-4-diphenylmethyl-2-oxazolidinone (404b):**



From **403b**<sup>173</sup> (29 mg, 0.094 mmol) and 2-iodopropane by the

**General Procedure** was obtained **404b** (5 mg, 15% yield, S,R/S,S =

24:1) as white crystals (m.p. = 114-115 °C );  $[\alpha]_D^{23} +51.4^\circ$  (*c* 0.07,

CHCl<sub>3</sub>); IR (film) 3505, 3316, 2961, 1756, 1495, 1454, 1405, 1219, 1091, 702 cm<sup>-1</sup>; <sup>1</sup>H

NMR (500 MHz, CDCl<sub>3</sub>)  $\delta$  7.33-7.14 (m, 10H), 4.58 (d, *J* = 5.8 Hz, 1H), 4.53 (m, 1H),

4.36 (t, *J* = 8.9 Hz, 1H), 4.22 (dd, *J* = 9.1, 3.4 Hz, 1H), 3.61 (d, *J* = 3.3 Hz, 1H), 2.70

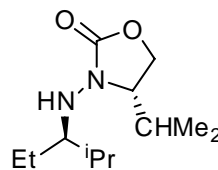
(q, *J* = 5.7, 4.4 Hz, 1H), 1.77-1.70 (m, 1H); <sup>13</sup>C NMR (500 MHz, CDCl<sub>3</sub>)  $\delta$  157.0,

140.8, 139.2, 128.9, 128.7, 128.3, 127.4, 127.0, 64.4, 64.2, 59.4, 51.5, 28.1, 21.4, 18.0,

17.7, 10.3; MS (CI) *m/z* (relative intensity) 353.7 ([M+H]<sup>+</sup>, 100%); Anal. Calcd for

C<sub>22</sub>H<sub>28</sub>N<sub>2</sub>O<sub>2</sub>: C, 74.97; H, 8.01; N, 7.95. Found: C, 74.85; H, 8.06; N, 7.74.

**(4*S*,3'*R*)-3-(2'-Methyl-3'-pentylamino)-4-isopropyl-2-oxazolidinone (404c):**



From **303c**<sup>173</sup> (147 mg, 0.80 mmol) and 2-iodopropane by the

**General Procedure** was obtained **404c** (28 mg, 16% yield, as a

colorless oil.  $[\alpha]_D^{23}$ ; IR (film) 3488, 3300, 2962, 1757, 1465, 1399,

1220, 1090, 1046 cm<sup>-1</sup>; <sup>1</sup>H NMR (500 MHz, CDCl<sub>3</sub>)  $\delta$  4.15 (t, *J* = 8.8 Hz, 1H), 3.99

(dd, *J* = 9.0, 4.2 Hz, 1H), 3.83 (s broad, 1H), 3.61 (m, 1H), 2.68 (q, *J* = 5.2 Hz, 1H),

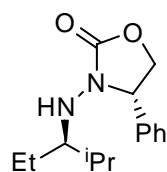
2.23-2.17 (m, 1H), 1.76-1.70 (m, 1H), 1.43-1.30 (m, 2H), .90-.83 (m, 12 H), 0.79 (d, *J*

= 6.9 Hz, 3H); <sup>13</sup>C NMR (500 MHz, CDCl<sub>3</sub>)  $\delta$  158.6, 65.1, 62.3, 61.8, 28.2, 27.4, 21.6,

18.1, 17.7, 14.9, 10.1; MS (CI) *m/z* (relative intensity) 229.2 ([M+H]<sup>+</sup>, 100%); Anal.

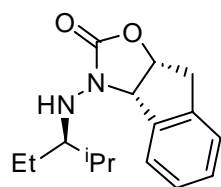
Calcd for C<sub>12</sub>H<sub>24</sub>N<sub>2</sub>O<sub>2</sub>: C, 63.12; H, 10.59; N, 12.27. Found: C, 63.09; H, 10.69; N, 12.11.

**(4S,3'R)-3-(2'-Methyl-3'-pentylamino)-4-phenyl-2-oxazolidinone (404d).**



From **403d**<sup>173</sup> (83 mg, 0.40 mmol) and 2-iodopropane by the **General Procedure** was obtained **404d** (35 mg 35% yield, S,R/S,S = 15:1) as a colorless oil.  $[\alpha]_D^{23} +32.00^\circ$  (c 0.03, CHCl<sub>3</sub>); IR (film) 3304, 2922, 1761, 1459, 1391, 1240, 1086, 1039, 755 cm<sup>-1</sup>; <sup>1</sup>H NMR (500 MHz, CDCl<sub>3</sub>)  $\delta$  7.35-7.24 (m, 5H), 4.72(dd, *J* = 8.4, 6.4 Hz, 1H), 4.53 (t, *J* = 8.7 Hz, 1H), 4.14 (dd, *J* = 8.8, 6.4 Hz, 1H), 3.68 (s, 1H), 2.46-2.43 (m, 1H), 1.61-1.55 (m, 1H), 1.27 (m, 1H), 0.75 (d, *J* = 6.9 Hz, 3H), 0.67 (d, *J* = 6.8 Hz, 3H), 0.64 (t, *J* = 7.3 Hz, 3H); <sup>13</sup>C NMR (500 MHz, CDCl<sub>3</sub>)  $\delta$  158.3, 137.2, 129.1, 127.5, 68.5, 64.4, 61.4, 28.3, 20.9, 18.2, 17.2, 10.2; MS (CI) *m/z* (relative intensity) 263.1 ([M+H]<sup>+</sup>, 100%); Anal. Calcd for C<sub>15</sub>H<sub>22</sub>N<sub>2</sub>O<sub>2</sub>: C, 68.67; H, 8.45; N, 10.68. Found: C, 68.89; H, 8.53; N, 10.51.

**(4S,3'R)-3-(2'-Methyl-3'-pentylamino)-4-phenyl-2-oxazolidinone (404e).**



From **403e**<sup>173</sup> (131 mg, 0.57 mmol) and 2-iodopropane by the **General Procedure** was obtained **404e** (80 mg, 50% yield, S,R/S,S = 20:1) as a colorless oil.  $[\alpha]_D^{23} -28.9^\circ$  (c 0.03, CHCl<sub>3</sub>); IR (film) 3490, 3304, 2961, 1753, 1462, 1381, 1201, 1106, 1035, 757, 726 cm<sup>-1</sup>; <sup>1</sup>H NMR (500 MHz, CDCl<sub>3</sub>)  $\delta$  7.60 (d, *J* = 7.5 Hz, 1H), 7.28-7.17 (m, 4H), 5.16 (dt, *J* = 6.5, 5.1 Hz, 1H), 5.02 (d, *J* = 6.9 Hz, 1H), 3.94 (s, 1H), 3.30 (dd, *J* = 17.9, 6.1 Hz, 1H), 3.23 (d, *J* =

17.5 Hz, 1H), 2.85 (m, 1H), 1.80-1.73 (m, 1H), 1.56-1.44 (m, 1H), 0.96 (t,  $J = 7.4$  Hz, 3H), 0.91 (d,  $J = 6.9$  Hz, 6H);  $^{13}\text{C}$  NMR (500 MHz,  $\text{CDCl}_3$ )  $\delta$  157.5, 140.2, 138.3, 129.5, 127.2, 126.1, 125.3, 65.6, 64.9, 38.9, 28.2, 21.7, 18.2, 18.1, 10.1; MS (CI)  $m/z$  (relative intensity) 275.4 ( $[\text{M}+\text{H}]^+$ , 100%); Anal. Calcd for  $\text{C}_{16}\text{H}_{22}\text{N}_2\text{O}_2$ : C, 70.04; H, 8.08; N, 10.21. Found: C, 69.85; H, 8.10; N, 10.08.

## REFERENCES

- (1) Curtius, T. *Chem. Ber.* **1883**, *16*, 2230.
- (2) Curtius, T. *J. Prakt. Chem.* **1889**, *39*, 107.
- (3) Thiele, J. *Ber. Dtsch. Chem. Ges.* **1911**, *44*, 2522.
- (4) Boersch, H. *Monatsh. Chem* **1935**, *65*, 311.
- (5) Clusius, K.; Lüthi, U. *Helv. Chim. Acta* **1957**, *40*, 445.
- (6) Wolff, L. *Justus Liebigs Ann. Chem.* **1902**, 325, 129.
- (7) Kirmse, W. *Eur. J. Org. Chem.* **2002**, 2193.
- (8) Di, M. P.; Rein, K. S. *Tetrahedron Lett.* **2004**, *45*, 4703.
- (9) Djerassi, C.; Scholz, C. R. *J. Org. Chem.* **1949**, *14*, 660.
- (10) Sandoval, A.; Rosenkranz, G.; Djerassi, C. *J. Am. Chem. Soc.* **1951**, *73*, 2383.
- (11) Mueller, G. P.; Riegel, B. *J. Am. Chem. Soc.* **1954**, *76*, 3686.
- (12) Wang, G.-W.; Li, Y.-J.; Peng, R.-F.; Liang, Z.-H.; Liu, Y.-C. *Tetrahedron* **2004**, *60*, 3921.
- (13) Hook, J. M.; Mander, L. N.; Urech, R. *J. Am. Chem. Soc.* **1980**, *102*, 6628.
- (14) Gutsche, C. D. *Org. React.* **1954**, 364.
- (15) Smith, P. A. S.; Baer, D. R. *Org. React.* **1960**, *11*, 157.
- (16) Coveney, D. J., *Comprehensive Organic Synthesis*. Pergamon: Oxford, 1991; Vol. 3, p 777.
- (17) Müller, E.; Bauer, M.; Rundel, W. *Tetrahedron Lett.* **1960**, 34.
- (18) House, H. O.; Grubbs, E. J.; Gannon, W. F. *J. Am. Chem. Soc.* **1960**, *82*, 4099.
- (19) Moebius, D. C.; Kingsbury, J. S. *J. Am. Chem. Soc.* **2009**, *131*, 878.
- (20) Mock, W. L.; Hartman, M. E. *J. Org. Chem.* **1977**, *42*, 459.
- (21) Doyle, M. P.; Trudell, M. L.; Terpstra, J. W. *J. Org. Chem.* **1983**, *48*, 5146.
- (22) Jiang, N.; Wang, J. *Tetrahedron Lett.* **2002**, *43*, 1285.

- (23) Schöllkopf, U.; Frasnelli, H. *Angew. Chem., Int. Ed. Engl.* **1970**, 9, 301.
- (24) Heydt, A.; Weber, B.; Regitz, M. *Chem. Ber.* **1982**, 115, 2965.
- (25) Fink, J.; Regitz, M. *Synthesis* **1985**, 569.
- (26) Buchner, E. *Ber. Dtsch. Chem. Ges.* **1895**, 28, 215.
- (27) Padwa, A.; Sá, M. M.; David Weingarten, M. *Tetrahedron* **1997**, 53, 2371.
- (28) Wenkert, E.; McPherson, C. A. *J. Am. Chem. Soc.* **1972**, 94, 8084.
- (29) Pellicciari, R.; Natalini, B.; Sadeghpour, B. M.; Marinozzi, M.; Snyder, J. P.; Williamson, B. L.; Kuethe, J. T.; Padwa, A. *J. Am. Chem. Soc.* **1996**, 118, 1.
- (30) Ye, T.; McKervey, M. A. *Tetrahedron* **1992**, 48, 8007.
- (31) Padwa, A.; Kulkarni, Y. S.; Zhang, Z. *J. Org. Chem.* **1990**, 55, 4144.
- (32) Singh, A. K.; Bakshi, R. K.; Corey, E. J. *J. Am. Chem. Soc.* **1987**, 109, 6187.
- (33) Pellicciari, R.; Natalini, B.; Cecchetti, S.; Fringuelli, R. *J. Chem. Soc. Perkin Trans. I* **1985**, 493.
- (34) Nagao, K.; Chiba, M.; Kim, S. W. *Synthesis* **1983**, 197.
- (35) Pellicciari, R.; Natalini, B.; Sadeghpour, B. M.; Rosato, G. C.; Ursini, A. *J. Chem. Soc., Chem. Commun.* **1993**, 1798.
- (36) Nenitzescu, C. D., *Carbonium Ions*. Wiley-Interscience: New York, 1968; Vol. 1, p 1.
- (37) Stang, P. J.; Rappoport, Z.; Hanack, M.; Subramanian, L. B., *Vinyl Cations*. Academic Press: New York, 1979.
- (38) Edens, M.; Boerner, D.; Chase, C. R.; Nass, D.; Schiavelli, M. D. *J. Org. Chem.* **1977**, 42, 3403.
- (39) Marcuzzi, F.; Melloni, G. *J. Am. Chem. Soc.* **1976**, 98, 3295.
- (40) Verhelst, W. F.; Drenth, W. *J. Am. Chem. Soc.* **1974**, 96, 6692.
- (41) Peterson, P. E.; Bopp, R. J. *J. Am. Chem. Soc.* **1967**, 89, 1283.
- (42) Pasto, D. J.; Miles, M. F.; Chou, S.-K. *J. Org. Chem.* **1977**, 42, 3098.
- (43) Poutsma, M. L.; Ibarbia, P. A. *J. Am. Chem. Soc.* **1971**, 93, 440.
- (44) Hanack, M.; Spang, W. *Chem. Ber.* **1980**, 113, 2015.

- (45) Collins, C. J.; Benjamin, B. M.; Hanack, M.; Stutz, H. *J. Am. Chem. Soc.* **1977**, *99*, 1669.
- (46) Bertrand, M.; Santelli, M. *Tetrahedron* **1974**, *30*, 227.
- (47) Ragonnet, B.; Santelli, M.; Bertrand, M. *Helv. Chim. Acta* **1974**, *57*, 557.
- (48) Bertrand, M.; Rouvier, C. S. *Bull. Soc. Chim. Fr.* **1973**, 1800.
- (49) Hanack, L. R. S. M. *J. Chem. Ed* **1975**, *52*, 80.
- (50) Grob, C. A.; Cseh, G. *Helv. Chim. Acta* **1964**, *47*, 194.
- (51) Hassdenteufel, J. R.; Hanack, M. *Tetrahedron Lett.* **1980**, 503.
- (52) Salaun, J.; Hanack, M. *J. Org. Chem.* **1975**, *40*, 1994.
- (53) Rappoport, Z.; Kaspi, J.; Tsidoni, D. *J. Org. Chem.* **1984**, *49*, 80.
- (54) Rappoport, Z.; Apeloig, Y.; Greenblatt, J. 1980; Vol. 102, p 3837.
- (55) Staudinger, H.; Gaule, A. *Ber. Dtsch. Chem. Ges.* **1916**, *49*, 1897.
- (56) Hendrickson, J. B. *J. Am. Chem. Soc.* **1986**, *108*, 6748.
- (57) R. E. Claus; Schreiber, S. L. In *Organic Syntheses, Collective Volume 7*; Wiley: 1990, p 168.
- (58) Maison, W. *Eur. J. Org. Chem.* **2007**, 2276.
- (59) Corey, E. J.; Mitra, R. B.; Uda, H. *J. Am. Chem. Soc.* **1964**, *86*, 485.
- (60) Draghici, C.; Brewer, M. *J. Am. Chem. Soc.* **2008**, *130*, 3766.
- (61) Grob, C. A.; Schiess, P. W. *Angew. Chem., Int. Ed. Engl.* **1967**, *6*, 1.
- (62) Beckmann, E. *Chem. Ber.* **1886**, 988.
- (63) Kirihaara, M.; Niimi, K.; Momose, T. *Chem. Comm.* **1997**, 599.
- (64) Franck, R. W.; Johnson, W. S. *Tetrahedron Lett.* **1963**, 545.
- (65) Grob, C. A.; Csapilla, J.; Cseh, G. *Helv. Chim. Acta* **1964**, *47*, 1590.
- (66) Laurent, A. J.; Drean, I. M. L.; Selmi, A. *Tetrahedron Lett.* **1991**, *32*, 3071.
- (67) LeGoff, E. *J. Am. Chem. Soc.* **1962**, *84*, 3786.
- (68) Nakayama, J.; Yamaoka, S.; Nakanishi, T.; Hoshino, M. *J. Am. Chem. Soc.* **1988**, *110*, 6598.
- (69) Kamijo, S.; Dudley, G. B. *J. Am. Chem. Soc.* **2006**, *128*, 6499.



- (70) Eschenmoser, A.; Felix, D.; Ohloff, G. *Helv. Chim. Acta* **1967**, *50*, 708.
- (71) Felix, D.; Shreiber, J.; Ohloff, G.; Eschenmoser, A. *Helv. Chim. Acta* **1971**, *54*, 2896.
- (72) Tanabe, M.; Crowe, D. F.; Dehn, R. L. *Tetrahedron Lett.* **1967**, 3943.
- (73) Tanabe, M.; Crowe, D. F.; Dehn, R. L.; Detre, G. *Tetrahedron Lett.* **1967**, 3739.
- (74) Mander, L. N.; McLachlan, M. M. *J. Am. Chem. Soc.* **2003**, *125*, 2400.
- (75) Minger, T. L.; Phillips, A. J. *Tetrahedron Lett.* **2002**, *43*, 5357.
- (76) Pfeiffer, M. W. B.; Phillips, A. J. *J. Am. Chem. Soc.* **2005**, *127*, 5334.
- (77) Salamone, S. G.; Dudley, G. B. *Org. Lett* **2005**, *7*, 4443.
- (78) Krapcho, A. P. *Synthesis* **1974**, 383.
- (79) Krapcho, A. P. *Synthesis* **1976**, 425.
- (80) Sannigrahi, M. *Tetrahedron* **1999**, *55*, 9007.
- (81) Rubottom, G. M. *Tetrahedron Lett.* **1974**, 4319.
- (82) Sharpless, K. B.; Amberg, W.; Bennani, Y. L.; Crispino, G. A.; Hartung, J.; Jeong, K. S.; Kwong, H. L.; Morikawa, K.; Wang, Z. M. *J. Org. Chem.* **1992**, *57*, 2768.
- (83) Demir, A. S.; Reis, O.; Igdir, A. C. *Tetrahedron* **2004**, *60*, 3427.
- (84) Glazier, E. R. *J. Org. Chem.* **1962**, *27*, 4397.
- (85) Numazawa, M.; Nagaoka, M.; Osawa, Y. *J. Org. Chem.* **1982**, *47*, 4024.
- (86) Shi, B. F.; Tang, P. P.; Hu, X. Y.; Liu, J. O.; Yu, B. *J. Org. Chem.* **2005**, *70*, 10354.
- (87) Regitz, M.; Maas, G., *Diazo Compounds: Properties and Synthesis* Academic Press: Orlando, 1986.
- (88) Gradillas, A.; Perez-Castells, J. *Angew. Chem., Int. Ed. Engl.* **2006**, *45*, 8086.
- (89) Parenty, A.; Moreau, X.; Campagne, J. M. *Chem. Rev.* **2006**, *106*, 911.
- (90) El-Gamal, A. A. H.; Wang, S. K.; Duh, C. Y. *Chem. Pharm. Bull.* **2007**, *55*, 890.

- (91) Reino, J. L.; Duran-Patron, R. M.; Daoubi, M.; Collado, I. G.; Hernandez-Galan, R. *J. Org. Chem.* **2006**, *71*, 562.
- (92) Neumann, H.; Seebach, D. *Tetrahedron Lett.* **1976**, *52*, 4839.
- (93) Marino, J. P.; Nguyen, H. N. *J. Org. Chem.* **2002**, *67*, 6291.
- (94) Nicola, T.; Schwarzrock, D.; Keller, M.; Eberbach, W. *Tetrahedron* **2001**, *57*, 1771.
- (95) Trost, B. M.; Shi, Y. *J. Am. Chem. Soc.* **1993**, *115*, 12491.
- (96) Johnson, T.; Cheshire, D. R.; Stocks, M. J.; Thurston, V. T. *Synlett* **2001**, 646.
- (97) Inokuchi, T.; Kawafuchi, H.; Torii, S. *J. Org. Chem.* **1991**, *56*, 4983.
- (98) Jang, H.-Y.; Hughes, F. W.; Gong, H.; Zhang, J.; Brodbelt, J. S.; Krische, M. J. *J. Am. Chem. Soc.* **2005**, *127*, 6174.
- (99) Paterson, I.; Cowden, C. J.; Woodrow, M. D. *Tetrahedron Lett.* **1998**, *39*, 6037.
- (100) Tufariello, J. J.; Trybulski, E. J. *J. Org. Chem.* **1974**, *39*, 3378.
- (101) Brown, C. A.; Yamashita, A. *J. Am. Chem. Soc.* **1975**, *97*, 891.
- (102) Ma, D. W.; Lu, X. Y. *Tetrahedron* **1990**, *46*, 6319.
- (103) Dabdoub, M. J.; Dabdoub, V. B.; Comasseto, J. V. *Tetrahedron Lett.* **1992**, *33*, 2261.
- (104) Tucci, F. C.; Chieffi, A.; Comasseto, J. V.; Marino, J. P. *J. Org. Chem.* **1996**, *61*, 4975.
- (105) Terao, J.; Kambe, N.; Sonoda, N. *Tetrahedron Lett.* **1996**, *37*, 4741.
- (106) Yamada, K.; Ojika, M.; Ishigaki, T.; Yoshida, Y.; Ekimoto, H.; Arakawa, M. *J. Am. Chem. Soc.* **1993**, *115*, 11020.
- (107) Huisgen, R., *1,3-Dipolar Cycloaddition Chemistry*. Wiley: New York, 1984; Vol. 1, p 1.
- (108) Lown, J. W., *1,3-Dipolar Cycloaddition Chemistry*. Wiley: New York, 1984; Vol. 1, p 653.

- (109) Houk, K. N.; Yamaguchi, K., *1,3-Dipolarcycloaddition Chemistry*. Wiley: New York, 1984; Vol. 2, p 407.
- (110) Bianchi, G.; Gandolfi, R., *1,3-Dipolar Cycloaddition Chemistry*. Wiley: New York, 1984; Vol. 2, p 451.
- (111) Gothelf, K. V.; Jorgensen, K. A. *Chem. Rev.* **1998**, 98, 863.
- (112) Coldham, I.; Hufton, R. *Chem. Rev.* **2005**, 105, 2765.
- (113) Woodward, R. B.; Hoffmann, R., *The Conservation of Orbital Symmetry*. Verlag Chemie: Weinheim, Germany, 1970.
- (114) Fleming, I., *Frontier Orbitals and Organic Chemical Reactions*. Wiley: New York, 1976.
- (115) Bashiardes, G.; Safir, I.; Barbot, F.; Laduranty, J. *Tetrahedron Lett.* **2004**, 45, 1567.
- (116) Grigg, R.; Surendrakumar, S.; Thianpatanagul, S.; Vipond, D. *J. Chem. Soc., Chem. Commun.* **1987**, 47.
- (117) Grigg, R.; Idle, J.; McMeekin, P.; Vipond, D. *J. Chem. Soc., Chem. Commun.* **1987**, 49.
- (118) Bashiardes, G.; Safir, I.; Barbot, F.; Laduranty, J. *Tetrahedron Lett.* **2003**, 44, 8417.
- (119) Confalone, P. N.; Huie, E. M. *J. Am. Chem. Soc.* **1984**, 106, 7175.
- (120) Marx, M. A.; Grillot, A.-L.; Louer, C. T.; Beaver, K. A.; Bartlett, P. A. *J. Am. Chem. Soc.* **1997**, 119, 6153.
- (121) Annunziata, R.; Ferrari, M.; Papeo, G.; Resmini, M.; Sisti, M. *Synthetic Communications* **1997**, 27, 23.
- (122) Seebach, D.; Boes, M.; Naef, R.; Schweizer, W. B. *J. Am. Chem. Soc.* **1983**, 105, 5390.
- (123) Vedejs, E.; Dax, S. L. *Tetrahedron Lett.* **1989**, 30, 2627.
- (124) Smith, E. D.; Shewbart, K. L. *J. Chromatogr. Sci.* **1969**, 7, 704.
- (125) Vronen, P. J. E.; Koval, N.; de Groot, A. *Arkivoc* **2004**, 24.

- (126) Jadhav, S. J.; Sharma, R. P.; Salunkhe, D. K. *CRC Crit. Rev. Toxicol.* **1981**, 9, 21.
- (127) Mensinga, T. T.; Sips, A. J. A. M.; Rompelberg, C. J. M.; van Twillert, K.; Meulenbelt, J.; van den Top, H. J.; van Egmond, H. P. *Regul. Toxicol. Pharmacol.* **2005**, 41, 66.
- (128) Morris, T. *Br. Med. J.* **1859**, 140, 719.
- (129) Morris, S. C.; Lee, T. H. *Food Technol. Australia* **1984**, 36, 118.
- (130) Smith, D. B.; Roddick, J. G.; Jones, J. L. *Trends Food Sci. Technol.* **1996**, 7, 126.
- (131) Dao, L.; Friedman, M. *J. Agric. Food Chem.* **1994**, 42, 633.
- (132) Chataing, B.; Concepcion, J. L.; Cristancho, N. B. d.; Usubillaga, N. B. *Revista de la Facultad de Farmacia* **1997**, 32, 18.
- (133) Gubarev, M. I.; Enioutina, E. Y.; Taylor, J. L.; Visic, D. M.; Daynes, R. *A. Phytother. Res.* **1998**, 12, 79.
- (134) McGehee, D. S.; Krasowski, M. D.; Fung, D. L.; Wilson, B.; Gronert, G. A.; Moss, J. *Anesthesiology* **2000**, 93, 510.
- (135) Rajanathanan, P.; Attard, G. S. *Vaccine* **2000**, 18, 140.
- (136) Lee, K.-R.; Kozukue, N.; Han, J.-S.; Park, J.-H.; Chang, E.-y.; Baek, E.-J.; Chang, J.-S.; Friedman, M. *J. Agric. Food Chem.* **2004**, 52, 2832.
- (137) Schreiber, K.; Ronsch, H. *Tetrahedron* **1965**, 645.
- (138) Pelletier, S. W.; Jacobs, W. A. *J. Am. Chem. Soc.* **1953**, 75, 4442.
- (139) Kessar, S. V.; Rampal, A. L.; Ghandi, S. S.; Mahajan, R. K. *Tetrahedron* **1970**, 27, 2153.
- (140) Alvaro, G.; Savoia, D. *Synlett* **2002**, 651.
- (141) Davis, F. A.; Zhou, P.; Chen, B. C. *Chemical Society Reviews* **1998**, 27, 13.
- (142) Enders, D.; Reinhold, U. *Tetrahedron: Asymmetry* **1997**, 8, 1895.
- (143) Bloch, R. *Chem. Rev.* **1998**, 98, 1407.

- (144) Corey, E. J.; Decicco, C. P.; Newbold, R. C. *Tetrahedron Lett.* **1991**, 32, 5287.
- (145) Friestad, G. K. *Tetrahedron* **2001**, 57, 5461.
- (146) Fallis, A. G.; Brinza, I. M. *Tetrahedron* **1997**, 53, 17543.
- (147) Renauld, P.; Sibi, M., *Radicals in Organic Synthesis*. Wiley-VCH: New York, 2001.
- (148) Curran, D. P.; Porter, N. A.; Giese, B., *Stereochemistry of Radical Reactions: Concepts, Guidelines, and Synthetic Applications*. VCH: New York, 1995.
- (149) Liu, G. C.; Cogan, D. A.; Ellman, J. A. *J. Am. Chem. Soc.* **1997**, 119, 9913.
- (150) Moody, C. J.; Gallagher, P. T.; Lightfoot, A. P.; Slawin, A. M. Z. *J. Org. Chem.* **1999**, 64, 4419.
- (151) Keith, J. M.; Jacobsen, E. N. *Org. Lett* **2004**, 6, 153.
- (152) Hamada, T.; Manabe, K.; Kodayashi, S. *J. Am. Chem. Soc.* **2004**, 126, 7768.
- (153) Berger, R.; Duff, K.; Leighton, J. L. *J. Am. Chem. Soc.* **2004**, 126, 5686.
- (154) Ballini, R.; Bosica, G.; Fiorini, D.; Palmieri, A.; Petrini, M. *Chem. Rev.* **2005**, 105, 933.
- (155) Williams, A. L.; Johnston, J. N. *J. Am. Chem. Soc.* **2004**, 126, 1612.
- (156) Antilla, J. C.; Wulff, W. D. *Angew. Chem., Int. Ed. Engl.* **2000**, 39, 4518.
- (157) Miyabe, H.; Ueda, M.; Naito, T. *Synlett* **2004**, 1140.
- (158) Miyabe, H.; Shibata, R.; Sangawa, M.; Ushiro, C.; Naito, T. *Tetrahedron* **1998**, 54, 11431.
- (159) Miyabe, H.; Fujii, K.; Naito, T. *Org. Lett* **1999**, 1, 569.
- (160) Alves, M. J.; Gilchrist, T. L.; Sousa, J. H. *J. Chem. Soc. Perkin Trans. 1* **1999**, 1305.
- (161) Miyabe, H.; Ushiro, C.; Naito, T. *Chem. Comm.* **1997**, 1789.
- (162) Bertrand, M. P.; Coantic, S.; Feray, L.; Nougulier, R.; Perfetti, P. *Tetrahedron* **2000**, 56, 3951.

- (163) Rademacher, P.; Pfeffer, H.-U.; Enders, D.; Eichenaur, H. *J. Chem. Res., Synop.* **1979**, 222.
- (164) Guerin, B.; Ogilvie, W. W.; Guindon, Y., *Radicals in Organic Synthesis*. Wiley-VCH: New York, 2001; p 441.
- (165) Ding, H.; Friestad, G. K. *Org. Lett* **2004**, 6, 637.
- (166) Sturino, C. F.; Fallis, A. G. *J. Am. Chem. Soc.* **1994**, 116, 7447.
- (167) Burk, M. J.; Feaster, J. E. *J. Am. Chem. Soc.* **1992**, 114, 6266.
- (168) Evans, D. A.; Kim, A. S., *Encyclopedia of Reagents for Organic Synthesis*. Wiley: New York, 1995; Vol. 1, p 345.
- (169) Sibi, M. P.; Jasperse, C. P.; Ji, J. G. *J. Am. Chem. Soc.* **1995**, 117, 10779.
- (170) Sibi, M. P.; Ji, J. G.; Sausker, J. B.; Jasperse, C. P. *J. Am. Chem. Soc.* **1999**, 121, 7517.
- (171) Shen, Y. H.; Friestad, G. K. *J. Org. Chem.* **2002**, 67, 6236.
- (172) Hynes, J.; Doubleday, W. W.; Dyckman, A. J.; Godfrey, J. D.; Grosso, J. A.; Kiau, S.; Leftheris, K. *J. Org. Chem.* **2004**, 69, 1368.
- (173) Friestad, G. K.; Draghici, C.; Soukri, M.; Qin, J. *J. Org. Chem.* **2005**, 70, 6330.
- (174) Hojo, M.; Harada, H.; Ito, H.; Hosomi, A. *J. Am. Chem. Soc.* **1997**, 119, 5459.
- (175) Paquette, L. A.; Hartung, R. E.; Hofferberth, J. E.; Vilotijevic, I.; Yang, J. *J. Org. Chem.* **2004**, 69, 2454.
- (176) Leino, R.; Luttikhedde, H. J. G.; Lehtonen, A.; Ekholm, P.; Näsman, J. H. *J. Organomet. Chem.* **1998**, 558, 181.
- (177) Murahashi, S.; Noji, S.; Hirabayashi, T.; Komiya, N. *Tetrahedron: Asymmetry* **2005**, 16, 3527.
- (178) Branco, L. C.; Afonso, C. A. M. *J. Org. Chem.* **2004**, 69, 4381.
- (179) Takikawa, H.; Hachisu, Y.; Bode, J. W.; Suzuki, K. *Angew. Chem., Int. Ed. Engl.* **2006**, 45, 3492.

- (180) Brown, M. J.; Harrison, T.; Overman, L. E. *J. Am. Chem. Soc.* **1991**, *113*, 5378.
- (181) Chau, A.; Paquin, J.-F.; Lautens, M. *J. Org. Chem.* **2006**, *71*, 1924.
- (182) Lauktien, G.; Volk, F. J.; Frahm, A. W. *Tetrahedron: Asymmetry* **1997**, *8*, 3457.
- (183) Gregoire, B.; Carre, M. C.; Caubere, P. *J. Org. Chem.* **1986**, *51*, 1419.

## APPENDIX

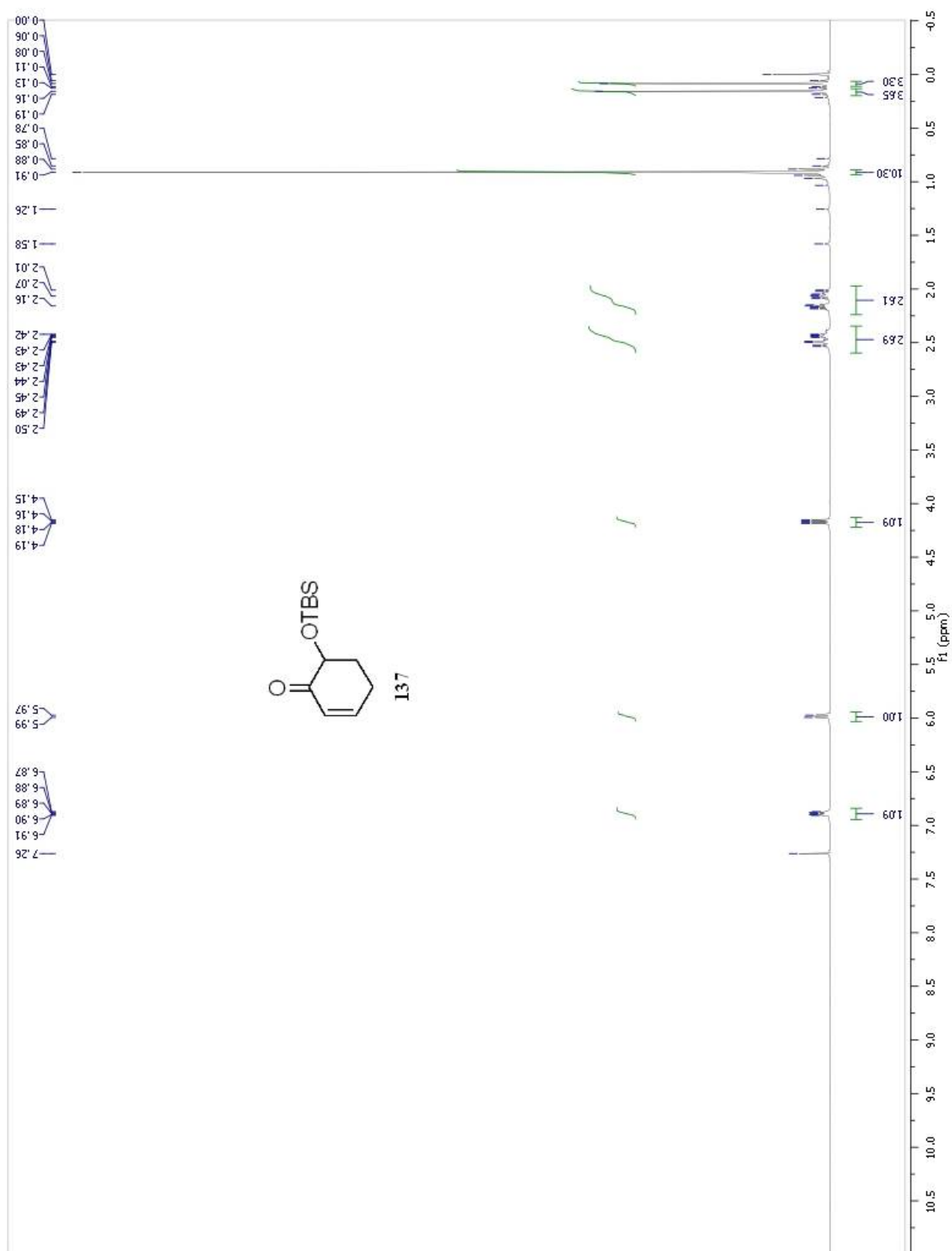
Listed in order of appearance are the NMR spectra of:

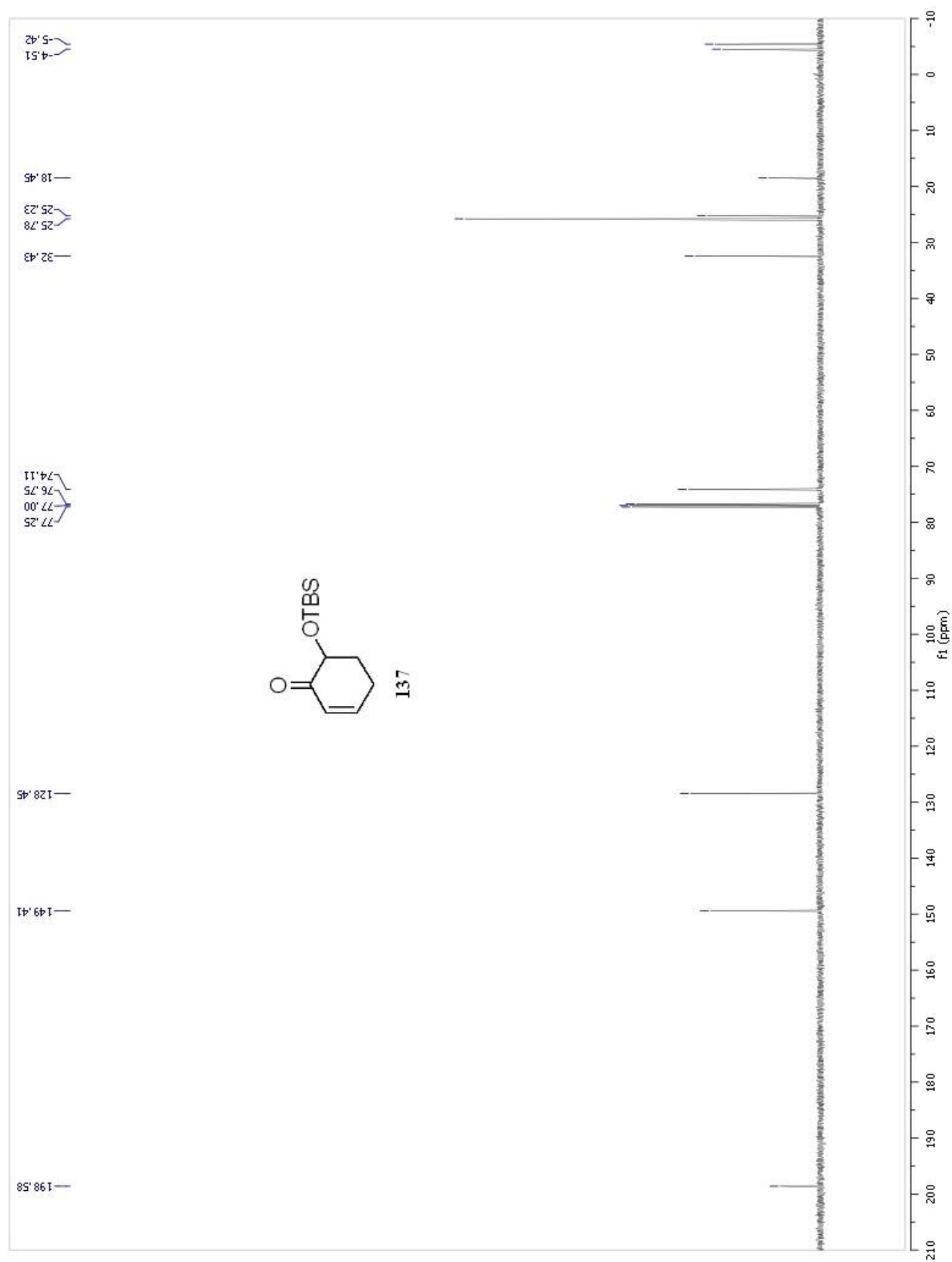
**137, 150, 154, 112, 128s, 129, 150, 154, 155, 156, 157s, 158a, 158s, 159s, 160, 162, 163, 164, 165, 166, 167, 181a, 181s, 183, 184, 190a, 190b, 199, 202, 206, 301, 302, 309, 317, 319, 320, 321, 322, 323a, 325, 328, 355, 404b, 404c, 404d, 404e.**

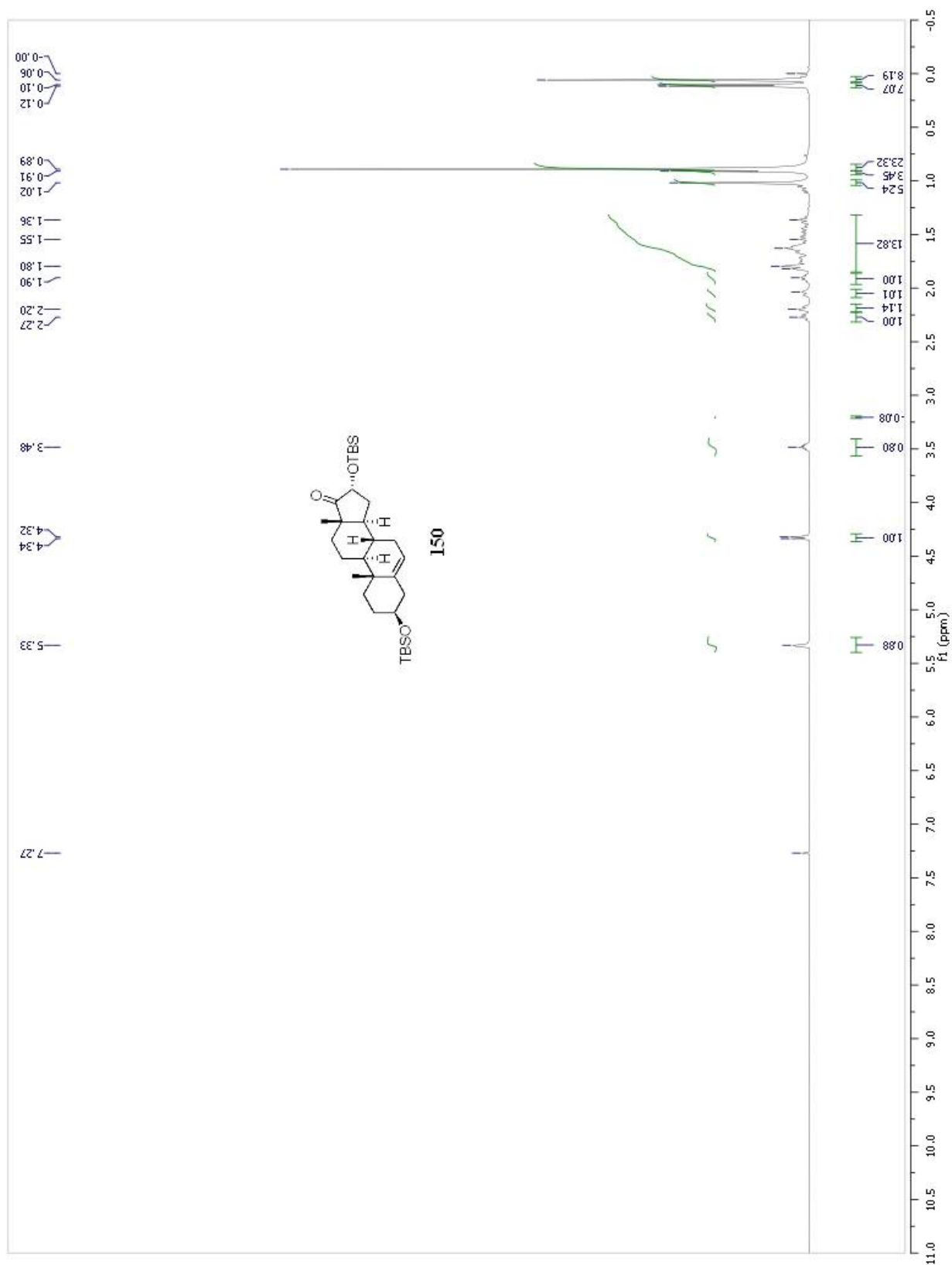
and crystallographic data for:

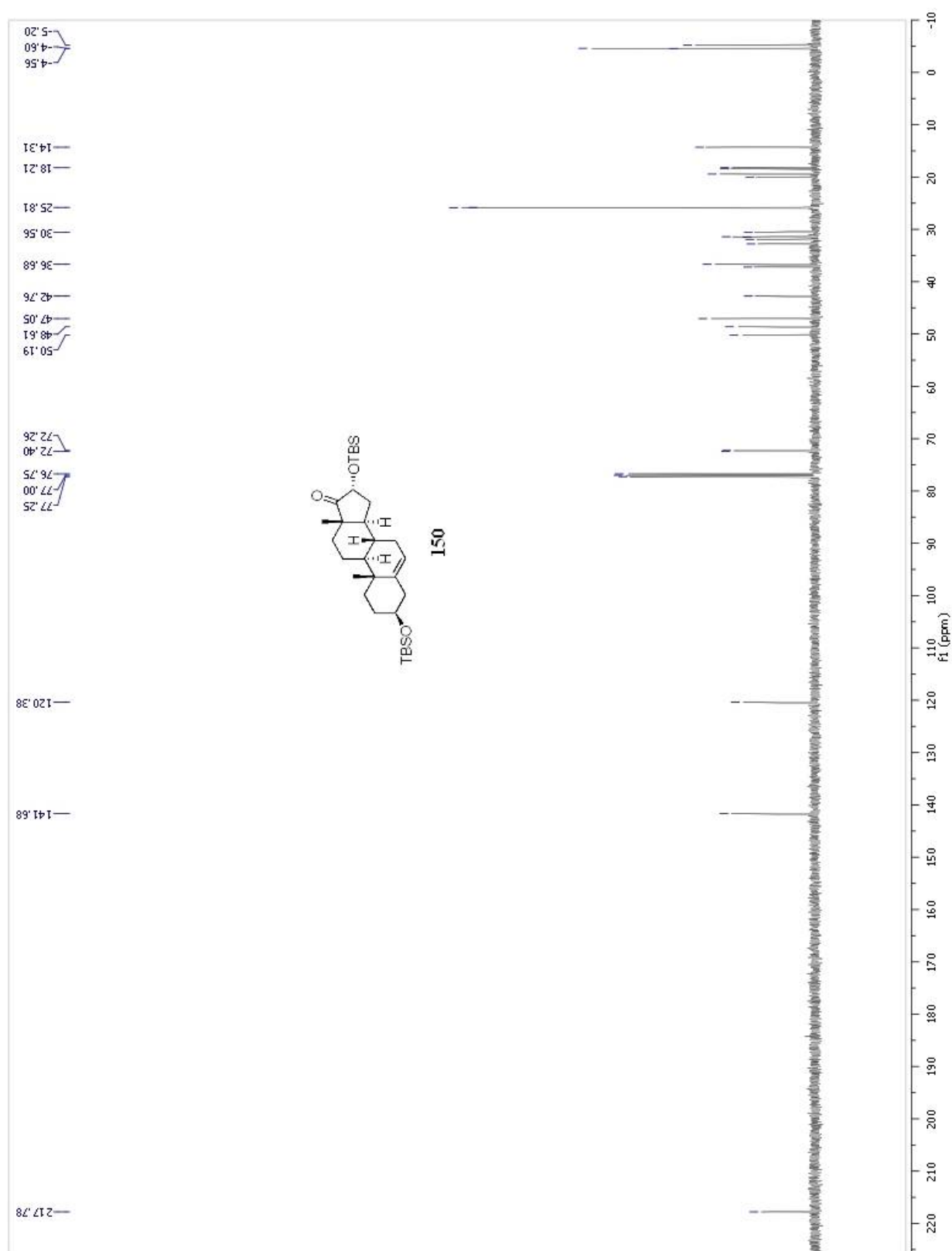
**157s, 158s.**

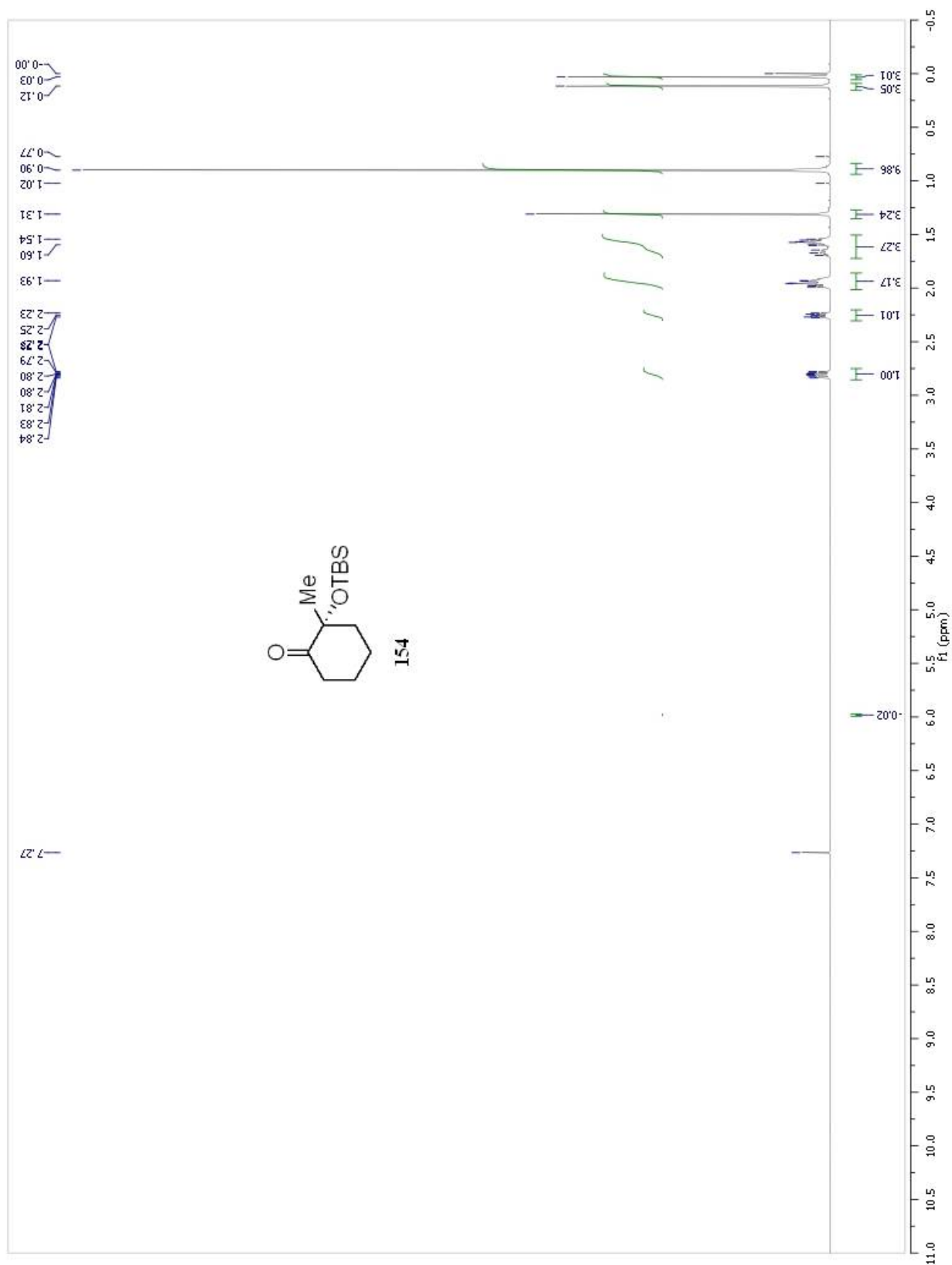


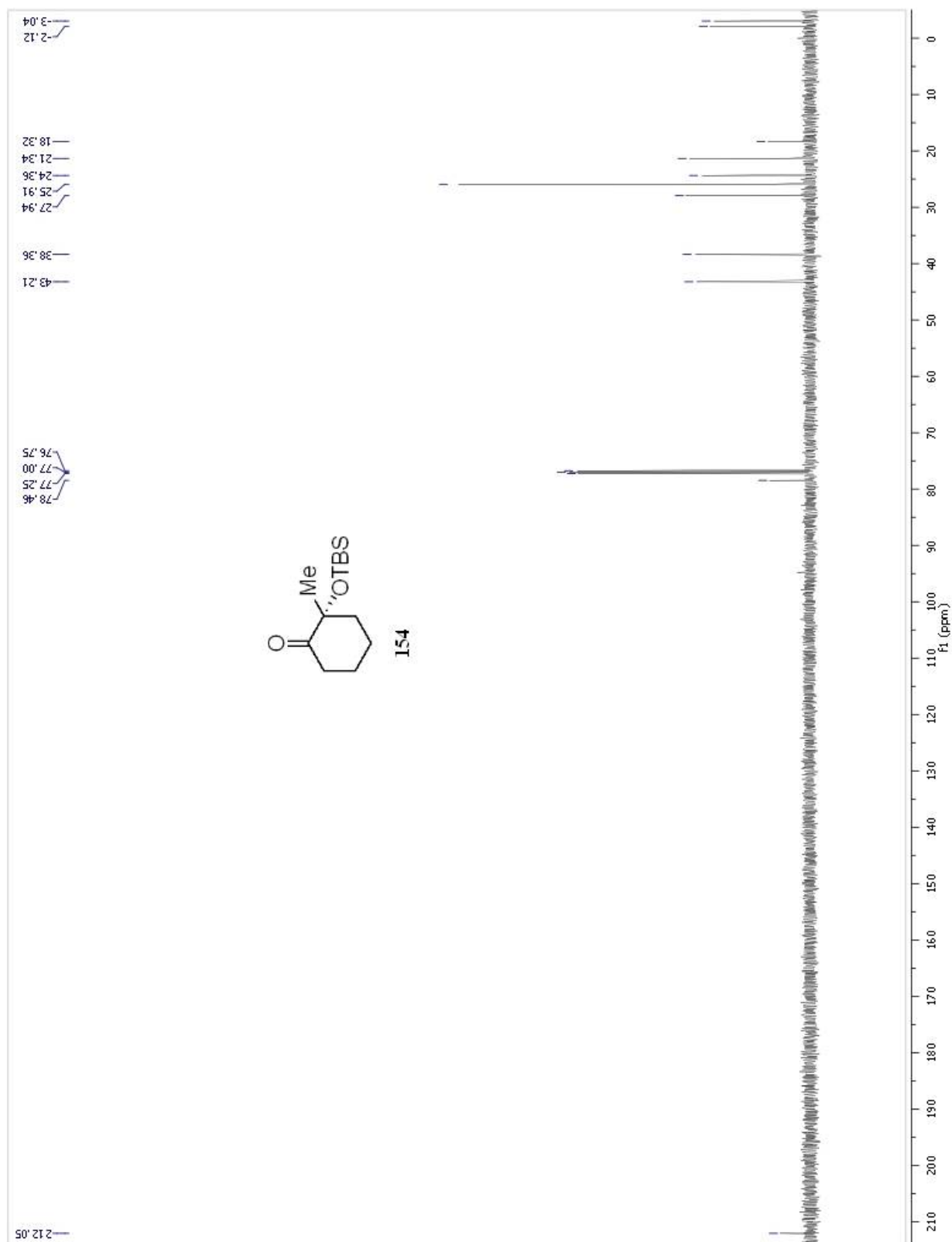




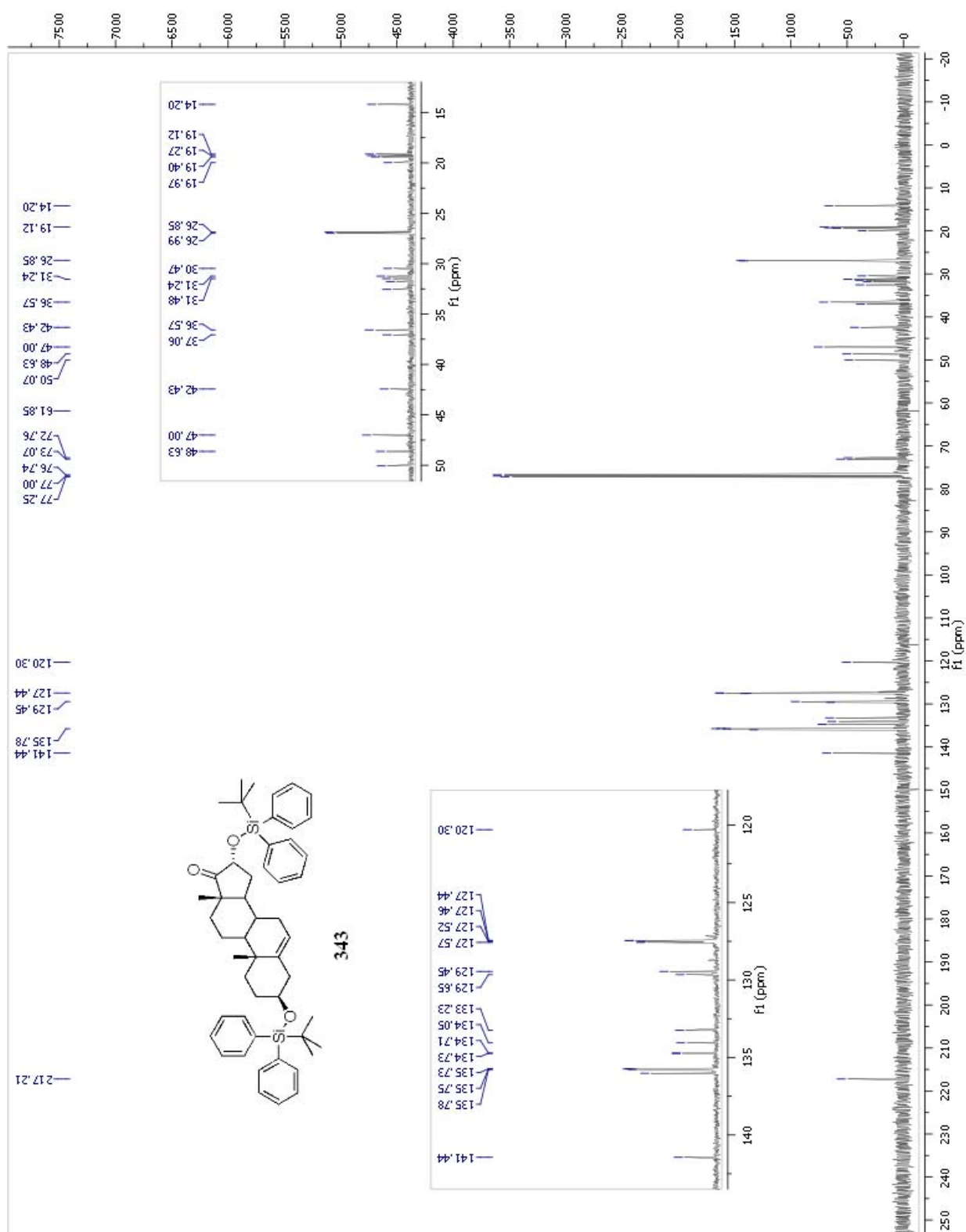






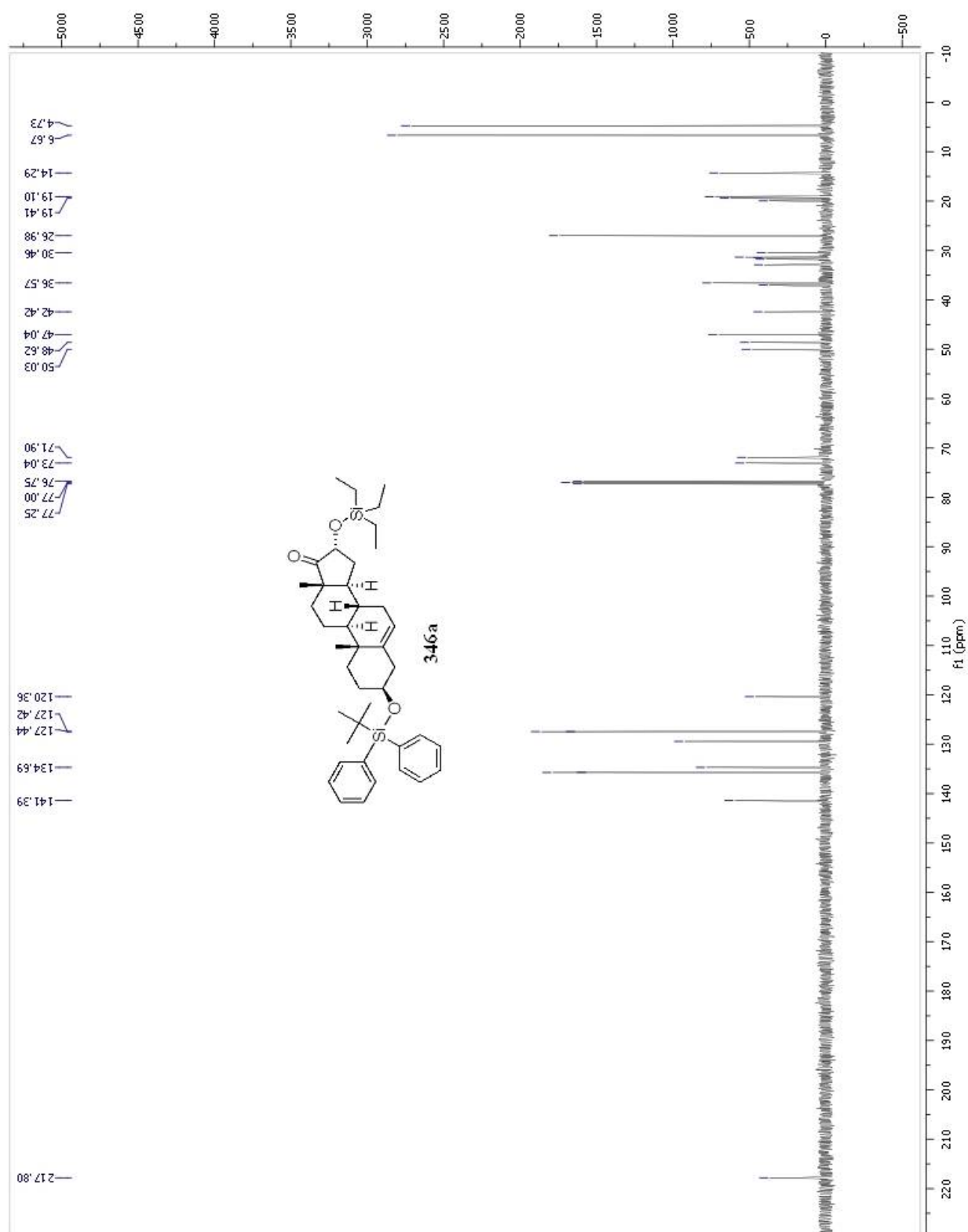


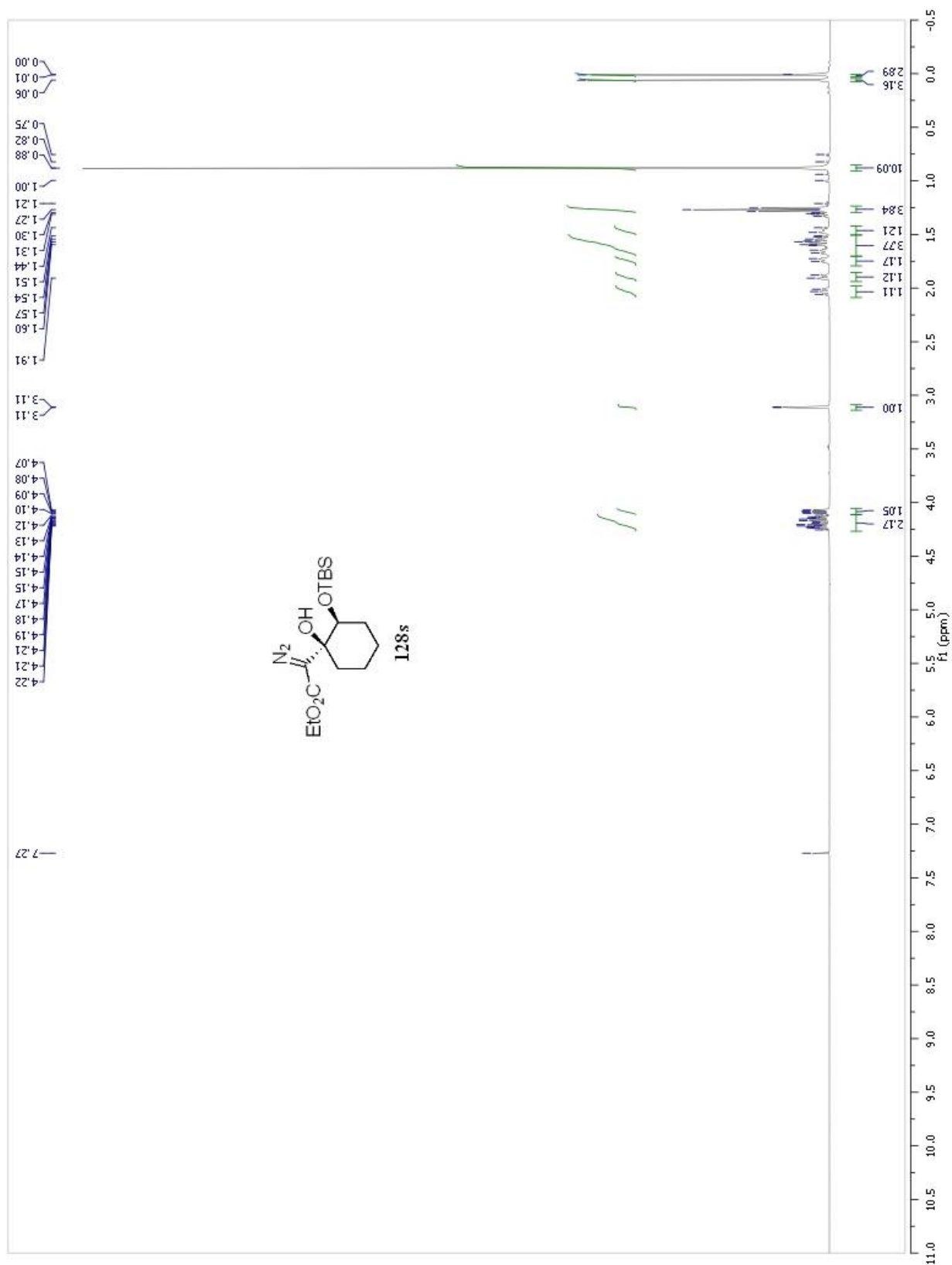


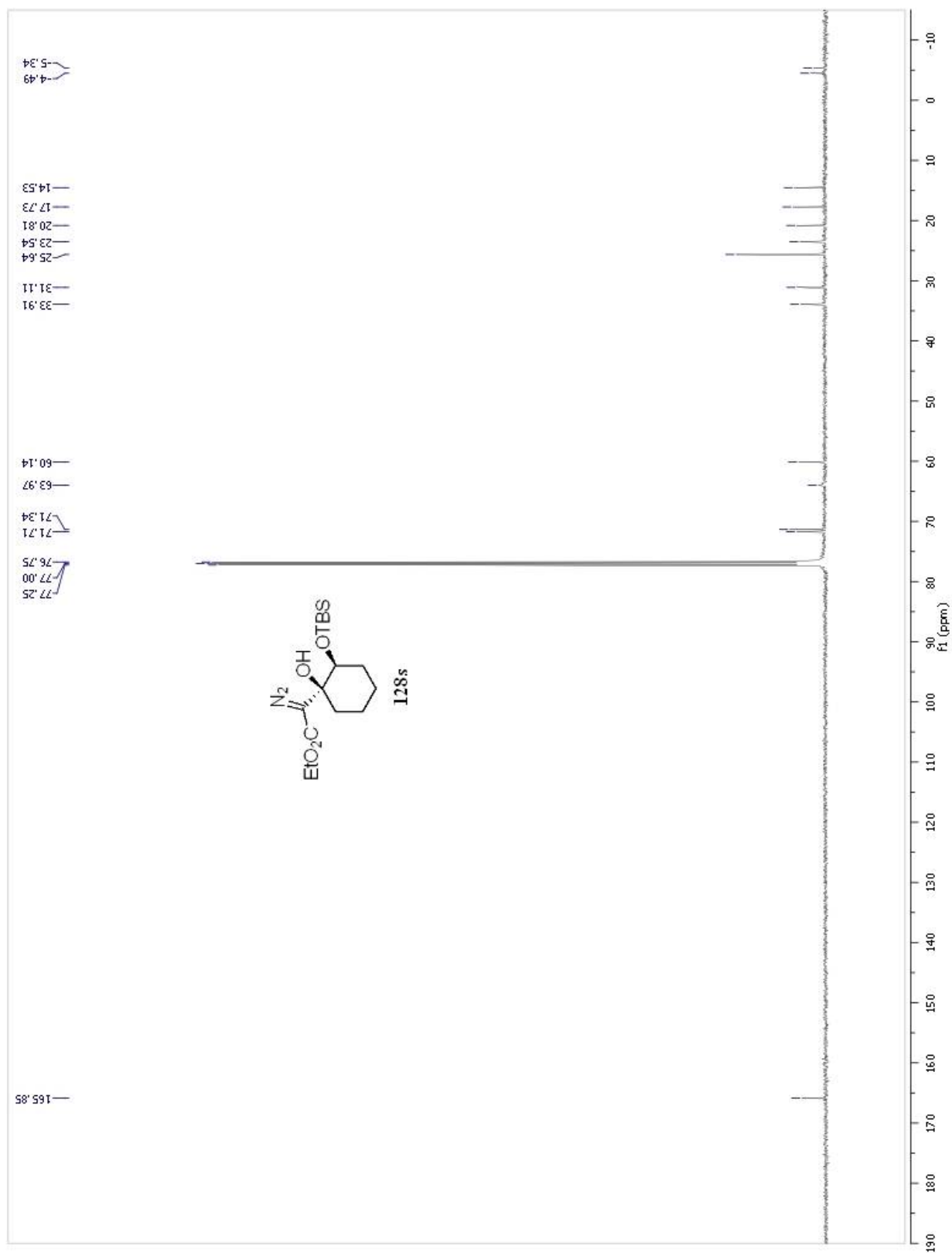


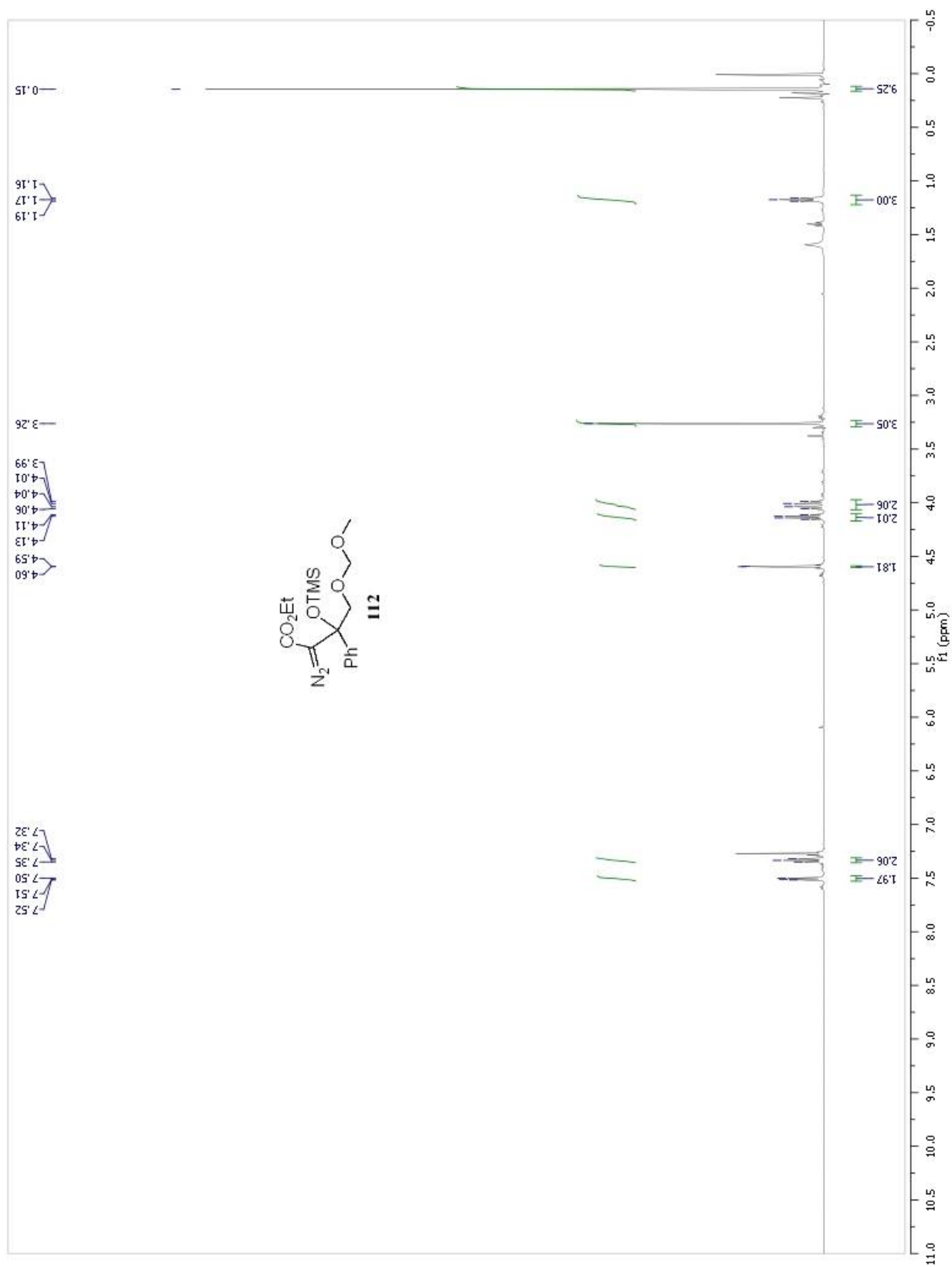


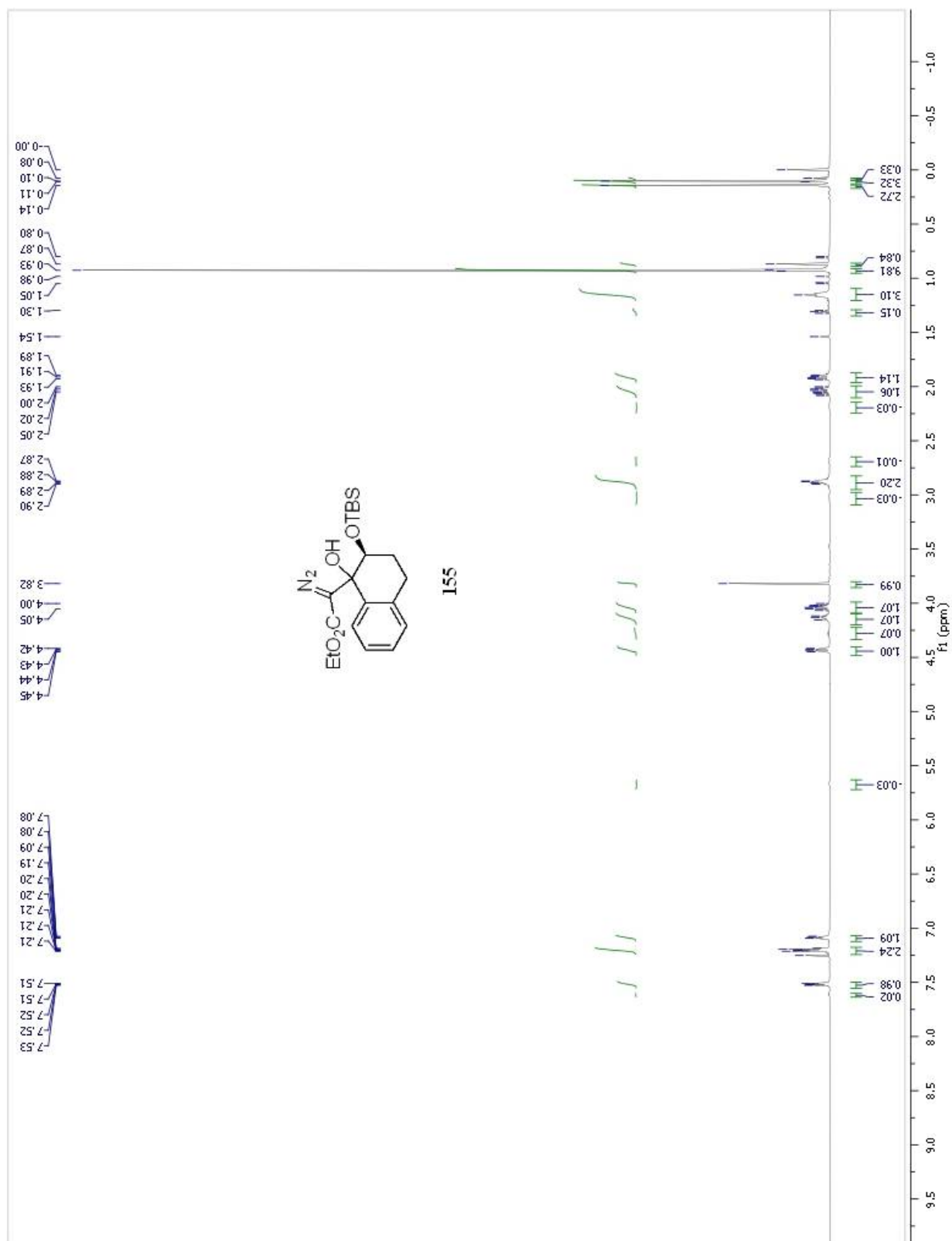


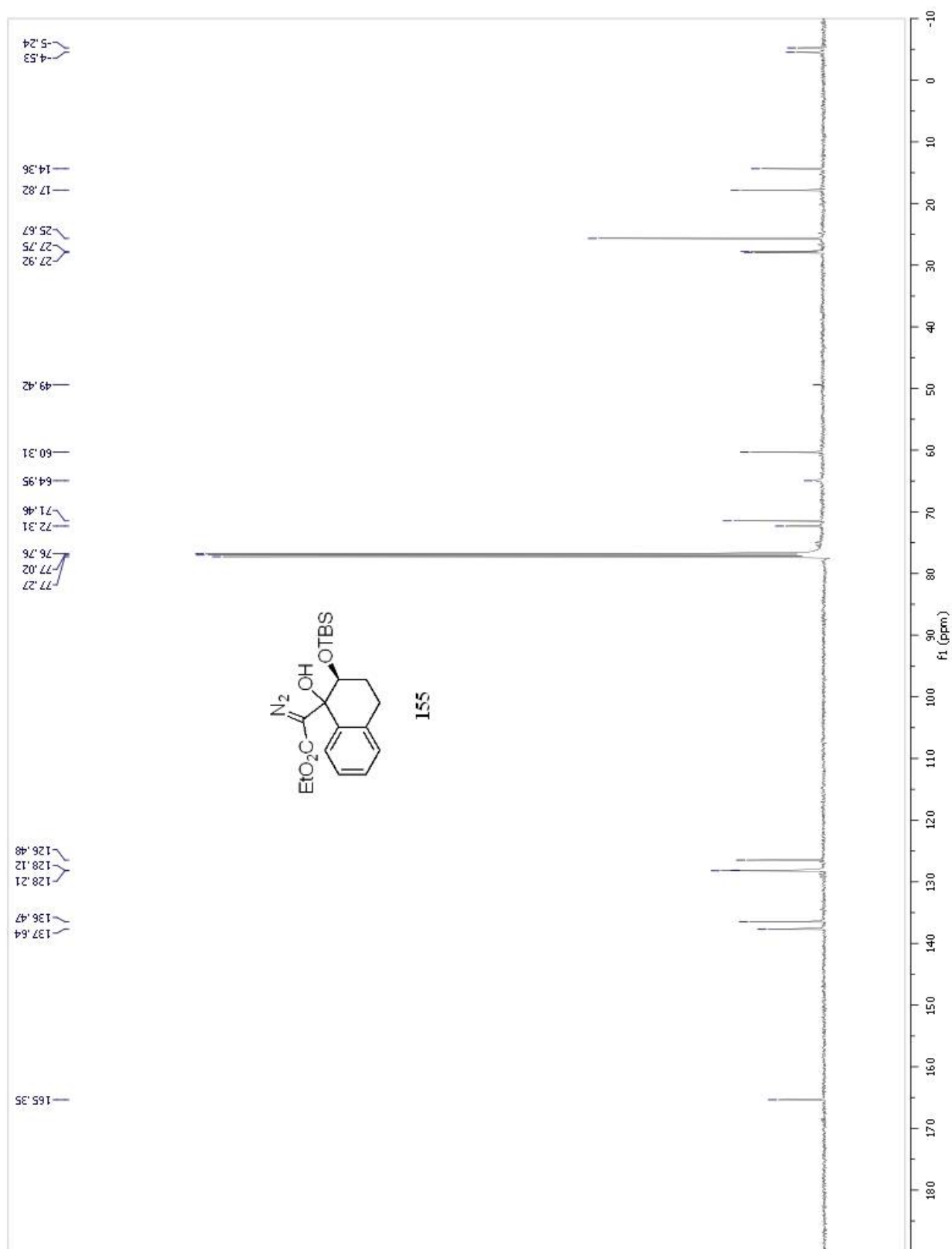


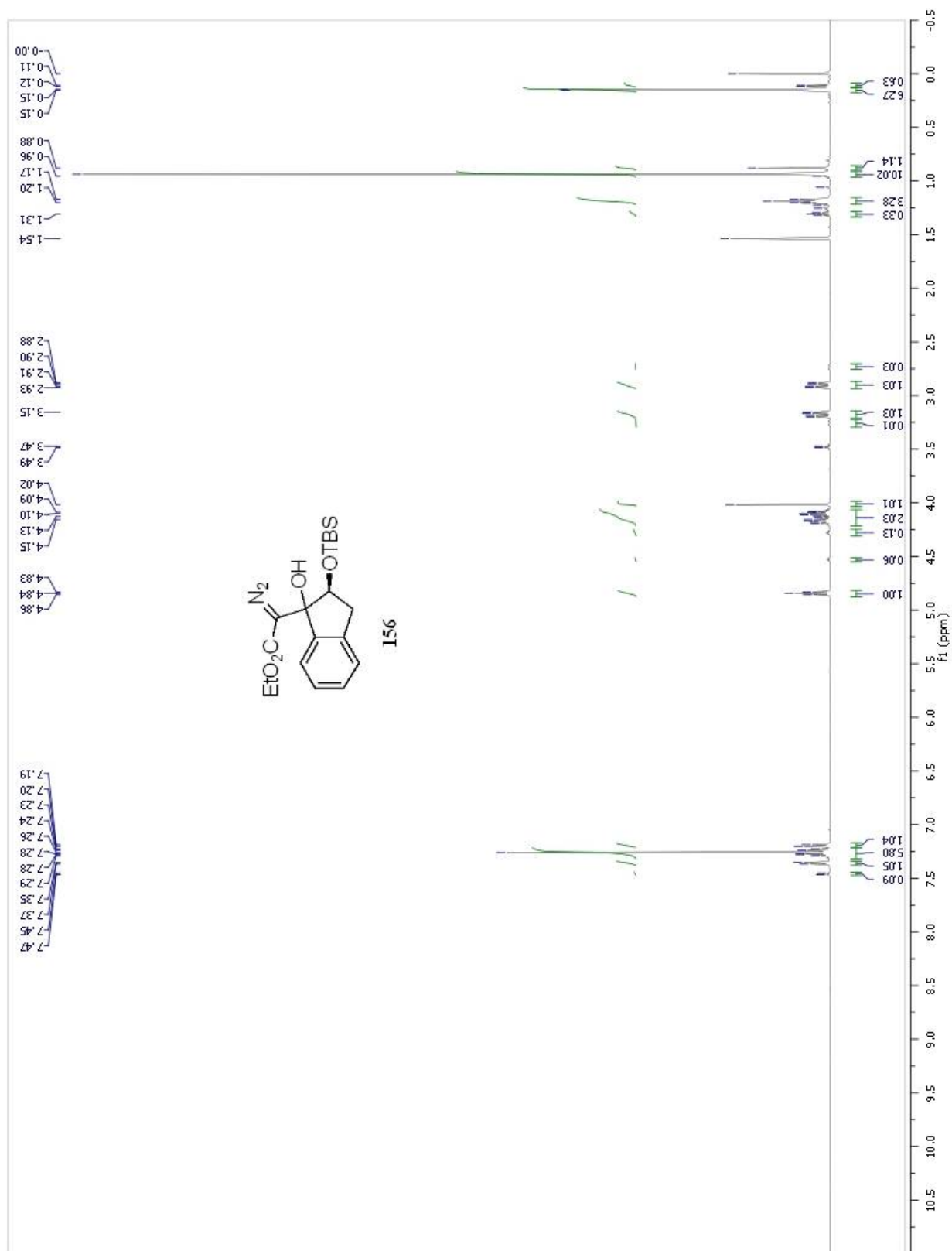






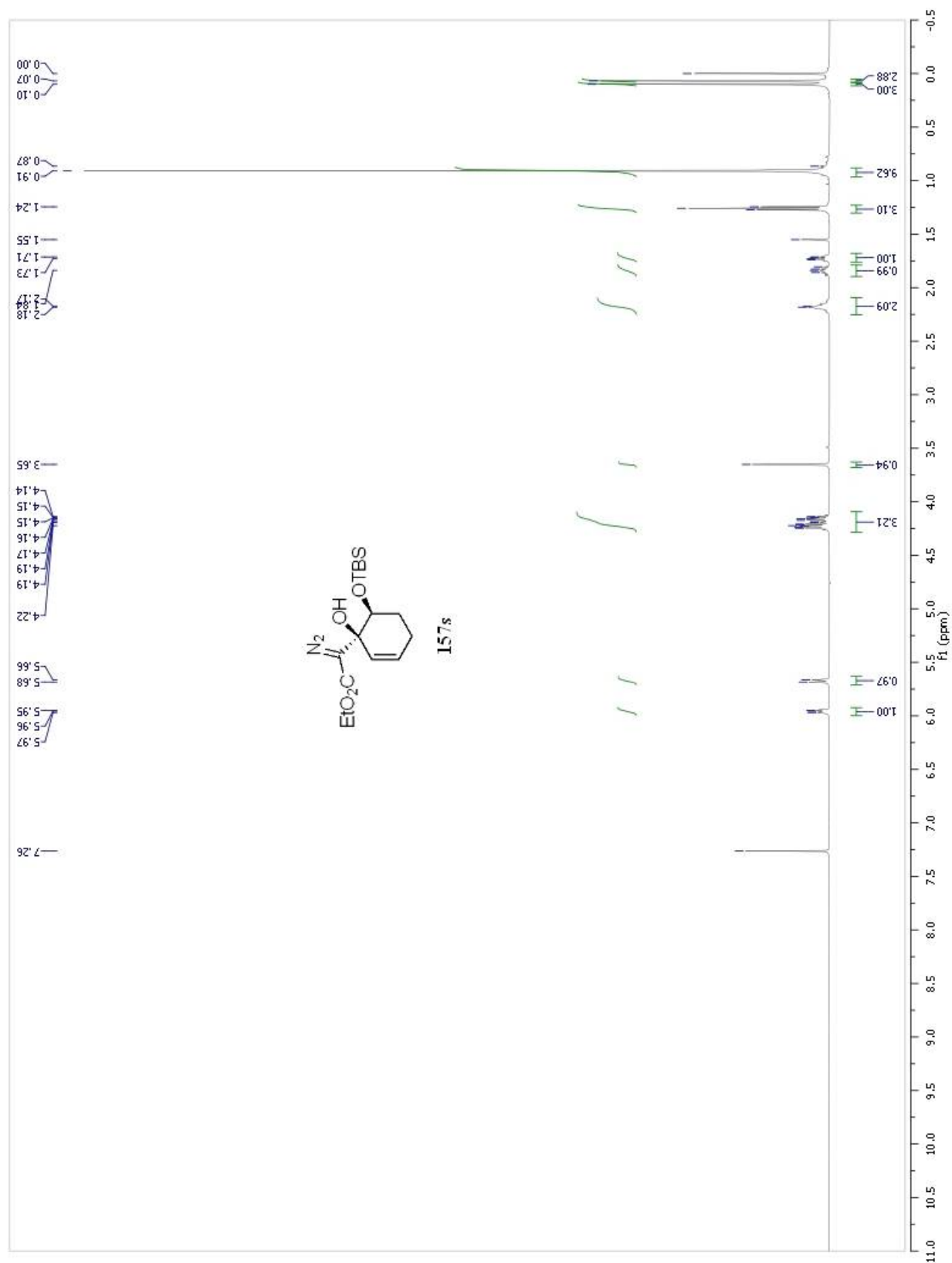


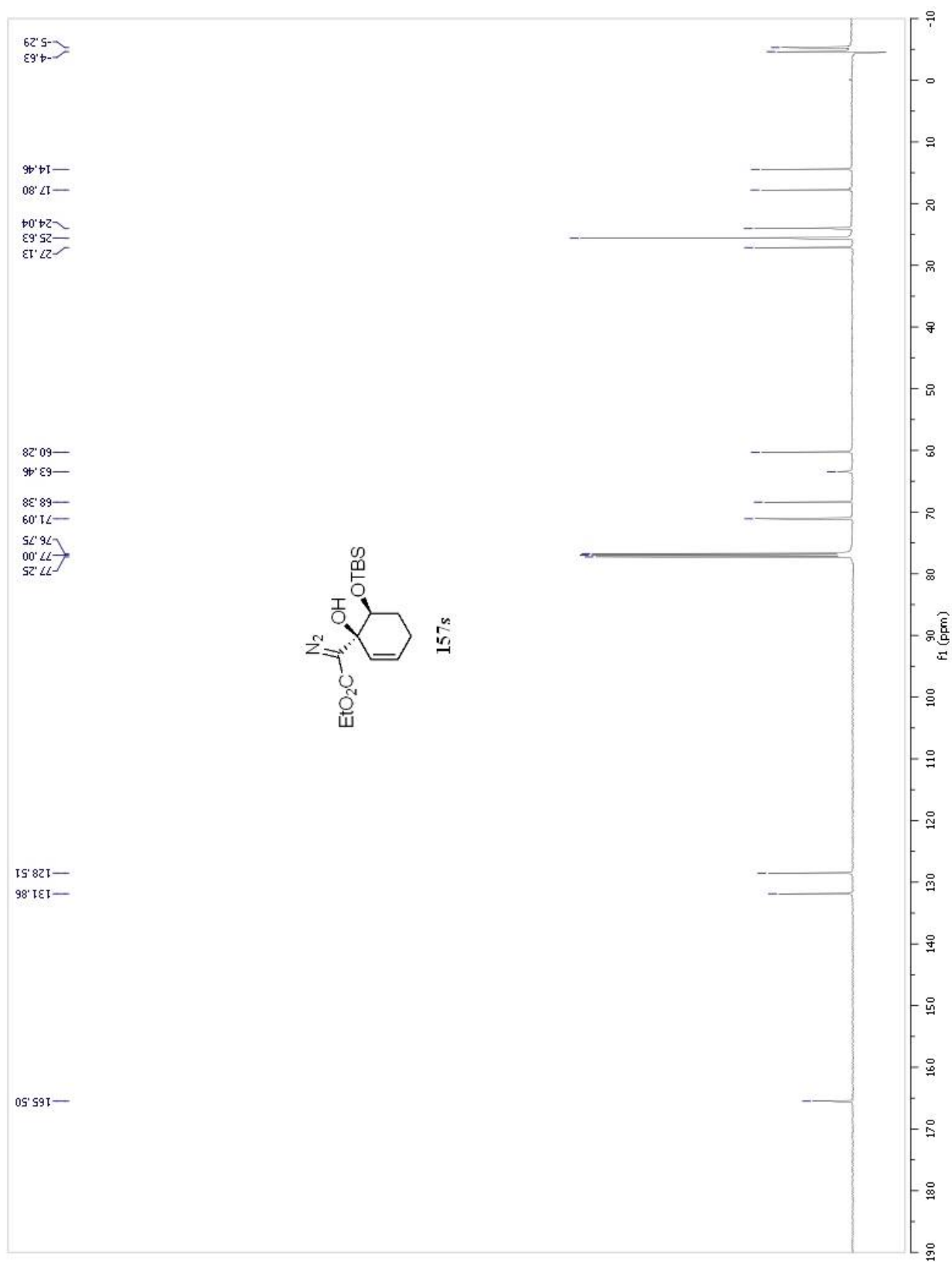


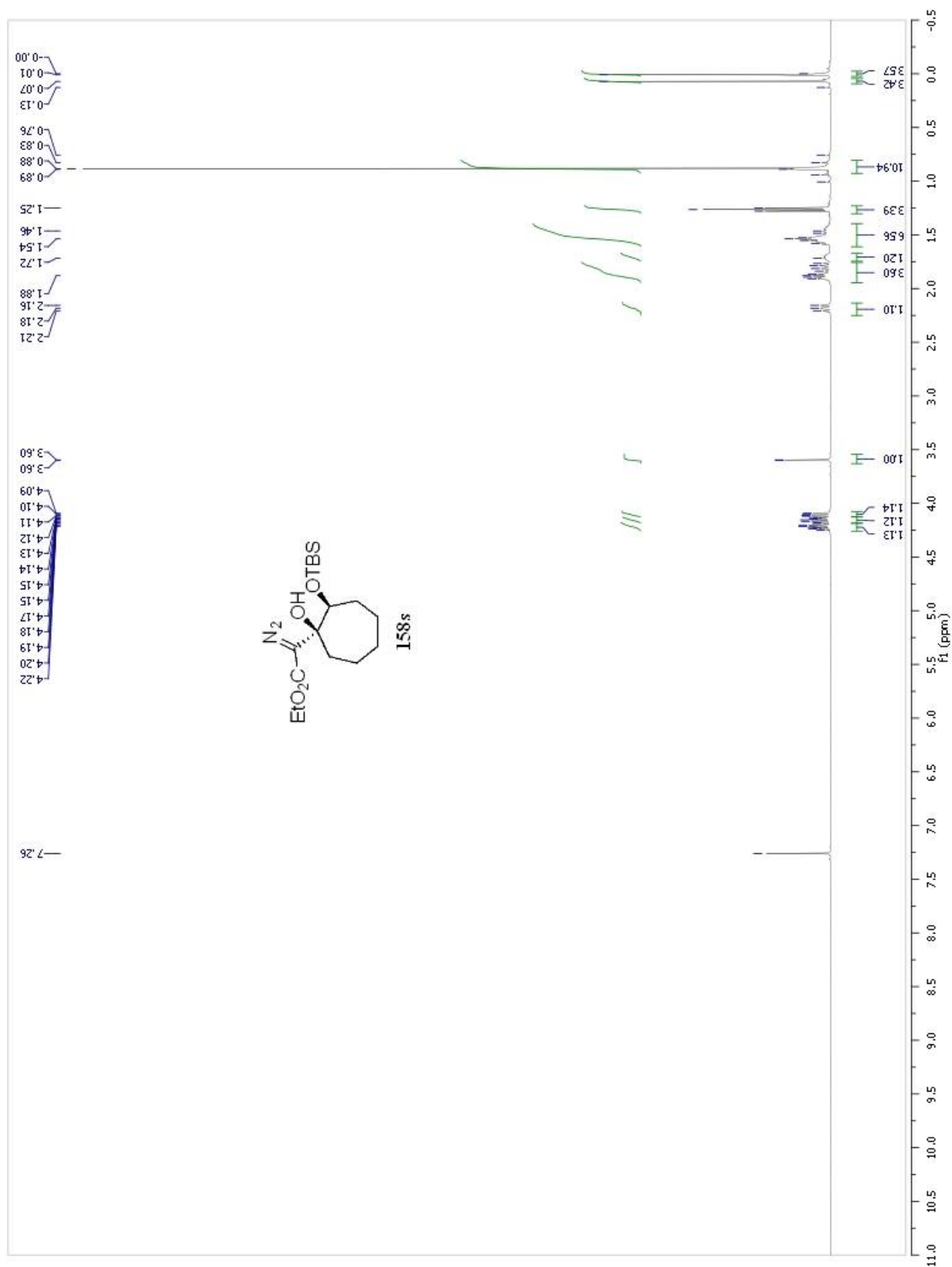


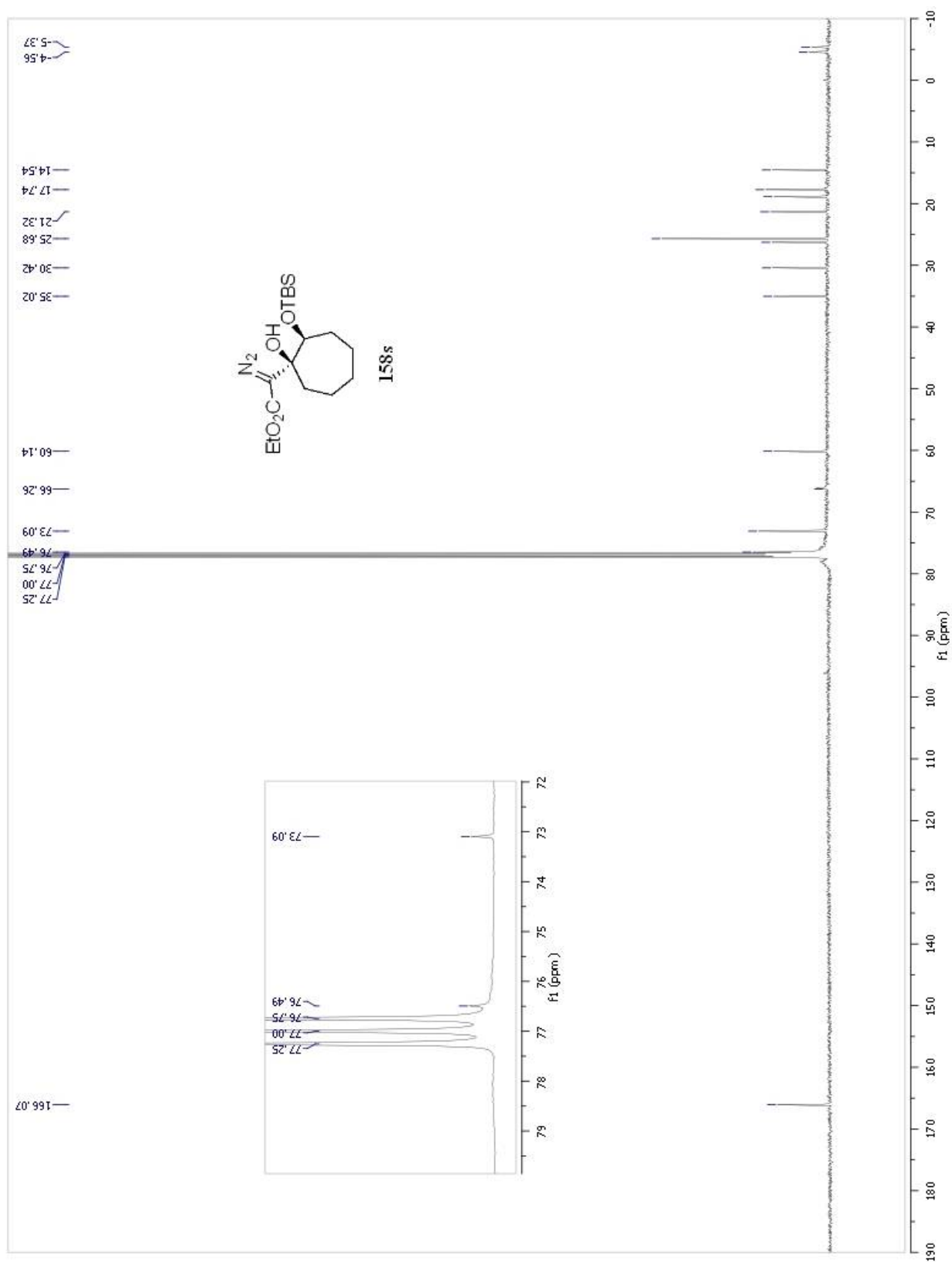


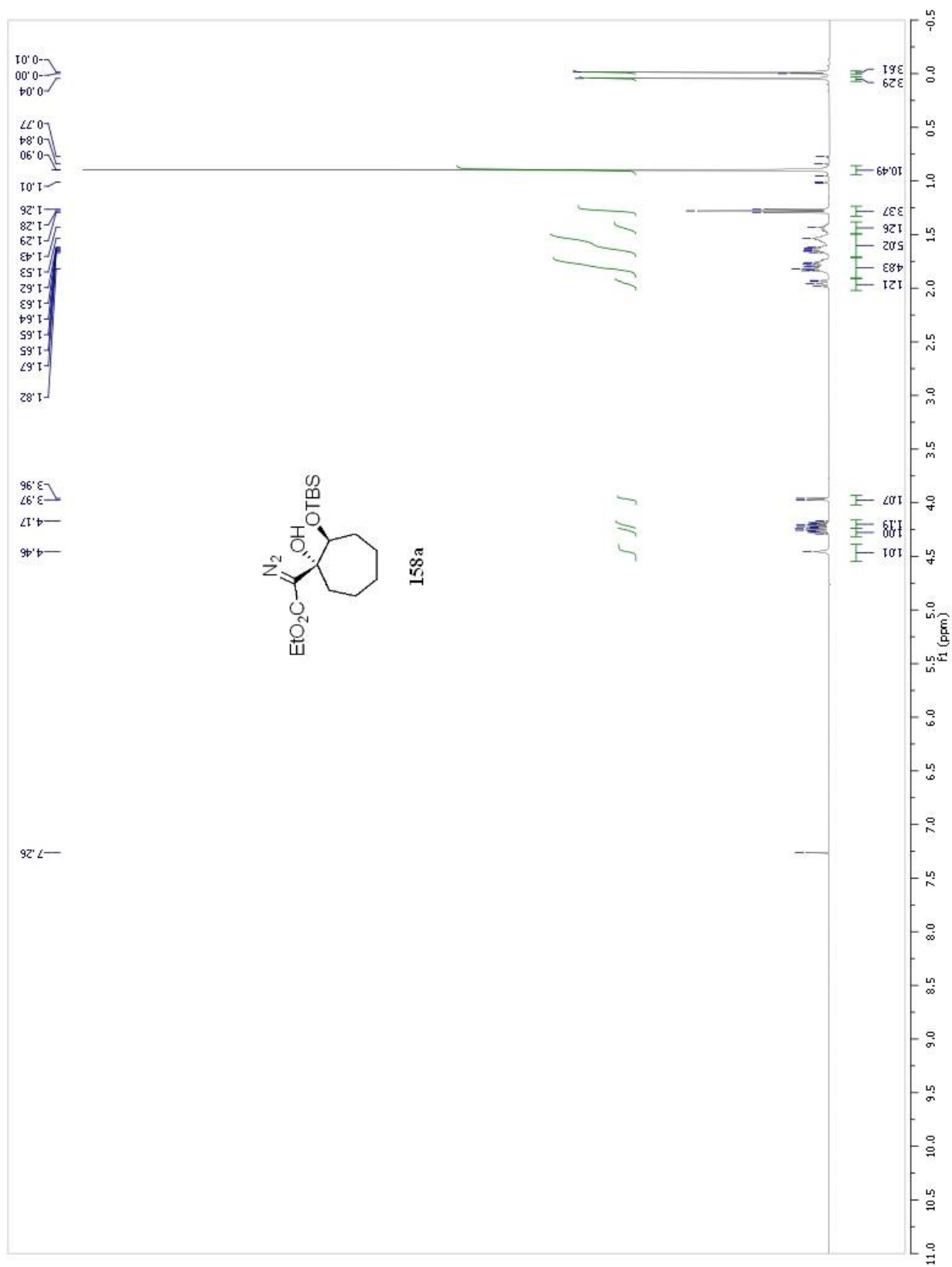


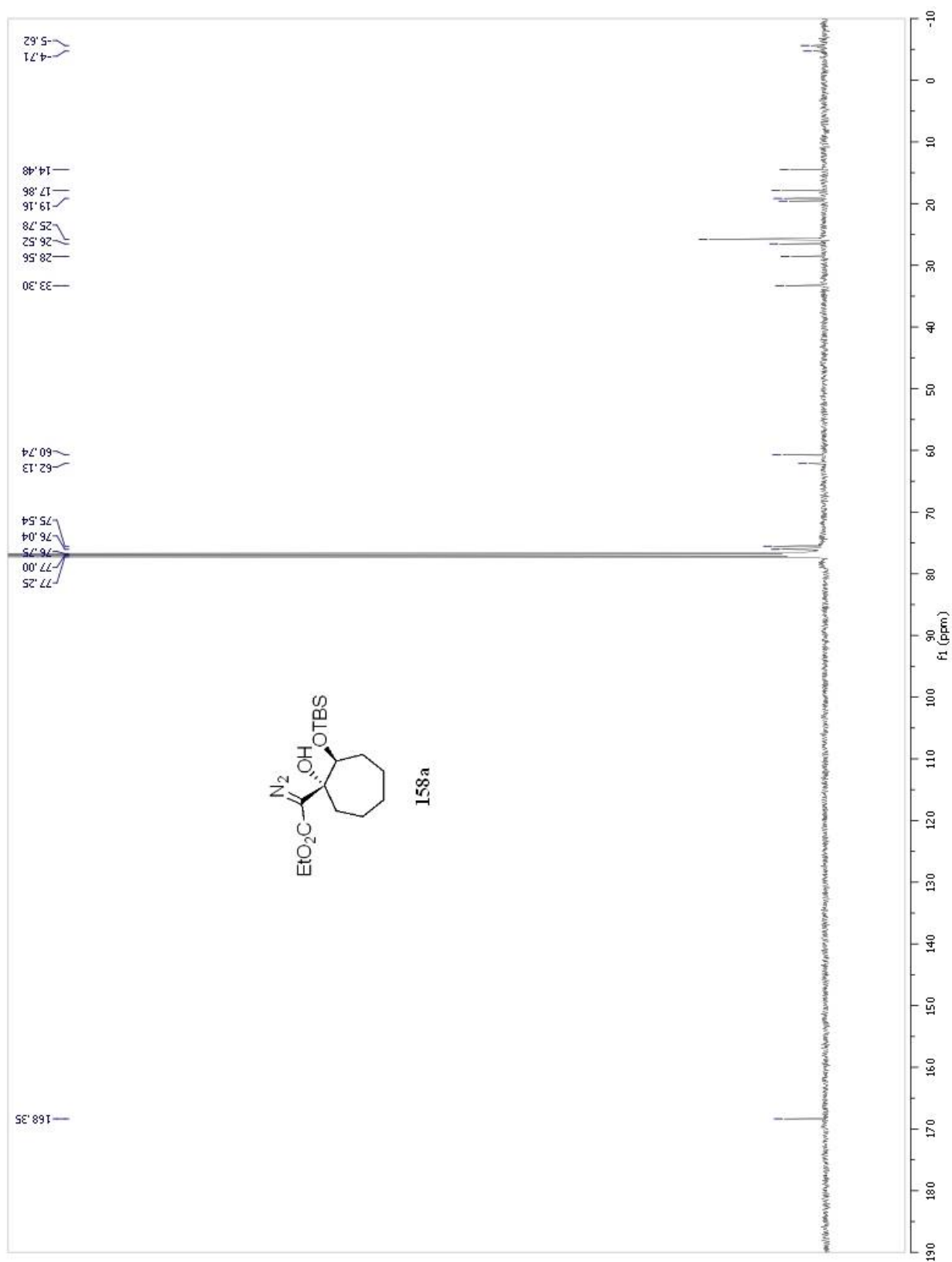


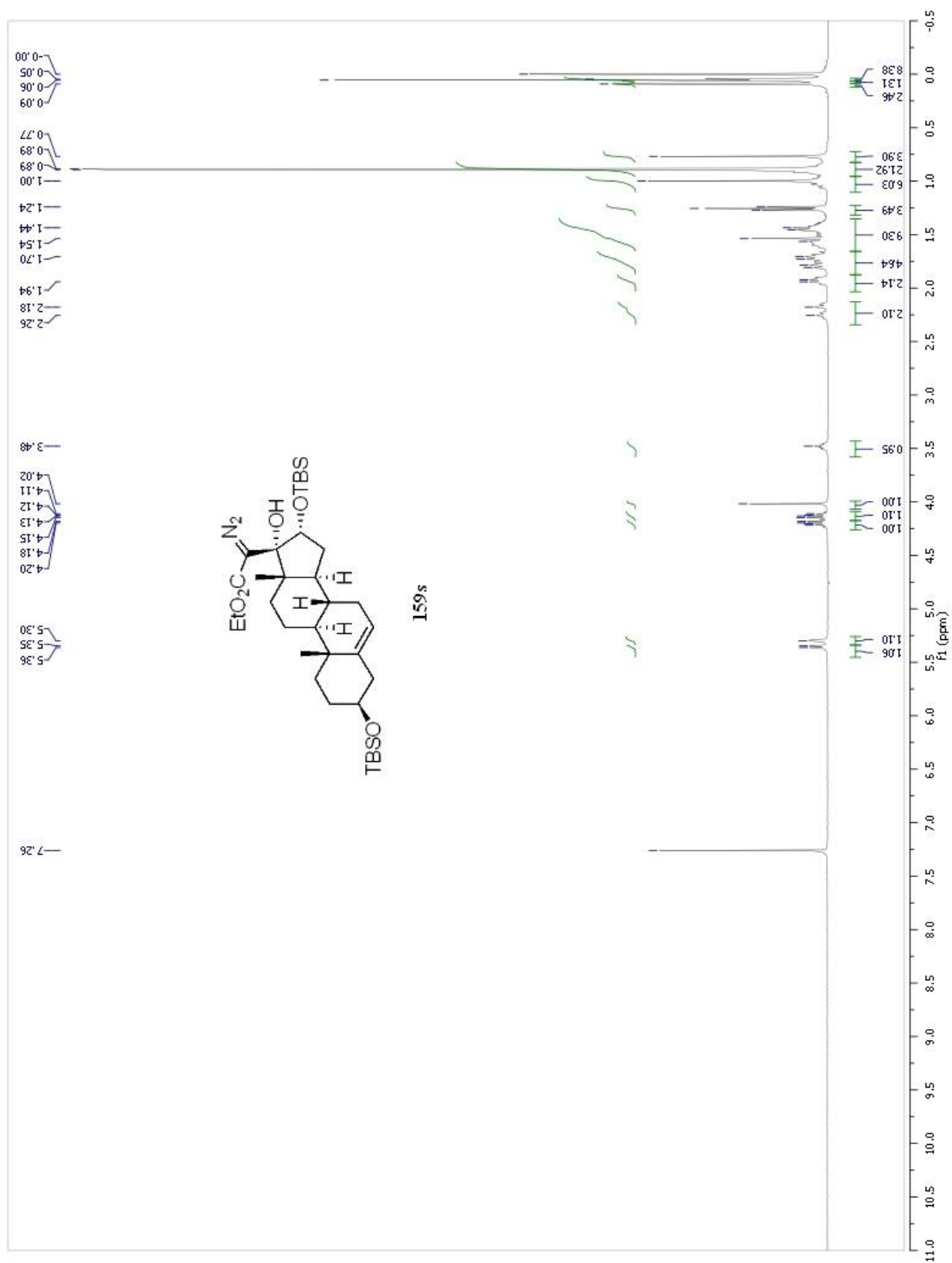




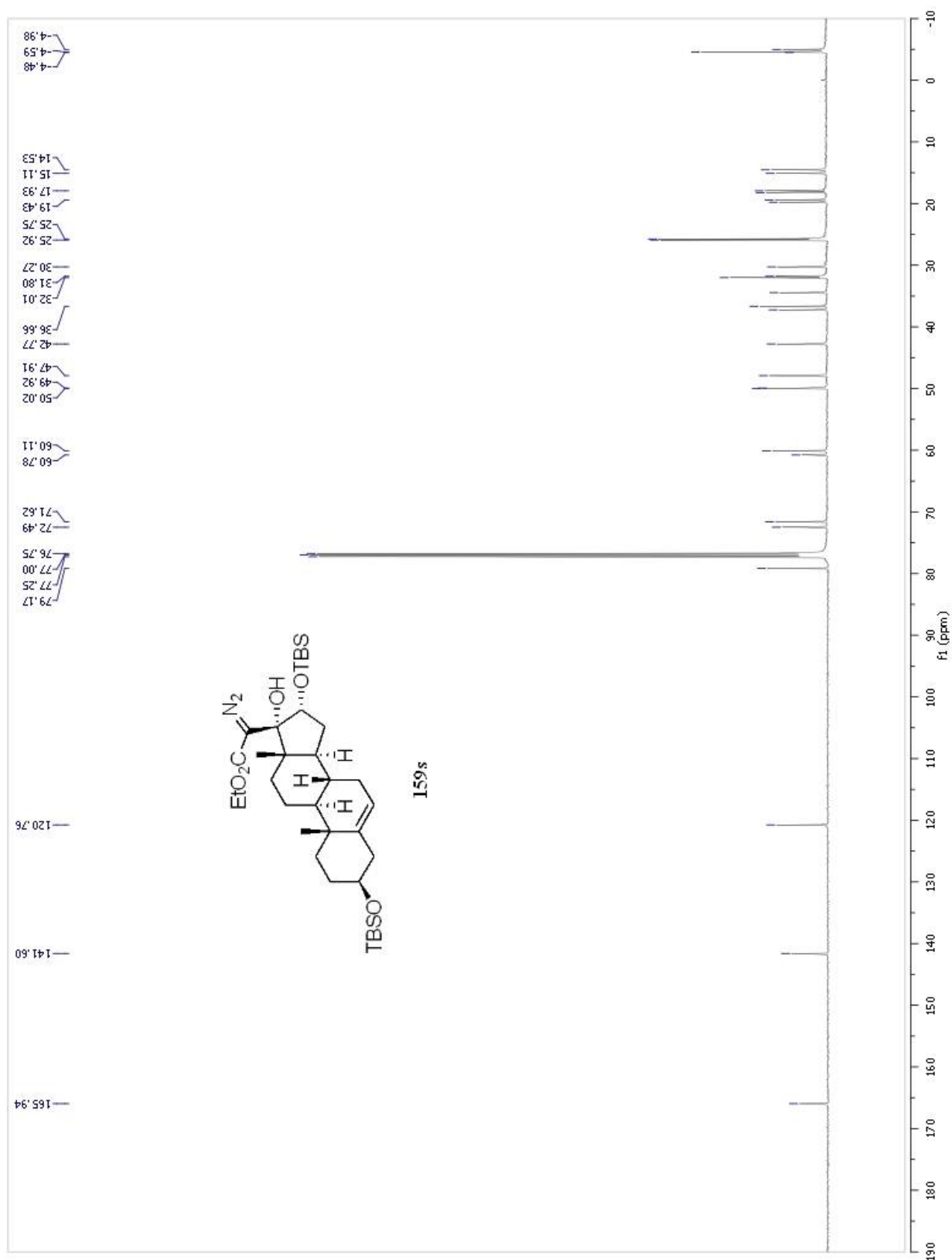




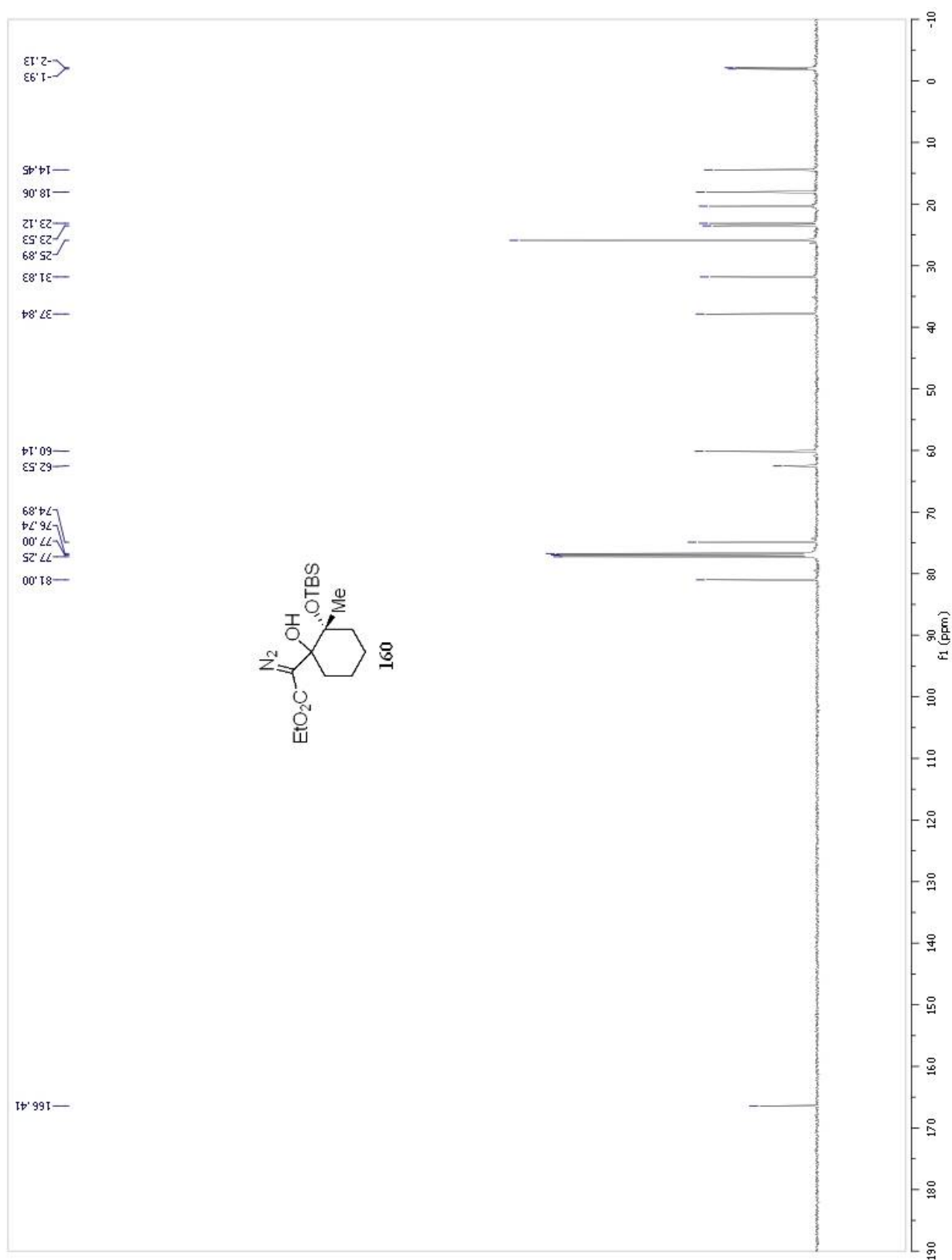


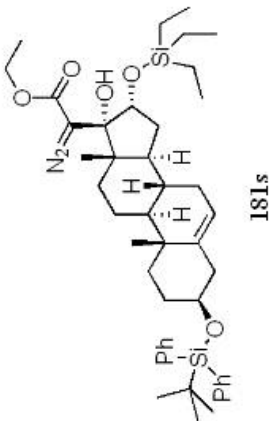






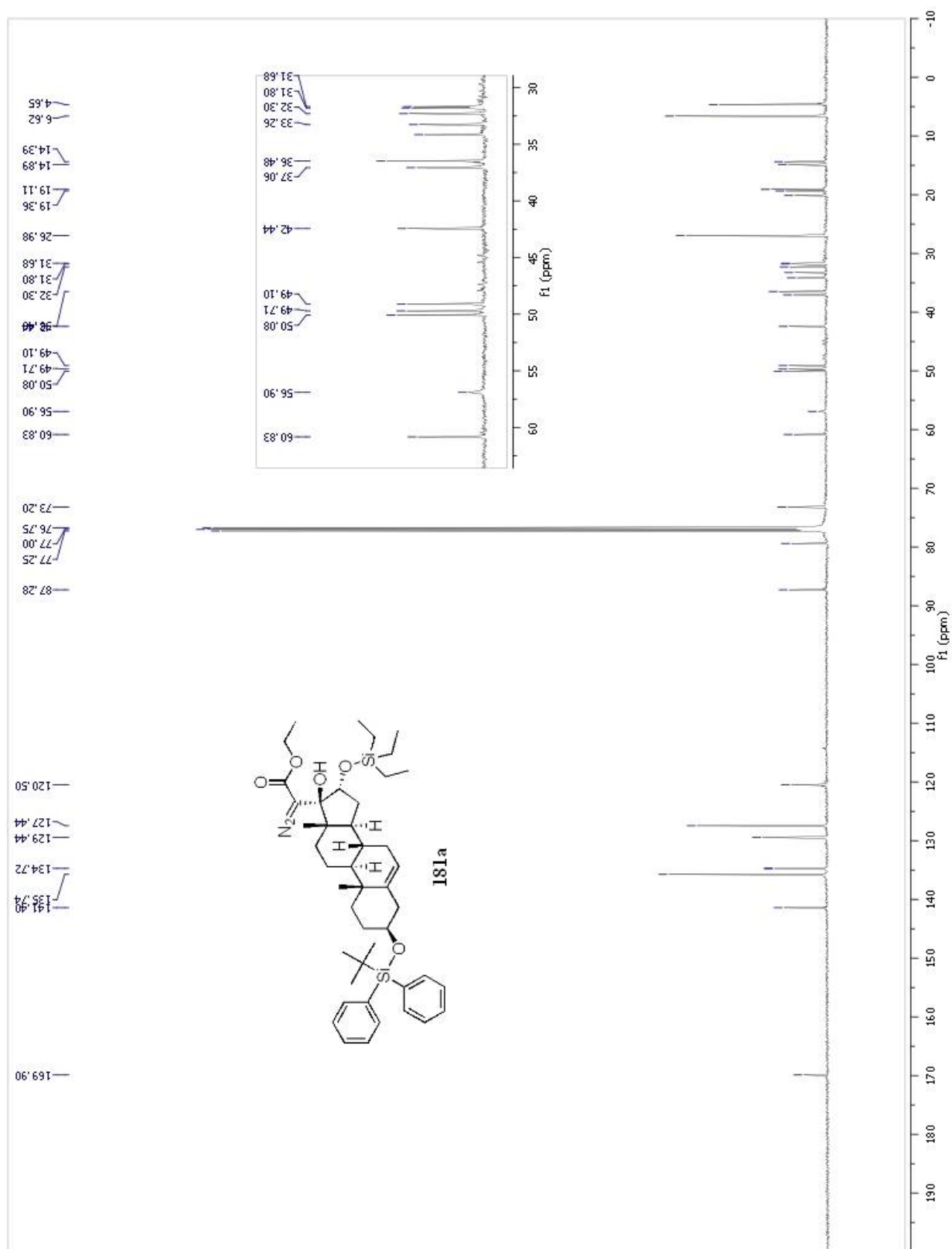


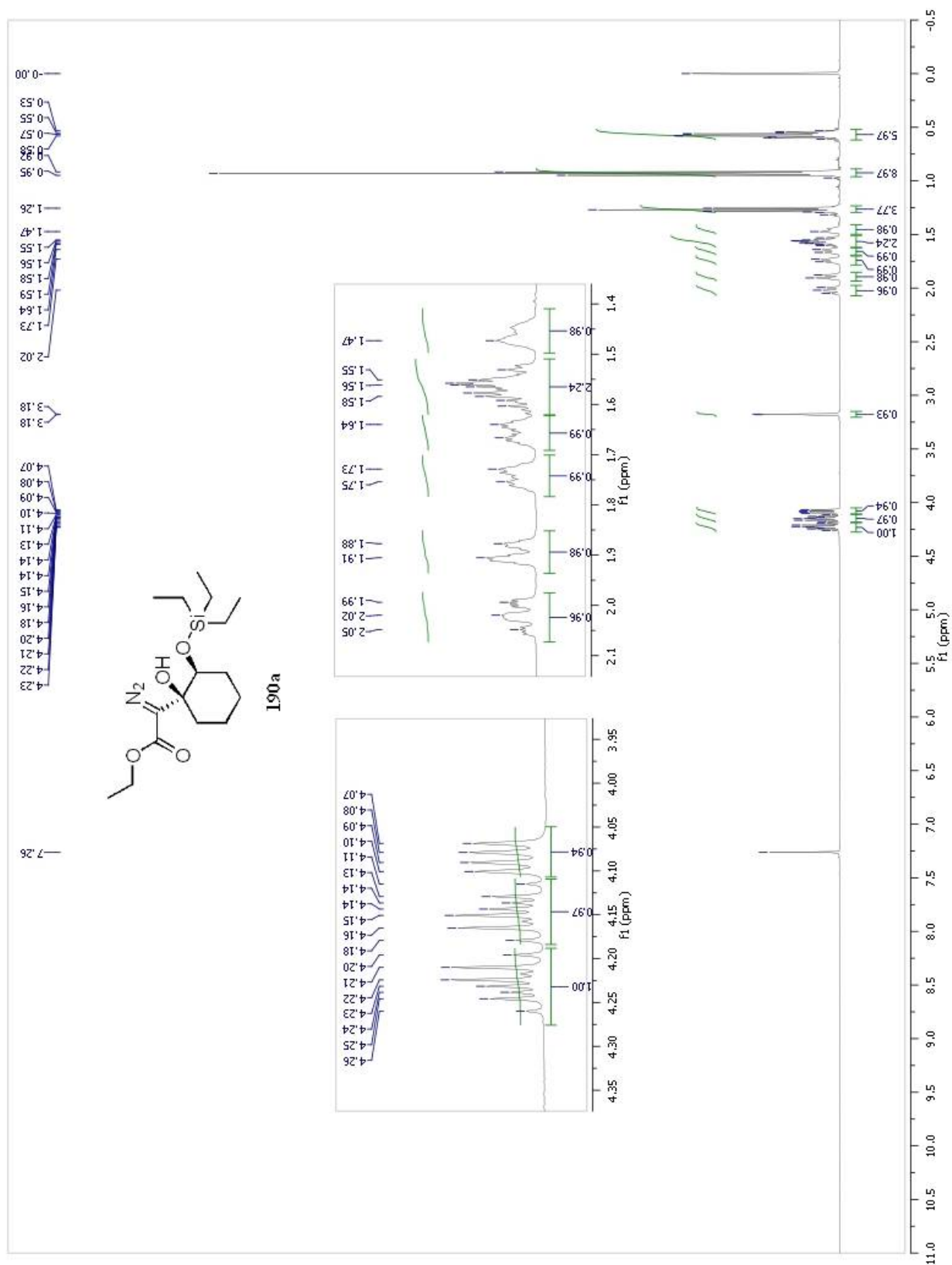




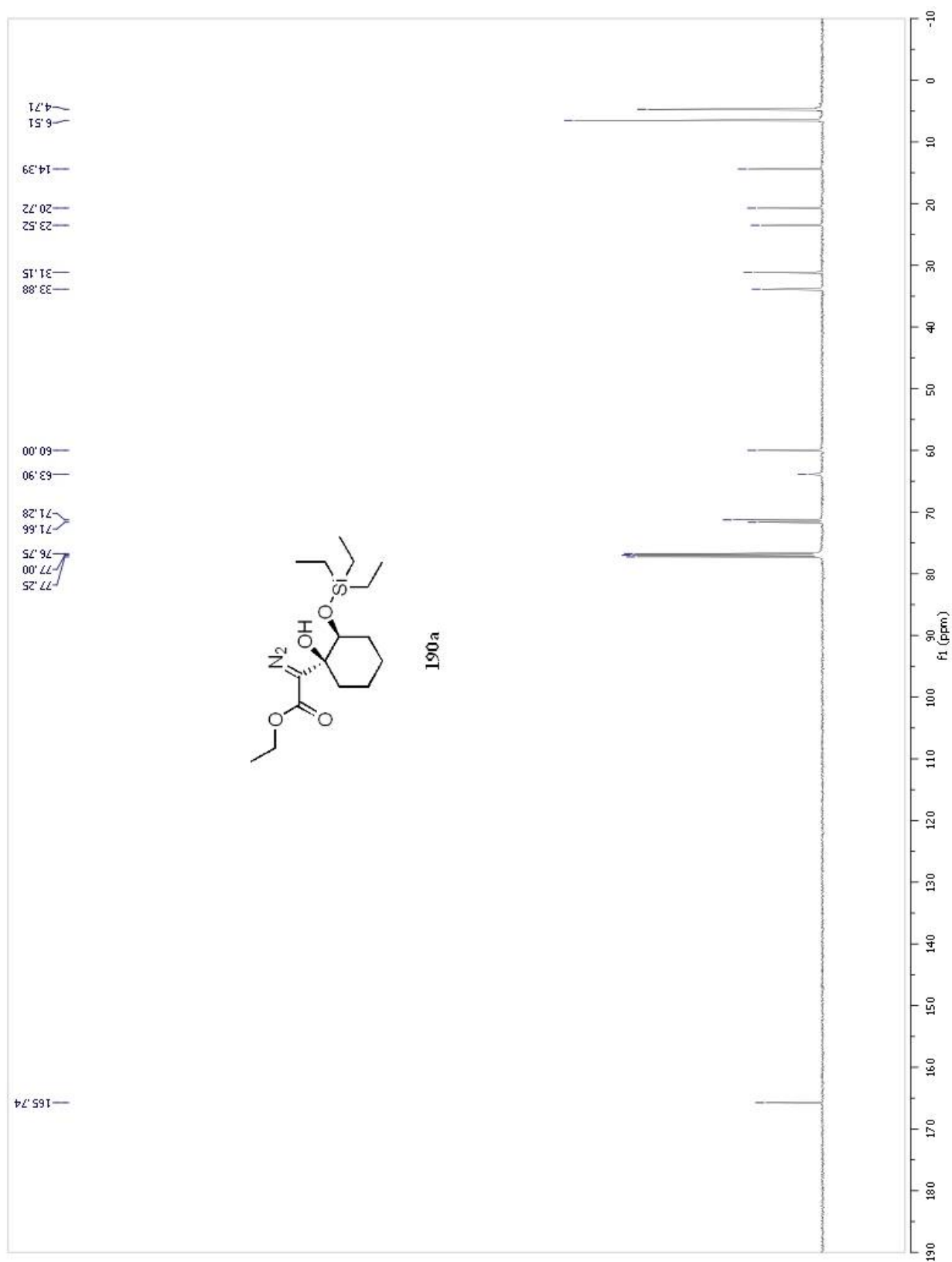




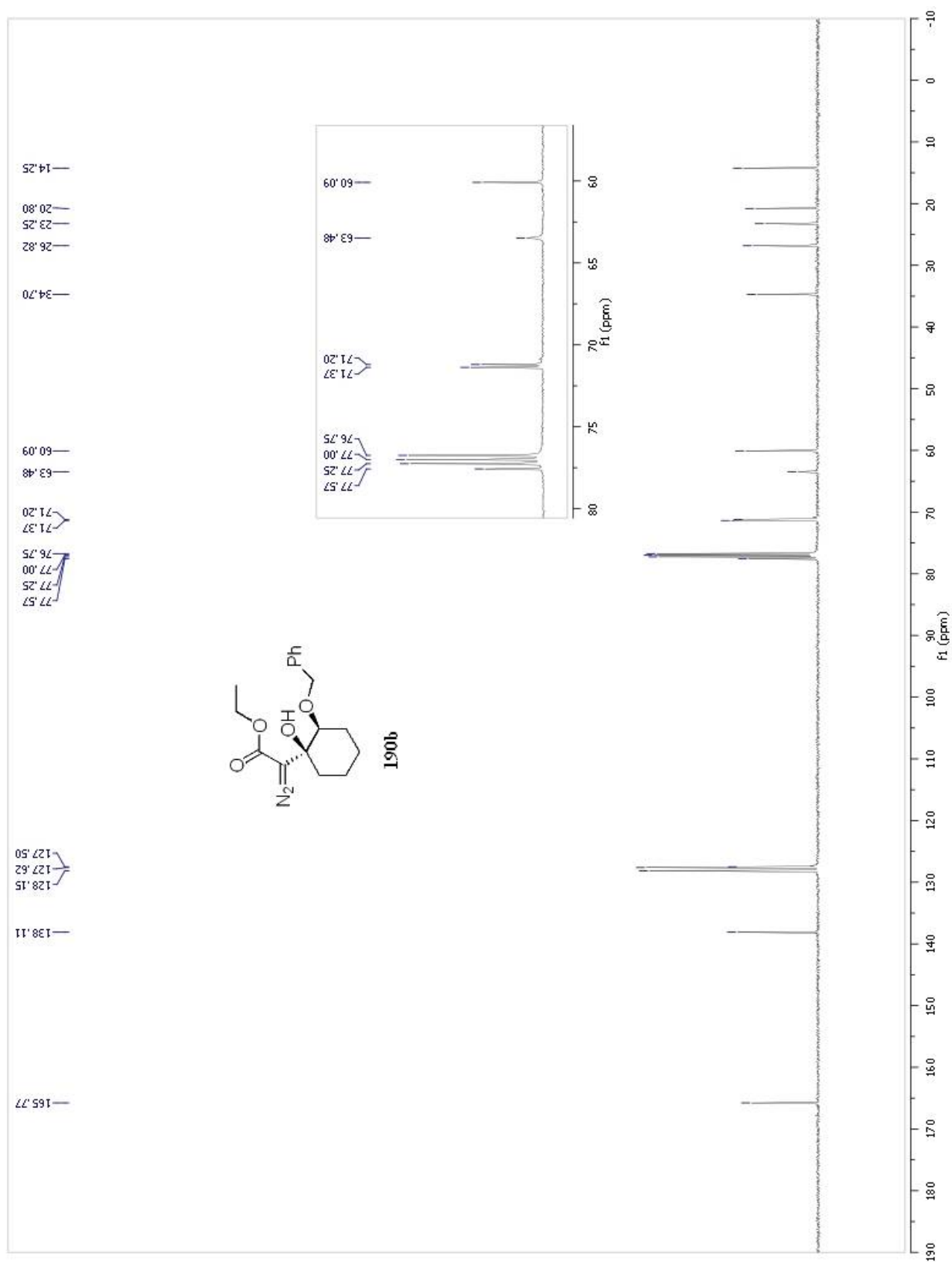




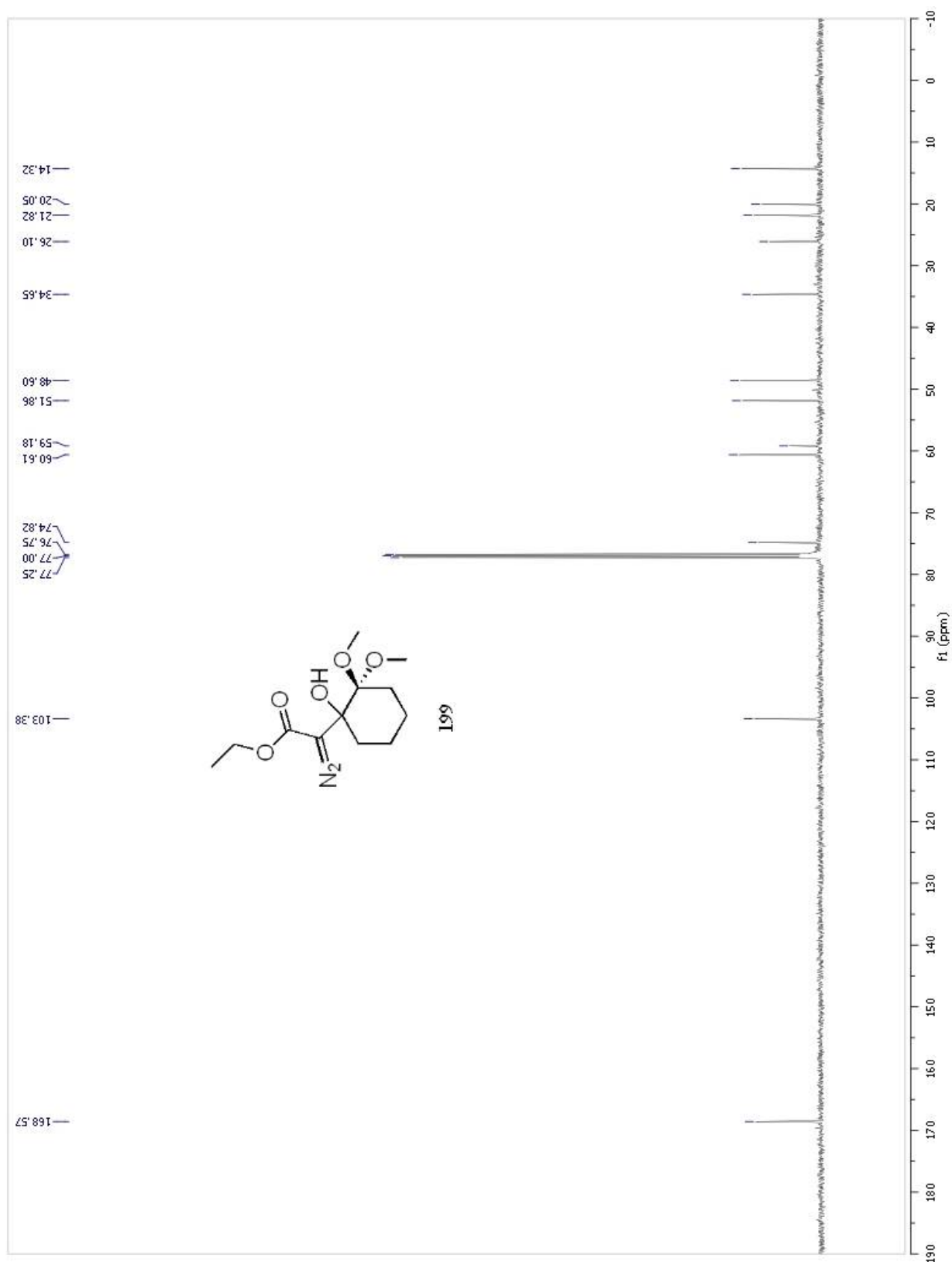


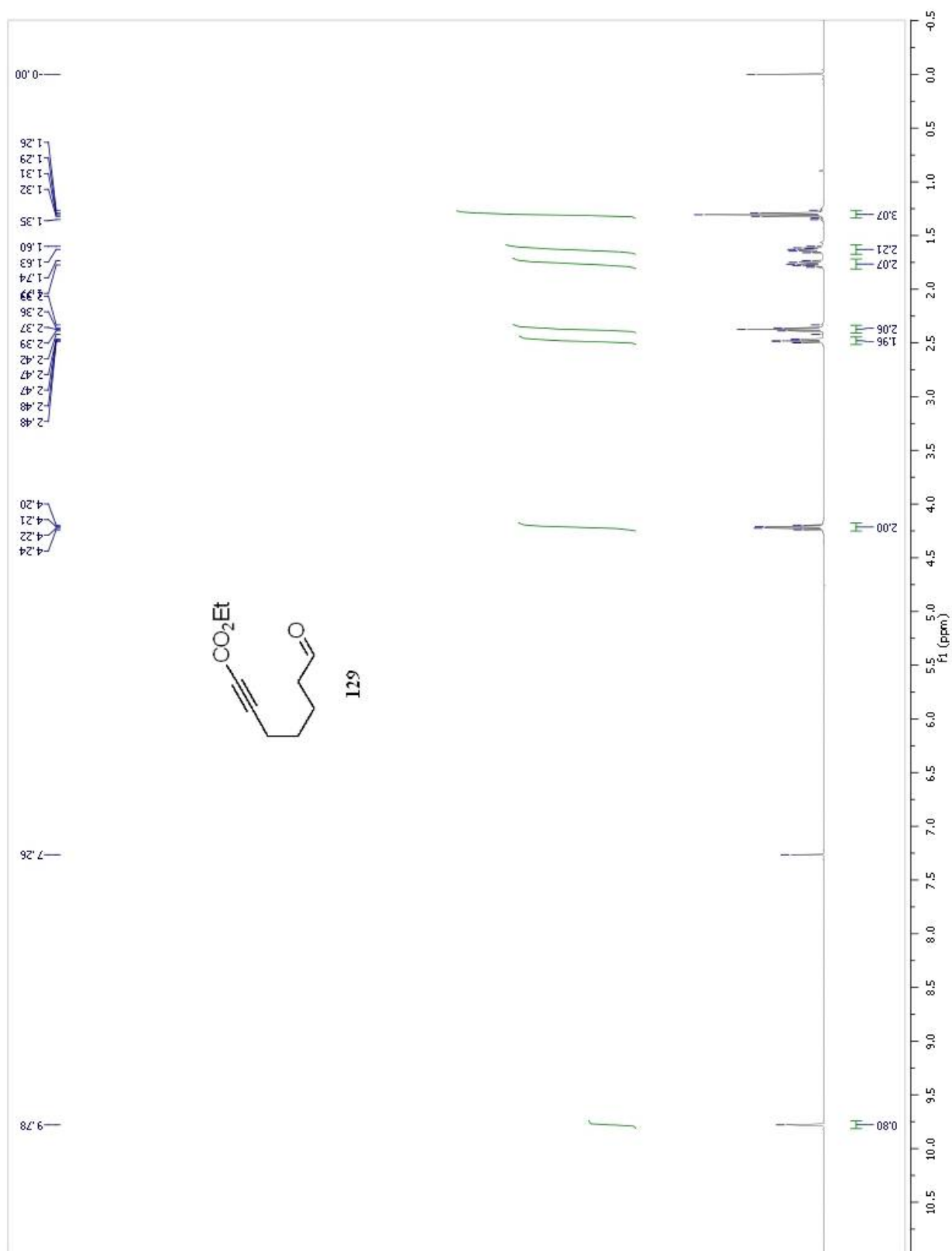


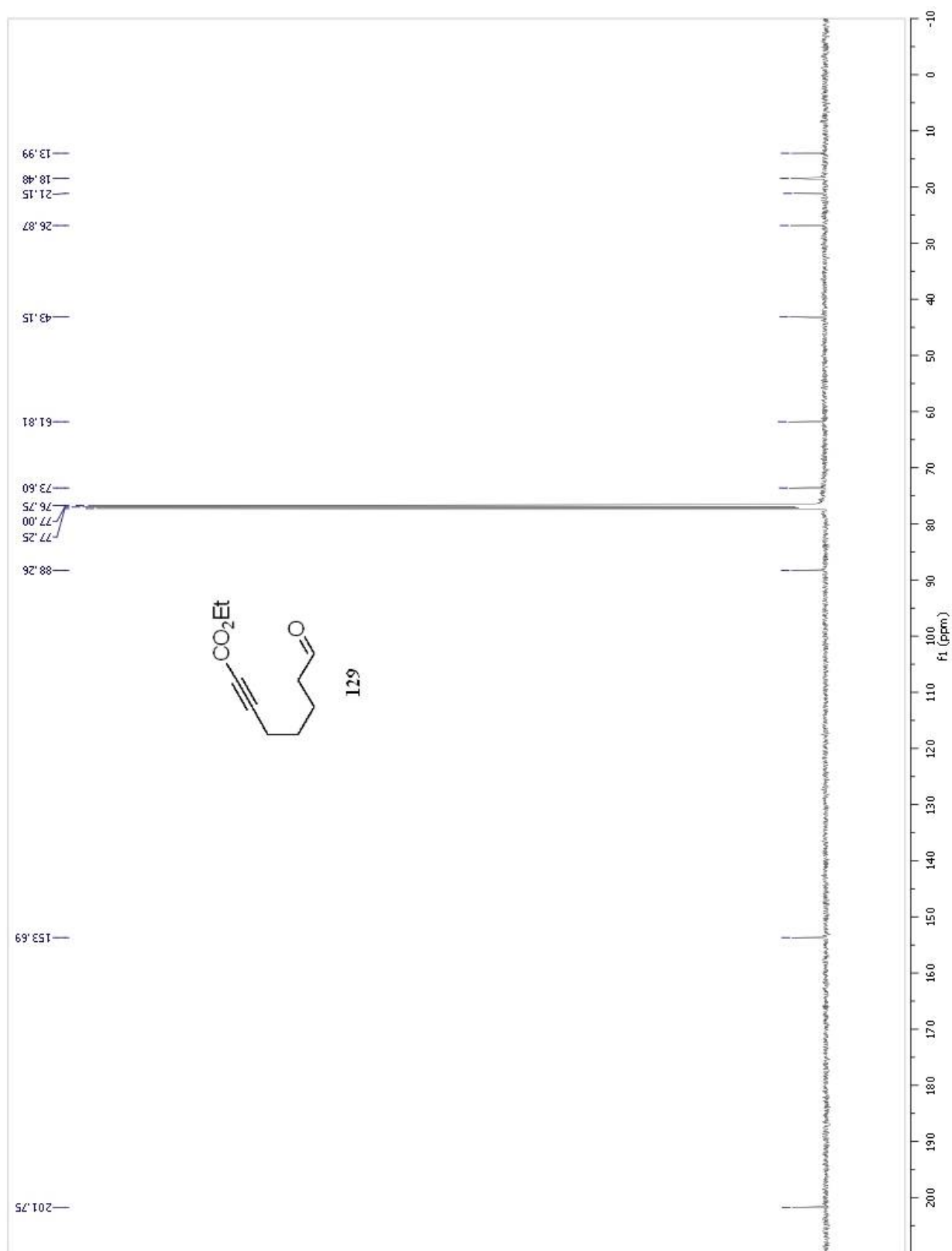


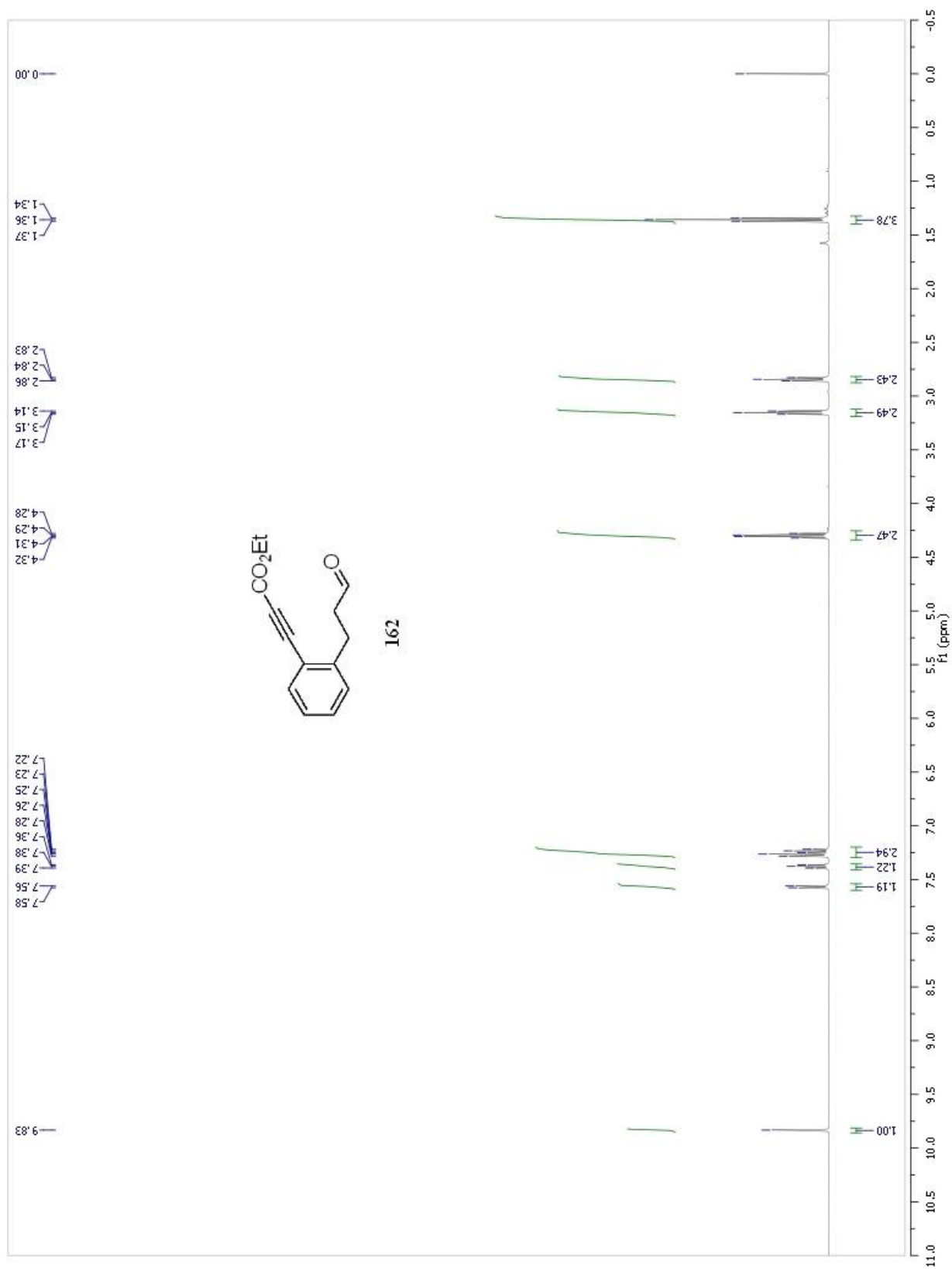




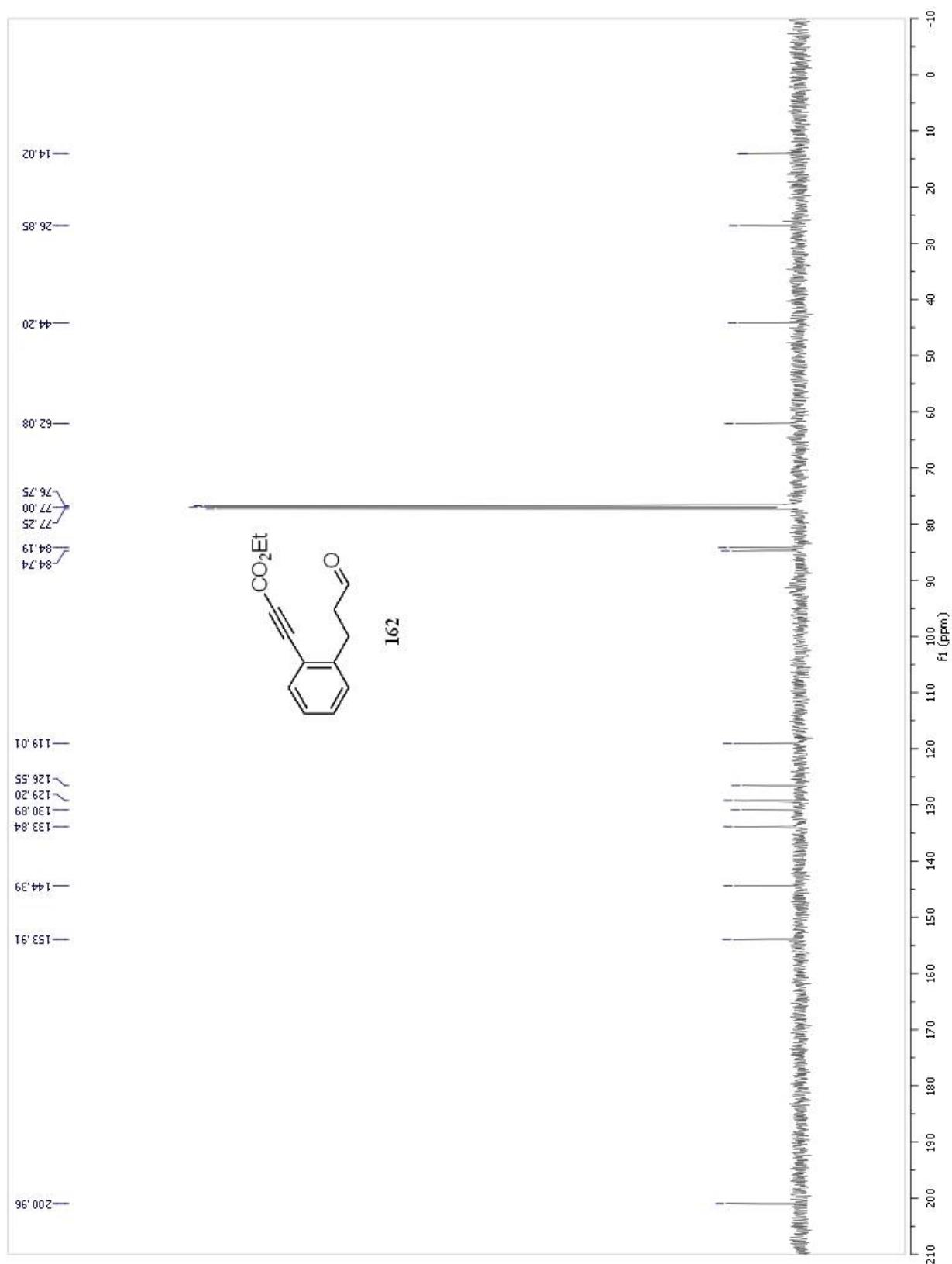


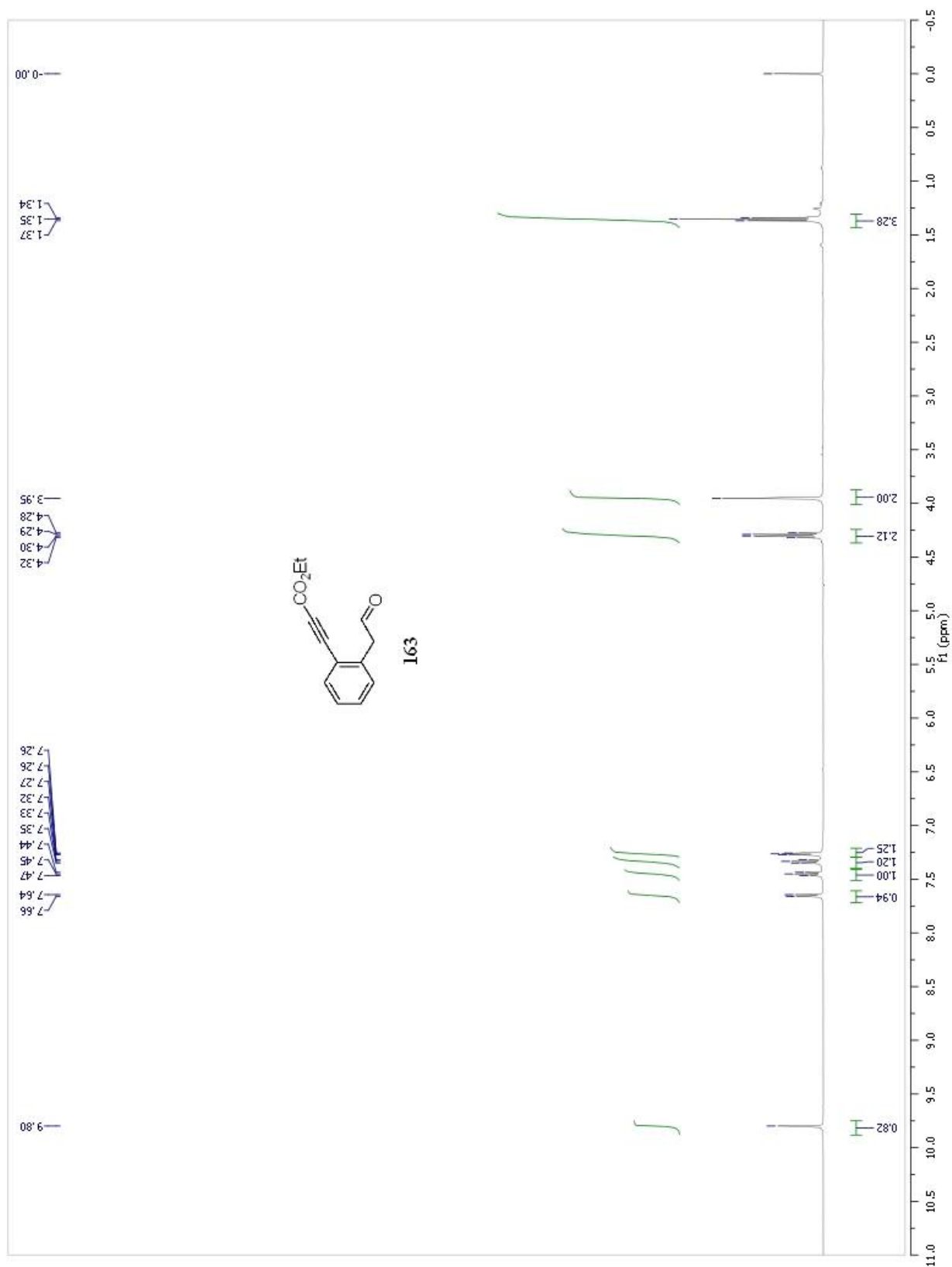


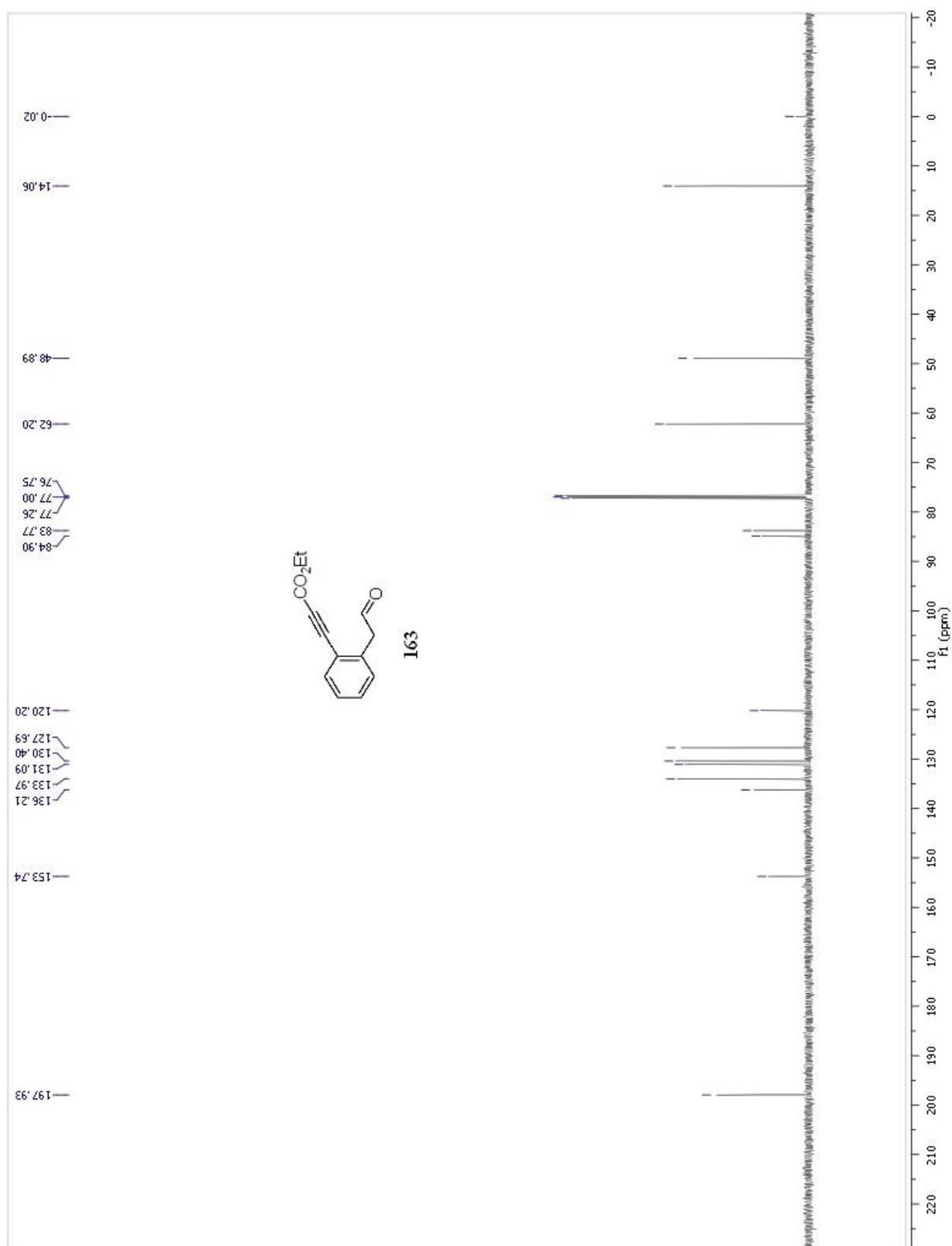


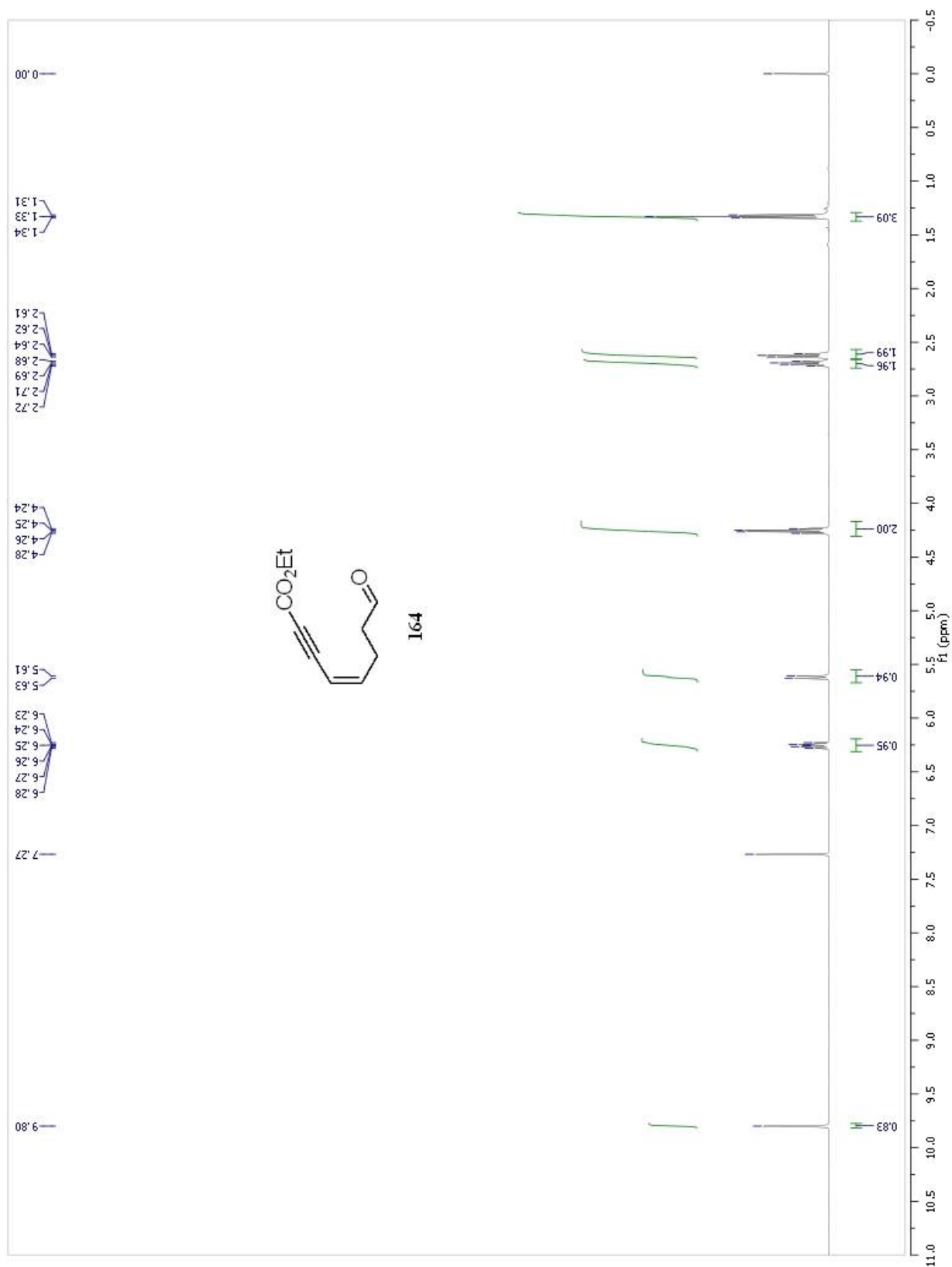


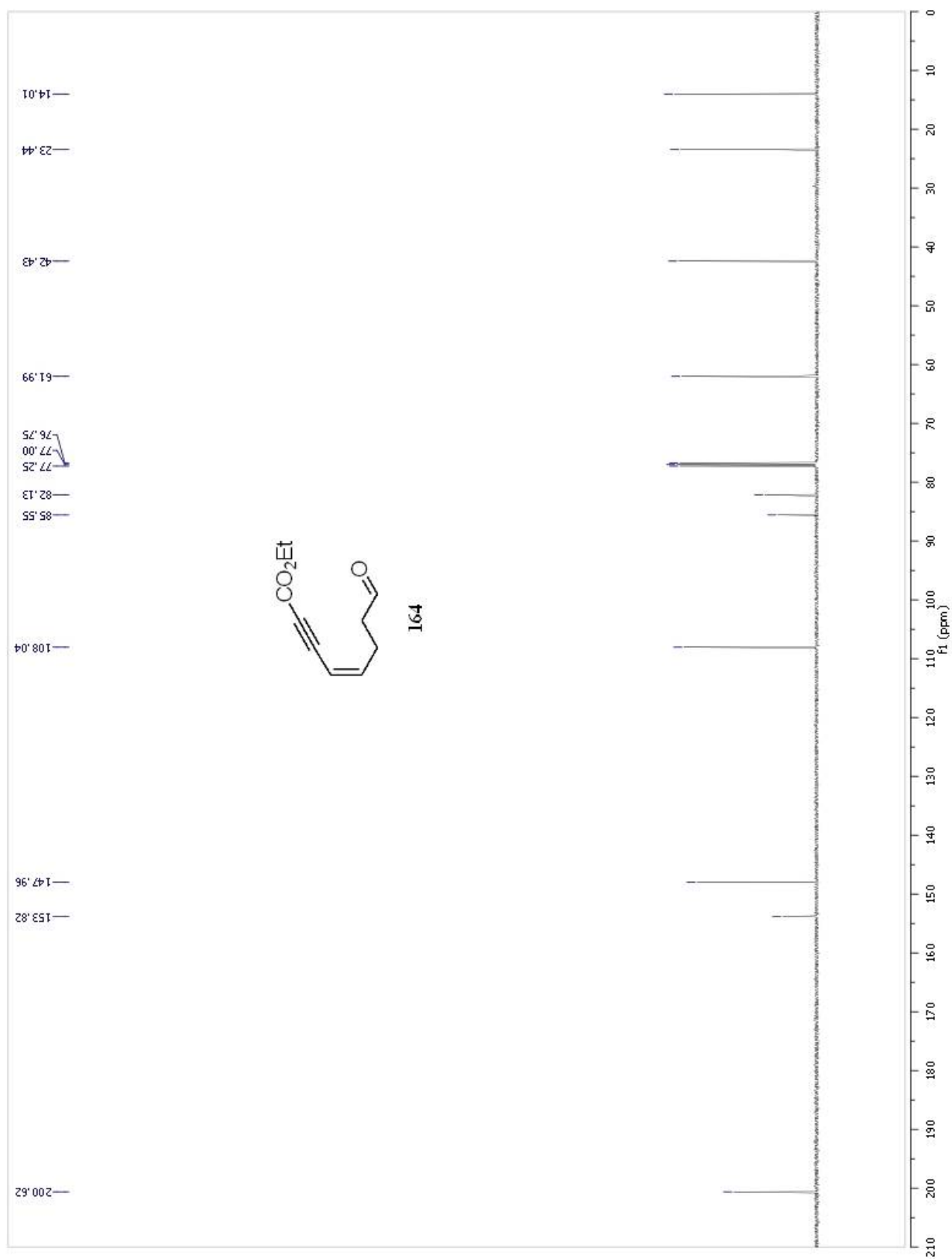


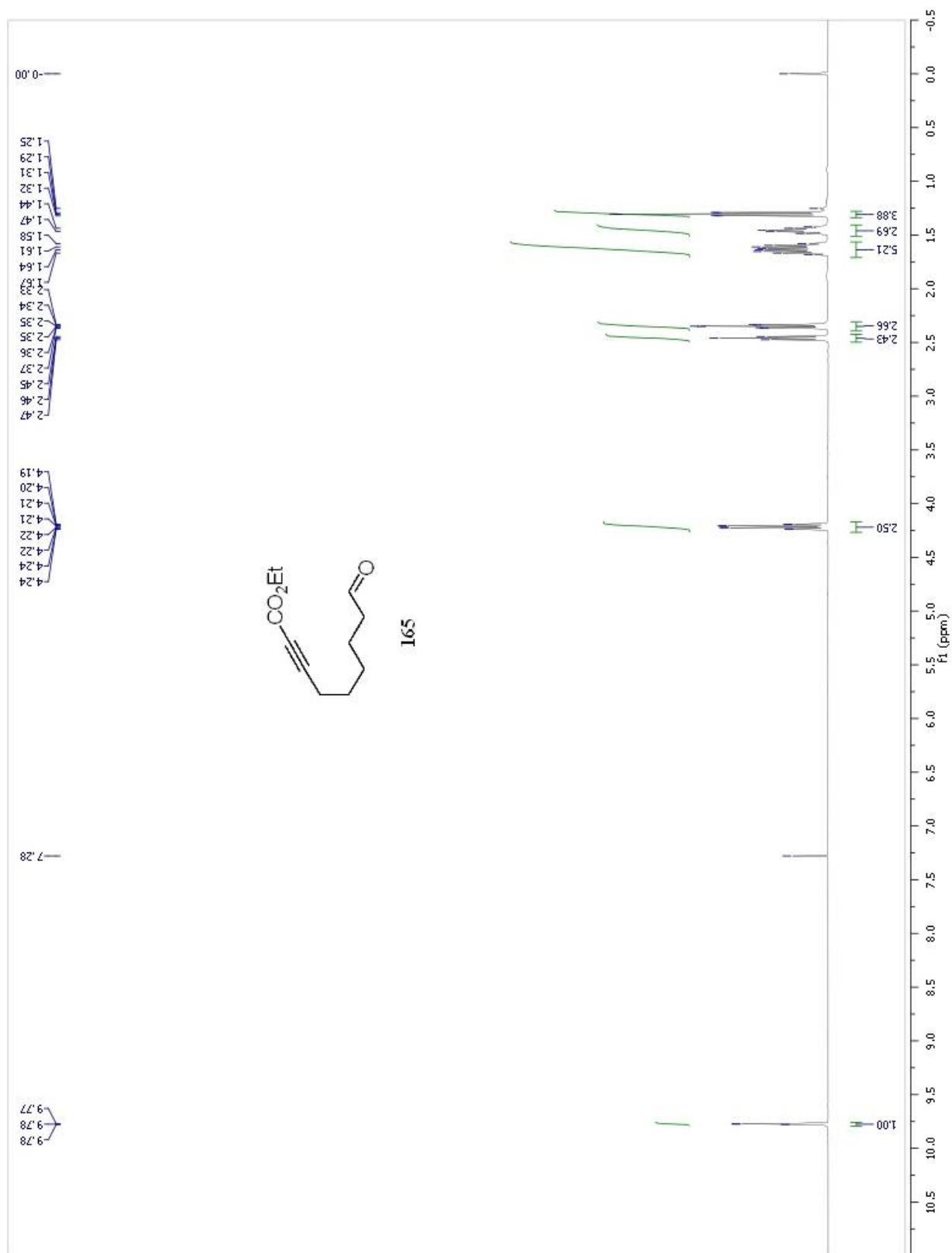


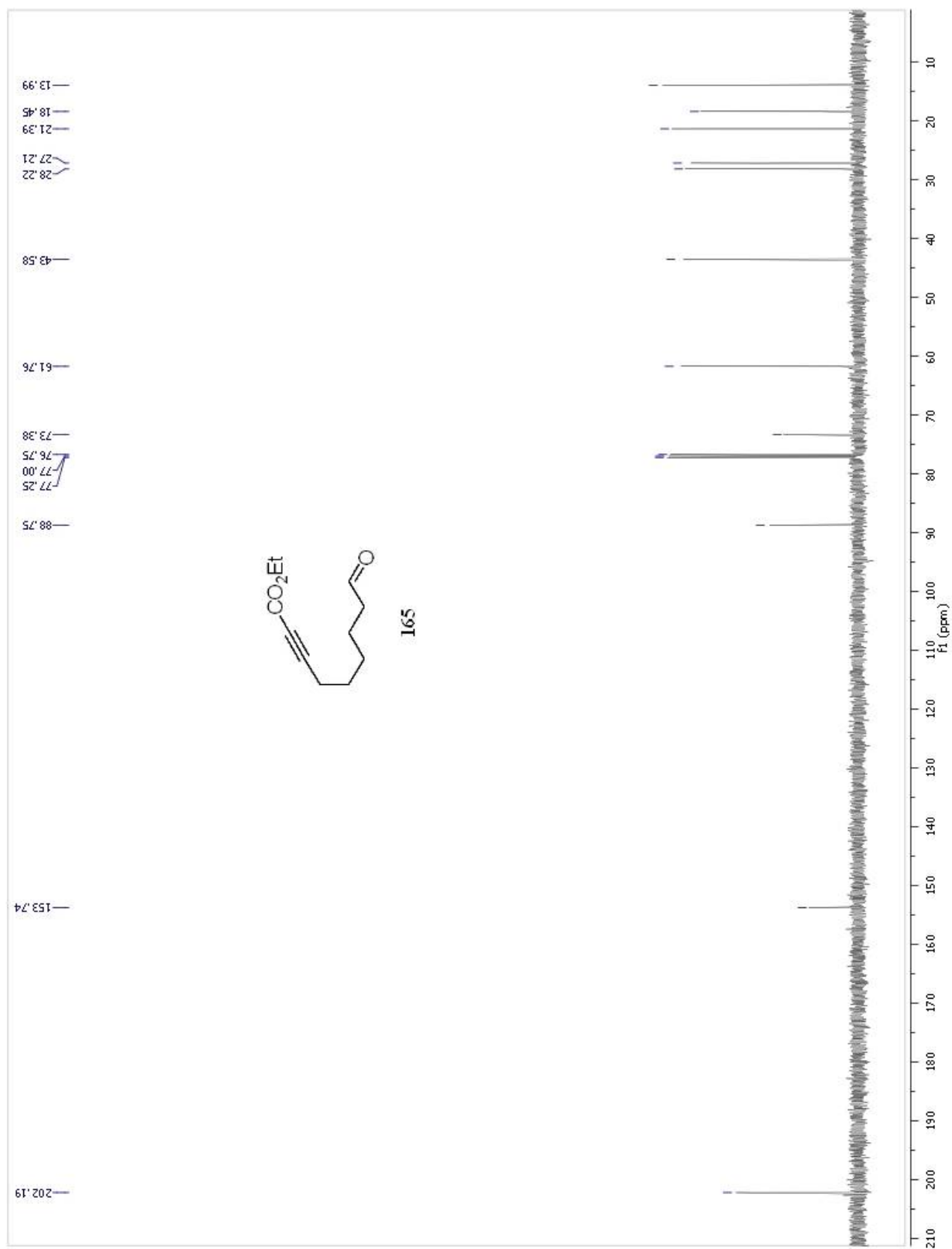


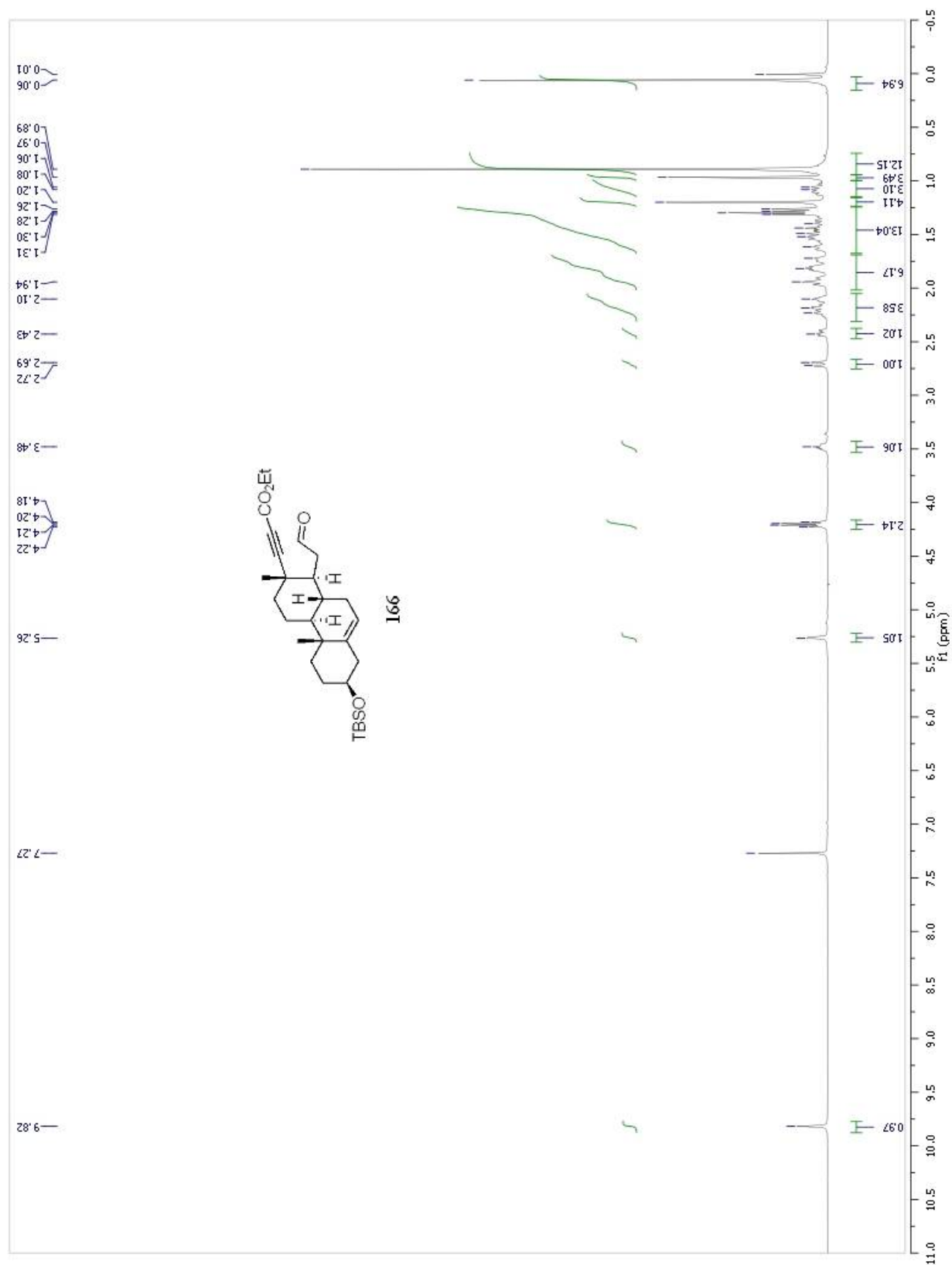




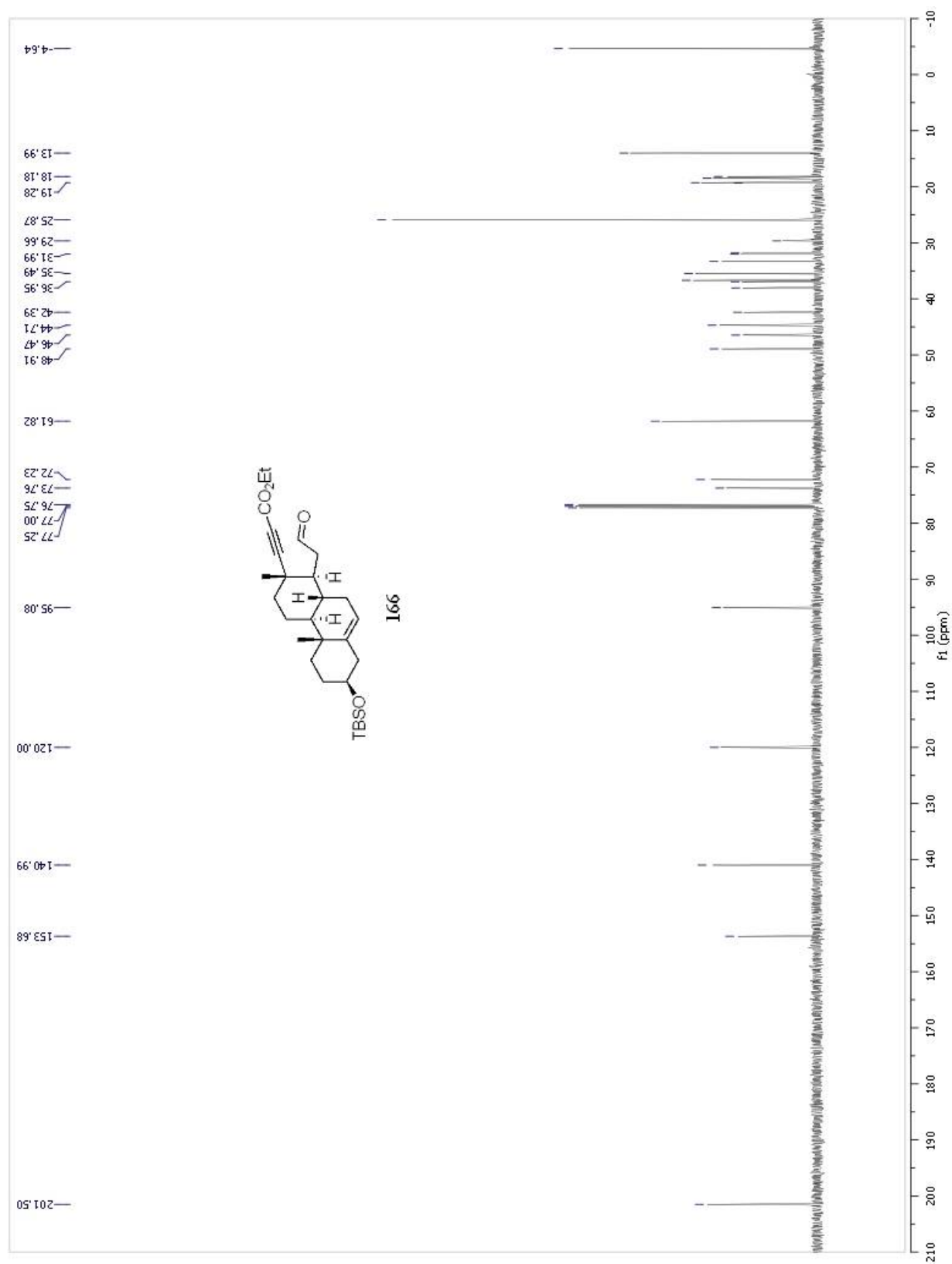


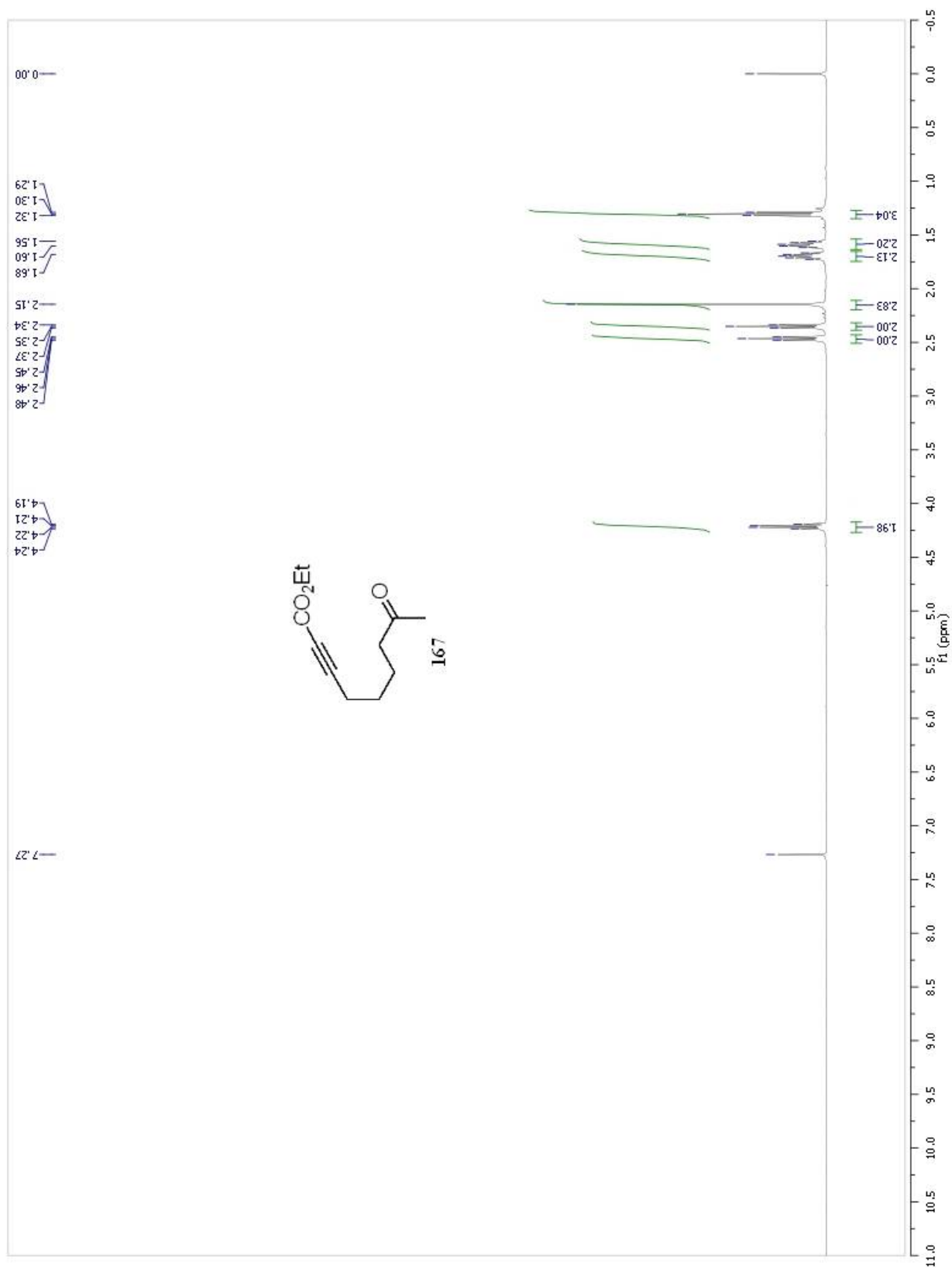


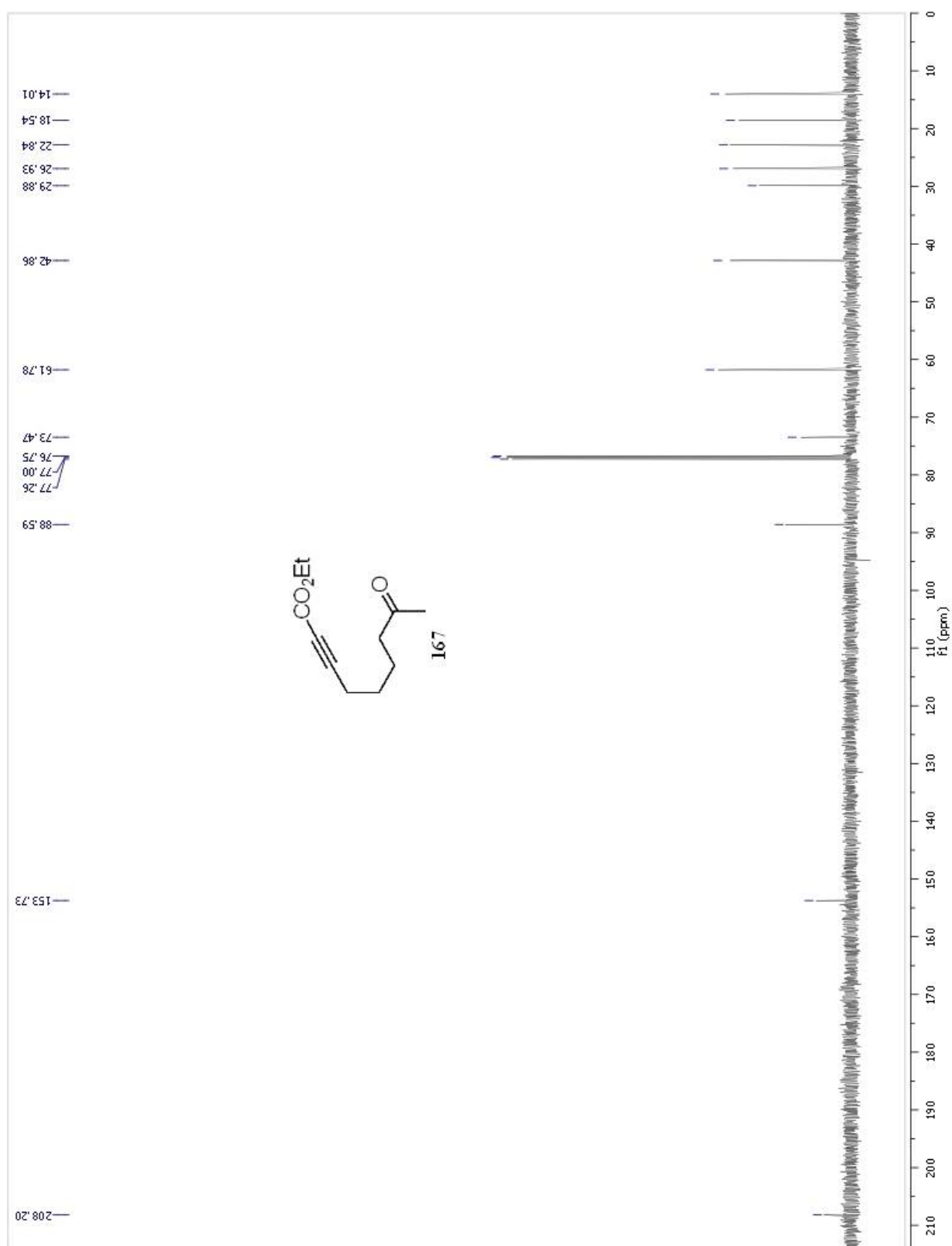


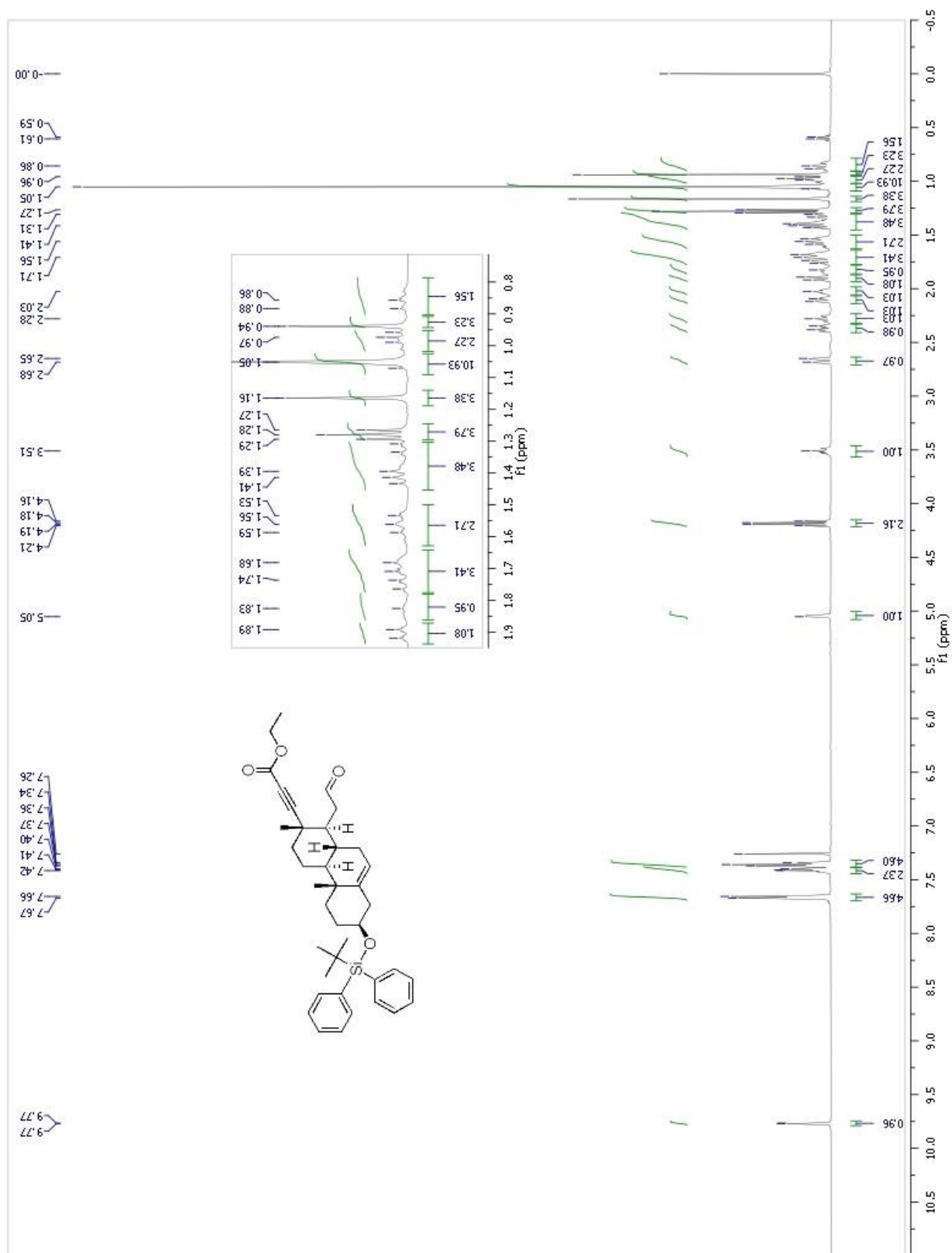


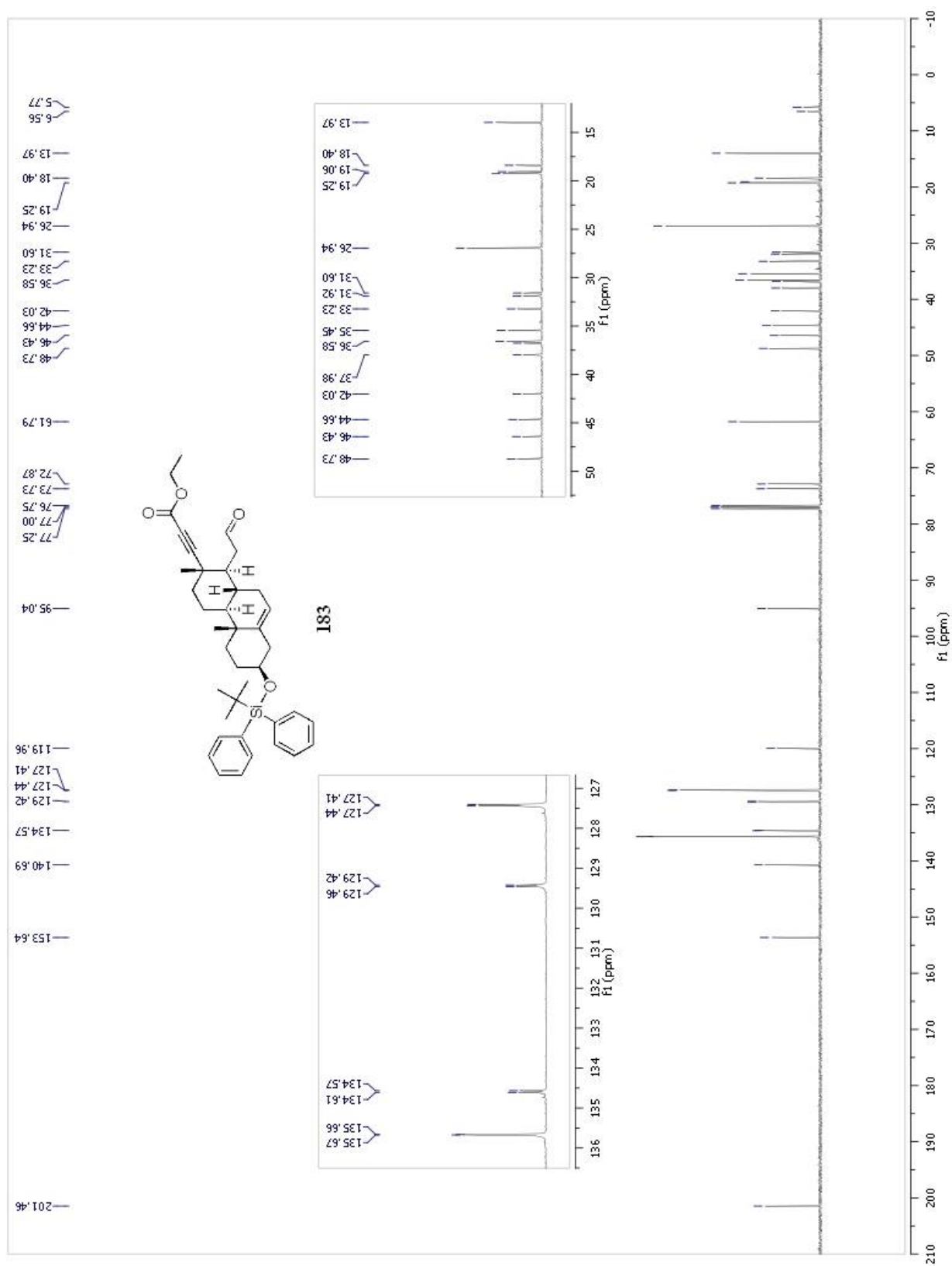




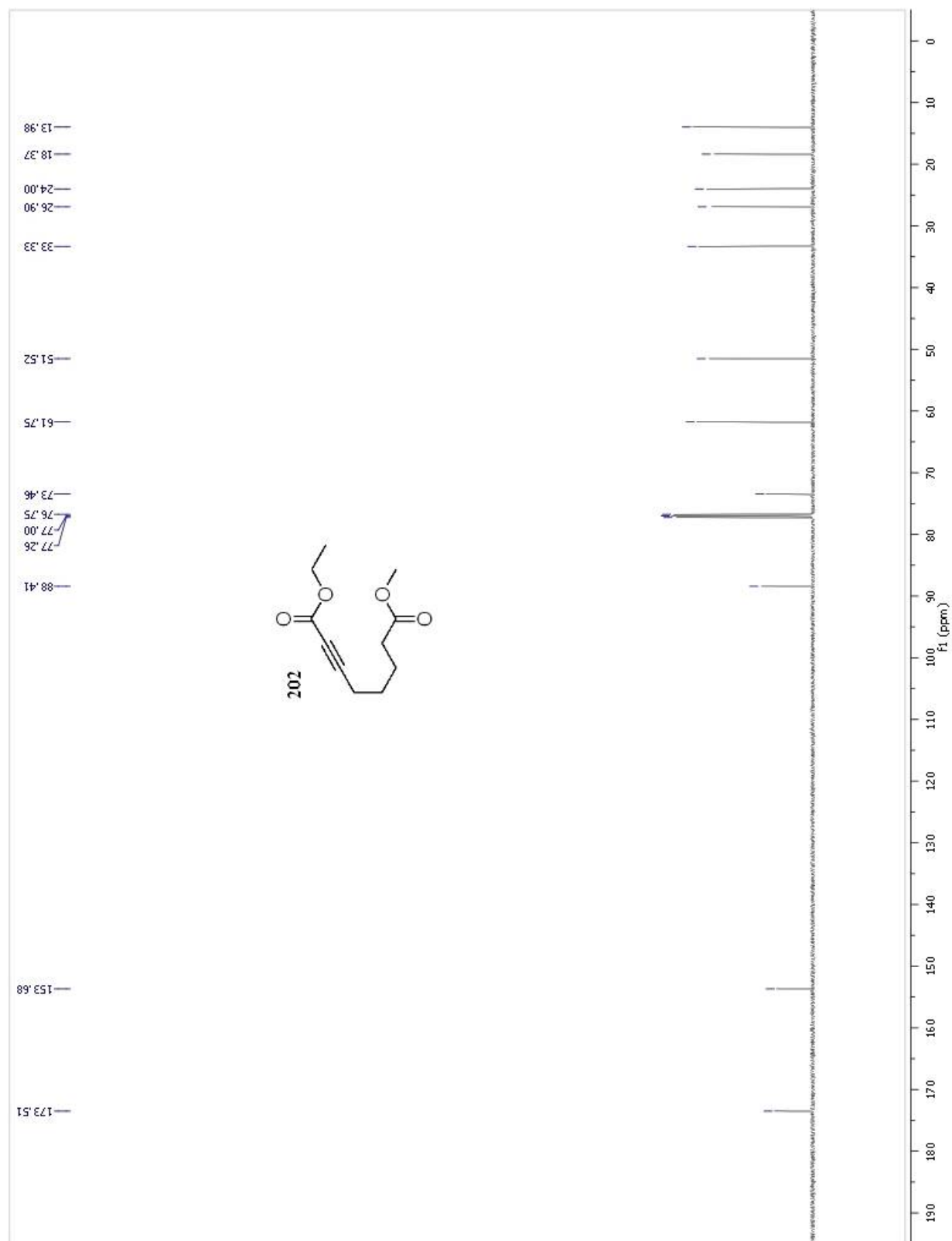


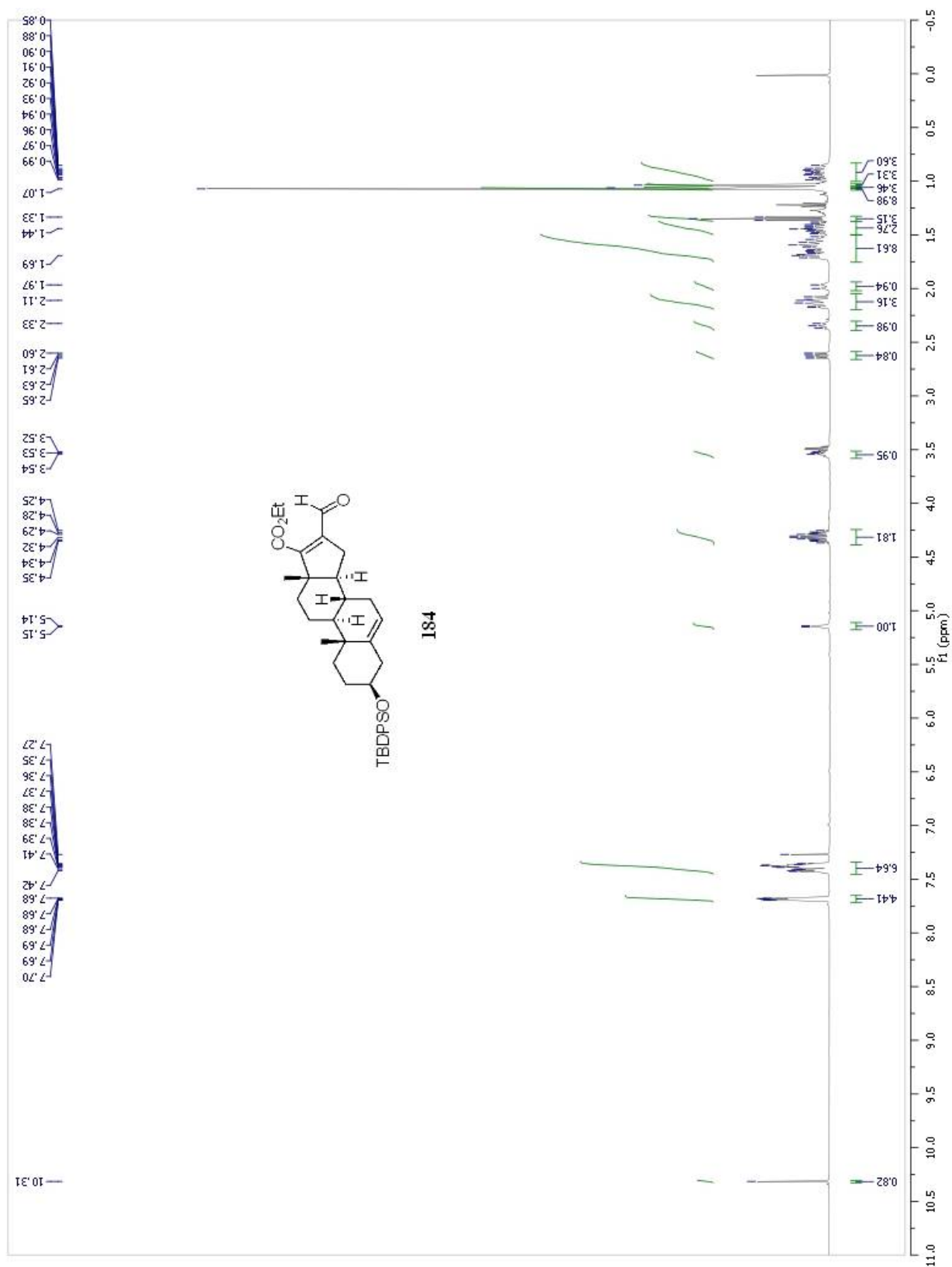




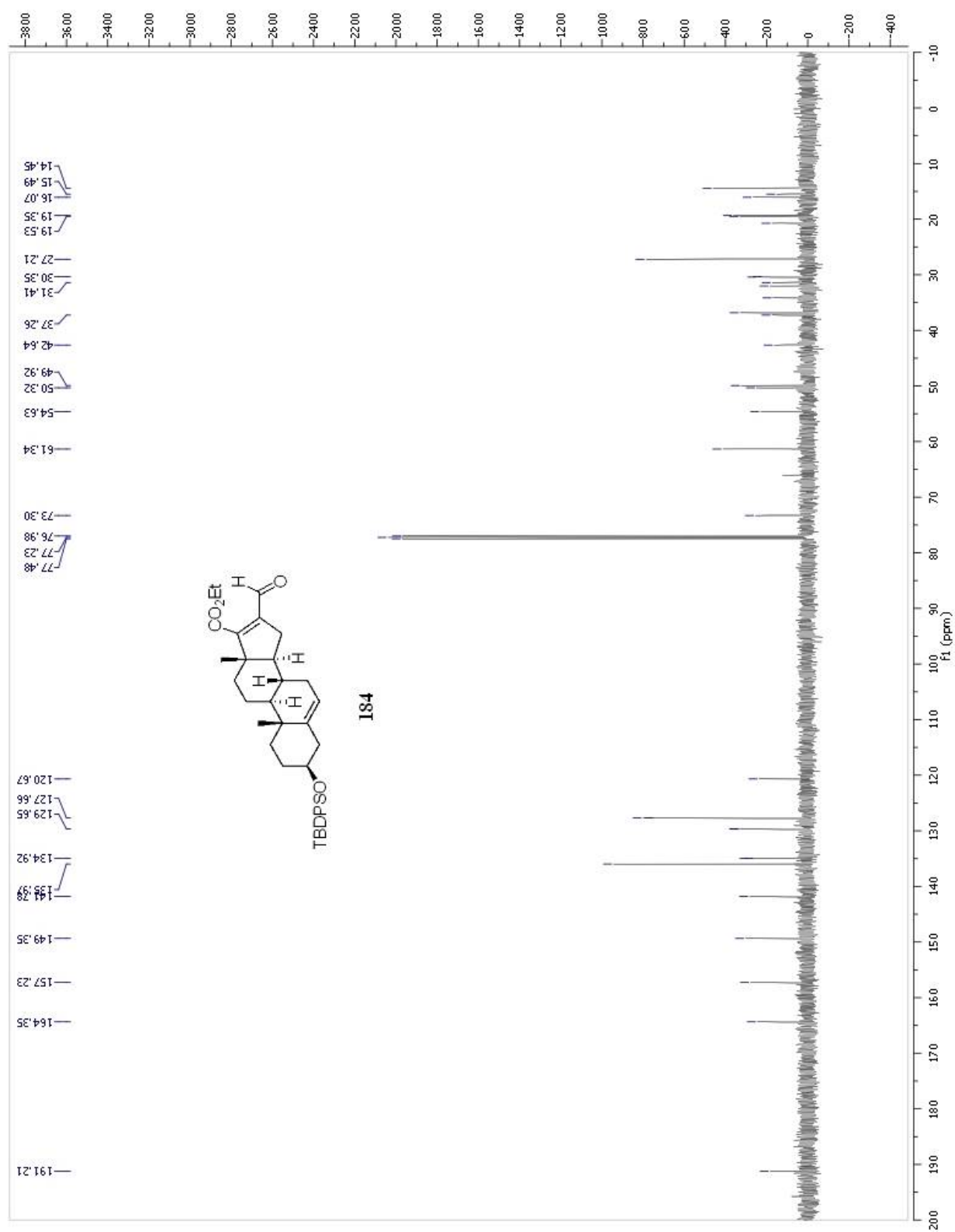


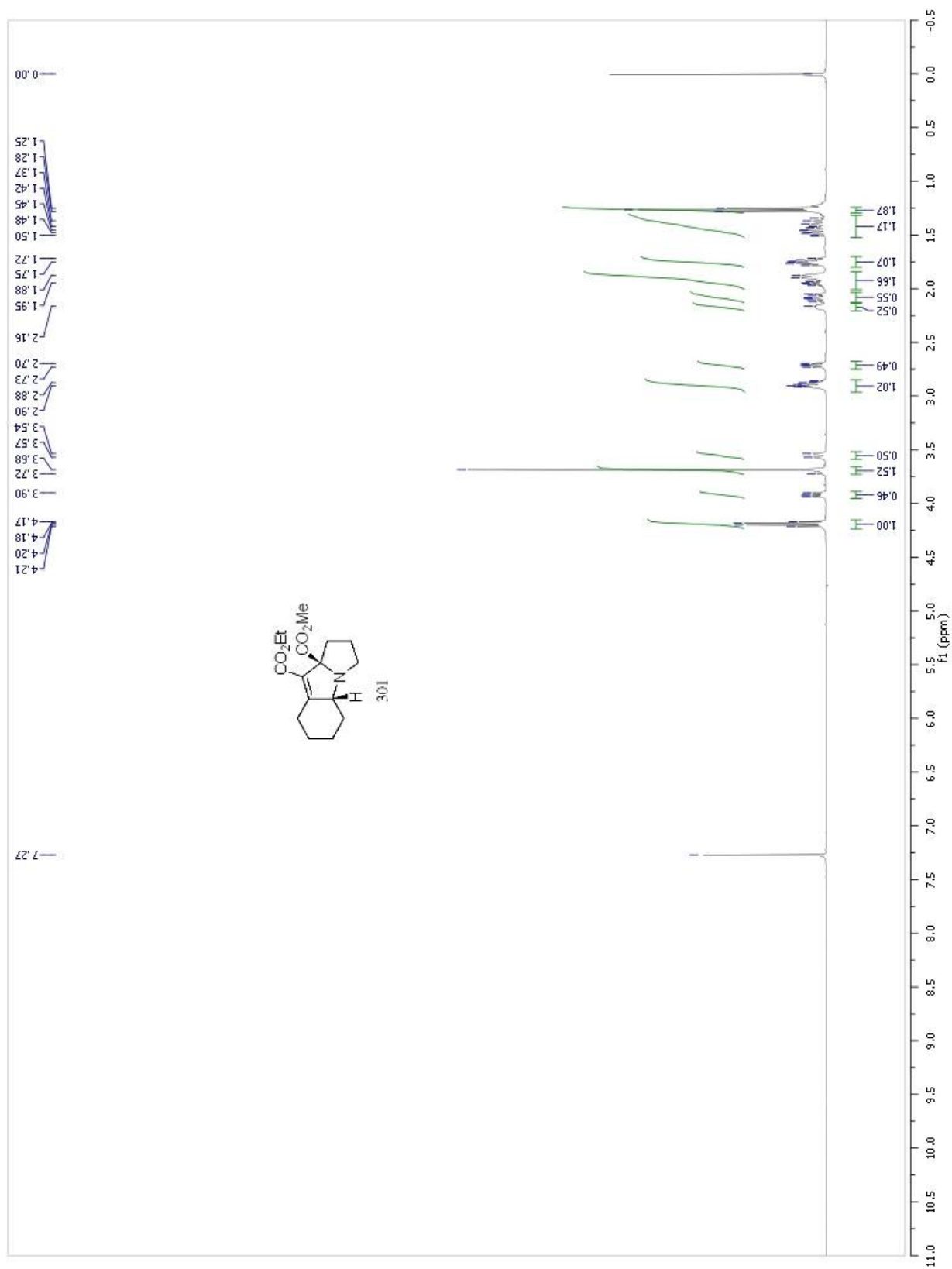


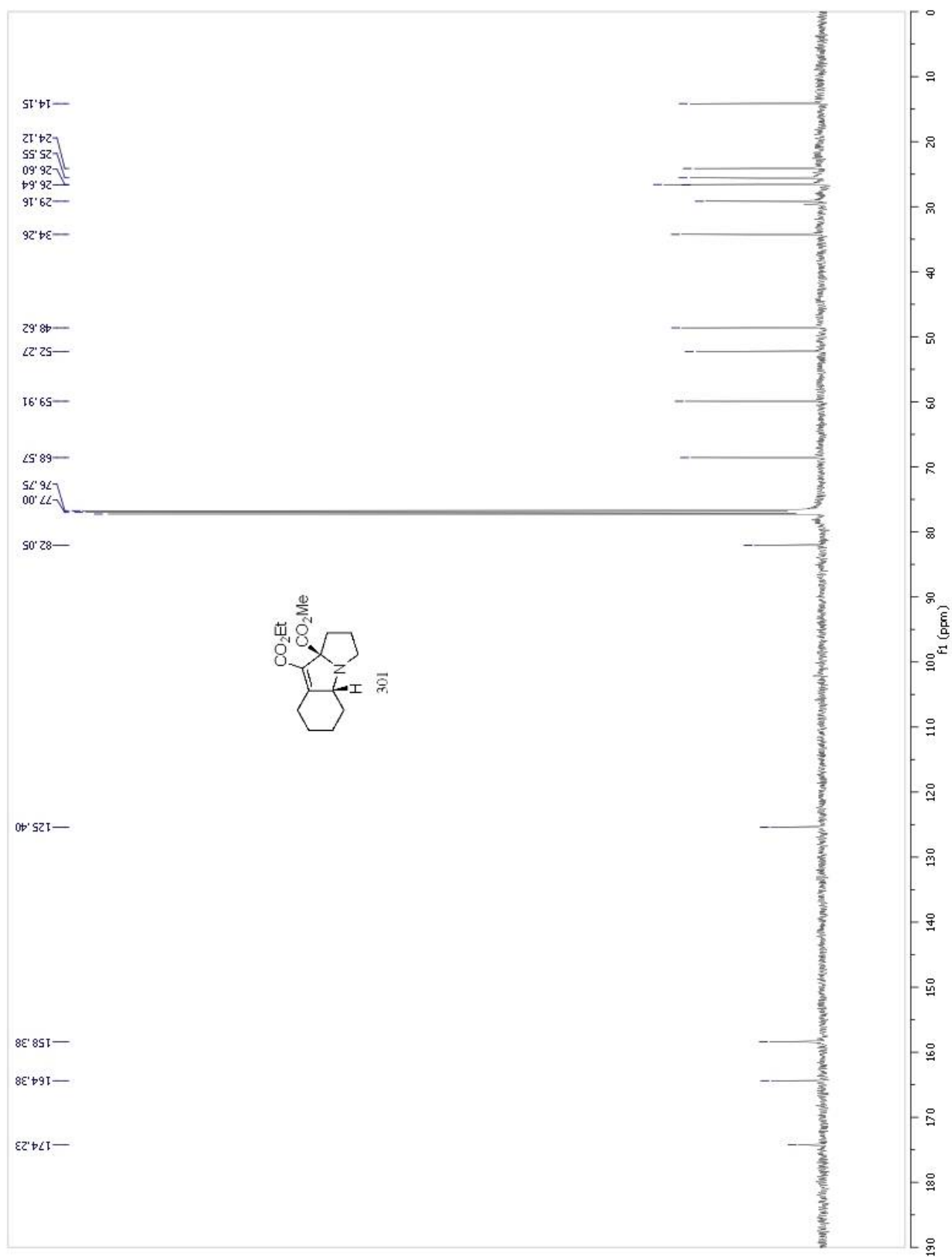


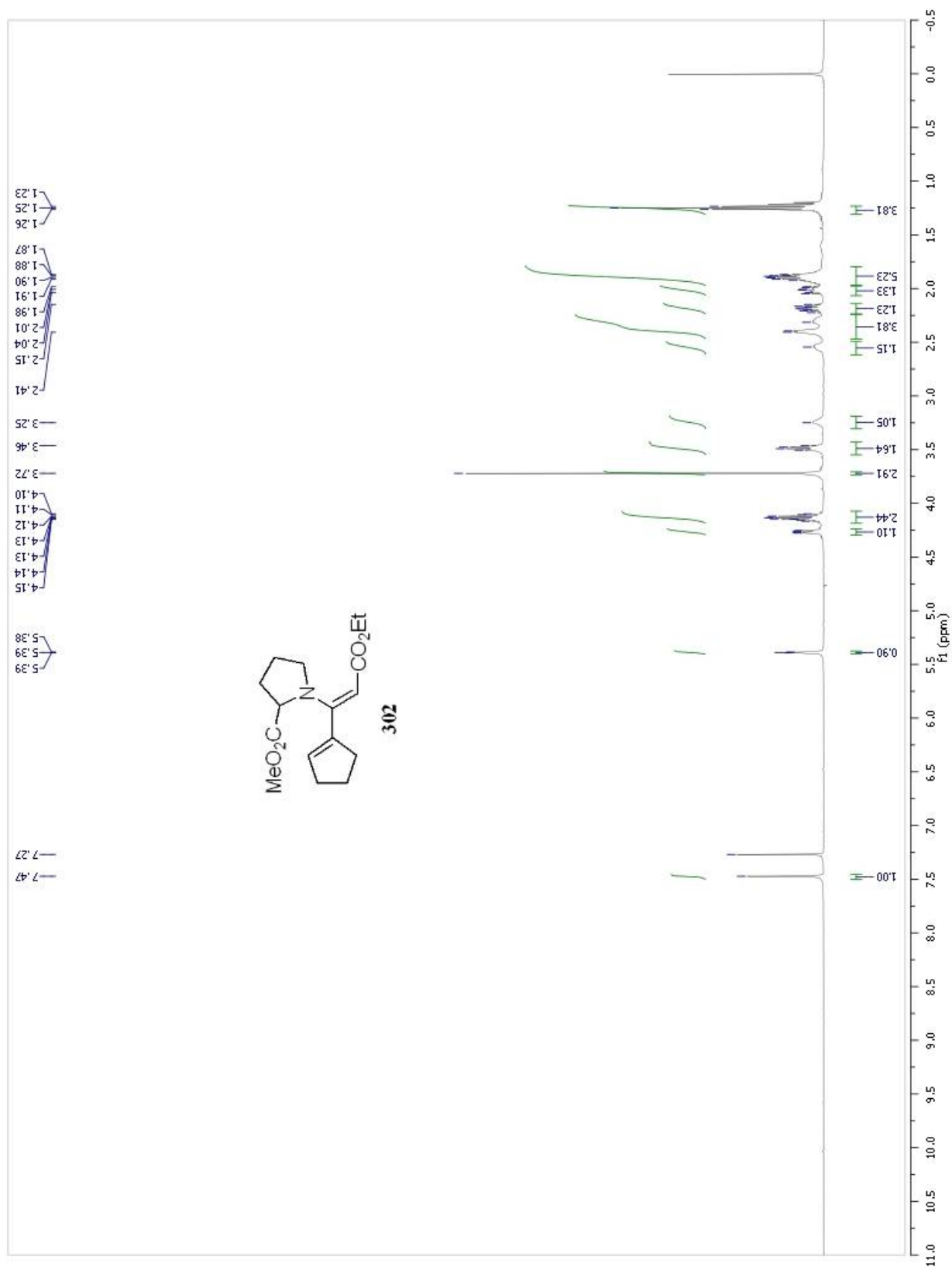


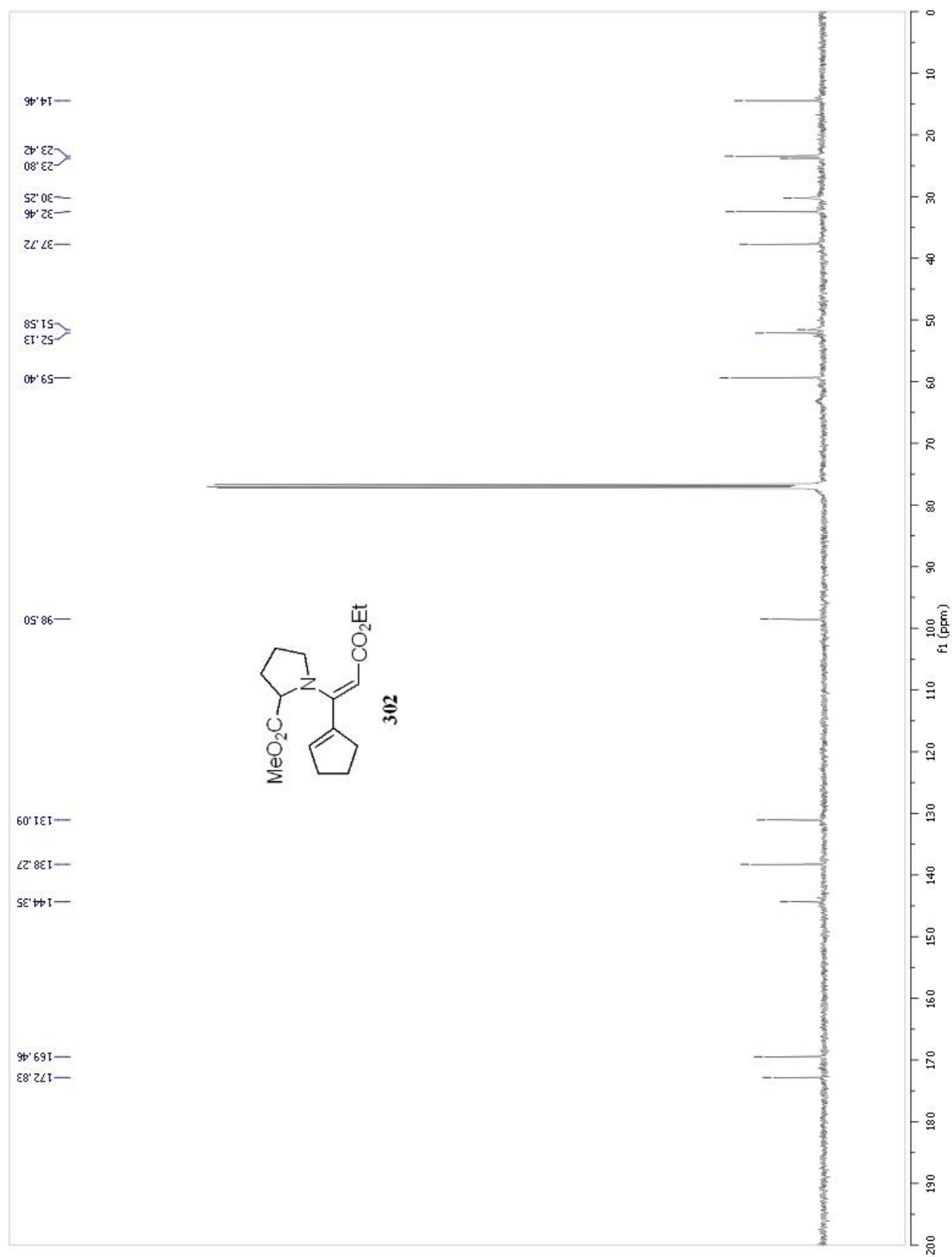


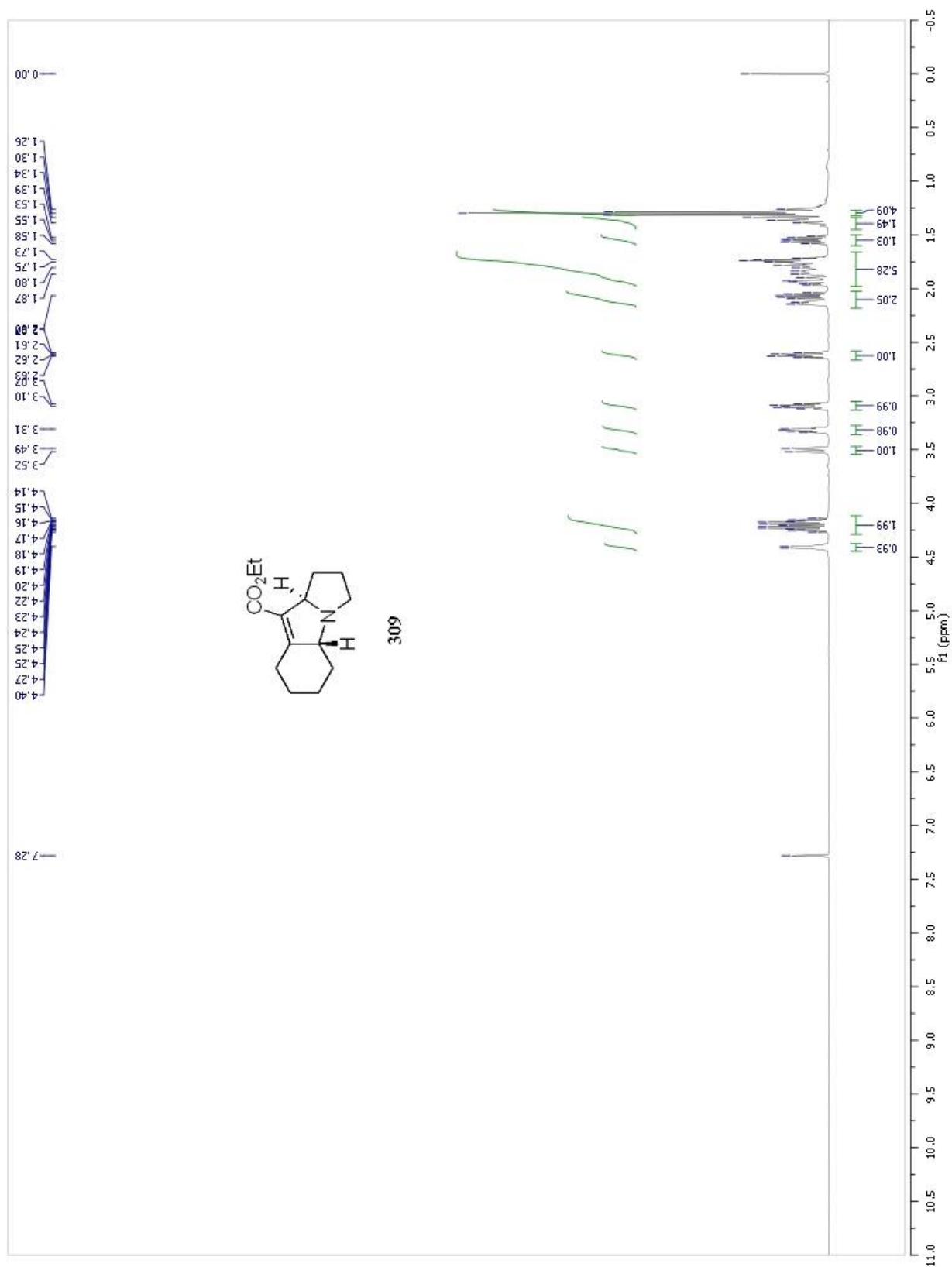


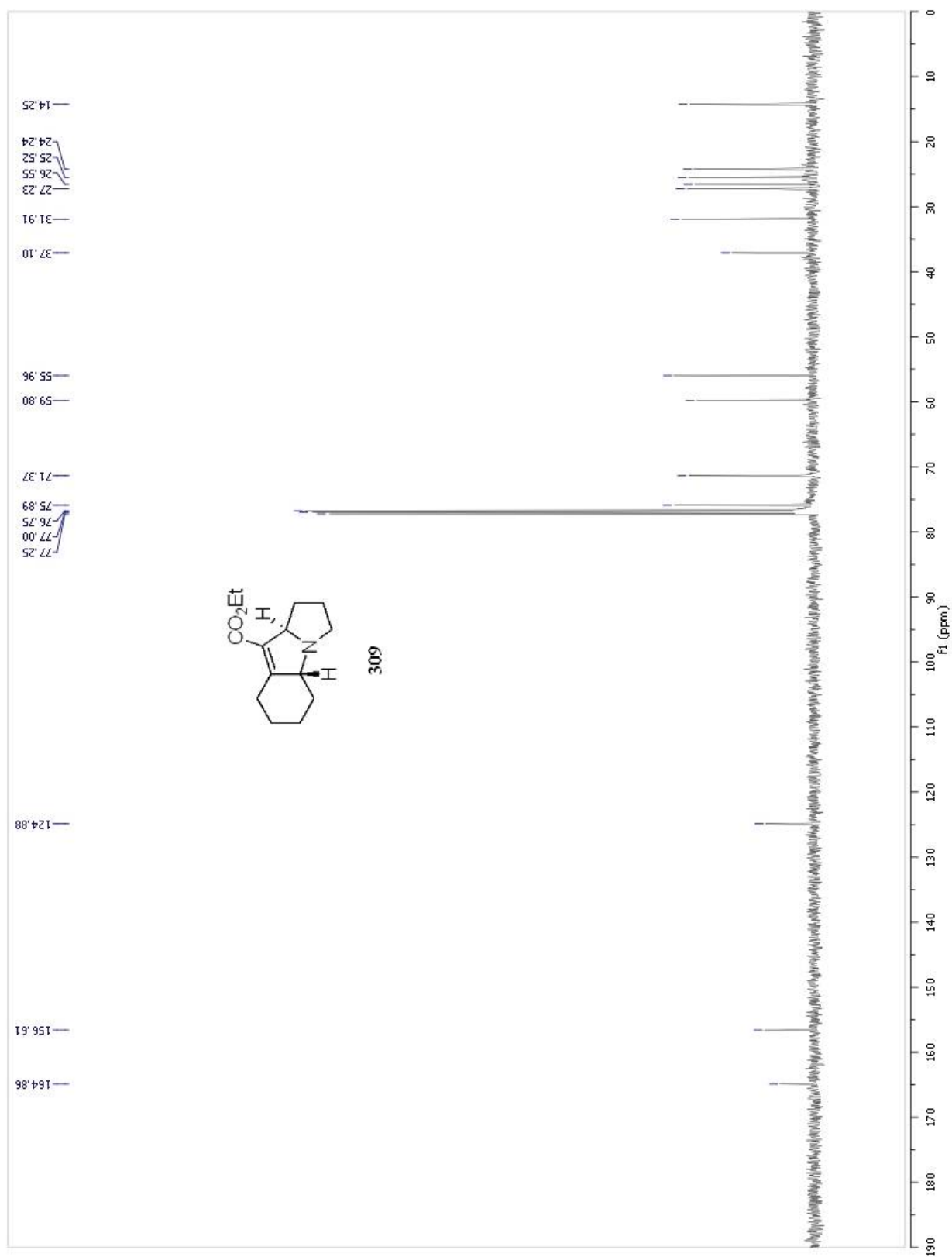


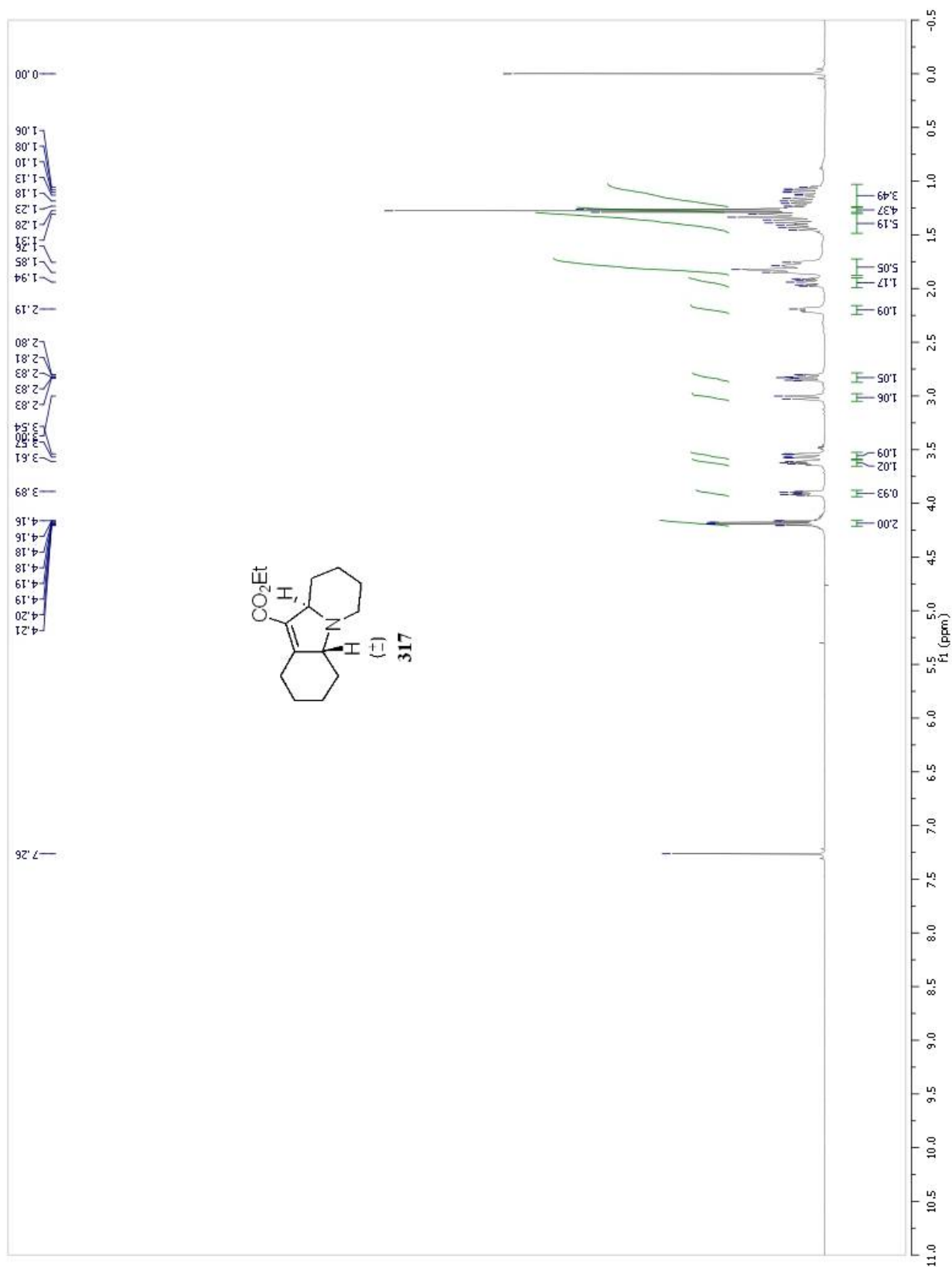




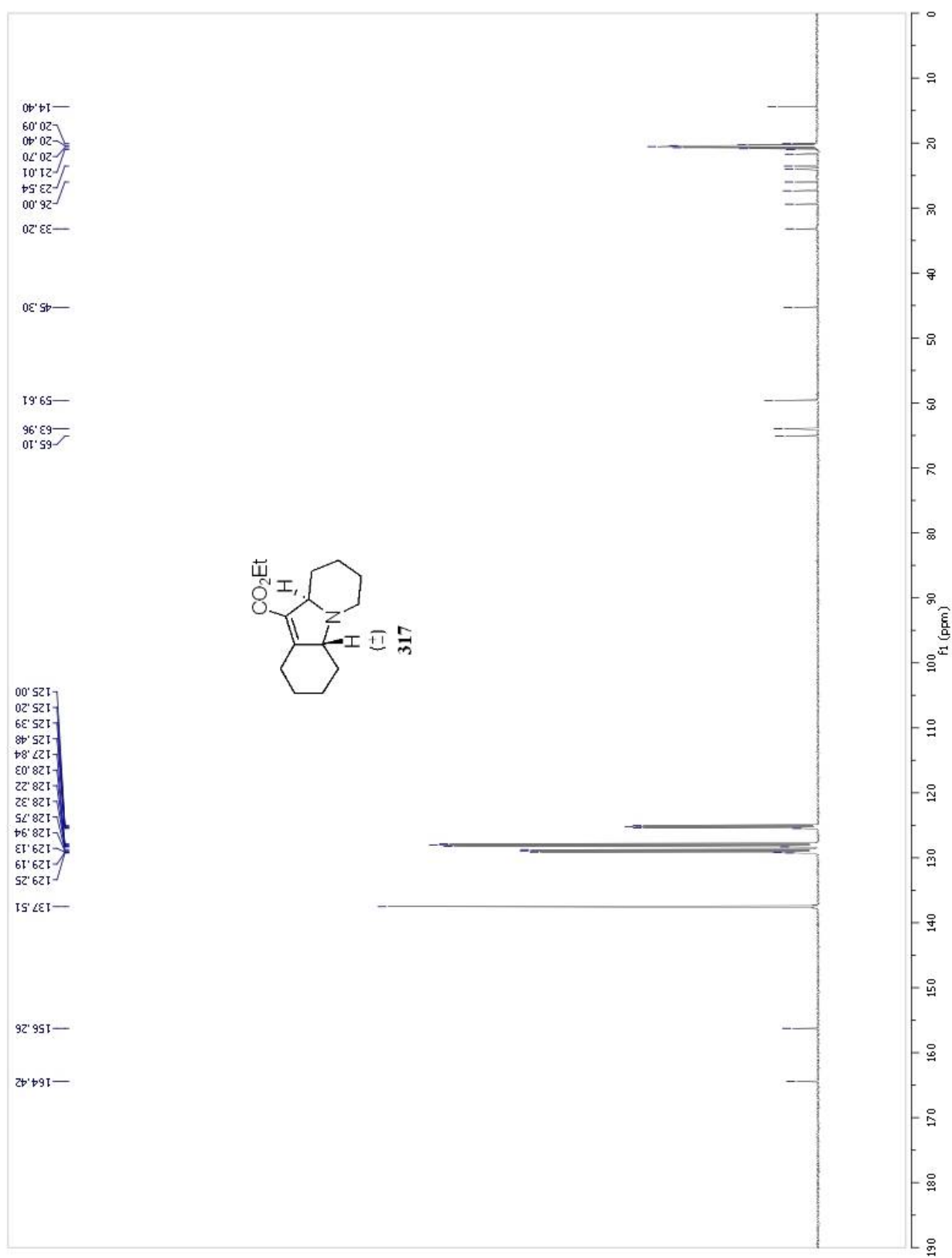


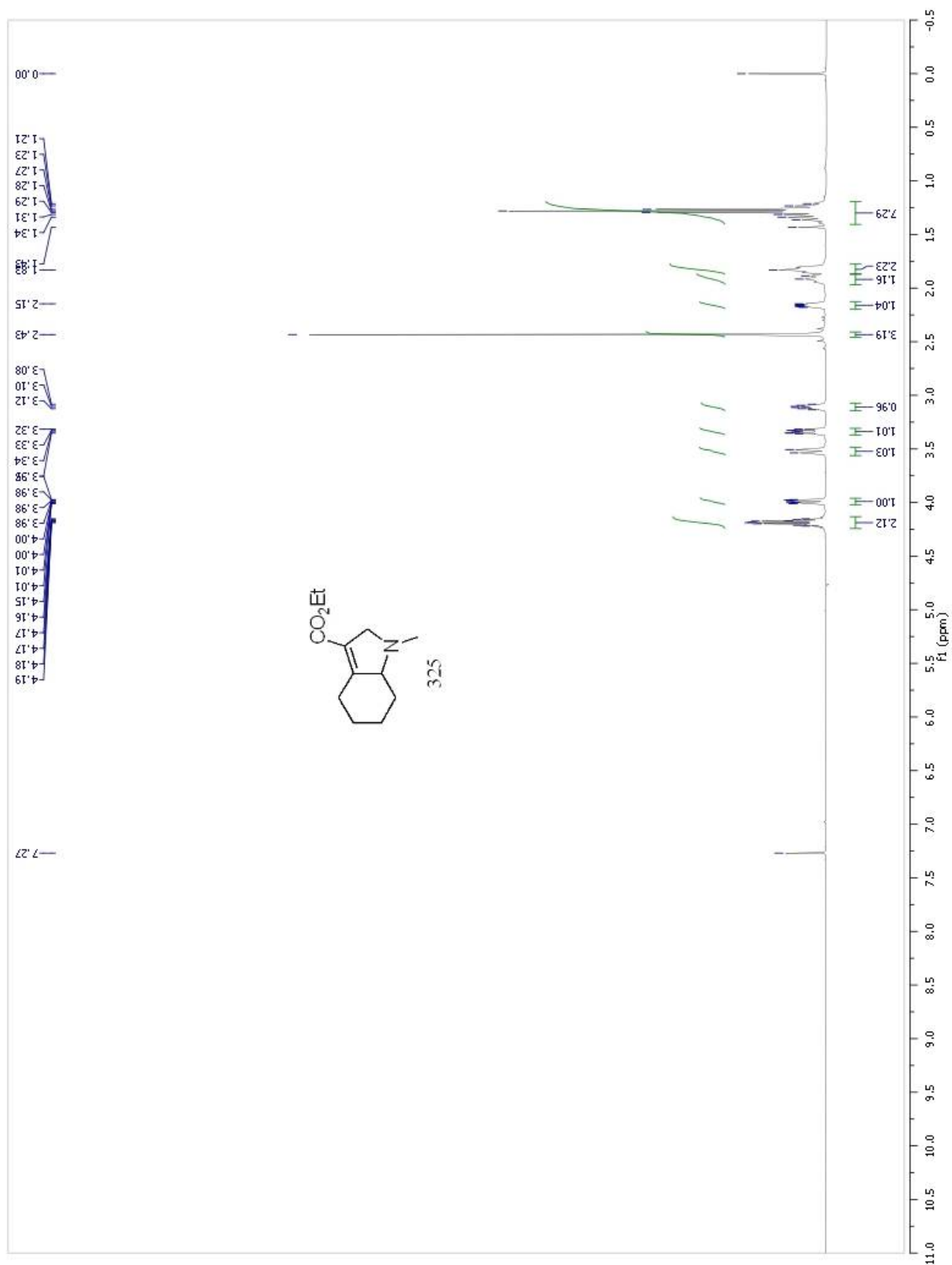


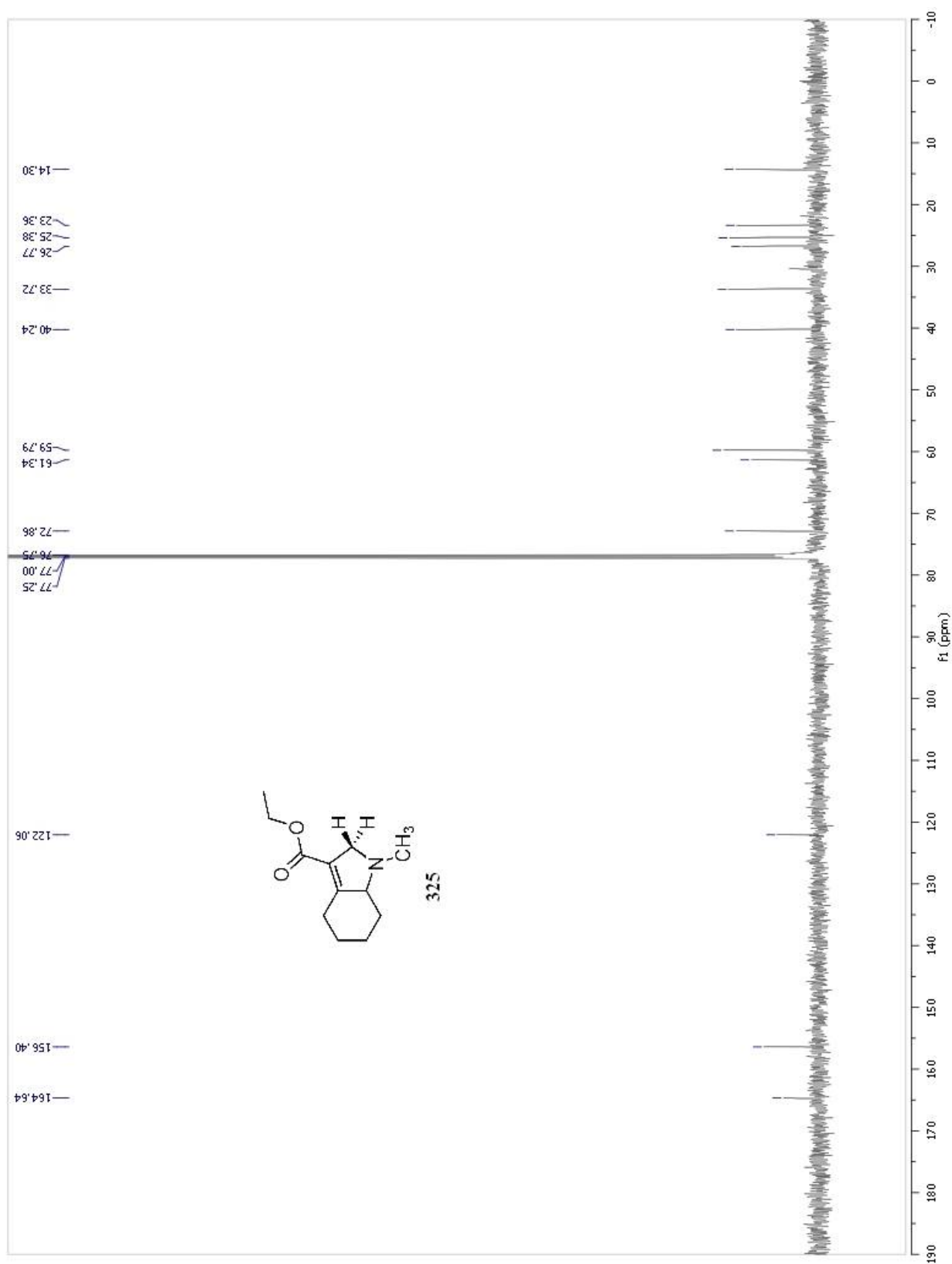


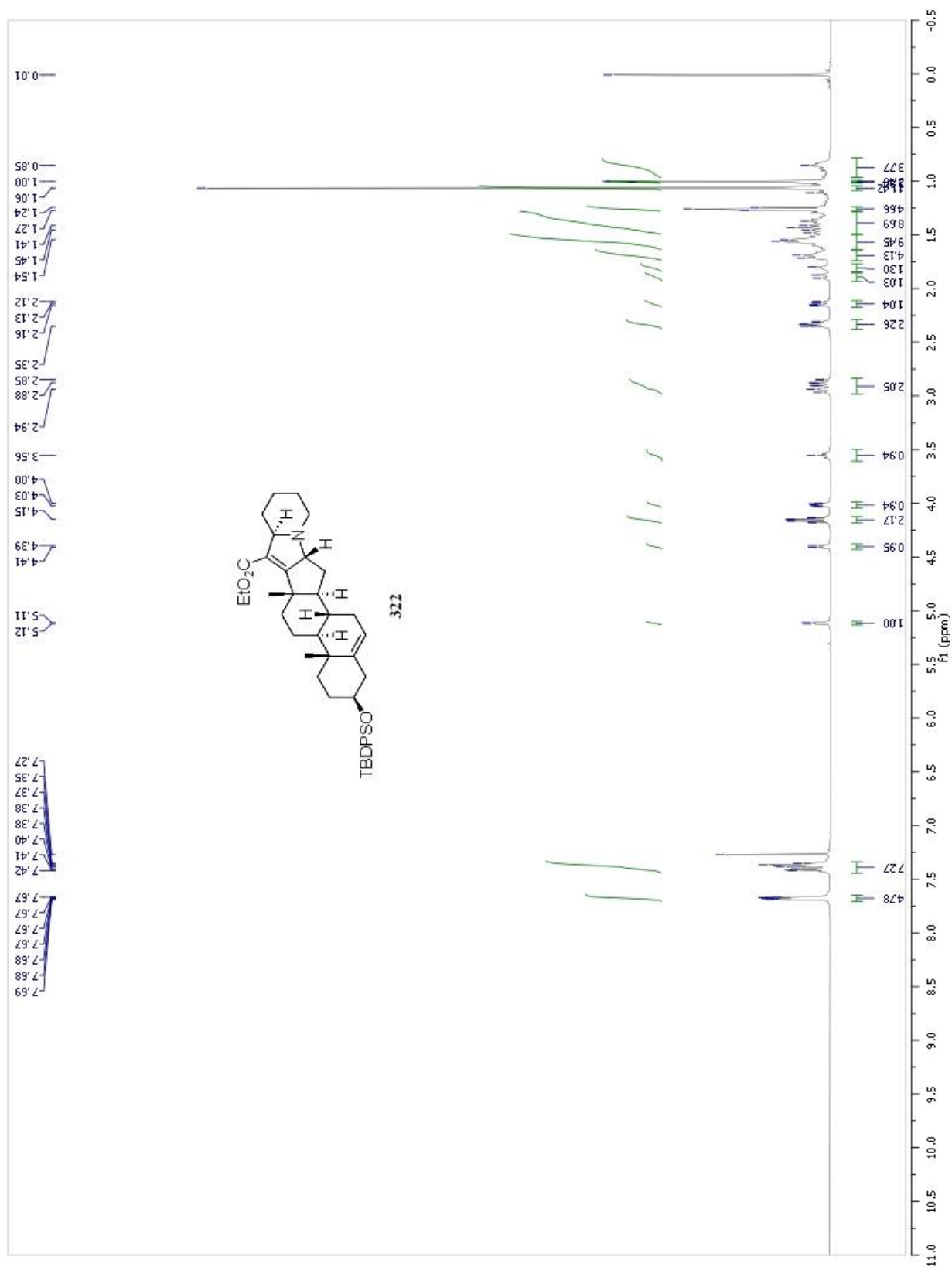


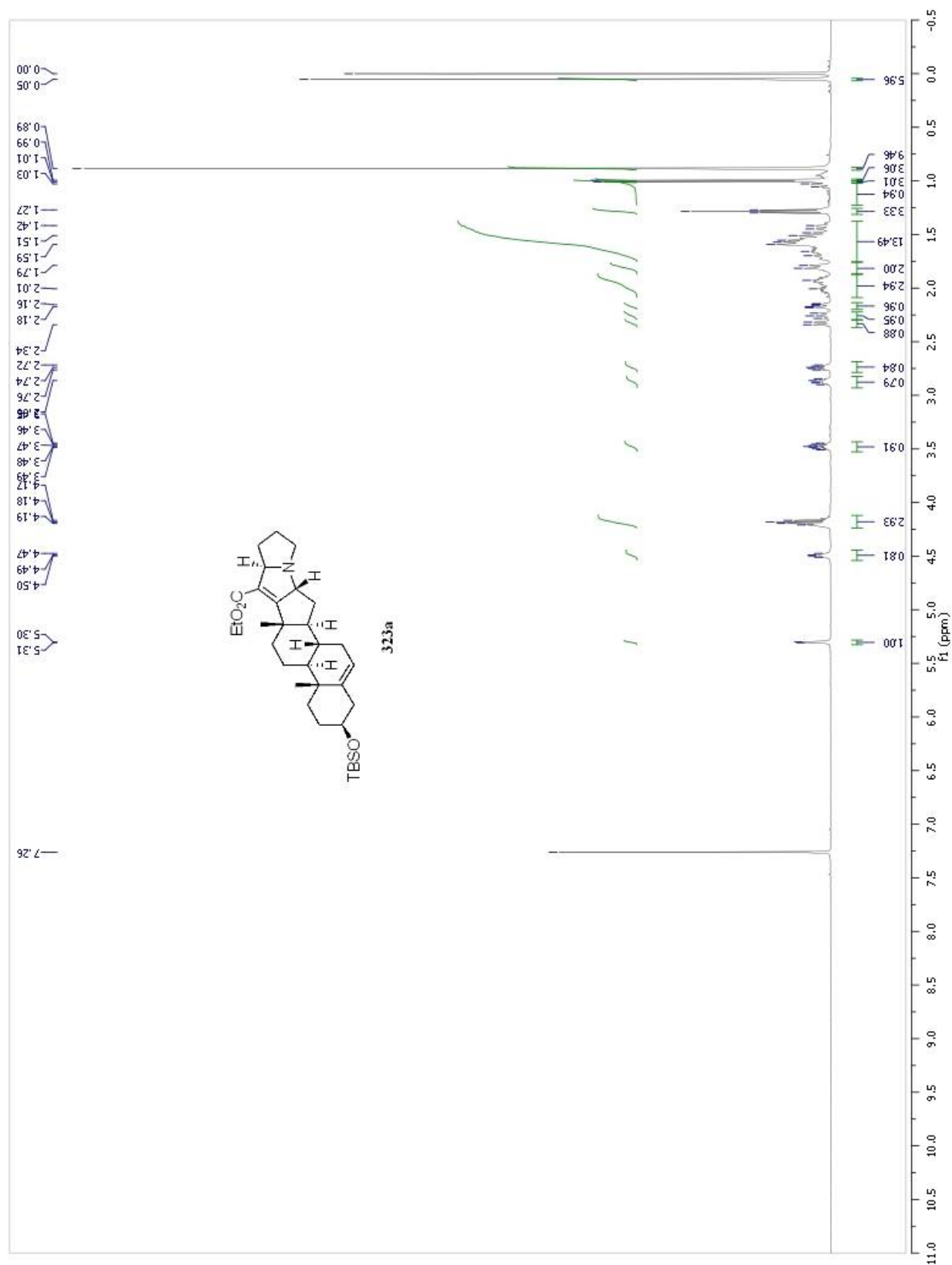


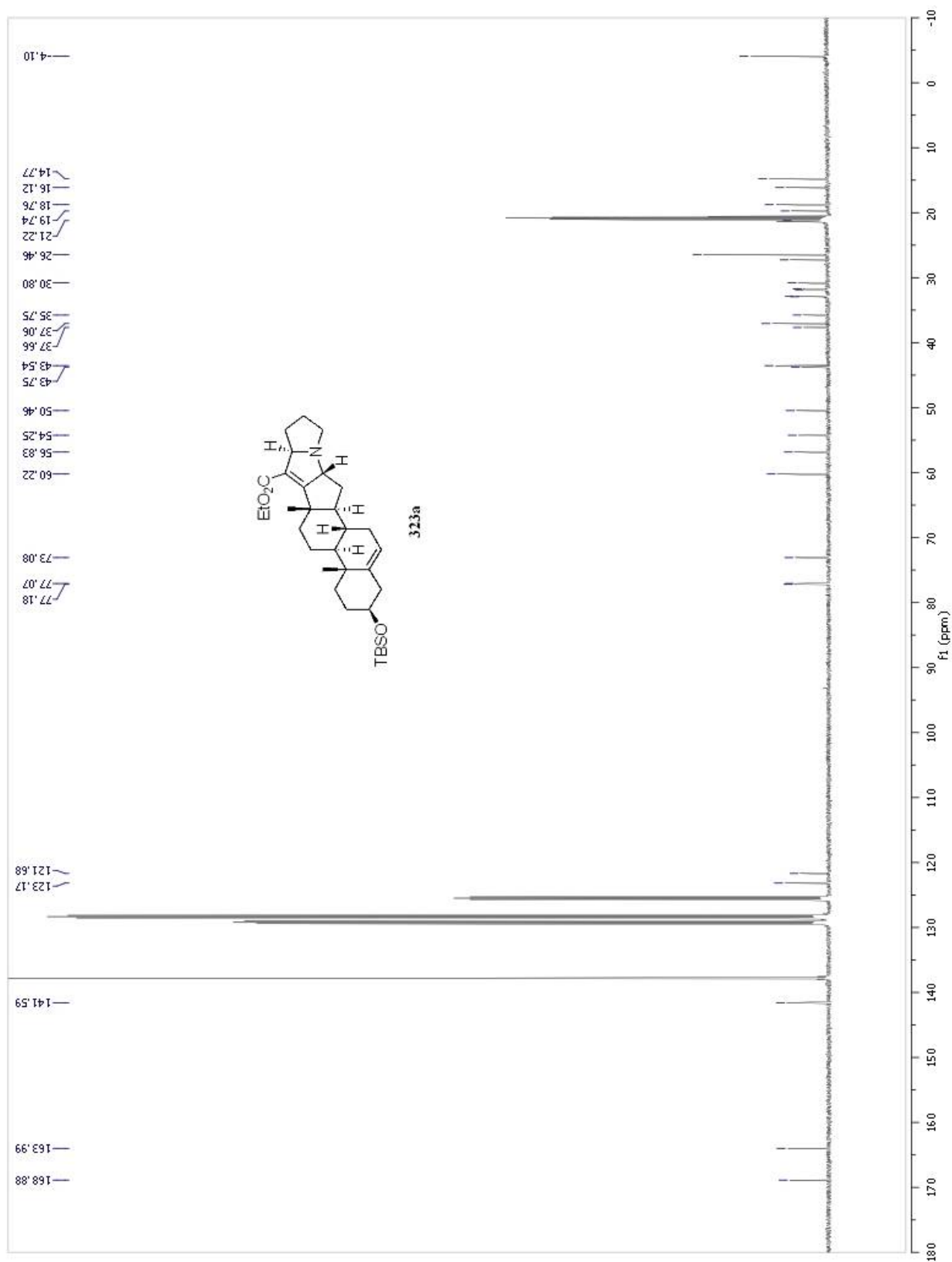


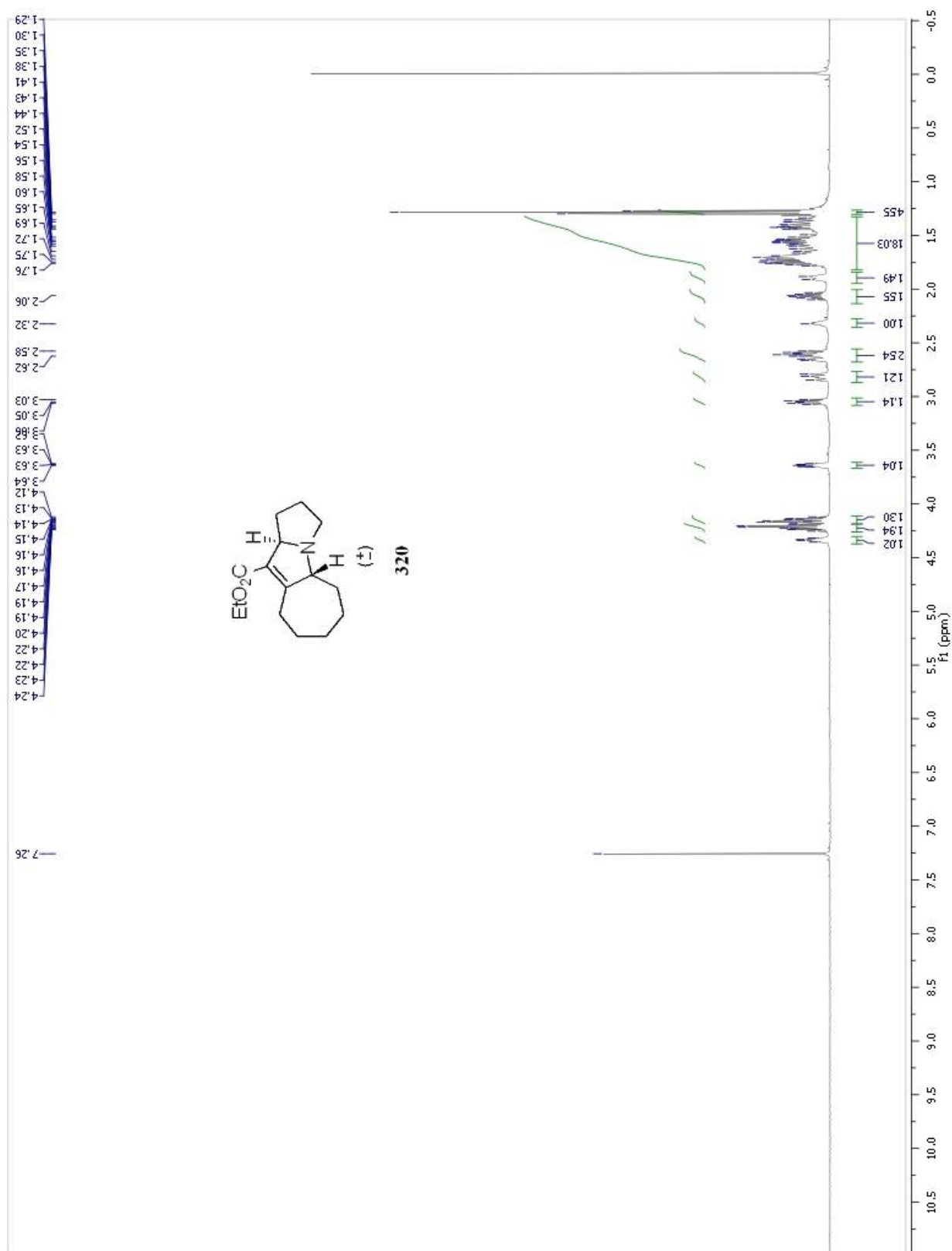


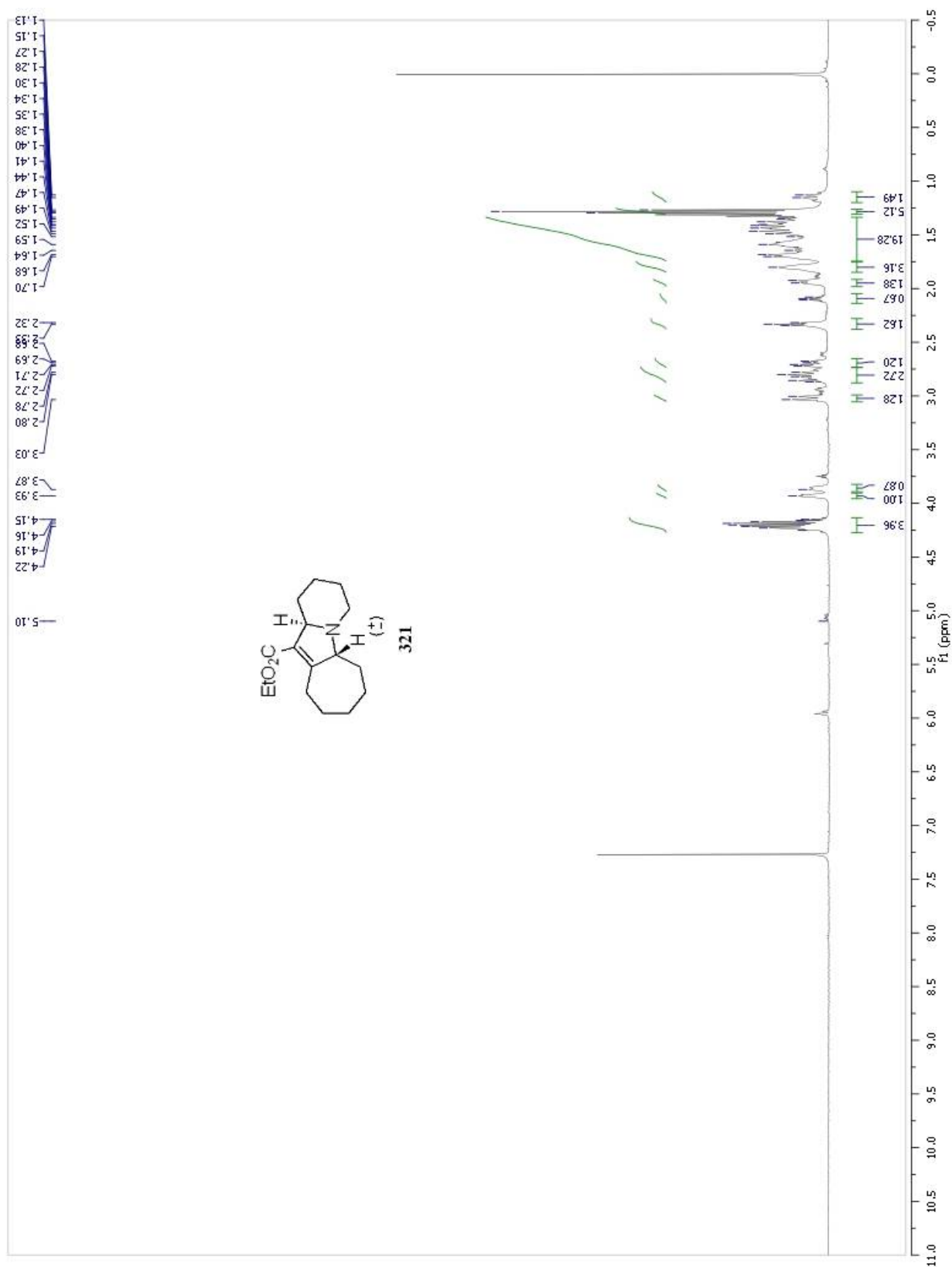




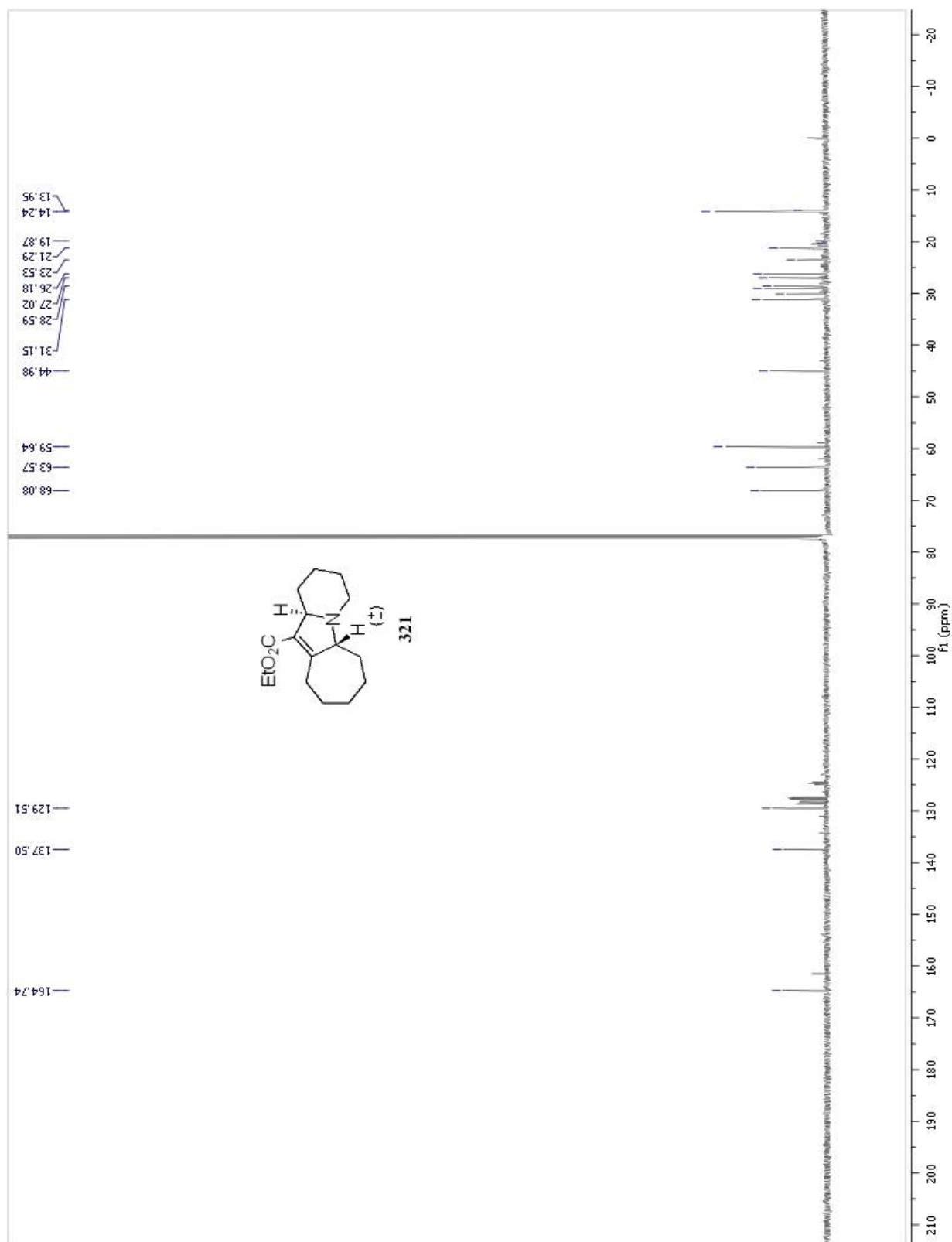


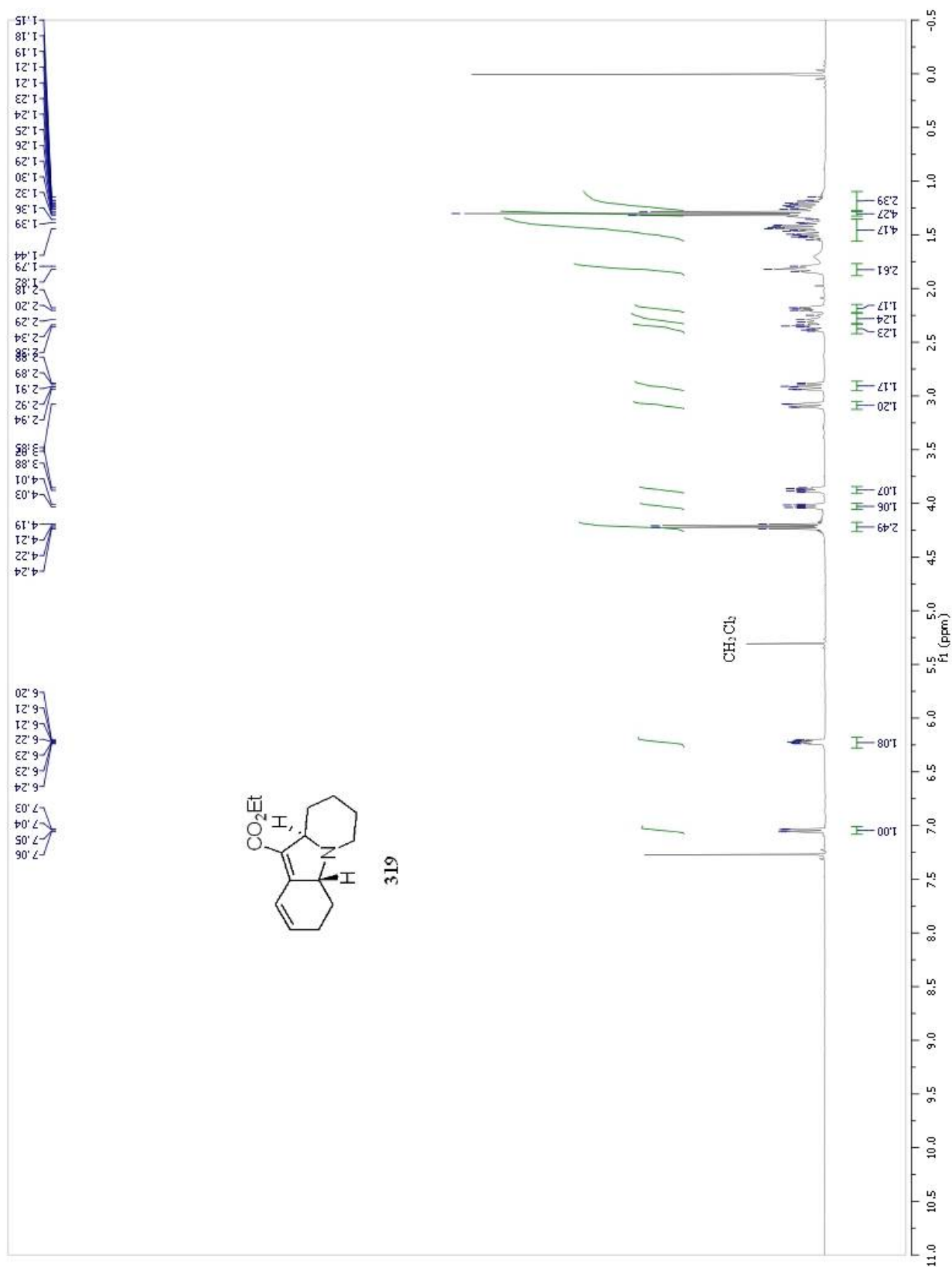


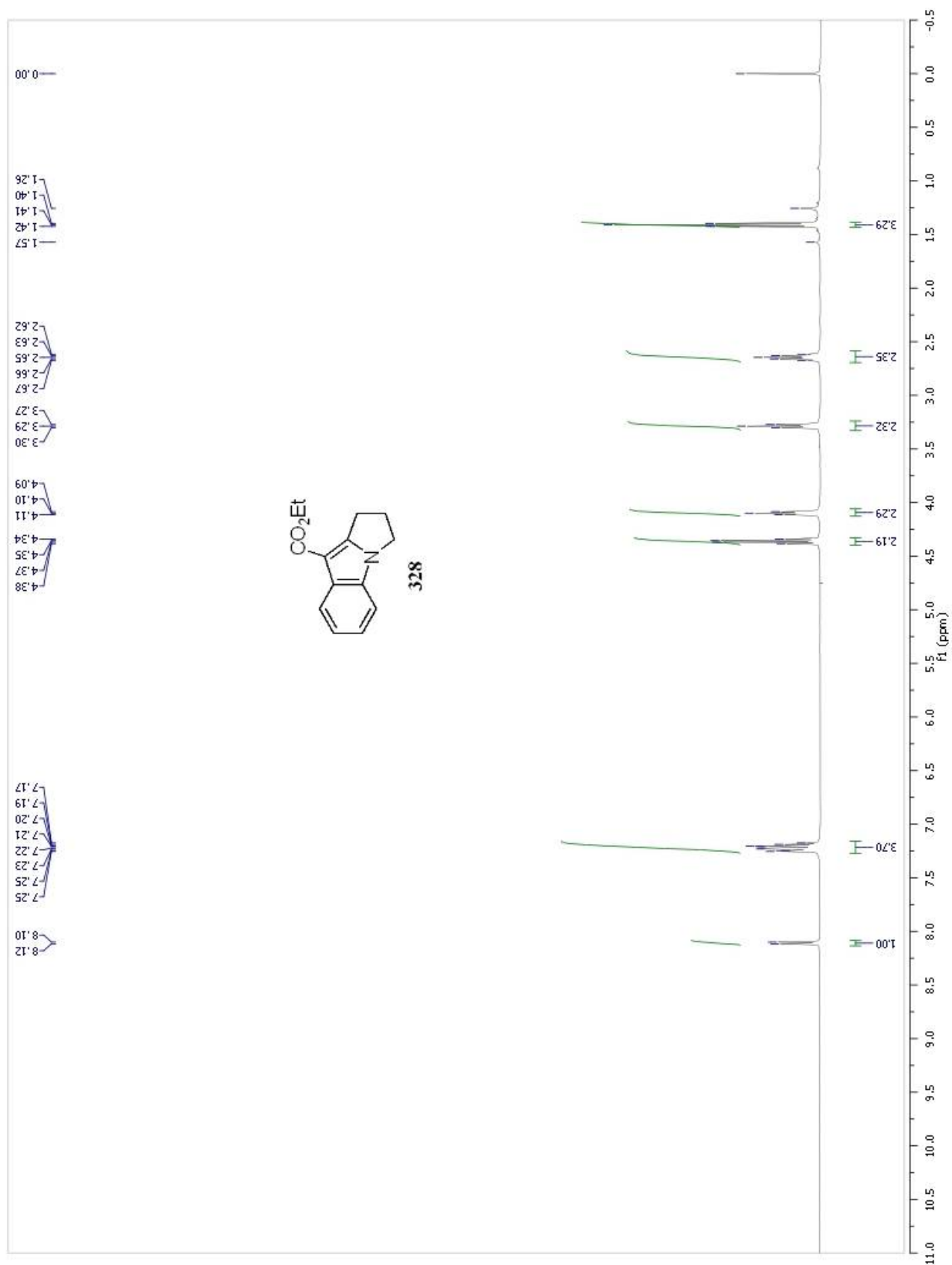


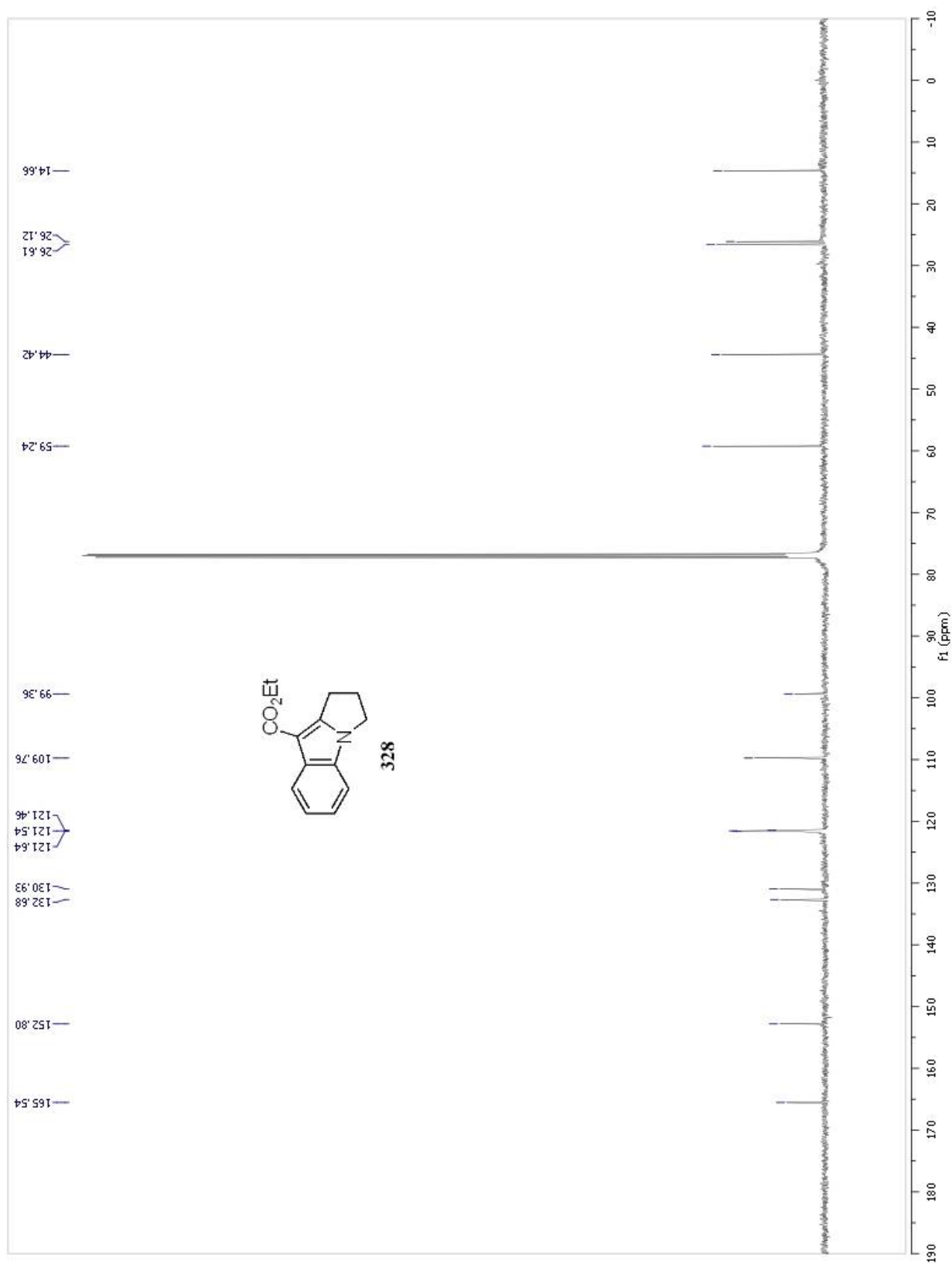


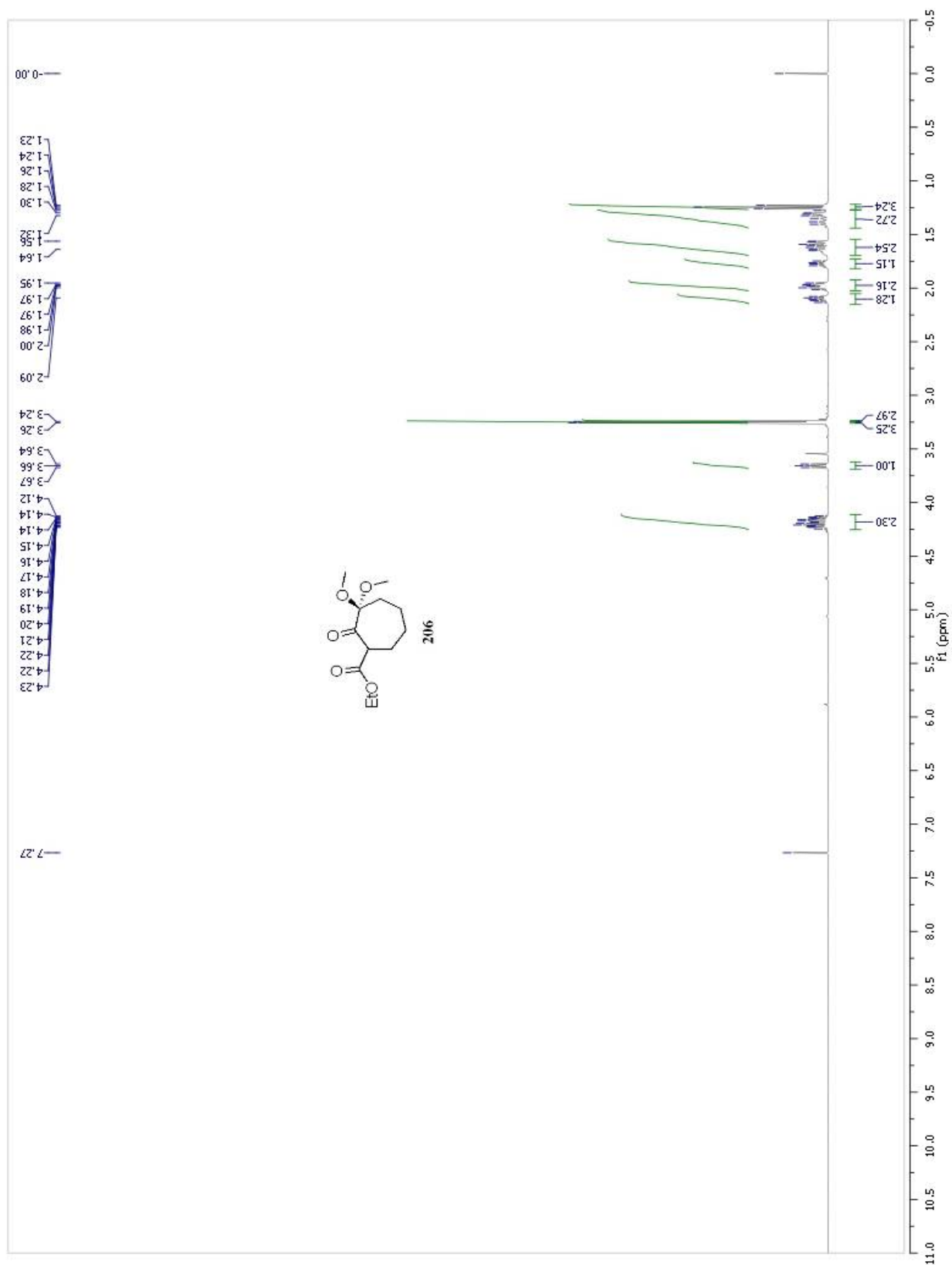




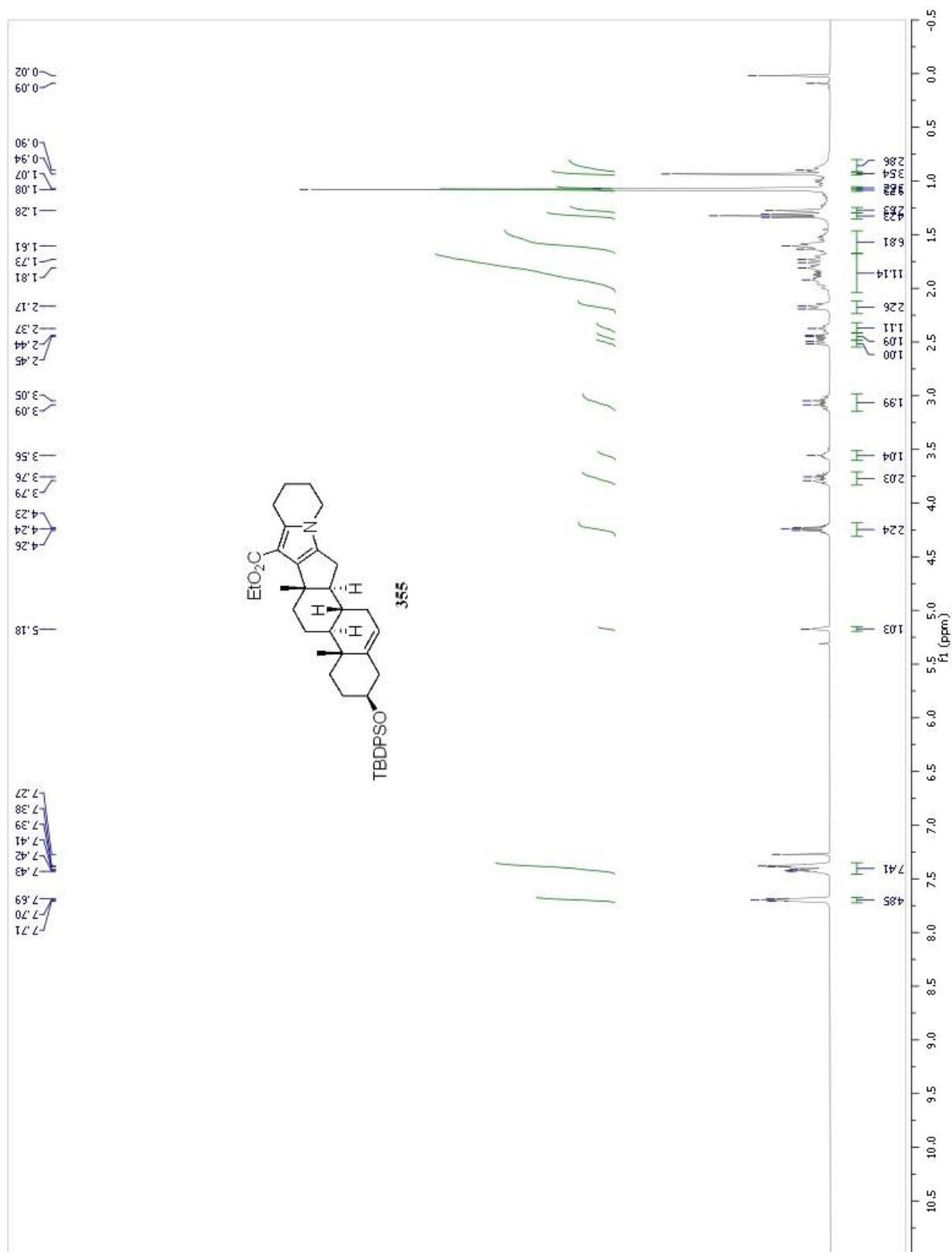


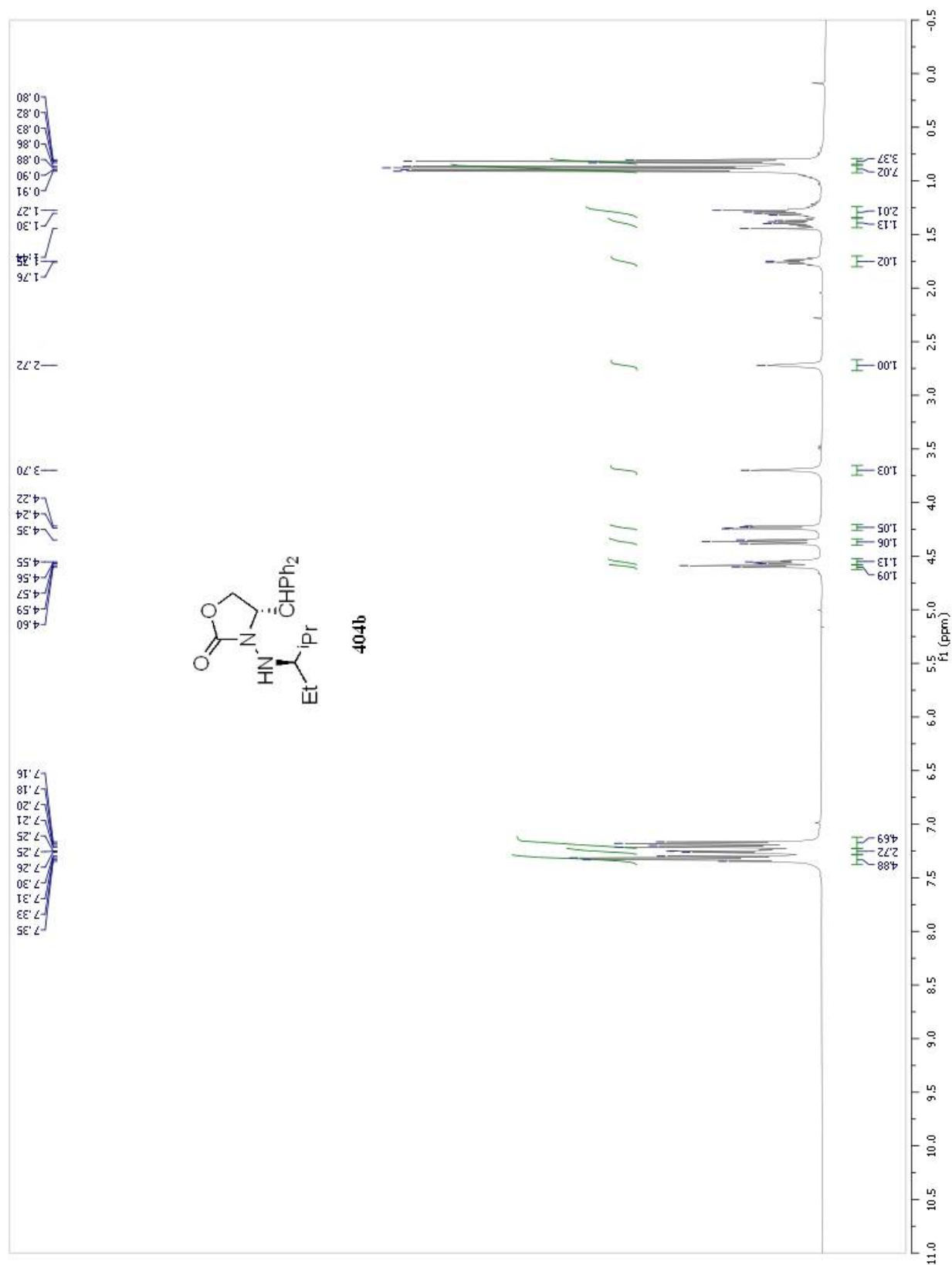




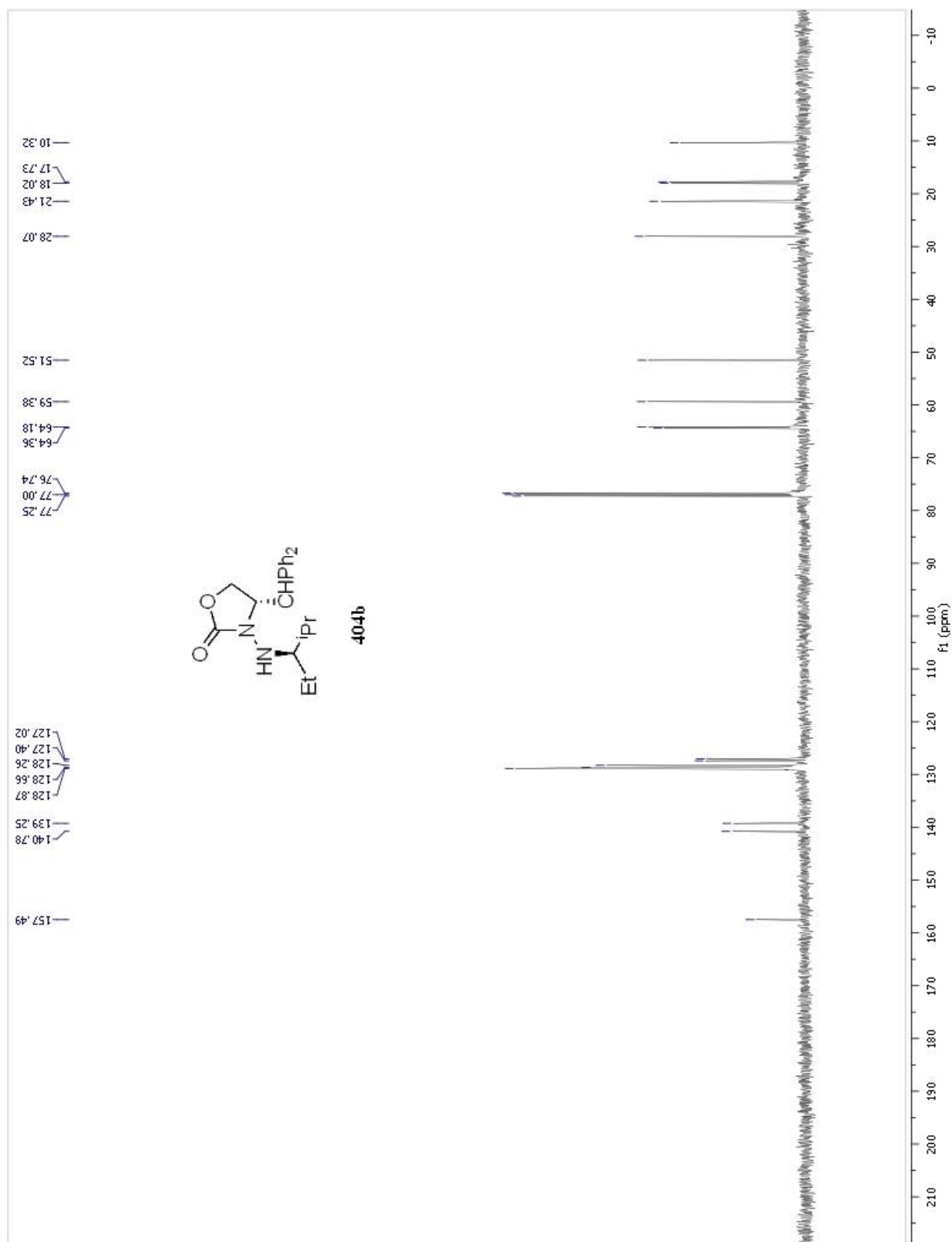


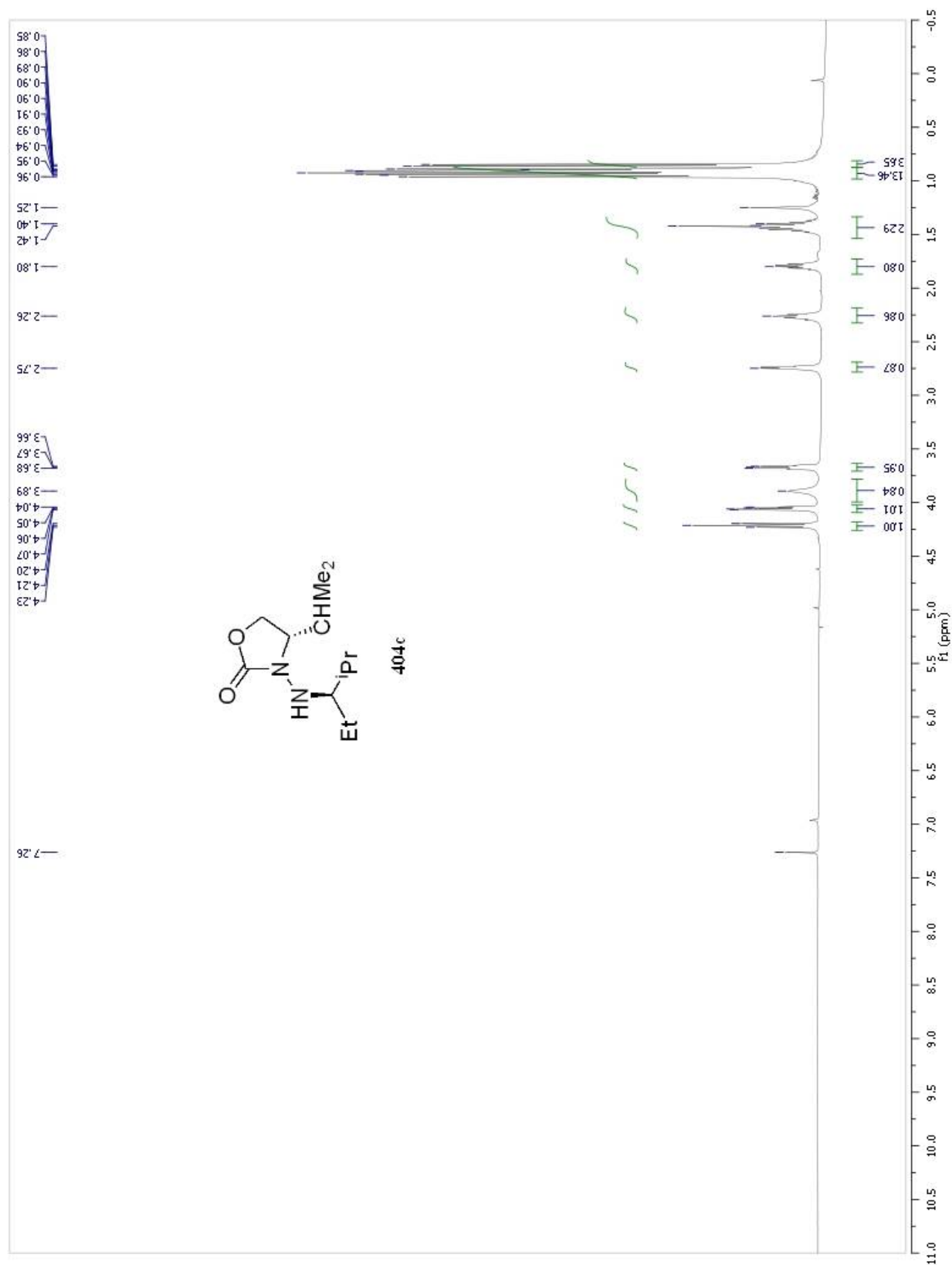


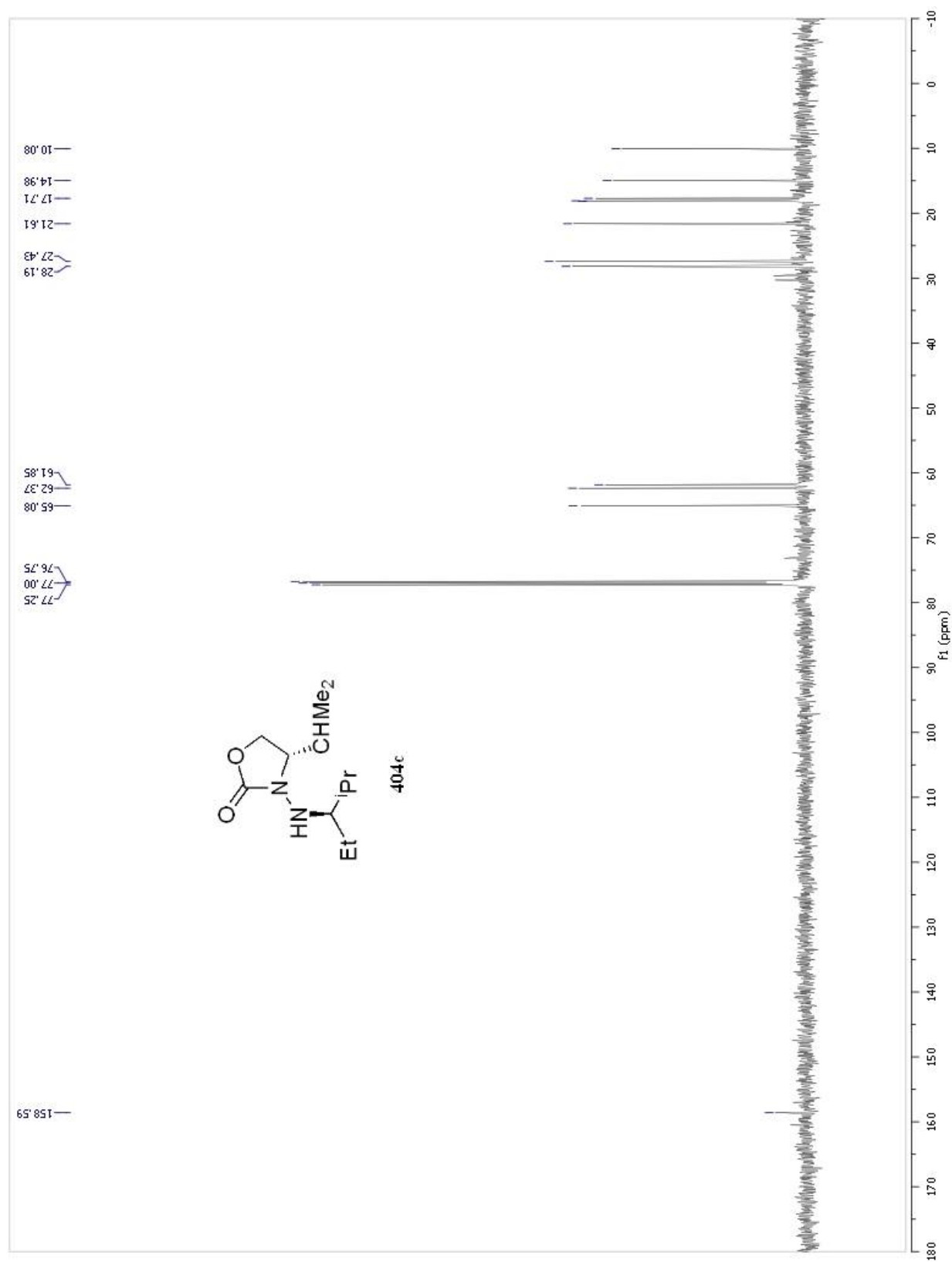


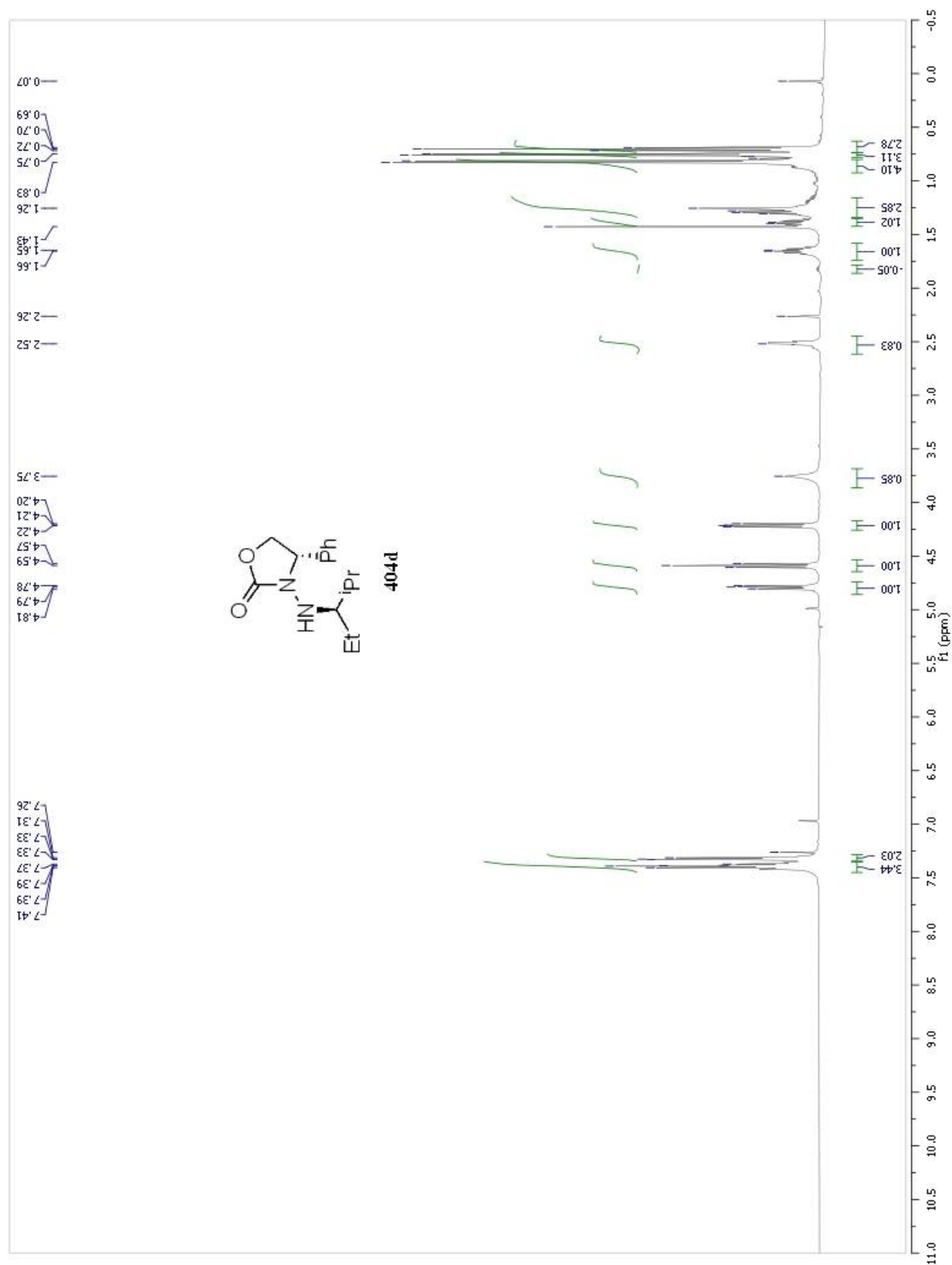




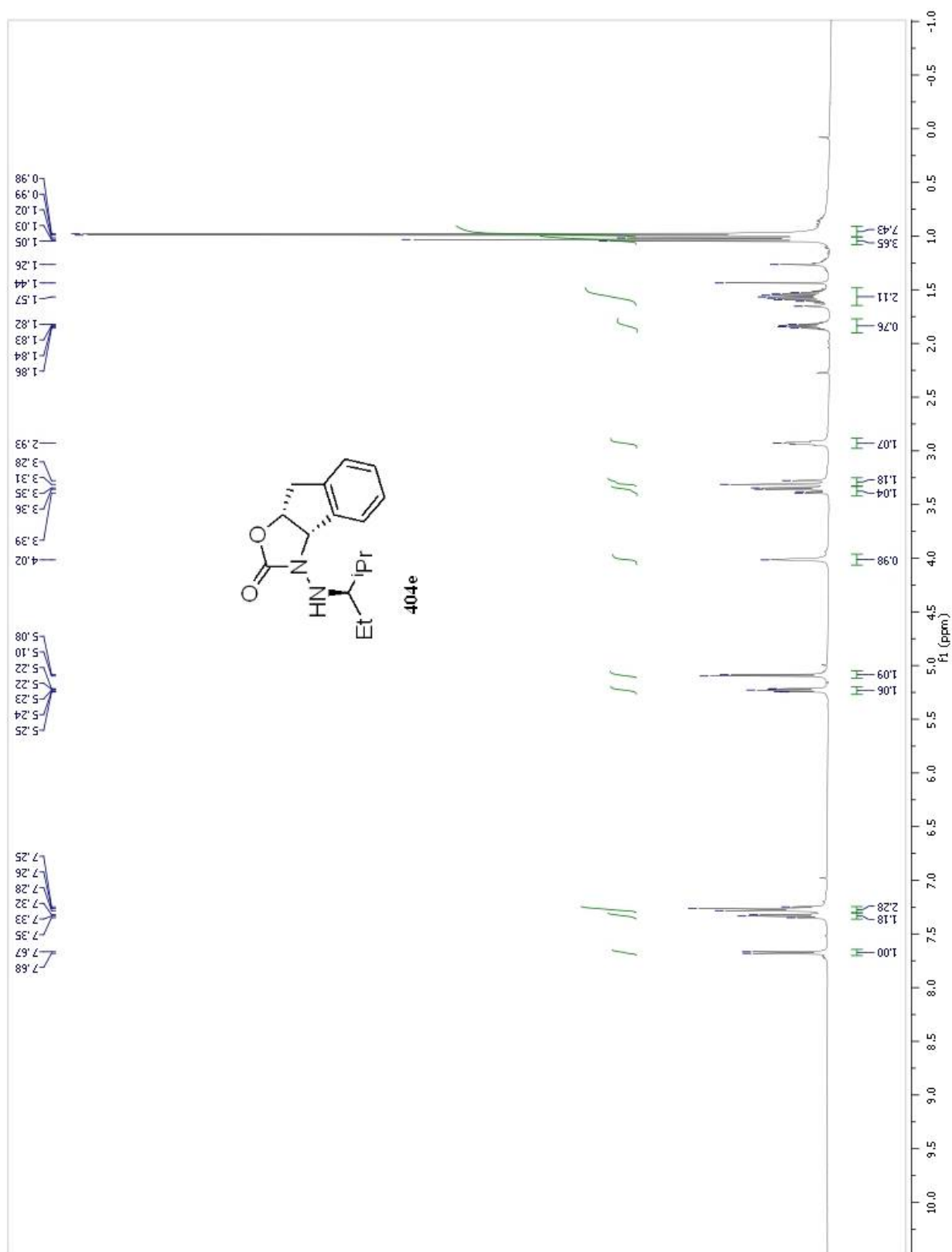


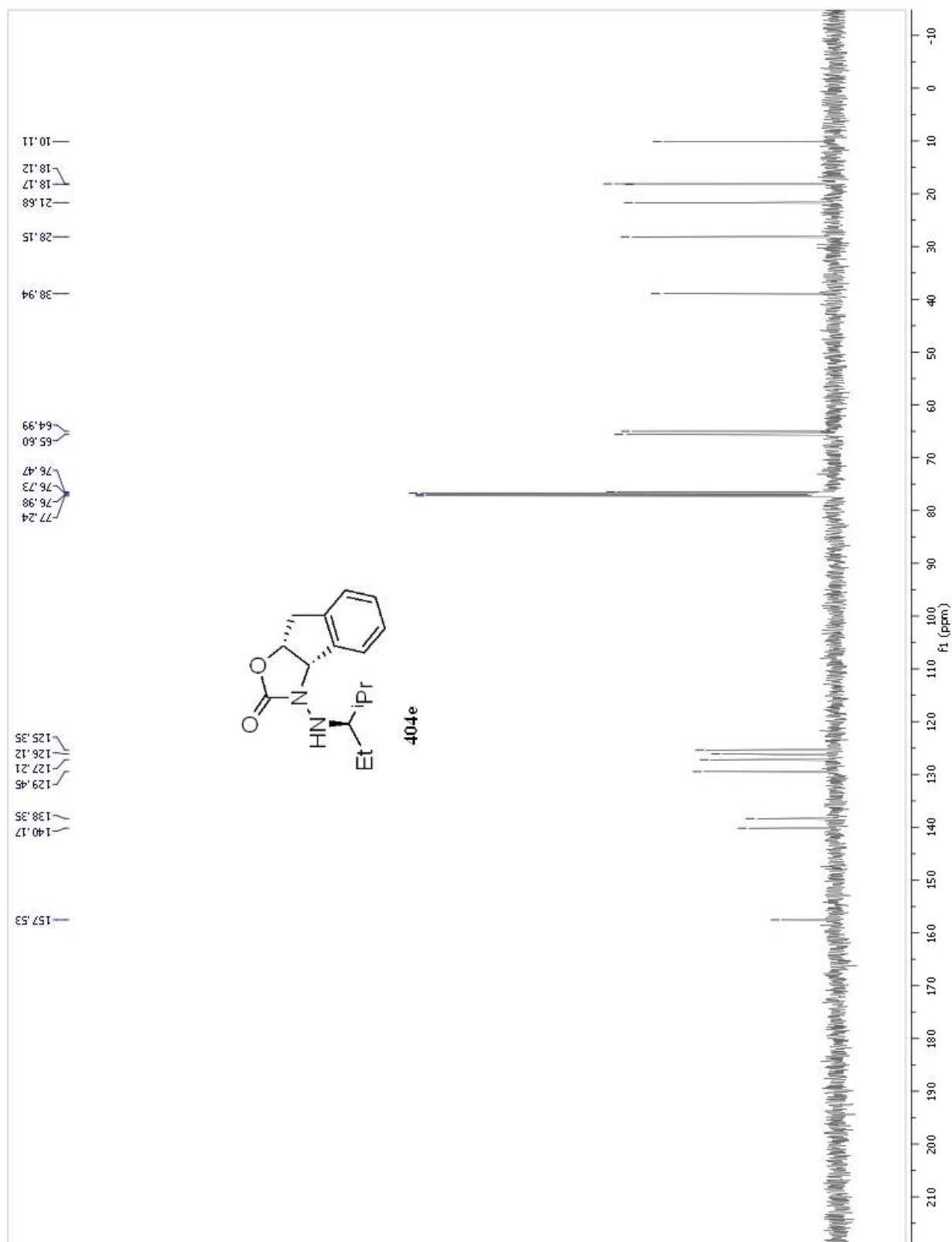




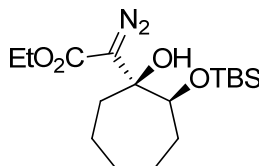








**Crystallographic data for ethyl 2-(*cis*-2-(*tert*-butyldimethylsilyloxy)-1-hydroxycycloheptyl)-2-diazoacetate (158s):**



**Experimental**

A colorless crystal of approximate dimensions 0.24 x 0.33 x 0.37 mm was mounted on a glass fiber and transferred to a Bruker SMART APEX II diffractometer. The APEX2<sup>1</sup> program package was used to determine the unit-cell parameters and for data collection (15 sec/frame scan time for a sphere of diffraction data). The raw frame data was processed using SAINT<sup>2</sup> and SADABS<sup>3</sup> to yield the reflection data file. Subsequent calculations were carried out using the SHELXTL<sup>4</sup> program. The diffraction symmetry was *mmm* and the systematic absences were consistent with the orthorhombic space group *P*2<sub>1</sub>2<sub>1</sub>2<sub>1</sub> that was later determined to be correct.

The structure was solved by direct methods and refined on F<sup>2</sup> by full-matrix least-squares techniques. The analytical scattering factors<sup>5</sup> for neutral atoms were used throughout the analysis. Hydrogen atoms were located from a difference-Fourier map and refined (*x,y,z* and *U*<sub>iso</sub>).

At convergence, wR2 = 0.0597 and Goof = 1.050 for 346 variables refined against 6016 data (0.70Å), R1 = 0.0220 for those 5866 data with I > 2.0σ(I). The absolute structure could not be assigned by inversion of the model or by refinement of the Flack parameter<sup>6</sup>. The structure was refined using the TWIN<sup>4</sup> command, BASF = 0.51(5).

**References**

APEX2 Version 2008.1-0, or 2.2-0 Bruker AXS, Inc.; Madison, WI 2008.

1. SAINT Version 7.51a, Bruker AXS, Inc.; Madison, WI 2007.
2. Sheldrick, G. M. SADABS, Version 2007/4, Bruker AXS, Inc.; Madison, WI 2007.
3. Sheldrick, G. M. SHELXTL, Version 6.12, Bruker AXS, Inc.; Madison, WI 2001.



4. International Tables for X-Ray Crystallography 1992, Vol. C., Dordrecht: Kluwer Academic Publishers.

5. Flack, H. D. Acta. Cryst., A39, 876-881, 1983.

**Definitions:**

$$wR2 = [\Sigma[w(F_o^2 - F_c^2)^2] / \Sigma[w(F_o^2)^2]]^{1/2}$$

$$R1 = \Sigma||F_o| - |F_c|| / \Sigma|F_o|$$

Goof = S =  $[\Sigma[w(F_o^2 - F_c^2)^2] / (n-p)]^{1/2}$  where n is the number of reflections and p is the total number of parameters refined.

The thermal ellipsoid plot is shown at the 50% probability level.

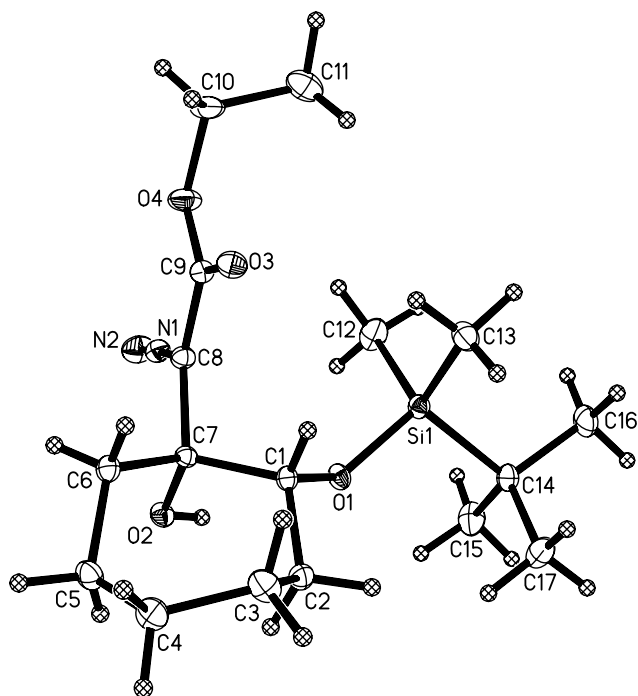


Table 1. Crystal data and structure refinement for **158s**.

Identification code	mb1	
Empirical formula	C <sub>17</sub> H <sub>32</sub> N <sub>2</sub> O <sub>4</sub> Si	
Formula weight	356.54	
Temperature	103(2) K	
Wavelength	0.71073 Å	
Crystal system	Orthorhombic	
Space group	<i>P</i> 2 <sub>1</sub> 2 <sub>1</sub> 2 <sub>1</sub>	
Unit cell dimensions	a = 10.4838(4) Å	α = 90°.
	b = 12.1220(4) Å	β = 90°.
	c = 15.5976(6) Å	γ = 90°.
Volume	1982.22(13) Å <sup>3</sup>	
Z	4	
Density (calculated)	1.195 Mg/m <sup>3</sup>	
Absorption coefficient	0.140 mm <sup>-1</sup>	
F(000)	776	
Crystal color	colourless	
Crystal size	0.37 x 0.33 x 0.24 mm <sup>3</sup>	
Theta range for data collection	4.10 to 30.51°	
Index ranges	-14 ≤ <i>h</i> ≤ 14, -17 ≤ <i>k</i> ≤ 17, -22 ≤ <i>l</i> ≤ 22	
Reflections collected	27951	
Independent reflections	6016 [R(int) = 0.0187]	
Completeness to theta = 30.51°	99.6 %	
Absorption correction	Semi-empirical from equivalents	
Max. and min. transmission	0.9671 and 0.9500	
Refinement method	Full-matrix least-squares on F <sup>2</sup>	
Data / restraints / parameters	6016 / 0 / 346	
Goodness-of-fit on F <sup>2</sup>	1.050	
Final R indices [I > 2σ(I) = 5866 data]	R1 = 0.0220, wR2 = 0.0591	
R indices (all data, 0.70 Å)	R1 = 0.0228, wR2 = 0.0597	
Absolute structure parameter	0.51(5)	
Largest diff. peak and hole	0.293 and -0.153 e.Å <sup>-3</sup>	

Table 2. Atomic coordinates ( $\times 10^4$ ) and equivalent isotropic displacement parameters ( $\text{\AA}^2 \times 10^3$ ) for mb1.  $U(\text{eq})$  is defined as one third of the trace of the orthogonalized  $U^{ij}$  tensor.

	x	y	z	$U(\text{eq})$
Si(1)	2490(1)	9464(1)	2360(1)	12(1)
O(1)	3571(1)	9715(1)	3111(1)	13(1)
O(2)	5940(1)	10492(1)	3416(1)	13(1)
O(3)	5627(1)	7291(1)	2104(1)	17(1)
O(4)	6196(1)	8322(1)	946(1)	20(1)
N(1)	6225(1)	10097(1)	1816(1)	14(1)
N(2)	6436(1)	10889(1)	1469(1)	21(1)
C(1)	4456(1)	8961(1)	3493(1)	11(1)
C(2)	4213(1)	8946(1)	4460(1)	14(1)
C(3)	4866(1)	7985(1)	4925(1)	18(1)
C(4)	6242(1)	8195(1)	5217(1)	19(1)
C(5)	7006(1)	8981(1)	4648(1)	17(1)
C(6)	6902(1)	8753(1)	3682(1)	14(1)
C(7)	5801(1)	9353(1)	3231(1)	11(1)
C(8)	5959(1)	9201(1)	2257(1)	13(1)
C(9)	5904(1)	8176(1)	1784(1)	14(1)
C(10)	6087(1)	7367(1)	389(1)	23(1)
C(11)	4754(1)	7281(1)	32(1)	24(1)
C(12)	3033(1)	10087(1)	1327(1)	22(1)
C(13)	2246(1)	7952(1)	2226(1)	18(1)
C(14)	970(1)	10155(1)	2732(1)	15(1)
C(15)	1143(1)	11415(1)	2730(1)	23(1)
C(16)	-138(1)	9857(1)	2124(1)	21(1)
C(17)	625(1)	9778(1)	3644(1)	21(1)

Table 3. Bond lengths [Å] and angles [°] for **158s**.

Si(1)-O(1)	1.6577(6)
Si(1)-C(13)	1.8632(8)
Si(1)-C(12)	1.8684(9)
Si(1)-C(14)	1.8918(8)
O(1)-C(1)	1.4318(9)
O(2)-C(7)	1.4185(8)
O(3)-C(9)	1.2181(10)
O(4)-C(9)	1.3538(9)
O(4)-C(10)	1.4526(10)
N(1)-N(2)	1.1234(10)
N(1)-C(8)	1.3161(10)
C(1)-C(2)	1.5304(10)
C(1)-C(7)	1.5438(10)
C(2)-C(3)	1.5331(11)
C(3)-C(4)	1.5346(12)
C(4)-C(5)	1.5291(12)
C(5)-C(6)	1.5358(11)
C(6)-C(7)	1.5349(10)
C(7)-C(8)	1.5393(10)
C(8)-C(9)	1.4452(10)
C(10)-C(11)	1.5081(14)
C(14)-C(17)	1.5374(11)
C(14)-C(15)	1.5380(11)
C(14)-C(16)	1.5420(11)
O(1)-Si(1)-C(13)	110.72(3)
O(1)-Si(1)-C(12)	109.09(4)
C(13)-Si(1)-C(12)	110.05(4)
O(1)-Si(1)-C(14)	106.18(3)
C(13)-Si(1)-C(14)	110.74(4)
C(12)-Si(1)-C(14)	109.99(4)
C(1)-O(1)-Si(1)	128.28(5)

C(9)-O(4)-C(10)	117.08(7)
N(2)-N(1)-C(8)	177.04(8)
O(1)-C(1)-C(2)	108.05(6)
O(1)-C(1)-C(7)	106.56(6)
C(2)-C(1)-C(7)	114.61(6)
C(1)-C(2)-C(3)	113.64(6)
C(2)-C(3)-C(4)	115.76(7)
C(5)-C(4)-C(3)	115.03(6)
C(4)-C(5)-C(6)	114.86(7)
C(7)-C(6)-C(5)	114.71(6)
O(2)-C(7)-C(6)	106.90(6)
O(2)-C(7)-C(8)	107.87(6)
C(6)-C(7)-C(8)	108.37(6)
O(2)-C(7)-C(1)	109.85(6)
C(6)-C(7)-C(1)	114.83(6)
C(8)-C(7)-C(1)	108.80(6)
N(1)-C(8)-C(9)	116.84(6)
N(1)-C(8)-C(7)	116.08(6)
C(9)-C(8)-C(7)	127.02(6)
O(3)-C(9)-O(4)	124.32(7)
O(3)-C(9)-C(8)	123.90(7)
O(4)-C(9)-C(8)	111.78(7)
O(4)-C(10)-C(11)	110.40(8)
C(17)-C(14)-C(15)	108.94(7)
C(17)-C(14)-C(16)	108.81(7)
C(15)-C(14)-C(16)	108.75(7)
C(17)-C(14)-Si(1)	110.46(5)
C(15)-C(14)-Si(1)	109.83(5)
C(16)-C(14)-Si(1)	110.01(5)

---

Table 4. Anisotropic displacement parameters ( $\text{\AA}^2 \times 10^3$ ) for mb1. The anisotropic displacement factor exponent takes the form:  $-2\pi^2 [h^2 a^{*2} U^{11} + \dots + 2 h k a^* b^* U^{12}]$

	$U^{11}$	$U^{22}$	$U^{33}$	$U^{23}$	$U^{13}$	$U^{12}$
Si(1)	11(1)	14(1)	12(1)	1(1)	-1(1)	1(1)
O(1)	11(1)	12(1)	16(1)	0(1)	-3(1)	1(1)
O(2)	14(1)	10(1)	16(1)	-1(1)	-1(1)	-1(1)
O(3)	19(1)	13(1)	18(1)	-2(1)	0(1)	0(1)
O(4)	27(1)	21(1)	13(1)	-5(1)	5(1)	-4(1)
N(1)	15(1)	16(1)	13(1)	-1(1)	2(1)	0(1)
N(2)	28(1)	19(1)	17(1)	2(1)	5(1)	-3(1)
C(1)	10(1)	11(1)	13(1)	1(1)	-1(1)	0(1)
C(2)	13(1)	18(1)	12(1)	1(1)	1(1)	-1(1)
C(3)	22(1)	18(1)	16(1)	5(1)	-3(1)	-3(1)
C(4)	19(1)	22(1)	16(1)	4(1)	-3(1)	3(1)
C(5)	16(1)	19(1)	15(1)	1(1)	-4(1)	1(1)
C(6)	12(1)	15(1)	15(1)	0(1)	-1(1)	2(1)
C(7)	11(1)	10(1)	11(1)	-1(1)	0(1)	-1(1)
C(8)	14(1)	12(1)	12(1)	0(1)	1(1)	-1(1)
C(9)	12(1)	16(1)	13(1)	-3(1)	0(1)	1(1)
C(10)	28(1)	25(1)	17(1)	-9(1)	4(1)	-2(1)
C(11)	33(1)	23(1)	17(1)	1(1)	-5(1)	-4(1)
C(12)	18(1)	31(1)	17(1)	8(1)	0(1)	3(1)
C(13)	17(1)	16(1)	22(1)	-3(1)	-3(1)	0(1)
C(14)	11(1)	16(1)	17(1)	2(1)	-1(1)	1(1)
C(15)	18(1)	16(1)	34(1)	0(1)	1(1)	2(1)
C(16)	13(1)	25(1)	25(1)	-1(1)	-4(1)	2(1)
C(17)	17(1)	28(1)	20(1)	3(1)	4(1)	3(1)

Table 5. Hydrogen coordinates ( $\times 10^4$ ) and isotropic displacement parameters ( $\text{\AA}^2 \times 10^{-3}$ ) for **158s**.

	x	y	z	U(eq)
H(2)	5339(14)	10801(11)	3283(8)	22(3)
H(1A)	4338(11)	8243(9)	3278(7)	11(2)
H(2A)	4456(12)	9702(10)	4716(8)	22(3)
H(2B)	3279(14)	8841(11)	4524(8)	28(3)
H(3A)	4397(13)	7763(11)	5428(8)	27(3)
H(3B)	4791(15)	7352(12)	4526(9)	36(4)
H(4A)	6693(14)	7531(12)	5251(8)	29(3)
H(4B)	6249(13)	8490(11)	5791(8)	25(3)
H(5A)	6762(12)	9721(11)	4750(8)	23(3)
H(5B)	7908(11)	8924(10)	4810(7)	15(3)
H(6A)	7628(12)	8987(10)	3416(7)	16(3)
H(6B)	6793(12)	7974(10)	3557(8)	20(3)
H(10A)	6734(15)	7504(13)	-75(9)	31(3)
H(10B)	6383(15)	6689(13)	708(10)	39(4)
H(11A)	4484(13)	7925(11)	-247(8)	26(3)
H(11B)	4173(13)	7127(11)	446(8)	24(3)
H(11C)	4746(14)	6669(13)	-379(9)	34(4)
H(12A)	3674(14)	9671(12)	1035(9)	36(4)
H(12B)	2331(16)	10187(13)	900(10)	46(4)
H(12C)	3419(15)	10815(13)	1412(10)	39(4)
H(13A)	1902(13)	7634(12)	2724(9)	30(3)
H(13B)	1585(15)	7835(12)	1739(9)	34(4)
H(13C)	3036(14)	7581(12)	2086(9)	32(3)
H(15A)	1870(14)	11631(11)	3097(9)	29(3)
H(15B)	1299(14)	11664(12)	2158(9)	35(4)
H(15C)	390(14)	11829(11)	2971(9)	34(4)
H(16A)	60(12)	10038(10)	1550(8)	21(3)
H(16B)	-924(15)	10300(13)	2319(10)	43(4)

H(16C)	-316(16)	9021(13)	2144(10)	45(4)
H(17A)	-174(13)	10122(11)	3831(8)	27(3)
H(17B)	1322(13)	10003(12)	4044(8)	27(3)
H(17C)	495(14)	9015(12)	3666(9)	31(3)

---

Table 6. Torsion angles [°] for **158s**.

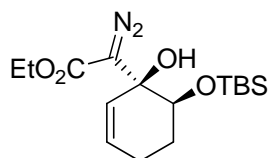
C(13)-Si(1)-O(1)-C(1)	14.23(7)
C(12)-Si(1)-O(1)-C(1)	-107.01(7)
C(14)-Si(1)-O(1)-C(1)	134.49(6)
Si(1)-O(1)-C(1)-C(2)	-121.39(6)
Si(1)-O(1)-C(1)-C(7)	114.98(6)
O(1)-C(1)-C(2)-C(3)	166.40(6)
C(7)-C(1)-C(2)-C(3)	-74.99(8)
C(1)-C(2)-C(3)-C(4)	87.23(8)
C(2)-C(3)-C(4)-C(5)	-31.14(10)
C(3)-C(4)-C(5)-C(6)	-46.52(10)
C(4)-C(5)-C(6)-C(7)	89.44(9)
C(5)-C(6)-C(7)-O(2)	54.58(8)
C(5)-C(6)-C(7)-C(8)	170.61(6)
C(5)-C(6)-C(7)-C(1)	-67.54(8)
O(1)-C(1)-C(7)-O(2)	51.00(7)
C(2)-C(1)-C(7)-O(2)	-68.45(7)
O(1)-C(1)-C(7)-C(6)	171.50(6)
C(2)-C(1)-C(7)-C(6)	52.05(8)
O(1)-C(1)-C(7)-C(8)	-66.88(7)
C(2)-C(1)-C(7)-C(8)	173.67(6)
N(2)-N(1)-C(8)-C(9)	167.6(16)
N(2)-N(1)-C(8)-C(7)	-15.2(17)
O(2)-C(7)-C(8)-N(1)	2.39(9)
C(6)-C(7)-C(8)-N(1)	-113.00(7)
C(1)-C(7)-C(8)-N(1)	121.52(7)
O(2)-C(7)-C(8)-C(9)	179.34(7)



C(6)-C(7)-C(8)-C(9)	63.94(9)
C(1)-C(7)-C(8)-C(9)	-61.54(9)
C(10)-O(4)-C(9)-O(3)	4.24(12)
C(10)-O(4)-C(9)-C(8)	-175.76(7)
N(1)-C(8)-C(9)-O(3)	-177.47(7)
C(7)-C(8)-C(9)-O(3)	5.61(13)
N(1)-C(8)-C(9)-O(4)	2.53(10)
C(7)-C(8)-C(9)-O(4)	-174.40(7)
C(9)-O(4)-C(10)-C(11)	88.53(9)
O(1)-Si(1)-C(14)-C(17)	-53.42(6)
C(13)-Si(1)-C(14)-C(17)	66.83(6)
C(12)-Si(1)-C(14)-C(17)	-171.32(6)
O(1)-Si(1)-C(14)-C(15)	66.76(6)
C(13)-Si(1)-C(14)-C(15)	-172.99(6)
C(12)-Si(1)-C(14)-C(15)	-51.14(7)
O(1)-Si(1)-C(14)-C(16)	-173.57(5)
C(13)-Si(1)-C(14)-C(16)	-53.32(7)
C(12)-Si(1)-C(14)-C(16)	68.53(7)

---

**Crystallographic data for Ethyl 2-(6-(tert-butyldimethylsilyloxy)-1-hydroxycyclohex-2-enyl)-2-diazoacetate (157s):**



**Experimental**

A colorless crystal of approximate dimensions 0.22 x 0.26 x 0.27 mm was mounted on a glass fiber and transferred to a Bruker SMART APEX II diffractometer. The APEX2<sup>1</sup> program package was used to determine the unit-cell parameters and for data collection (20 sec/frame scan time for a sphere of diffraction data). The raw frame data was processed using SAINT<sup>2</sup> and SADABS<sup>3</sup> to yield the reflection data file. Subsequent calculations were carried out using the SHELXTL<sup>4</sup> program. The diffraction symmetry was  $2/m$  and the systematic absences were consistent with the monoclinic space group  $P2_1/c$  that was later determined to be correct.

The structure was solved by direct methods and refined on  $F^2$  by full-matrix least-squares techniques. The analytical scattering factors<sup>5</sup> for neutral atoms were used throughout the analysis. Hydrogen atoms were located from a difference-Fourier map and refined ( $x, y, z$  and  $U_{iso}$ ).

At convergence,  $wR2 = 0.0938$  and  $Goof = 1.044$  for 320 variables refined against 4685 data ( $0.75\text{\AA}$ ),  $R1 = 0.0330$  for those 4140 data with  $I > 2.0\sigma(I)$ .

**References**

1. APEX2 Version 2.2-0 Bruker AXS, Inc.; Madison, WI 2007.
2. SAINT Version 7.46a, Bruker AXS, Inc.; Madison, WI 2007.
3. Sheldrick, G. M. SADABS, Version 2007/4, Bruker AXS, Inc.; Madison, WI 2007.
4. Sheldrick, G. M. SHELXTL, Version 6.12, Bruker AXS, Inc.; Madison, WI 2001.
5. International Tables for X-Ray Crystallography 1992, Vol. C., Dordrecht: Kluwer Academic Publishers.

## Definitions

$$wR2 = [\Sigma[w(F_o^2 - F_c^2)^2] / \Sigma[w(F_o^2)^2]]^{1/2}$$

$$R1 = \Sigma||F_o| - |F_c|| / \Sigma|F_o|$$

Goof = S =  $[\Sigma[w(F_o^2 - F_c^2)^2] / (n-p)]^{1/2}$  where n is the number of reflections and p is the total number of parameters refined.

The thermal ellipsoid plot is shown at the 50% probability level.

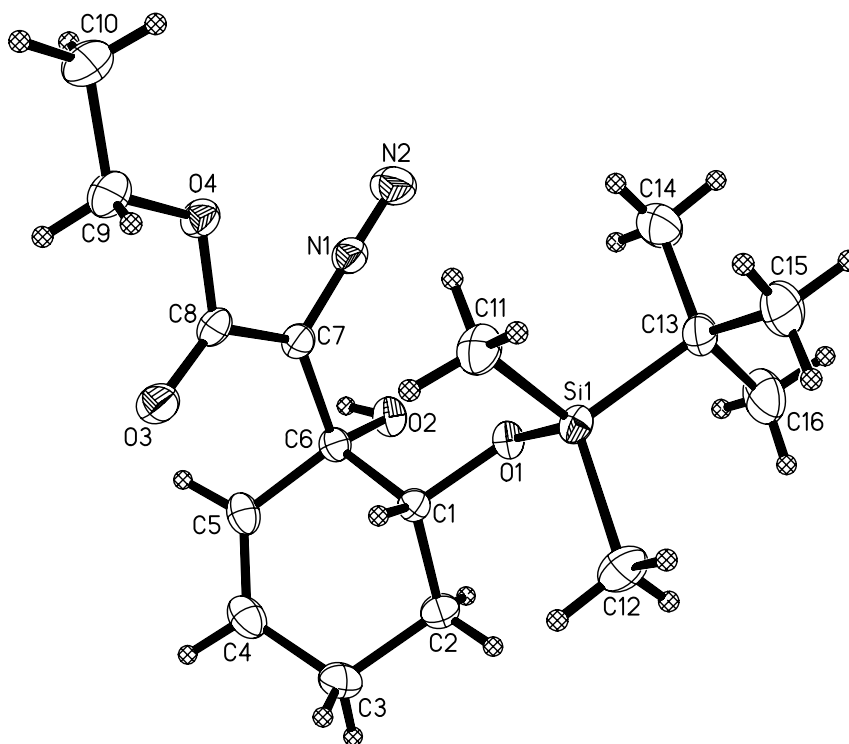


Table 1. Crystal data and structure refinement for **157s**.

Identification code	mb2	
Empirical formula	C <sub>16</sub> H <sub>28</sub> N <sub>2</sub> O <sub>4</sub> Si	
Formula weight	340.49	
Temperature	163(2) K	
Wavelength	0.71073 Å	
Crystal system	Monoclinic	
Space group	<i>P</i> 2 <sub>1</sub> / <i>c</i>	
Unit cell dimensions	<i>a</i> = 9.0925(6) Å <i>b</i> = 21.3372(15) Å <i>c</i> = 10.5045(7) Å	$\alpha = 90^\circ$ . $\beta = 111.3760(10)^\circ$ . $\gamma = 90^\circ$ .
Volume	1897.8(2) Å <sup>3</sup>	
<i>Z</i>	4	
Density (calculated)	1.192 Mg/m <sup>3</sup>	
Absorption coefficient	0.143 mm <sup>-1</sup>	
<i>F</i> (000)	736	
Crystal color	colorless	
Crystal size	0.27 x 0.26 x 0.22 mm <sup>3</sup>	
Theta range for data collection	3.98 to 28.28°	
Index ranges	-12 ≤ <i>h</i> ≤ 12, -28 ≤ <i>k</i> ≤ 28, -13 ≤ <i>l</i> ≤ 13	
Reflections collected	22747	
Independent reflections	4685 [ <i>R</i> (int) = 0.0262]	
Completeness to theta = 28.28°	99.7 %	
Absorption correction	Semi-empirical from equivalents	
Max. and min. transmission	0.9691 and 0.9623	
Refinement method	Full-matrix least-squares on <i>F</i> <sup>2</sup>	
Data / restraints / parameters	4685 / 0 / 320	
Goodness-of-fit on <i>F</i> <sup>2</sup>	1.044	
Final <i>R</i> indices [ <i>I</i> > 2σ( <i>I</i> ) = 4140 data]	<i>R</i> 1 = 0.0330, <i>wR</i> 2 = 0.0899	
<i>R</i> indices (all data; 0.75Å)	<i>R</i> 1 = 0.0378, <i>wR</i> 2 = 0.0938	
Largest diff. peak and hole	0.409 and -0.179 e.Å <sup>-3</sup>	

Table 2. Atomic coordinates ( $\times 10^4$ ) and equivalent isotropic displacement parameters ( $\text{\AA}^2 \times 10^3$ ) for **157s**.  $U(\text{eq})$  is defined as one third of the trace of the orthogonalized  $U_{ij}$  tensor.

	x	y	z	U(eq)
Si(1)	3785(1)	6322(1)	7990(1)	20(1)
O(1)	4700(1)	6798(1)	7282(1)	20(1)
O(2)	6773(1)	7351(1)	6347(1)	23(1)
O(3)	9151(1)	7078(1)	10739(1)	28(1)
O(4)	9761(1)	6137(1)	10090(1)	23(1)
N(1)	8083(1)	6337(1)	7574(1)	23(1)
N(2)	8032(1)	5957(1)	6818(1)	34(1)
C(1)	5540(1)	7333(1)	7994(1)	18(1)
C(2)	4601(1)	7932(1)	7499(1)	26(1)
C(3)	5480(2)	8483(1)	8377(1)	31(1)
C(4)	7209(2)	8468(1)	8623(1)	29(1)
C(5)	7959(1)	7975(1)	8394(1)	24(1)
C(6)	7118(1)	7373(1)	7782(1)	19(1)
C(7)	8134(1)	6801(1)	8415(1)	20(1)
C(8)	9036(1)	6700(1)	9843(1)	20(1)
C(9)	10675(2)	6005(1)	11520(1)	30(1)
C(10)	11645(2)	5436(1)	11568(2)	42(1)
C(11)	5248(1)	5949(1)	9546(1)	29(1)
C(12)	2309(2)	6765(1)	8480(1)	32(1)
C(13)	2804(1)	5724(1)	6627(1)	26(1)
C(14)	4034(2)	5372(1)	6215(2)	38(1)
C(15)	1894(2)	5250(1)	7158(2)	39(1)
C(16)	1647(2)	6056(1)	5367(1)	41(1)

Table 3. Bond lengths [Å] and angles [°] for **157s**.

Si(1)-O(1)	1.6516(7)
Si(1)-C(12)	1.8609(12)
Si(1)-C(11)	1.8680(12)
Si(1)-C(13)	1.8818(11)
O(1)-C(1)	1.4250(12)
O(2)-C(6)	1.4250(12)
O(3)-C(8)	1.2152(13)
O(4)-C(8)	1.3501(12)
O(4)-C(9)	1.4545(13)
N(1)-N(2)	1.1236(14)
N(1)-C(7)	1.3162(13)
C(1)-C(2)	1.5203(14)
C(1)-C(6)	1.5317(14)
C(2)-C(3)	1.5272(16)
C(3)-C(4)	1.4986(18)
C(4)-C(5)	1.3227(17)
C(5)-C(6)	1.5135(14)
C(6)-C(7)	1.5286(14)
C(7)-C(8)	1.4394(14)
C(9)-C(10)	1.4913(18)
C(13)-C(16)	1.5316(17)
C(13)-C(14)	1.5334(17)
C(13)-C(15)	1.5353(16)
O(1)-Si(1)-C(12)	110.15(5)
O(1)-Si(1)-C(11)	109.93(5)
C(12)-Si(1)-C(11)	109.24(6)
O(1)-Si(1)-C(13)	104.52(4)
C(12)-Si(1)-C(13)	111.43(6)
C(11)-Si(1)-C(13)	111.50(5)
C(1)-O(1)-Si(1)	121.23(6)
C(8)-O(4)-C(9)	115.14(8)

N(2)-N(1)-C(7)	177.45(11)
O(1)-C(1)-C(2)	111.59(8)
O(1)-C(1)-C(6)	108.66(8)
C(2)-C(1)-C(6)	110.04(8)
C(1)-C(2)-C(3)	109.63(9)
C(4)-C(3)-C(2)	111.89(10)
C(5)-C(4)-C(3)	124.28(10)
C(4)-C(5)-C(6)	122.61(10)
O(2)-C(6)-C(5)	111.09(8)
O(2)-C(6)-C(7)	107.38(8)
C(5)-C(6)-C(7)	111.17(8)
O(2)-C(6)-C(1)	107.17(8)
C(5)-C(6)-C(1)	109.90(8)
C(7)-C(6)-C(1)	110.03(8)
N(1)-C(7)-C(8)	117.03(9)
N(1)-C(7)-C(6)	116.13(9)
C(8)-C(7)-C(6)	126.66(9)
O(3)-C(8)-O(4)	122.98(9)
O(3)-C(8)-C(7)	124.31(10)
O(4)-C(8)-C(7)	112.71(9)
O(4)-C(9)-C(10)	107.47(10)
C(16)-C(13)-C(14)	108.94(11)
C(16)-C(13)-C(15)	109.12(10)
C(14)-C(13)-C(15)	108.97(10)
C(16)-C(13)-Si(1)	109.25(8)
C(14)-C(13)-Si(1)	110.74(8)
C(15)-C(13)-Si(1)	109.80(9)

---

Table 4. Anisotropic displacement parameters ( $\text{\AA}^2 \times 10^3$ ) for mb2. The anisotropic displacement factor exponent takes the form:  $-2\pi^2 [h^2 a^{*2} U^{11} + \dots + 2 h k a^* b^* U^{12}]$

	$U^{11}$	$U^{22}$	$U^{33}$	$U^{23}$	$U^{13}$	$U^{12}$
Si(1)	16(1)	22(1)	21(1)	2(1)	6(1)	0(1)
O(1)	18(1)	21(1)	19(1)	-1(1)	6(1)	-3(1)
O(2)	24(1)	27(1)	17(1)	2(1)	8(1)	-3(1)
O(3)	27(1)	34(1)	21(1)	-1(1)	8(1)	7(1)
O(4)	22(1)	25(1)	21(1)	3(1)	6(1)	4(1)
N(1)	21(1)	24(1)	22(1)	2(1)	6(1)	3(1)
N(2)	40(1)	30(1)	28(1)	-3(1)	7(1)	8(1)
C(1)	18(1)	18(1)	18(1)	0(1)	6(1)	0(1)
C(2)	23(1)	23(1)	28(1)	3(1)	6(1)	5(1)
C(3)	37(1)	20(1)	36(1)	0(1)	10(1)	5(1)
C(4)	37(1)	20(1)	25(1)	0(1)	7(1)	-5(1)
C(5)	25(1)	24(1)	21(1)	1(1)	6(1)	-6(1)
C(6)	19(1)	19(1)	17(1)	1(1)	6(1)	-1(1)
C(7)	17(1)	22(1)	20(1)	0(1)	7(1)	1(1)
C(8)	15(1)	26(1)	22(1)	2(1)	9(1)	1(1)
C(9)	29(1)	34(1)	23(1)	5(1)	3(1)	4(1)
C(10)	41(1)	36(1)	36(1)	6(1)	-1(1)	12(1)
C(11)	27(1)	31(1)	26(1)	7(1)	6(1)	0(1)
C(12)	28(1)	38(1)	36(1)	2(1)	18(1)	4(1)
C(13)	21(1)	24(1)	29(1)	-1(1)	6(1)	-4(1)
C(14)	36(1)	34(1)	46(1)	-13(1)	17(1)	-5(1)
C(15)	31(1)	31(1)	53(1)	0(1)	15(1)	-11(1)
C(16)	38(1)	39(1)	31(1)	0(1)	-5(1)	-6(1)



Table 5. Hydrogen coordinates ( $\times 10^4$ ) and isotropic displacement parameters ( $\text{\AA}^2 \times 10^3$ ) for **157s**.

	x	y	z	U(eq)
H(2)	7520(20)	7489(8)	6196(17)	42(4)
H(1A)	5790(14)	7295(5)	8953(12)	12(3)
H(2A)	4474(17)	7998(7)	6548(15)	32(4)
H(2B)	3591(19)	7884(7)	7557(15)	33(4)
H(3A)	5331(19)	8477(7)	9265(17)	41(4)
H(3B)	5043(19)	8874(7)	7944(16)	39(4)
H(4A)	7793(18)	8841(7)	9013(15)	31(4)
H(5A)	9083(18)	7981(7)	8571(15)	32(4)
H(9A)	11310(19)	6371(8)	11905(16)	41(4)
H(9B)	9940(20)	5947(8)	12006(17)	50(5)
H(10A)	12270(20)	5344(8)	12525(19)	55(5)
H(10B)	12310(20)	5497(9)	11080(20)	60(5)
H(10C)	10970(20)	5082(9)	11170(20)	61(5)
H(11A)	5750(20)	6246(8)	10234(18)	47(5)
H(11B)	6040(20)	5707(8)	9339(16)	44(4)
H(11C)	4750(20)	5658(8)	10002(17)	48(4)
H(12A)	2790(20)	7103(8)	9136(17)	41(4)
H(12B)	1530(20)	6949(8)	7711(17)	44(4)
H(12C)	1850(20)	6496(9)	8950(20)	61(5)
H(14A)	4750(20)	5151(8)	6997(18)	46(4)
H(14B)	4660(20)	5655(8)	5868(17)	50(5)
H(14C)	3530(20)	5062(8)	5488(18)	50(5)
H(15A)	1340(20)	4947(8)	6442(18)	50(5)
H(15B)	2630(20)	5012(8)	7964(18)	50(5)
H(15C)	1140(20)	5454(9)	7474(19)	56(5)

H(16A)	770(20)	6285(8)	5576(19)	54(5)
H(16B)	1130(20)	5740(9)	4639(19)	54(5)
H(16C)	2170(20)	6368(9)	4970(20)	61(5)

---

Table 6. Torsion angles [°] for **157s**.

C(12)-Si(1)-O(1)-C(1)	57.80(8)
C(11)-Si(1)-O(1)-C(1)	-62.63(8)
C(13)-Si(1)-O(1)-C(1)	177.60(7)
Si(1)-O(1)-C(1)-C(2)	-102.23(9)
Si(1)-O(1)-C(1)-C(6)	136.26(7)
O(1)-C(1)-C(2)-C(3)	174.83(9)
C(6)-C(1)-C(2)-C(3)	-64.47(12)
C(1)-C(2)-C(3)-C(4)	44.33(13)
C(2)-C(3)-C(4)-C(5)	-14.73(17)
C(3)-C(4)-C(5)-C(6)	3.20(18)
C(4)-C(5)-C(6)-O(2)	96.99(12)
C(4)-C(5)-C(6)-C(7)	-143.50(10)
C(4)-C(5)-C(6)-C(1)	-21.44(14)
O(1)-C(1)-C(6)-O(2)	52.96(10)
C(2)-C(1)-C(6)-O(2)	-69.49(10)
O(1)-C(1)-C(6)-C(5)	173.78(8)
C(2)-C(1)-C(6)-C(5)	51.33(11)
O(1)-C(1)-C(6)-C(7)	-63.48(10)
C(2)-C(1)-C(6)-C(7)	174.07(8)
N(2)-N(1)-C(7)-C(8)	-152(3)
N(2)-N(1)-C(7)-C(6)	32(3)
O(2)-C(6)-C(7)-N(1)	-19.55(12)
C(5)-C(6)-C(7)-N(1)	-141.26(9)
C(1)-C(6)-C(7)-N(1)	96.76(10)
O(2)-C(6)-C(7)-C(8)	165.62(9)
C(5)-C(6)-C(7)-C(8)	43.92(13)

C(1)-C(6)-C(7)-C(8)	-78.06(12)
C(9)-O(4)-C(8)-O(3)	1.21(14)
C(9)-O(4)-C(8)-C(7)	-179.24(9)
N(1)-C(7)-C(8)-O(3)	-177.81(10)
C(6)-C(7)-C(8)-O(3)	-3.03(16)
N(1)-C(7)-C(8)-O(4)	2.64(13)
C(6)-C(7)-C(8)-O(4)	177.42(9)
C(8)-O(4)-C(9)-C(10)	-168.40(11)
O(1)-Si(1)-C(13)-C(16)	-60.04(10)
C(12)-Si(1)-C(13)-C(16)	58.91(11)
C(11)-Si(1)-C(13)-C(16)	-178.75(9)
O(1)-Si(1)-C(13)-C(14)	59.96(9)
C(12)-Si(1)-C(13)-C(14)	178.90(9)
C(11)-Si(1)-C(13)-C(14)	-58.75(10)
O(1)-Si(1)-C(13)-C(15)	-179.67(8)
C(12)-Si(1)-C(13)-C(15)	-60.72(10)
C(11)-Si(1)-C(13)-C(15)	61.62(10)